Role of Doc2β in Regulated Exocytosis of Large Dense-Core Vesicles in Bovine Adrenal Chromaffin cells

by

Sompol Tapechum

A dissertation submitted for the degree of Doctor of Philosophy

Department of Biomedical Sciences, Faculty of Medicine

The University of Edinburgh

2003

DECLARATION

This study was carried out under the supervision of Dr Michael J. Shipston and Dr Robert H. Chow in the Membrane Biology Group, Division of Biomedical Sciences, University of Edinburgh and the Department of Physiology & Biophysics, University of Southern California, USA between October 1998 and October 2002.

The experimental work presented in this thesis is my own and this thesis has been composed by myself.

Sompol TAPECHUM

Membrane Biology Group

Division of Biomedical Sciences

Hugh Robson Building

University of Edinburgh

Edinburgh EH8 9XD

April 2003

Table of Contents

Table of Contents i

List of Tables xii

List of Figures xiv

List of Abbreviations xxi

Abstract 1

Chapter 1 Introduction 3

1.1 Exocytosis 4

1.1.1 Constitutive exocytosis 5

1.1.2 Regulated exocytosis 5

1.2 Molecular mechanism of regulated exocytosis 10

1.2.1 Proteins involved in vesicle docking 10

1.2.1.1 Munc18 11

1.2.1.2 Rab3 12

1.2.2 Priming of secretory vesicles 14

1.2.2.1 NSF and SNAP 15

1.2.2.2 Protein Kinase C 16

1.2.2.3 Phosphatidylinositol kinases 17

1.2.2.4 Munc13 17

1.2.3 Proteins involved in the fusion reaction 22

1.2.4 C2 domain proteins 23

1.2.4.1 Synaptotagmin 25

1.2.4.2 Rabphilin3A 26

1.3 Doc2 27

1.3.1 Doc2α 27

1.3.1.1 Ca^{2+}-dependent phospholipid-binding 28

1.3.1.2 Doc2α-Munc13 interaction 29

1.3.1.3 Doc2α-Munc18 interaction 29

1.3.1.4 Doc2α-Dynein interaction 30

1.3.1.5 Roles of Doc2α in regulated exocytosis 30

1.3.2 DOC2β 34

1.3.2.1 Ca^{2+}-dependent phospholipid binding 35

1.3.2.2 Interaction with Munc13 35

1.3.2.3 Interaction with Munc18 36

1.3.2.4 Interaction with a motor protein Dynein 36

1.3.3 Doc2γ 36

1.3.4 Roles of Doc2β in regulated exocytosis 37

1.3.5 Proposed functions of Doc2β in regulated exocytosis..... 37

1.3.5.1 Vesicle recruitment and docking 37

1.3.5.2 Vesicle priming 38

Chapter 2 Materials and Methods 42

2.1 MATERIALS 43

2.1.1 Bacterial strains 43

2.1.1.1 SCS110 (Stratagene, La Jolla, CA, US.) 43

2.1.1.2 DH5α (Clontech, Palo Alto, CA, US.) 43

2.1.2 Cell line 43

2.1.3 Plasmid vectors..... 43

2.1.3.1 pIRES2-EGFP 43

2.1.3.2 Superlinker Phagemid pSL1180 44

2.1.3.3 pSCA1 and pSCAHelper 44

2.1.3.4 Doc2β gene, Doc2β-EGFP fusion gene and C2AB-EGFP fusion gene... 45

2.1.4 Molecular biology reagents 45

2.1.4.1 Plasmid DNA Purification kits.....45

2.1.4.2 Enzymes 46

2.1.4.3 DNA Electrophoresis 46

2.1.4.4 DNA extraction from agarose 47

2.1.4.5 Protein Electrophoresis and Western Blotting 47

2.1.5 Bacterial Culture Media and Related products..... 47

2.1.6 Mammalian Cell Culture media and Cell culture supplementary..... 48

2.1.7 Chemicals and Solutions 48

2.2 METHODS.....50

2.2.1 Construction of Recombinant plasmid vectors..... 50

2.2.1.1 Preparation of Plasmids for Restriction Digests.....51

2.2.1.2 Restriction Digests 51

2.2.1.3 DNA Electrophoresis 52

2.2.1.4 DNA Extraction from Agarose Gel.....52

2.2.1.5 Dephosphorylation of 5'-end....53

2.2.1.6 DNA Ligation....53

2.2.2 Bacterial Transformation....53

2.2.2.1 Preparation of Competent Bacteria....53

2.2.2.2 Transformation....54

2.2.3 Analysis of Transformants....54

2.2.4 DNA Sequencing....55

2.2.5 Large Scale DNA preparation....55

2.2.6 Long-term Storage of transformants....56

2.2.7 Viral packaging....56

2.2.7.1 HEK293T cell culture....56

2.2.7.2 Calcium Phosphate transfection....56

2.2.8 Viral Activation....58

2.2.9 Titering of viral particles....58

2.2.10 Detection of protein expression in SFV-infected cells....59

2.2.10.1 Preparation of cell lysate....59

2.2.10.2 SDS Polyacrylamide Gel Electrophoresis (SDS-PAGE)....59

2.2.10.3 Electroblotting 61

2.2.10.4 Indirect Enzyme Immunoassay detection of proteins on membrane 61

2.2.11 Primary culture of bovine adrenal chromaffin cells 62

2.2.12 Bovine adrenal chromaffin cells infection 63

2.2.13 Population Assay 64

2.2.13.1 High-K^+ stimulation 64

2.2.13.2 β-escin permeabilisation 64

2.2.13.3 Catecholamine assay 66

2.2.13.4 Calibration of the catecholamine concentration 67

2.2.14 Electrophysiological recording 67

2.2.14.1 Patch clamp 67

2.2.14.2 Membrane capacitance measurements 69

2.2.14.3 Measurement of the fusion-competent vesicle pool 69

2.2.14.4 Electrochemical detection of catecholamine release 77

2.2.14.5 Measurement of intracellular calcium 78

2.2.15 Imaging 83

2.2.16 Analysis *83*

2.2.16.1 Data Analysis 83

2.2.16.2 Statistical Analysis 83

Chapter 3 Protein expression using DNA-based Semliki Forest Virus (SFV) vectors 84

3.1 Introduction 85

3.2 Results 90

3.2.1 High viral titer was achieved by using calcium-phosphate transfection of HEK293T for viral packaging 93

3.2.2 Efficiency of SFV transduction system in primary cultured bovine adrenal chromaffin cells 94

3.2.3 Subcellular distribution of proteins expressed by SFV expression system 96

3.2.4 No obvious cytotoxic effect was observed in SFV-infected cells 100

3.2.5 Basal intracellular Ca^{2+} concentration ($[Ca^{2+}]_i$) was increased in viral infected cells 104

3.2.6 SFV infection affected calcium currents in bovine adrenal chromaffin cells 106

3.2.7 Sodium current was reduced by SFV infection 109

3.2.8 The catecholamine content was not affected by SFV infection 112

3.2.9 SFV infection did not affect catecholamine secretion 113

3.2.9.1 Effect of SFV infection on catecholamine secretion in cell-populations 113

3.2.9.2 Effect of SFV infection on single cell exocytosis 117

3.2.9.3 Single vesicle exocytosis 130

3.3 Conclusion 135

Chapter 4 Effects of Doc2β expression in bovine adrenal chromaffin cells 136

4.1 Introduction 137

4.2 Results 139

4.2.1 Doc2β did not affect cell morphology 139

4.2.2 Basal intracellular Ca^{2+} ($[Ca^{2+}]_i$) concentration was not altered by Doc2β expression 140

4.2.3 Doc2β did not affect calcium and sodium currents 141

4.2.4 Doc2β did not affect the total catecholamine content 144

4.2.5 Doc2β expression did not affect secretion..... 145

4.2.5.1Effect of Doc2β on catecholamine secretion in cell-population....145

4.2.5.2 Effect of Doc2β expression on single cell exocytosis 149

4.2.6 Effect of Doc2β expression on single vesicle exocytosis..... 156

4.3 Conclusion 160

Chapter 5 Effects of phorbol ester 161

5.1 Introduction.....162

5.2 Results 163

5.2.1 The fluorescence distribution in cells expressing Doc2β-EGFP was not affected by phorbol ester 163

5.2.2 Effect of Phorbol ester on exocytosis 165

5.2.2.1 High-K^+ stimulation.....165

5.2.2.2 β-escin permeabilisation 167

5.2.2.3 Step depolarisation.....169

5.3 Conclusion 173

Summarised results 174

Chapter 6 DISCUSSION 182

Discussion 183

6.1 Semliki forest virus (SFV) transduction system for Exocytosis study 183

6.2 Role of Doc2β in regulated exocytosis of large dense-core vesicles in bovine adrenal chromaffin cells 189

Conclusion 193

Perspectives 194

Chapter 7 APPENDICES 196

Appendix I

Patch clamp Membrane Capacitance Measurements 197

Appendix II

Electrochemical detection of catecholamines release from single bovine adrenal chromaffin cells 202

Appendix III

Analysis of amperometric currents 208

Data acquisition 208

File opening 210

Baseline characterisation 211

Identification of peak 211

Peak selection 211

Identification of the actual peak, the beginning and the end of the amperometric event 212

Measurement of amperometric parameters 213

Measurement of foot parameters 216

Acknowledgements 218

Chapter 8 Bibliography 219

Publications 234

High-efficiency Semliki Forest virus-mediated transduction in bovine adrenal chromaffin cells 235

Efficacy of Semliki Forest Virus Transduction of Bovine Adrenal Chromaffin Cells 240

Use of ANF-EGFP for the Visualization of Secretory Vesicles in Bovine Adrenal Chromaffin cells 246

List of Tables

Table 1: Leak currents 174

Table 2: Initial membrane capacitance 174

Table 3: Basal intracellular calcium concentration 174

Table 4: Calcium currents 175

Table 5: Sodium currents 175

Table 6: Total catecholamine content 175

Table 7: High-K^+ induced catecholamine secretion 176

Table 8: Catecholamine secretion by β-escin permeabilisation. 176

Table 9: Capacitance changes in response to 50-ms depolarization 177

Table 10: Fusion-competent vesicle pool size 177

Table 11: Capacitance response to intracellular dialysis with 10 μM Ca^{2+} 178

Table 12: Amperometric current response to intracellular dialysis. 178

Table 13: Amperometric current amplitude 179

Table 14: Amperometric current charge 179

Table 15: Amperometric current 50-90%risetime 179

Table 16: Amperometric current halfwidth 180

Table 17: Amperometric current decay time constant.....180

Table 18: Amperometric foot amplitude 180

Table 19: Amperometric foot duration 181

Table 20: Amperometric foot charge.....181

List of Figures

Figure 1-1 Synaptic vesicle trafficking....9

Figure 1-2 Munc13s and Munc13-syntaxin interaction....21

Figure 1-3 Structure of C2 domain and protein containing C2 domains in vesicular transport pathway....24

Figure 1-4 Sequence alignment of mouse Doc2 family....33

Figure 1-5 Hypothetical model of Doc2β function in regulated exocytosis....39

Figure 2-1 Capacitance response to train of depolarisation....70

Figure 2-2 Measurement of capacitance response to each depolarisation....71

Figure 2-3 Cumulative capacitance responses....72

Figure 2-4 Depression of secretory response during train of depolarisation....74

Figure 2-5 Paired-pulse depolarisation....75

Figure 2-6 Correlation of the fusion-competent pool calculated from the train and pair-pulse protocols....76

Figure 2-7 Fura-2 fluorescence excitation and emission spectrum....79

Figure 2-8 Fura-2 calibration....81

Figure 2-9 Intracellular calcium measurement....82

Figure 3-1 RNA and DNA-based SFV vectors 87

Figure 3-2 Viral packaging in RNA- and DNA-based SFV transduction system 89

Figure 3-3 Domain structures of Doc2β and Doc2β C2-domain translation products from the DNA-based SFV replicons 91

Figure 3-4 Doc2β sequence 92

Figure 3-5 High efficiency expression by SFV system 95

Figure 3-6 Subcellular distribution of EGFP 97

Figure 3-7 subcellular distribution of Doc2β-EGFP 98

Figure 3-8 Distribution of C2AB-EGFP and EGFP from the bicistronic construct containing Doc2β and EGFP 99

Figure 3-9 The distribution of initial membrane capacitance in non-infected cells .101

Figure 3-10 Histogram summarises the effect of SFV infection on initial cell size.102

Figure 3-11 Histogram summarises the effect of SFV infection on the leak currents 103

Figure 3-12 Histogram summarises the effect of SFV infection on basal $[Ca^{2+}]_i$ 105

Figure 3-13 Distribution of calcium currents in non-infected cells 106

Figure 3-14 Effect of SFV infection on calcium currents 107

Figure 3-15 The rundown of calcium currents after SFV infection 108

Figure 3-16 Effect of SFV infection on sodium currents 109

Figure 3-17 Effect of $[Ca^{2+}]_i$ on calcium and sodium currents.....111

Figure 3-18 Total catecholamine content in SFV-infected and non-infected bovine adrenal chromaffin cells.....112

Figure 3-19 High-K^+ induced similar catecholamine secretion in SFV-infected and non-infected bovine adrenal chromaffin cells 114

Figure 3-20 Catecholamine secretion from β-escin permeabilised cells.....116

Figure 3-21 Cell membrane capacitance measurement and amperometry.....117

Figure 3-22 Single cell secretion during whole-cell Ca^{2+}-dialysis experiments 119

Figure 3-23 Latency histogram of amperometric current.....120

Figure 3-24 Amperometric currents from SFV-infected and non-infected cells during Ca^{2+} dialysis experiments 121

Figure 3-25 Membrane capacitance responses from SFV-infected and non-infected cells during Ca^{2+} dialysis experiments.....122

Figure 3-26 Effect of SFV infection on depolarisation-induced secretion.....124

Figure 3-27 Capacitance and amperometric response to a train of depolarisations .125

Figure 3-28 distribution of the fusion-competent vesicle pool sizes in non-infected cells 126

Figure 3-29 The fusion-competent vesicle pool was not affected by SFV-infection 127

Figure 3-30 Histogram summarizes the secretion from non-infected cells with different calcium currents 129

Figure 3-31 Amperometric current amplitude in SFV-infected and non-infected cells 130

Figure 3-32 Amperometric current amplitude and charge from selected responses with amplitude higher than 20 pA 131

Figure 3-33 The amperometric foot signal was not affected by SFV infection 133

Figure 3-34 Effects of SFV infection on risetime, halfwidth and decay time constant of amperometric currents 134

Figure 4-1 Effect of Doc2β and Doc2β C2 domains on basal cellular properties.... 139

Figure 4-2 Basal intracellular calcium concentration in Doc2β-, C2AB- and EGFP-expressing cells 140

Figure 4-3 The calcium and sodium currents from cells expressing Doc2β and Doc2β-EGFP 141

Figure 4-4 Effect of Doc2β and Doc2β C2 domains on calcium currents 142

Figure 4-5 Histogram summarizes the effect of Doc2β and Doc2β C2 domains on sodium currents 143

Figure 4-6 Total catecholamine content was not affected by Doc2β and Doc2β C2 domains 144

Figure 4-7 Histogram summarizes the effect of Doc2β and Doc2β C2 domains on high-K^+ stimulated catecholamine secretion 146

Figure 4-8 Effect of Doc2β and Doc2β C2 domains on catecholamine secretion in β-escin permeabilised cells 148

Figure 4-9 Effect of Doc2β and Doc2β C2 domains on membrane capacitance changes in Ca^{2+}dialysis experiments 150

Figure 4-10 Amperometric response to Ca^{2+}dialysis in Doc2β-expressing cells 151

Figure 4-11 Depolarization-induced secretion in cells expressing Doc2β and Doc2β-EGFP 152

Figure 4-12 Effect of Doc2β and Doc2β C2 domains on depolarization-induced secretion 153

Figure 4-13 The size of the fusion-competent vesicle pool in cells expressing Doc2β from the bicistronic and the fusion construct 154

Figure 4-14 The effect of Doc2β on the fusion-competent vesicle pool 155

Figure 4-15 Overall amperometric current amplitude 156

Figure 4-16 Effect of Doc2β on amperometric current amplitude 157

Figure 4-17 Effect of Doc2β on kinetics of single vesicle exocytosis 158

Figure 4-18 The amperometric foot signal was not affected by Doc2β and Doc2β C2 domains 159

Figure 5-1 Effect of phorbol ester on distribution of Doc2β-EGFP 164

Figure 5-2 Effect of phorbol ester on catecholamine secretion induced by high-K^+ stimulation 166

Figure 5-3 Effect of phorbol ester on catecholamine secretion in β-escin permeabilised cells 168

Figure 5-4 Effect of phorbol ester on calcium currents and secretion responded to 50-ms depolarisation 170

Figure 5-5 Effect of phorbol ester on the size of the fusion-competent vesicle pool 172

Figure 7-1 Three-component equivalent circuit 197

Figure 7-2 Current response to a sinusoidal voltage stimulus of the resistor-capacitor (RC) circuit 198

Figure 7-3 Low resolution capacitance recording 201

Figure 7-4 Oxidation of catechol from catecholamine to a quinone derivatives. 202

Figure 7-5 Amperometric current recording from a chromaffin cell 203

Figure 7-6 Individual amperometric currents 206

Figure 7-7 Structure of the macro for amperometric analysis 209

Figure 7-8 Capacitance recording.....210

Figure 7-9 Identification of an individual amperometric event.....212

Figure 7-10 Measurement of amperometric charge.....213

Figure 7-11 Identification of 50 and 90% of the amperometric amplitude.....214

Figure 7-12 Exponential fitting of the amperometric current.....215

Figure 7-13 Determination of foot parameter.....216

List of Abbreviations

A	Ampere
ATP	Adenosine triphosphate
BCIP	5-bromo-4-chloro-3-indolyl phosphate
BHK	Baby hamster kidney cell line
Bis	N,N'-ethylenebis(acrylamide)
bp	Base pair
°C	Celcius
C-terminus	Carboxy-terminus
Ca^{2+}	Calcium ion
$[Ca^{2+}]_i$	Intracellular calcium concentration
CFM	Carbon fiber microelectrode
CMV	Cytomegalovirus
Da	Dalton
DAG	Diacylglycerol
Did	Doc2-interacting domain of Munc13
DMEM	Dulbecco's Modified Eagle Medium

DSR	Doc2-specific region
EDP	Anodic electrophoretic deposition paint
EDTA	Ethylenediaminetetraacetic acid
EGFP	Enhanced green fluorescent protein
EGTA	Ethylene glycol-bis(2-aminoethyl)-N,N,N',N'-tetraacetic acid
EPSP	Excitatory postsynaptic potential
F	Farad
g	gram
GABA	Gamma- aminobutyric acid
GTP	Guanosine triphosphate
GDP	Guanosine diphosphate
HEDTA	N-(2-hydroxyethyl)ethylenediamine-N,N',N'-triacetic acid
HEPES	4-(2-hydroxyethyl)piperazine-1-ethanesulfonic acid
HRP	Horse radish peroxidase
Hz	Hertz
IMEM	Iscove's Modified Eagle Medium
IRES	Internal ribosomal entry site

ITSX	Insulin-transferrin-selenium mixture
l	liter
LDCV	Large dense-core vesicle
LTP	Long-term potentiation
kb	Kilobases
Kd	Dissociation constant
m	Meter
M	Molar
MCS	Multiple cloning sites
Mid	Munc13-interacting domain of Doc2
NP-40	Nonidet P-40
NTB	Nitro blue tetrazolium
N-terminus	Amino-terminus
Ω	Ohm
Osm	Osmole
PAGE	Polyacrylamide Gel Electrophoresis
PBS	Phosphate buffer saline

PCR	Polymerase chain reaction
PE	Phorbol ester
PI	Phosphatidylinositol
PIP_2	Phosphatidylinositol-4,5-phosphate
PKC	Protein kinase C
PMA	Phorbol-12-myristate-13-acetate
PMSF	Phenylmethanesulfonyl fluoride
Rab-BD	Rab-binding domain
rpm	Revolutions per minute
RRP	Readily releasable pool of vesicles
s	Second
S	Seimen
SDS	Sodium dodecyl sulfate
SEM	Standard error of the mean
SFV	Semliki forest virus
SNAP	Soluble N-ethylmaleimide-sensitive fusion protein attachment protein

SNAP-25	Synaptosomal-associated membrane protein of 25 kDa
SNARE	SNAP receptor
SRP	Slowly releasable pool of vesicles
TEMED	Tetramethylethylenediamine
TGN	trans-Golgi network
V	Volt
VAMP	Vesicle-associated membrane protein
v/v	volume by volume
w/v	weight by volume

Abstract

Doc2β is a member of the double C2-domain (Doc2) protein family, a novel family of proteins having two C2 domains. Doc2β is highly enriched in brain where it is associated with synaptic vesicles. However, Doc2β is also expressed in non-neuronal tissues. Like its brain-specific counterpart Doc2α, Doc2β interacts with Ca^{2+}, phospholipids, Munc13 and Munc18, all of which are important elements for regulated exocytosis. While the significant role of Doc2α in regulated exocytosis was confirmed in PC12 cells, the role of Doc2β in regulated exocytosis is still unresolved. Given the high homology, the complementary distribution in brain, the similarities in Ca^{2+}-dependent phospholipid binding and interaction with other synaptic proteins between Doc2α and Doc2β, it is hypothesised that Doc2β performs a similar function in regulated exocytosis as Doc2α. The aim of this thesis is to study the possible roles of Doc2β in regulated exocytosis and to elucidate the mechanisms of action.

The adrenal chromaffin cell has been a popular model cell for the study of exocytosis. This cell contains catecholamine packaged in large dense-core vesicles (LDCVs) that undergo Ca^{2+}-dependent exocytosis based on molecular machinery similar to that of synaptic transmission. Heterologous protein expression was achieved by using a Semliki Forest Virus (SFV) vector system, yielding high efficiency expression and minimal interference of membrane trafficking. Secretion was studied in both cell-population and single-cell levels. At the cell-population level, secretion of catecholamine was detected by using spectrofluorimetry. High

resolution monitoring of secretion was achieved by using membrane capacitance measurements and electrochemical detection of catecholamine.

Expression of Doc2β fusion with green fluorescent protein (Doc2β-EGFP) in bovine adrenal chromaffin cell showed both cytoplasmic and nuclear localisation. Punctate cytoplasmic fluorescence was identified in some cells which indicated the association with some intracytoplasmic compartments. Deletion of the amino terminal of Doc2β (C2AB-EGFP) did not change the fluorescence distribution pattern. The expression of Doc2β did not affect calcium currents and intracellular calcium level. Secretion induced by 50 mM KCl depolarisation in intact cells or 1 μM free Ca^{2+} in β-escin-permeabilised cells was not different among cells expressing green fluorescent protein, cells expressing wild-type Doc2β and cells expressing N-terminal deletion of Doc2β (C2AB). Secretion induced by whole-cell dialysis with solution containing 10 μM free calcium was also not different among those groups. The fusion-competent vesicle pool was not significantly changed by the expression of Doc2β or C2AB. Application of phorbol ester similarly increased the fusion-competent vesicle pool and catecholamine secretion in all cell groups. The results from this study indicate that Doc2β is not essential for regulated exocytosis of LCDVs in bovine adrenal chromaffin cells.

Chapter 1

Introduction

1.1 Exocytosis

Plasma membrane performs fundamental functions in providing cell boundary and maintaining the difference between cytoplasm and extracellular environment. However, transportation across the plasma membrane occurs all the time. Small molecules are transported via specific channels, transporters or carriers. Membrane-permeable molecules are free to diffuse across the membrane. How the membrane-impermeable macromolecules, such as hormones and neurotransmitters, are transported across the plasma membrane has been a subject of extensive studies. In early 1950s, the vesicle hypothesis and quantal theory of neurotransmission was proposed. The basis of this theory came from the discovery that acetylcholine was released as an all or none quanta at the neuromuscular junction (Fatt and Katz 1952; Del Castillo and Katz 1954a; Del Castillo and Katz 1954b) and the discovery of the ultrastructural membrane-bounded organelles in synapses (De Robertis and Bennett 1954). Since then, the mechanisms of vesicle transportation and secretion have been characterised. The term **exocytosis** has been used to describe a process whereby the membrane-bounded organelles fuse with the plasma membrane and simultaneously release their contents into the extracellular space. Exocytosis is an important cellular function in variety of cells ranging from primitive to highly differentiated eukaryotic cells such as neurons and endocrine cells. Exocytosis exists in two pathways, constitutive and regulated exocytosis (Palade 1975).

1.1.1 Constitutive exocytosis

Constitutive exocytosis is a default pathway and is present in all kinds of cell. The rate of secretion closely follows the rate of synthesis of the secretory products. Constitutive exocytosis provides continuous fusion of vesicles with the plasma membrane (Gumbiner and Kelly 1982; Kelly 1985; Burgess and Kelly 1987). Constitutive exocytosis underlies a broad variety of physiological processes including cell surface growth, transportation of proteoglycans and glycoproteins to the extracellular space and transportation of newly synthesised proteins and lipid components of plasma membrane.

1.1.2 Regulated exocytosis

Regulated exocytosis is a process whereby the fusion of the designated membrane-bounded organelles with the plasma membrane is regulated by particular signals. The most well known signal in regulated exocytosis is Ca^{2+}. Regulated exocytosis is fundamental for neurotransmission, hormonal secretion and enzyme secretion from secretory cells of digestive system.

Regulated exocytosis involves a series of vesicle trafficking steps. In protein secreting cells, the secretory products such as hormones and enzymes are synthesised in the endoplasmic reticulum, processed in the Golgi apparatus and transported to the plasma membrane via secretory vesicles budding from trans-Golgi network (TGN) (review in Kelly 1985). These secretory vesicles contain a characteristic electron-dense material under the electron microscope and are called large dense-core vesicles (LDCVs). The biogenesis of synaptic vesicles in neurons is different from that of

LDCVs. Synaptic vesicles are generated from the early endosomes and plasma membrane recycling (review in Kelly 1991). A recent study shows that a vesicle membrane protein synaptophysin is transported via the large tubulovesicular organelles to the axon terminal. The synaptophysin is later present in the early endosomes and synaptic vesicles (Nakata, Terada et al. 1998). This study supports that the synaptic vesicles are produced within the synaptic terminal. Neurotransmitters are synthesised in the cytoplasm and transported into synaptic vesicles via the neurotransmitter transporters. Catecholamines are also packaged in the LDCVs of adrenal chromaffin cells by using the same mechanism (review in Aunis 1998; Aunis and Langley 1999).

Kinetics and electron microscopic studies in adrenal chromaffin cells reveal that secretory vesicles reside in different functional pools (Heinemann, von Ruden et al. 1993; Parsons, Coorssen et al. 1995; Sudhof 1995; Xu, Binz et al. 1998; Xu, Rammner et al. 1999; Voets 2000). The **reserve pool** is a pool of vesicles away from the plasma membrane that can be released only with very strong stimuli. **Docked-vesicles** are vesicles within a close proximity to the plasma membrane. **The primed-vesicles or the fusion-competent vesicles** are those docked-vesicles that are primed and ready for release upon stimulation. This pool is further divided into two functional pools according to the kinetics release in response to flash photolysis of caged-Ca^{2+} compounds, the **slowly releasable pool** (SRP) and the **readily releasable pool** (RRP) of vesicles. The presence of different functional pools of synaptic vesicles in neurons (Figure 1-1) is supported by several studies. Studies in neurons reveal at least two different functional pools of synaptic vesicles, the RRP and the reserve pool (Stevens and Tsujimoto 1995; Schneggenburger, Meyer et al. 1999).

The RRP is the primed synaptic vesicles that are ready to release upon stimulation. The number of the morphological docked vesicles is well corresponded with the number of synaptic vesicles in the RRP indicating the tight correlation between docking and priming in synapses (Schikorski and Stevens 1997; Murthy and Stevens 1999).

Upon stimulation, the increase in intracellular Ca^{2+} concentration signals the vesicles to fuse with the plasma membrane and release their contents into the extracellular space. The rate of exocytosis depends on the concentration of the intracellular Ca^{2+} to the power of two to four (Heidelberger, Heinemann et al. 1994; Heinemann, Chow et al. 1994). The rate of exocytosis at synapses is much faster than the rate of exocytosis in endocrine cells (Chow, Klingauf et al. 1994; Sabatini and Regehr 1996). This is probably because of the arrangement of the exocytotic machinery at the release sites is differrent between neurons and endocrine cells. In neurons, the calcium channels are colocalised with synaptic vesicles at the active zone. However, there might be other differences in the secretory machinery of synaptic vesicles and LDCVs.

After fusion with the plasma membrane and release of the secretory products, the vesicle membranes are retrieved via endocytosis. In protein secreting cells, the secretory vesicles are cycled through the Golgi complex before the next round of exocytosis. The synaptic vesicle membranes are recycled by at least three different pathways. The endosomal recycling is the slowest of all and is supported by the presence of an endosomal protein Rab5 on some synaptic vesicles (Fischer von Mollard, Stahl et al. 1994). The second pathway is the local recycling of synaptic

vesicles without an endosomal intermediate. This is supported by a study showing that FM1-43 labelled synaptic vesicles can be reexocytosis without dilution of the dye in the early endosomes (Murthy and Stevens 1998). The third recycling pathway utilised in neurons is the reuse pathway. In this pathway, the neurotransmitters are released through a fusion pore which is closed immediately after exocytosis. The synaptic vesicles then reuptake the neurotransmitters for another round of exocytosis without leaving the active zones (Pyle, Kavalali et al. 2000; Stevens and Williams 2000). The local recycling of chromaffin vesicles after exocytosis is also reported. In a study using horse-radish peroxidase (HRP) as a fluid phase marker for endocytosis, chomaffin vesicles containing HRP enter the pool of release ready vesicles immediately after the membranes are retrieved by endocytosis (von Grafenstein and Knight 1992).

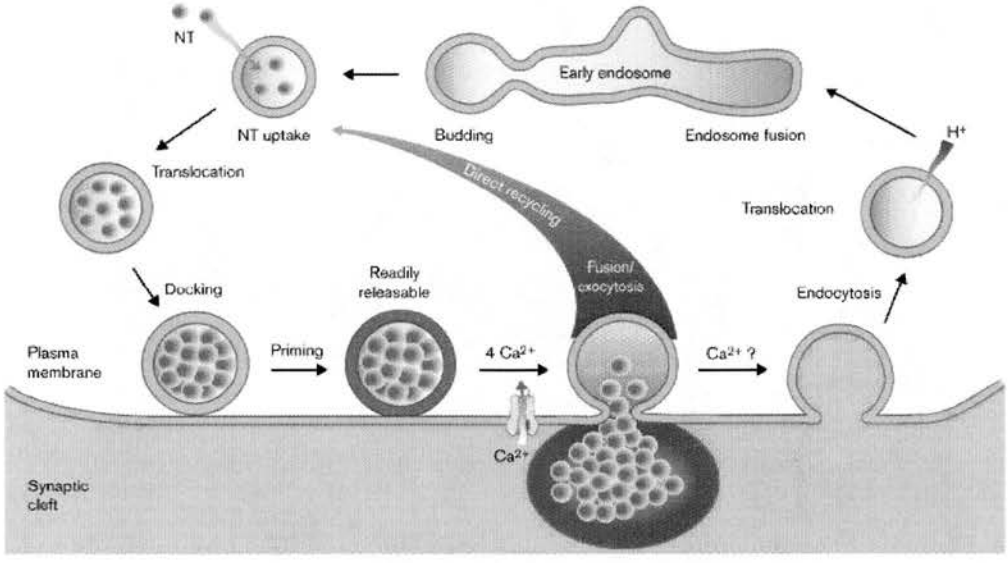

Figure 1-1 Synaptic vesicle trafficking

(Brose, Rosenmund et al. 2000)

Simple diagram displays different stages of synaptic vesicle maturation. Synaptic vesicles are produced from the early endosomes and endocytotic recycling from the plasma membrane. The neurotransmitters are transported into the synaptic vesicles. The mature synaptic vesicles are transported to the plasma membrane. The docked vesicles are primed and ready for fusion upon elevation of intracellular Ca^{2+} concentration. This traffic is also applied to regulated exocytosis in adrenal chromaffin cells.

1.2 Molecular mechanism of regulated exocytosis

The process of exocytosis represents a complex interplay between secretory vesicles and other cellular components. Several families of proteins are involved in regulated exocytosis. Most of these proteins are conserved evolutionarily and several families of protein are common in both regulated and constitutive pathway (review in Burgess and Kelly 1987). Although regulated secretion at synapses and endocrine cells is different in the vesicle biogenesis and the stimulus-secretion coupling, most of the proteins that function in neurotransmission at synapses are also present in endocrine cells (Lowe, Madeddu et al. 1988; Morgan and Burgoyne 1997; review in Gerber and Sudhof 2002). Taking advantage of advanced techniques in molecular genetic, molecular biology and electrophysiology, functions of several proteins involved in exocytosis are determined.

1.2.1 Proteins involved in vesicle docking

Before fusion with the plasma membrane, the secretory vesicles must first be translocated to the plasma membrane. Fluorescent and electron microscopic imaging in adrenal chromaffin cells show that there is a subset of vesicles in close proximity with the plasma membrane and less mobile compared to the rest of the vesicles (Plattner, Artalejo et al. 1997; Steyer, Horstmann et al. 1997; Oheim, Loerke et al. 1998). These vesicles are docked vesicles. In PC12 cells, the docked vesicles remain attached to plasma membrane even after homogenisation (Martin and Kowalchyk 1997). These docked vesicles undergo exocytosis upon stimulation with Ca^{2+}. In neurons, there is also a fraction of synaptic vesicles docked at the plasma membrane active zone (Murthy and Stevens 1999). The nature of vesicle docking

has been studied extensively both in neurons and endocrine cells. Several proteins are proposed to function in vesicle docking.

1.2.1.1 Munc18

Munc18 is a mammalian homologue of the yeast Sec1 protein. This family of proteins (Sec1/Munc18 or SM proteins) is conserved from yeast, *Drosophila*, *C. elegans* and mammal. Munc18 is about 60-70 kDa with no special domain structure. Three isoforms have been reported, Munc18-1, Munc18-2 and Munc18c. Munc18-1 is highly expressed in brain while Munc18-2 and Munc18c are expressed ubiquitously (Hata, Slaughter et al. 1993; Hata and Sudhof 1995; Tellam, McIntosh et al. 1995). Munc18 is important in regulated exocytosis. It is well established that Munc18 interacts with syntaxin, a plasma membrane component of the SNARE (soluble N-ethylmaleimide-sensitive fusion protein-attachment protein receptors) complex (Dulubova, Sugita et al. 1999; Yang, Steegmaier et al. 2000). Mutation of the yeast homologue of Munc18 completely blocks secretion (Ossig, Dascher et al. 1991; Schekman 1992). Deletion of Munc18-1 in mice also results in complete loss of neurotransmission. These mutant mice are paralysed and die soon after birth (Verhage, Maia et al. 2000). These results suggest the essential positive role of Munc18 in regulated exocytosis. However, some studies suggest that Munc18 and the Munc18-syntaxin interaction might serve as a negative regulator for the SNARE complex formation and exocytosis. In pancreatic β-cells introduction of Munc18 peptide or Munc18 antibody, which disrupts the Munc18-syntaxin interaction, leads to an enhancement of secretion (Zhang, Efanov et al. 2000). Overexpression of Munc18 homologue Rop in *Drosophila* reduces evoked neurotransmitter release

(Schulze, Littleton et al. 1994). It is possible that Munc18 performs multiple functions in regulated exocytosis mediated by several Munc18-interacting proteins (Wu, Littleton et al. 1998). Munc18 interacts with several plasma membrane proteins including syntaxin (Hata, Slaughter et al. 1993; Hata and Sudhof 1995; Wu, Littleton et al. 1998) and Mint (Okamoto, Matsuyama et al. 2000). Mint is a Munc18-interacting protein that is highly concentrated at the active zone. Mint also interacts with a plasma membrane neurexin and may function by recruiting Munc18 to the plasma membrane where exocytosis occurs (Biederer and Sudhof 2000). The ability to interact with several plasma membrane proteins might suggest the involment of Munc18 in vesicle docking. This hypothesis is supported by recent studies in adrenal chromaffin cells. Munc18-1 null mutant mice show significant reduction of the number of vesicles attached to the plasma membrane in adrenal chromaffin cells. On the other hand, overexpression of Munc18-1 increases secretion and the rate of vesicle recruitment in bovine adrenal chromaffin cells (Voets, Toonen et al. 2001a).

1.2.1.2 Rab3

Rab3 proteins are low molecular weight GTP-binding proteins. Several Rab3 proteins have been reported including Rab3A, Rab3B, Rab3C and Rab3D. These proteins are enriched in neurons and endocrine cells (Fischer von Mollard, Mignery et al. 1990; Darchen, Senyshyn et al. 1995). Rab3 is present both as soluble and membrane-bound forms. For membrane-bound form, it is associated with synaptic vesicles and secretory granules (Fischer von Mollard, Mignery et al. 1990; Martelli, Baldini et al. 2000). Rab3 cycles between GTP- and GDP-bound forms. It is

associated with vesicles in GTP-bound form and dissociated from vesicles after the GTP is hydrolysed to GDP (review in Fischer von Mollard, Stahl et al. 1994). This association-dissociation cycle might be important for membrane attachment and exocytosis. Mutant *C. elegans* lacking functional Rab3 show impairment of synaptic transmission and reduction of synaptic vesicles especially the population of synaptic vesicles near plasma membrane (Nonet, Staunton et al. 1997). This study supports the essential role of Rab3 in excocytosis and suggests that Rab3 might be involved in vesicle docking. Consistent with the study in *C. elegans*, overexpression of mutant Rab3A and Rab3D in PC12 cells reduces the number of docked vesicles while overexpression of wild type of both proteins increases total vesicles and the fraction of vesicles near the plasma membrane (Martelli, Baldini et al. 2000). However, a study in Rab3A knockout mice indicates a negative role of Rab3A in regulated exocytosis. In the Rab3A knockout mice, the size and the refilling of the RRP were not altered but the synaptic transmission was increased (Geppert, Goda et al. 1997). The variety of effects of Rab3 in regulated exocytosis might be due to the existence of multiple isoforms of Rab3 and the multiple effectors which remain to be investigated.

Recent studies suggest a potential role of **synaptotagmin** in vesicle docking. Synaptotagmin is a vesicle membrane protein containing tandem C2 domains. Synaptotagmin interacts with Ca^{2+} and phospholipids and has been shown to be important for the final Ca^{2+}-dependent step of exocytosis (Brose, Petrenko et al. 1992; Davletov and Sudhof 1993; Nonet, Grundahl et al. 1993; Chapman and Jahn 1994; Geppert, Goda et al. 1994; Fernandez-Chacon, Konigstorfer et al. 2001; Voets, Moser et al. 2001b). Besides Ca^{2+} and phospholipids, synaptotagmin also interacts

with several proteins including a plasma membrane protein neurexin (Petrenko, Perin et al. 1991). It was shown in *Drosophila* that the number of docked vesicles at synapses were reduced in null mutation of synaptotagmin (Reist, Buchanan et al. 1998). Another study in squid giant synapses shows that vesicle docking is mediated by the synaptotagmin C-terminus (Fukuda, Moreira et al. 2000a). Injection of a peptide corresponding to the synaptotagmin C-terminus into squid giant synapses blocks synaptic transmission and reduces number of docked synaptic vesicles at the active zones. It might be possible that synaptotagmin mediates vesicle docking by interacting with plasma membrane neurexin (Fukuda, Moreira et al. 2000a). Therefore, multiple factors are involved in vesicle docking. Studies of intracellular membrane trafficking also reveals several proteins, the tethering complex, that might be involved in vesicle tethering and docking (review in Whyte and Munro 2002).

1.2.2 Priming of secretory vesicles

Fusion-competent vesicles are vesicles that are ready to fuse with the plasma membrane when the intracellular Ca^{2+} concentration increases. Only a fraction of morphological docked vesicles are fusion-competent (Parsons, Coorssen et al. 1995; Dobrunz and Stevens 1997; Plattner, Artalejo et al. 1997; Ashery, Varoqueaux et al. 2000). Based on the studies in neurons and endocrine cells, the docked vesicles have to undergo a series of priming steps prior to the fusion step (review in Klenchin and Martin 2000). Several factors are involved in vesicle priming. Vesicle priming is ATP-dependent and reversible (Hay and Martin 1992; Xu, Binz et al. 1998; Xu, Rammner et al. 1999). Secretion in adrenal chromaffin cell was completely abolished after 5 minutes of whole-cell dialysis with non-hydrolysable ATP analogs

(Xu, Binz et al. 1998). Ca^{2+} is not only important for the final stage of exocytosis but also involved in the early steps possibly vesicle recruitment and priming (Hay and Martin 1992; von Ruden and Neher 1993). The involvement of Ca^{2+} in the vesicle priming and exocytosis indicates that there might be multiple Ca^{2+}-interacting proteins in vesicle trafficking. Vesicle priming is also sensitive to temperature (Hay and Martin 1992). The rate of vesicle refilling increases at higher temperature (Dinkelacker, Voets et al. 2000; Pyott and Rosenmund 2002). Numbers of proteins are involved in vesicle priming.

1.2.2.1 NSF and SNAP

NSF (N-ethylmaleimide-sensitive fusion protein) and SNAP (soluble N-ethylmaleimide-sensitive fusion protein-attachment protein) are synaptic proteins that catalyse the disassembly of SNARE complexes by using the energy from ATP hydrolysis (Sollner, Bennett et al. 1993; Barnard, Morgan et al. 1997). The disassembly of *cis*-SNARE complexes by NSF/SNAP may promote the formation of *tran*-SNARE complexes between the vesicle and plasma membrane SNARE component. It was shown in PC12 cells that NSF/SNAP functions in the ATP-dependent step prior to Ca^{2+}-activated exocytosis (Banerjee, Barry et al. 1996). Treatment of adrenal chromaffin cells with N-ethylmaleimide which inhibits NSF reduces the RRP refilling while pipette injection of α-SNAP increases the RRP and the RRP refilling (Xu, Ashery et al. 1999). More evidence that support the function of NSF/SNAP in vesicle priming come from the studies in *Drosophila* having a temperature-sensitive allele of NSF (Kawasaki, Mattiuz et al. 1998; Tolar and Pallanck 1998). At non-permissive temperature, synaptic vesicles accumulate at

synapses and the evoked responses decrease in an activity-dependent manner (Kawasaki, Mattiuz et al. 1998).

1.2.2.2 Protein Kinase C

It is proposed that protein phosphorylation is responsible for the ATP-dependent step of exocytosis. Several proteins involved in vesicle trafficking such as syntaxin, SNAP-25, synaptobrevin and Munc18 have been shown to be targets for the phosphorylation reaction (Nielander, Onofri et al. 1995; Shimazaki, Nishiki et al. 1996; Risinger and Bennett 1999; de Vries, Geijtenbeek et al. 2000). The role of protein kinase C (PKC) in exocytosis has been studied extensively. Phorbol ester, a protein kinase C activator, has been shown to enhance exocytosis by increasing the number of docked vesicles (Vitale, Seward et al. 1995; Tsuboi, Kikuta et al. 2001; Cochilla, Angleson et al. 2000), increase the RRP (Gillis, Mossner et al. 1996; Smith, Moser et al. 1998) and increase the high Ca^{2+}-sensitive pool of vesicles in adrenal chromaffin cells (Yang, Udayasankar et al. 2002). The secretory enhancement effect of phorbol ester is inhibited by PKC inhibitors. In hippocampal neurons, phorbol ester stimulation increases the RRP and the RRP refilling (Stevens and Sullivan 1998). Direct evidence of the involvement of PKC in regulated exocytosis comes from studies in permeabilised PC12 cells where reconstitution of the bath solution with PKC-deficient cytosol reduces the secretion (Nishizaki, Walent et al. 1992). On the other hand, a study in hippocampal neurons showed that PKC is not important in phorbol ester stimulation. In this study, the effect of phorbol ester enhanced synaptic transmission was completely abolished in hippocampal neurons expressing phorbol ester-binding deficient Munc13 (Rhee, Betz et al. 2002). Therefore, more studies

need to be done before one can conclude the precise function of PKC in regulated exocytosis. Besides PKC, other protein kinases have been shown to participate in regulated exocytosis (review in Turner, Burgoyne et al. 1999).

1.2.2.3 Phosphatidylinositol kinases

Phosphoinositides are group of phospholipids produced by phosphorylation of membrane phosphatidylinositol (PI) by using enzyme PI-kinases. The role of phosphoinositides in membrane trafficking has been demonstrated. Phosphatidylinositol-4,5-phosphate (PIP_2) is required for ATP-dependent priming of vesicles in adrenal chromaffin cells (Eberhard, Cooper et al. 1990). Reduction of the PIP_2 level by treatment with the bacterial phospholipase C or removal of ATP during priming step reduced the catecholamine secretion in permeabilised adrenal chromaffin cells. PI 4 kinase and PIP 5-kinase are responsible for the generation of PIP_2. In adrenal chromaffin cells, PI 4-kinase is tighly bound to LDCVs (Wiedemann, Schafer et al. 1996). Phosphoinositides can bind several proteins implicated in regulated exocytosis including protein containing C2 domain such as synaptotagmin and rabphilin3A (Schiavo, Gu et al. 1996; Chung, Song et al. 1998). All the evidence support the involvement of the phosphoinositides in regulated exocytosis. However, the precise mechanism of action remains to be elucidated.

1.2.2.4 Munc13

Munc13 is a brain-specific mammalian homologue of *C. elegans* unc13p. Three isoforms of Munc13 have been reported (Figure 1-2A), Munc13-1 (1735 amino acids, 196 kDa), Munc13-2 (1985 amino acids, 222 kDa) and Munc13-3 (2205

amino acids, 249 kDa). Recent discovery of Munc13 in adrenal chromaffin cells and a novel isoform of Munc13, Munc13-4, in lung and spleen suggests the ubiquitous expression of Munc13 (Ashery, Varoqueaux et al. 2000; Koch, Hofmann et al. 2000). In brain, Munc13 is highly enriched in synaptosomes where it is concentrated on the plasma membrane especially at the active zone (Brose, Hofmann et al. 1995). The distribution of Munc13 isoforms in brain is not uniform. Munc13-1 is expressed in all neurons. Munc13-2 is expressed in the rostral brain region while Munc13-3 expression is restricted to cerebellum (Augustin, Betz et al. 1999a). The heterogeneity of expression even occurs in the different synapses of the same neurons. While glutamatergic synapses utilise Munc13-1 in synaptic transmission, the GABAergic synapses use Munc13-2 isoform (Augustin, Rosenmund et al. 1999b; Varoqueaux, Sigler et al. 2002). Munc13 contains one C1 domain and two C2 domains similar to those of PKC. Munc13-1 has an extra C2 domain at its N-terminal. The C1 domain contains a zinc finger-like region that is responsible for binding with phorbol ester or diacylglycerol (DAG) (Kazanietz, Lewin et al. 1995; Betz, Ashery et al. 1998; Rhee, Betz et al. 2002). Application of phorbol ester induces translocation of Munc13 to plasma membrane (Betz, Ashery et al. 1998; Duncan, Betz et al. 1999a; Ashery, Varoqueaux et al. 2000). The phorbol ester-induced translocation of Munc13 requires only Munc13 C1-domain. Mutation of Munc13-1 C1 domain abolished the phorbol ester binding to Munc13-1 (Betz, Ashery et al. 1998). The C2 domains of Munc13 are homologous to those of PKC and synaptotagmin, but there is no evidence of Ca^{2+}-dependent phospholipid binding to these domains (Brose, Hofmann et al. 1995). The crucial role of Munc13 in regulated exocytosis is supported by several studies. Mutation of unc13p in *C.*

elegans causes an accumulation of synaptic vesicles at presynaptic terminals and paralysis of the mutants (Hosono, Sassa et al. 1987; Hosono and Kamiya 1991). These results indicate that Unc13 functions at the post-docking step of exocytosis. A similar result was obtained from Unc-13 null-mutant *Drosophila* (Aravamudan, Fergestad et al. 1999). In mouse hippocampal synapses, Munc13-1 null-mutation does not affect the number of docked vesicles but glutamatergic neurotransmission is severely inhibited while GABAergic neurotransmission is not affected (Augustin, Rosenmund et al. 1999b). However, double deletion of both Munc13-1 and Munc13-2 severely inhibits both glutamatergic and GABAergic neurotransmission in those synapses (Varoqueaux, Sigler et al. 2002). These results indicate that both isoforms of Munc13 are important for synaptic transmission. The function of Munc13 C1 domain as a phorbol ester/DAG receptor for neurotransmission is essential. Over-expression of Munc13-1 with an intact C1 domain enhances phorbol ester-mediated increase of neurotransmitter release at *Xenopus* neuromuscular junction (Betz, Ashery et al. 1998). Mice expressing phorbol ester/DAG binding-deficient Munc13-1 show a complete loss of phorbol ester- enhanced neurotransmission in hippocampal synapses (Rhee, Betz et al. 2002).

The mechanism of Munc13 actions in regulated exocytosis has been a subject of interest. Munc13 interacts with syntaxin, a plasma membrane component of the SNARE complex. The interaction of Munc13 with syntaxin is neither phorbol ester nor Ca^{2+}-dependent. This interaction may be important for core complex formation or docking of vesicles at the plasma membrane (Betz, Okamoto et al. 1997). The similarity between the Munc13 and Munc18 binding site on syntaxin suggests that these two proteins do not bind syntaxin at the same time. Munc13 binds to an

opened-conformation of syntaxin while Munc18 binds to the closed-conformation of syntaxin (Figure 1-2B) (Yang, Steegmaier et al. 2000; Richmond, Weimer et al. 2001). Expression of the opened conformation of syntaxin was able to rescue the paralytic phenotype of Unc13 mutation in *C. elegans* (Richmond, Weimer et al. 2001). It is proposed that Munc13-1 is involved in the vesicle priming step by promoting the opened- conformation of syntaxin which is capable of SNARE complex formation. Munc13 also interacts with Rim (Rab3-interacting molecules). Rim is another protein containing C2 domains that is highly enriched at plasma membrane active zone (Wang, Okamoto et al. 1997). Rim binds Rab3 in the GTP-bound form and might be important for synaptic vesicle docking at the active zone. Overexpression of N-termial domain containing Rab3-binding domain of Rim1 in PC-12 cells and adranal chromaffin cells enhanced secretion (Wang, Okamoto et al. 1997; Sun, Bittner et al. 2001). Munc13-1 interacts with Rim1 through its N-terminal Rim-binding region while the C-terminal region is responsible for the interaction with other proteins including Doc2 and syntaxin (Betz, Thakur et al. 2001). Disruption of the Munc13-1/Rim1 interaction by expression of the N-terminal Rim-binding region of Munc13-1 reduced the synaptic transmission and the RRP in hippocampal neurons (Betz, Thakur et al. 2001). Therefore, the Munc13-1/Rim1 interaction is important for synaptic transmission and might involve synaptic vesicle priming once the vesicles arrive at the active zone. The function of Munc13 in vesicle priming is also supported by recent studies in adrenal chromaffin cells. Overexpression of Munc13-1 in bovine adrenal chromaffin cells increases the SRP and the RRP without affecting the number of docked-vesicles (Ashery, Varoqueaux et al. 2000).

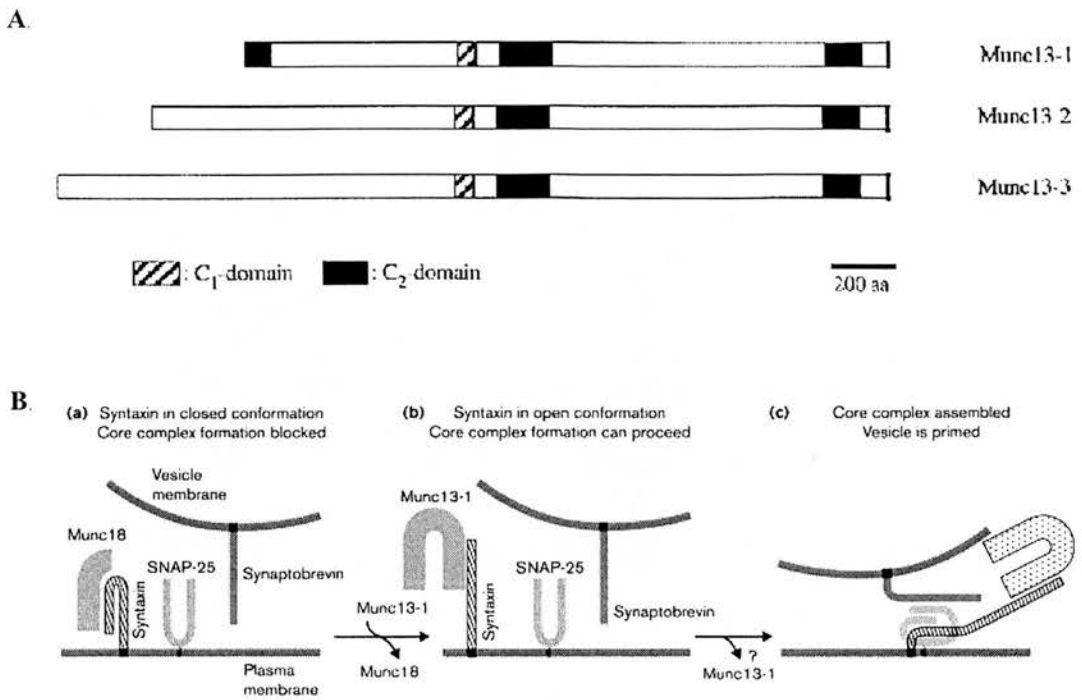

Figure 1-2 Munc13s and Munc13-syntaxin interaction

(Betz, Ashery et al. 1998; Brose, Rosenmund et al. 2000)

(A) Modular diagram represents functional domain of Munc13s. Note that Munc13-1 has an extra C2 domain at its N-terminus. The Doc2-interacting domain (Did) of Munc13 is the residues between two C-terminal C2 domains. (B) Diagram demonstrates the Munc13-syntaxin interaction. Munc18 interacts with the closed conformation of syntaxin and prevents the formation of SNARE complex (a). Munc13-1 interacts with the opened conformation of syntaxin (b). Syntaxin in the opened conformation is able to form the complex with other SNARE counterpart (c).

1.2.3 Proteins involved in the fusion reaction

Our knowledge about membrane fusion in exocytosis has advanced in recent years. Evidence from studies of exocytosis in secretory cells and intracellular membrane fusion reveal several families of proteins that are important for the membrane fusion. The **SNAREs** (soluble N-ethylmaleimide-sensitive fusion protein-attachment protein receptors) are known as the core complexes for membrane fusion. The essential role of SNAREs in membrane fusion is demonstrated in both intracellular membrane traffic and exocytosis (review in Jahn and Sudhof 1999). The best-characterised SNAREs are the neuronal SNAREs. SNAREs consist of two classes of proteins, vesicle membrane protein synaptobrevin (v-SNARE) and plasma membrane proteins syntaxin and SNAP-25 (t-SNAREs). The SNAREs are targets of clostridial toxin (Niemann, Blasi et al. 1994; Xu, Binz et al. 1998). A common characteristic of the SNARE proteins is the presence of SNARE motif. The four-helix bundle contributed by each SNARE counterpart (one from synaptobrevin, one from syntaxin and two from SNAP-25) provides machinery for membrane fusion (review in Weber, Zemelman et al. 1998). The timing of SNARE complex formation relative to the vesicle trafficking is still being argued. Studies in adrenal chromaffin cells reveal that the SNARE complexes exist in two forms prior to Ca^{2+}-induced exocytosis, loose and tight forms, both of which are fusion-competent and interconvertable (Niemann, Blasi et al. 1994; Xu, Binz et al. 1998; Xu, Rammner et al. 1999). The loose SNARE complexes are sensitive to cleavage by clostridial neurotoxins while the tight SNARE complexes are toxin-resistant. The tight and the loose forms of SNARE complexes contribute to the fast and slow phase of an exocytotic burst during flash photolysis of caged-Ca^{2+} experiment. Other proteins that interact with

the SNARE complexes, such as Munc18, Rab3 and complexin might also play an important part in vesicular fusion (Jahn and Sudhof 1999; Hu, Carroll et al. 2002).

1.2.4 C2 domain proteins

The importance of Ca^{2+}in regulated exocytosis has been recognised for a long time. In chemical synapses where regulated exocytosis is a basic mechanism for neurotransmitter release, removal of Ca^{2+} from the extracellular solution inhibits synaptic transmission (Del Castillo and Katz 1954a; Del Castillo and Katz 1954b; Katz and Miledi 1965). The rate of exocytosis in neurons and endocrine cells is dependent on Ca^{2+}concentration to the power of two to four (Heinemann, von Ruden et al. 1993; Heidelberger, Heinemann et al. 1994). Besides regulation of the final step of exocytosis, Ca^{2+} is also involved in vesicle recruitment (Neher and Zucker 1993; von Ruden and Neher 1993). Several families of Ca^{2+}-binding proteins are involved in regulated exocytosis, including proteins containing the C2 domain.

The C2 domain was originally defined in Ca^{2+}-dependent isoforms of protein kinase C (PKC) where it was the second of the four conserved domains of PKC (Coussens, Parker et al. 1986; Parker, Coussens et al. 1986). The kinase activity and phospholipid binding of these PKCs are Ca^{2+}-dependent and are mediated by the C2 domain (Newton 1995; Shao, Davletov et al. 1996). Single and multiple C2 domains were later discovered in number of proteins participating in variety of cellular processes including membrane trafficking (Figure 1-3B), lipid second messengers, GTPase activation and protein phosphorylation (review in Nalefski and Falke 1996).

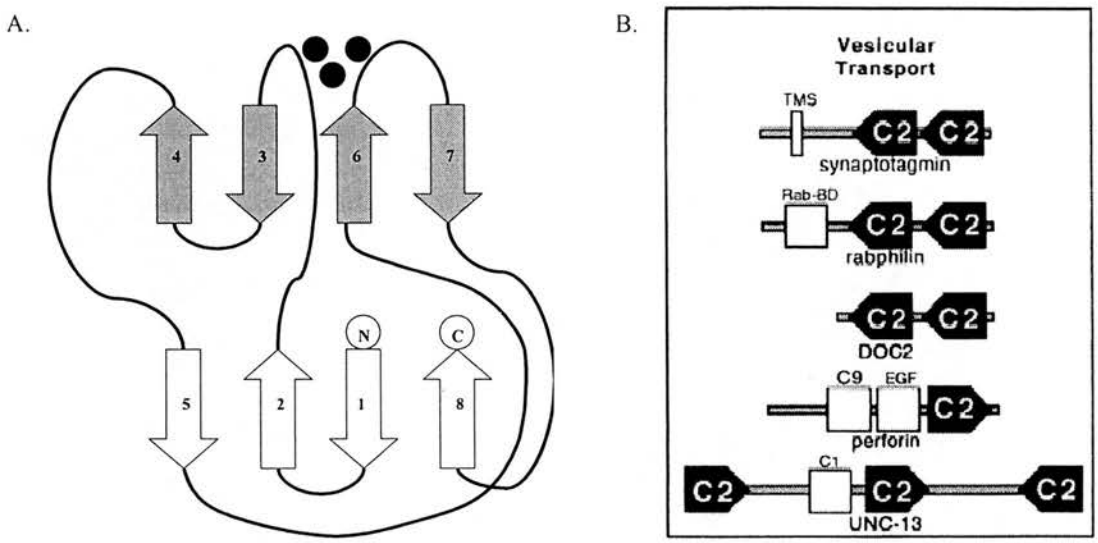

Figure 1-3 Structure of C2 domain and protein containing C2 domains in vesicular transport pathway

(Sutton, Davletov et al. 1995; Nalefski and Falke 1996)

(A) Diagram represents structure of topology I C2 domain. Each block arrow represents each β-strand that forms β-sandwich structure. N and C indicate amino and carboxy terminal, respectively. Ca^{2+} ions are represented by filled-circles. The Ca^{2+}-binding domain is formed by the residues connecting strand β2-β3 and β6-β7. (B) Examples of protein containing C2 domains involved in the vesicular transport pathway. The diagrams show the functional domains of those proteins. The filled boxes that point to the right and left represent topology I and II of the C2 domains, respectively. *TMS* = transmembrane segment, *Rab-BD* = Rab-binding domain.

The C2 domain is a putative Ca^{2+} and phospholipid-binding motif of about 130 residues. The structure of C2 domains in all proteins containing C2 domain identified fall into two topologies based on an X-ray crystallographic study of the first C2 domain of synaptotagmin I (topology I) and the C2 domain of phosphoinositide-specific phospholipase C-δ1(topology II) (Sutton, Davletov et al. 1995; Essen, Perisic et al. 1996). Both topologies form eight-stranded antiparallel β-sandwich structures with a slight difference at the connection of β-strands (Figure 1-3A).

The C2 domain has the ability to bind a variety of intracellular signalling molecules such as Ca^{2+}, phospholipids, phosphoinositides and intracellular proteins. The Ca^{2+}-binding domains are at the loops connecting strands (Figure 1-3A). In synaptotagmin I, the Ca^{2+}co-ordination residues are five aspatate (Asp) residues. These residues are conserved among several proteins containing C2 domains. Substitution of these aspartate residues with asparagine (Asn) in synaptotagmin I first C2 domain abolishes the Ca^{2+}-dependent phospholipid binding ability of the protein (Sutton, Davletov et al. 1995).

1.2.4.1 Synaptotagmin

Synaptotagmin I C2 domain is one of the best-characterised C2 domains. Synaptotagmin is an integral membrane protein of synaptic vesicles containing two cytosolic C2 domains (Perin, Fried et al. 1990). Several isoforms of synaptotagmin have been identified in regulated secretory pathway. The first C2 domain (C2A) of synaptotagmin binds phospholipid vesicles upon addition of Ca^{2+} (Brose, Petrenko et

al. 1992; Davletov and Sudhof 1993; Chapman and Jahn 1994). The Ca^{2+}-dependency of phospholipid binding by synaptotagmin I is consistent with that of neurotransmission (Davis, Bai et al. 1999). The second C2 domain (C2B) of synaptotagmin, which is also capable of Ca^{2+}-dependent activity, interacts with several synaptic proteins including calcium channels, clathrin adaptor protein (AP-2), β-SNAP and other synaptotagmin molecules. Mutation studies reveal that synaptotagmin is important for neurotransmission especially the rapid phase of Ca^{2+}-dependent neurotransmitter release (Nonet, Grundahl et al. 1993; Geppert, Goda et al. 1994; Fernandez-Chacon, Konigstorfer et al. 2001; Voets, Moser et al. 2001b).

1.2.4.2 Rabphilin3A

Another C2 domain-containing protein involved in eukaryotic membrane trafficking is rabphilin3A. Rabphilin3A is a Rab3A-binding protein highly enriched in brain where it is associated with synaptic vesicles (Mizoguchi, Yano et al. 1994). Rab3A is a small guanosine triphosphate (GTP)-binding protein implicated in neurotransmission. Rabphilin3A contains two C-terminal C2 domains similar to synaptotagmin but does not have a transmembrane domain. The N-terminus of rabphilin3A possesses a Rab3A-binding domain. Rabphilin3A binds phospholipids in a Ca^{2+}-dependent manner (Yamaguchi, Shirataki et al. 1993; Chung, Song et al. 1998). Overexpression of rabphilin3A in adrenal chromaffin cells enhances catecholamine secretion (Chung, Takai et al. 1995). It is proposed that GTP-bound Rab3A stabilises the complex with rabphilin3A on the secretory vesicles. Hydrolysis of GTP dissociates Rab3A from rabphilin3A and allows exocytosis to proceed (Chung, Stabila et al. 1997).

Although the C2 domain is discovered in many Ca^{2+}-binding proteins, some C2 domain-containing proteins can function independent of Ca^{2+}. Non-classical PKCs contain C2 domains but do not have Ca^{2+}-dependent functions. The Second C2 domain (C2B) of synaptotagmin binds syntaxin, AP-2 and phosphoinositides in a Ca^{2+}-independent manner. The first C-terminal C2 domain from all three Munc13 isoforms fails to bind phospholipids in response to Ca^{2+} (Brose, Hofmann et al. 1995). These pieces of evidence imply the roles for C2 domain-containing proteins other than Ca^{2+}-dependent function.

1.3 Doc2

Doc2 (Double C2) is a recently discovered family of proteins containing two C2 domains (Orita, Sasaki et al. 1995). Doc2 has an N-terminal sequences unique among Doc2 family members (Doc2-specific region; DSR) and two C-terminal C2 domains (C2A and C2B) of type I topology (Orita, Sasaki et al. 1995; Nalefski and Falke 1996; Verhage, de Vries et al. 1997). These two C2 domains are highly homologous to those of synaptotagmin and rabphilin3A. Doc2 does not contain a transmembrane domain as in synaptotagmin or a Rab3A-binding domain as in rabphilin3A. At least three isoforms have been reported; Doc2α, Doc2β and Doc2γ (Figure 1-4) (Orita, Sasaki et al. 1995; Sakaguchi, Orita et al. 1995; Fukuda and Mikoshiba 2000b).

1.3.1 Doc2α

Doc2α is a brain-specific isoform of the Doc2 family. Doc2α has 400 residues with a molecular weight of 44 kDa (Orita, Sasaki et al. 1995). The distribution within

brain is not uniform. Doc2α is highly expressed in cortex, brain stem, CA3-CA4 areas of hippocampus, dentate gyrus, ventral hypothalamic nuclei (Naito, Orita et al. 1997; Verhage, de Vries et al. 1997). Doc2α is associated with synaptic vesicles (Orita, Sasaki et al. 1995; Sakaguchi, Orita et al. 1995; Verhage, de Vries et al. 1997). The association between Doc2α and synaptic vesicles is mediated by the C2 domains (Duncan, Betz et al. 1999a). The spatiotemporal distribution of Doc2α was studied in rat brain (Korteweg, Denekamp et al. 2000). Doc2α, like the other exocytotic machinery, was detected at the late embryonic stage and in postnatal rats consistent with synaptogenesis. Doc2α possesses several properties required for Ca^{2+}-dependent exocytosis.

1.3.1.1 Ca^{2+}-dependent phospholipid-binding

Doc2α C2-domains conserve the Ca^{2+}-binding residues similar to those of synaptotagmin I and rabphilin3A (Sakaguchi, Orita et al. 1995). Doc2α binds phospholipids in a Ca^{2+}-dependent manner (Orita, Sasaki et al. 1995). The Ca^{2+}-dependency of phospholipid binding is different from that of synaptotagmin I. The Ca^{2+} concentration for half-maximal phospholipid binding of Doc2α is about 1 μM while synaptotagmin I binds phospholipids with half-maximal binding at Ca^{2+} concentration of 74 μM (Davis, Bai et al. 1999). The difference in the Ca^{2+}-dependency of phospholipid binding between Doc2α and synaptotagmin I implies that these two proteins participate in different stages of regulated exocytosis.

1.3.1.2 Doc2α-Munc13 interaction

Doc2α interacts with Munc13 through the N-terminal Munc13-interacting domain (Mid) of Doc2α and the Doc2-interacting domain (Did) of Munc13 (Orita, Sasaki et al. 1995; Mochida, Orita et al. 1998). This interaction is regulated by the Munc13 C1 domain. Binding of phorbol ester (PE) or diacylglycerol (DAG) with the C1 domain induces the Doc2α-Munc13 interaction. Deletion of the C1 domain abolishes phorbol ester-mediated Doc2α-Munc13 interaction. The Doc2α-Munc13 interaction is Ca^{2+}-dependent (Orita, Naito et al. 1997). One explanation is that Ca^{2+} helps translocation of Doc2α to plasma membrane, where Munc13 is, through the interaction with the C2 domain (Conesa-Zamora, Gomez-Fernandez et al. 2000). Another explanation is that phosphoinositide-specific phospholipase C, the enzyme that produces DAG, needs Ca^{2+} for the action (Mochida, Orita et al. 1998).

1.3.1.3 Doc2α-Munc18 interaction

Doc2α interacts with the brain-specific isoform of Munc18 (Munc18-1) (Verhage, de Vries et al. 1997). The interaction is Ca^{2+}-independent. Only the C2A domain of Doc2α is needed for the interaction with Munc18-1 while nearly the full-length of Munc18-1 is needed for the interaction. Similarly, the full-length of Munc18 is needed for the interaction with syntaxin (Hata and Sudhof 1995). Therefore, Doc2α and syntaxin compete for Munc18. The Munc18-syntaxin interaction is stronger than the Doc2α-Munc18 interaction. Formation of the SNARE complexes reduces the affinity of syntaxin-Munc18 and favours the formation of the Doc2α-Munc18 complex. In situ hybridisation studies in *Xenopus* brain reveals that both Doc2 and

Munc18 homologues are co-expressed in the same neurons and the level of both mRNAs are up-regulated by stimuli that increase the secretory function of neurons (Berghs, Korteweg et al. 1999). A similar expression pattern is also observed in endocrine cells of the pituitary gland.

1.3.1.4 Doc2α-Dynein interaction

Doc2α interacts with tctex-1, a light-chain of the motor protein dynein, through the Doc2α N-terminus (Nagano, Orita et al. 1998). This interaction was observed in both a cell-free system and in intact cells. Dynein is a minus end-directed microtubule-based motor protein that is involved in vesicle transportation from the early to late endosomes (Aniento, Emans et al. 1993). Overexpression of the N-terminal or C-terminal fragments of Doc2α in baby hamster kidney cells (BHK) disrupts the transportation between trans-Golgi network (TGN) and late endosomes (Nagano, Orita et al. 1998). Dynein also has a variety of functions besides membrane trafficking such as mitotic spindle formation (Heald, Tournebize et al. 1996), chromosomal segregation and distribution of intracellular organelles. The interaction between Doc2α and dynein implies a possible role of Doc2α in intracellular transportation.

1.3.1.5 Roles of Doc2α in regulated exocytosis

Several lines of evidence support the role of Doc2α in regulated exocytosis. Over-expression of Doc2α in PC12 cells enhanced high K^+-induced and phorbol ester-induced secretion of co-expressed growth hormone without any effect on basal

secretion and endocytosis (Orita, Sasaki et al. 1996; Orita, Naito et al. 1997). On the other hand, over-expression of Doc2α-antisense, which decreased the production of Doc2α, inhibited high K^+-induced secretion. Electrophysiological study of synaptic transmission in the hippocampus of homozygous null-Doc2α mutant mice revealed a steeper depression of postsynaptic response at high frequency stimulation and impairment of long-term potentiation (LTP) (Sakaguchi, Manabe et al. 1999). The steeper declination during high frequency stimulation and the effect on long-term potentiation is hypothesised to be the result of the impairment of vesicle recruitment in the mutant mice. Consistent with the electrophysiological findings, these mutant mice showed impairment in passive avoidance tests. The inhibition of high K^+-induced exocytosis by over-expression of N- or C-terminal deletions of Doc2α in PC12 cell suggests that Doc2α enhances Ca^{2+}-dependent exocytosis through the interaction with other components of exocytotic machinery (Orita, Sasaki et al. 1996). The N-terminus of Doc2α interacts with Munc13 and dynein whereas the C-terminus containing C2 domains interacts with Ca^{2+}, phospholipids and Munc18.

The Doc2α-Munc13 interaction is important for Ca^{2+}-dependent exocytosis and believed to be a molecular mechanism of phorbol ester-enhanced neurotransmitter release (Hori, Takai et al. 1999). Disruption of the Doc2α-Munc13 interaction by introduction of Doc2α-Mid or Munc13-Did inhibited Ca^{2+}-dependent exocytosis in PC12 cells (Orita, Sasaki et al. 1996; Orita, Naito et al. 1997; Hori, Takai et al. 1999). Introduction of Doc2α-Mid peptide to presynaptic neurons of the superior cervical ganglia inhibited excitatory postsynaptic potential (EPSP) (Mochida, Orita et al. 1998). The delay between the introduction of the peptide and the inhibitory

effect, which is accelerated by increasing the frequency of stimulation, implies the involvement of Doc2α-Munc13 in the step prior to final fusion step.

However, Doc2α does not seem to be crucial for synaptic transmission as homozygous null-Doc2α mutant mice showed normal phenotype and synaptic transmission at low frequency stimulation (Sakaguchi, Manabe et al. 1999).

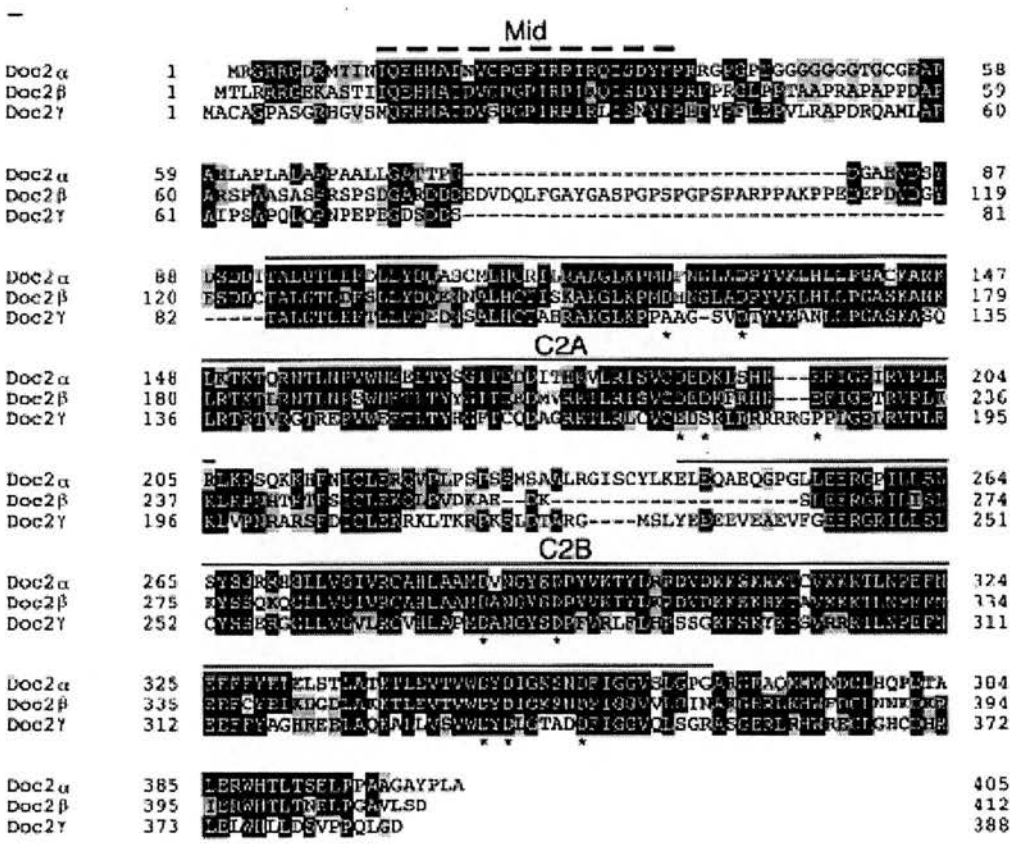

Figure 1-4 Sequence alignment of mouse Doc2 family

(Fukuda and Mikoshiba 2000b)

The sequence alignment of mouse Doc2α, Doc2β and Doc2γ is displayed. The black and the shaded background indicate the residues which half of the sequences are conserved or similar, respectively. Asterisks indicate the conserved aspartate (D) or glutamate (E) residues responsible for Ca^{2+} binding. The broken lines indicate the Munc13-interacting domain (Mid) at the N-terminal. The solid lines indicate the first (C2A) and second (C2B) C2 domains, respectively.

1.3.2 DOC2β

Doc2β is a ubiquitous isoform of Doc2 family. Doc2β has a molecular weight of 46 kDa and contains 412 amino acids, which are highly homologous to its brain specific counterpart Doc2α, especially at the N-terminal Doc2-specific region and both C2 domains (Figure 1-4) (Sakaguchi, Orita et al. 1995). Doc2β is expressed in nearly all tissues but abundantly expressed in brain. The distribution within brain of Doc2β is nonuniform and complementary with the distribution of Doc2α (Verhage, de Vries et al. 1997). Doc2β is highly expressed in caudate, putamen, limbic structures, cerebellum, dentate gyrus, CA1-CA2 areas of hippocampus, amygdala and ethorhinal cortex (Naito, Orita et al. 1997; Verhage, de Vries et al. 1997). Fractionation studies demonstrated that the distribution of Doc2β within neurons is similar to the distribution of Doc2α in that it is highly enriched in the synaptic vesicle fraction (Sakaguchi, Orita et al. 1995; Verhage, de Vries et al. 1997). The distribution of Doc2β was also studied in non-neuronal cells. Doc2β is present in cytoplasm when expressed in PC12 cells similar to the distribution of Doc2α (Orita, Sasaki et al. 1996; Fukuda, Saegusa et al. 2001). HEK293 cells expressing Doc2β fusion with green fluorescent protein reporter (EGFP) demonstrate a cytoplasmic punctate fluorescence distribution which implies the association of Doc2β with some intracellular organelles (Duncan, Betz et al. 1999a). The punctate distribution pattern needs only the C-terminal containing C2 domains of Doc2β. Doc2β was detected throughout the neuroepithelium before the reported development of synapses in rat embryoes. This spatiotemperal distribution of Doc2β implies a non-secretory role of

Doc2β in synapses. The level of both Doc2α and Doc2β in rat brain decrease during postnatal period and the pattern of distribution gradually becomes the adult complementary pattern of Doc2α and Doc2β (Korteweg, Denekamp et al. 2000). Doc2β posses several properties similar to Doc2α.

1.3.2.1 Ca^{2+}-dependent phospholipid binding

Doc2β C2-domains conserve Ca^{2+}-binding residues similar to those of Doc2α, synaptotagmin I and rabphilin3A. Only the C2A domain of Doc2β is responsible for Ca^{2+}-dependent phospholipid binding (Kojima, Fukuda et al. 1996). The Ca^{2+}-dependency of phospholipid binding is similar to that of Doc2α (Orita, Sasaki et al. 1995; Sakaguchi, Orita et al. 1995).

1.3.2.2 Interaction with Munc13

All members of Doc2 family have the Munc13-interacting domain (Mid) within the N-terminal Doc2 specific region. Mid and Doc2-interacting domain (Did) show sequence homology among all isoforms of Doc2 and Munc13, respectively. Doc2β is able to interact with Munc13 similar to Doc2α (Orita, Naito et al. 1997). In HEK293 cells expressing both Doc2β and Munc13, application of phorbol ester induces a translocation of Doc2β to plasma membrane (Duncan, Betz et al. 1999a). Deletion of Doc2β N-terminal containing Mid renders the Doc2β distribution insensitive to phorbol ester.

1.3.2.3 Interaction with Munc18

Doc2β is able to interact with both brain-specific (Munc18-1) and ubiquitous (Munc18-2) isoforms of Munc18 (Verhage, de Vries et al. 1997). The interaction is Ca^{2+}-independent and requires the first C2 domain (C2A) of Doc2β similar to Doc2α-Munc18 interaction.

1.3.2.4 Interaction with a motor protein Dynein

Doc2β interacts with the tctex-1 of motor protein dynein similar to Doc2α (Nagano, Orita et al. 1998). This interaction might indicate the role of Doc2β in intracellular transportation in non-secretory cells.

1.3.3 Doc2γ

Doc2γ has 388 residues and has a molecular mass of 43 kDa. The N-terminal Doc2-specific domain is 80% homologous to those of Doc2α and Doc2β (Figure 1-4). Doc2γ is expressed ubiquitously but it is highly enriched in heart. The level of Doc2γ expression is constant throughout the embryonic stages. Doc2γ C2A domain lacks three of five putative Ca^{2+}-binding residues which are conserved in Doc2α and Doc2β and does not possess a Ca^{2+}-dependent phospholipid-binding property (Fukuda and Mikoshiba 2000b). The C2B domain conserves the five putative Ca^{2+}-binding residues but does not show Ca^{2+}-dependent phospholipid binding as also evidenced in Doc2α and Doc2β. Doc2γ is exclusively associated with the nucleus (Fukuda, Saegusa et al. 2001). The nuclear localisation is mediated by the substitution of the residues in the Ca^{2+}-binding loop of the C2A domain with a

cluster of basic amino acids. Doc2γ interacting proteins have not been identified. The sequence homology of Doc2γ N-terminal with those of Doc2α and Doc2β implies that Doc2γ may be able to interact with Munc13.

1.3.4 Roles of Doc2β in regulated exocytosis

The role of Doc2β in regulated exocytosis has not been studied. Given the high homology, the complementary distribution in brain, the similarities in Ca^{2+}-dependent phospholipid binding and the interaction with other synaptic proteins between Doc2α and Doc2β, it is hypothesised that Doc2β performs a similar function in regulated exocytosis as Doc2α.

1.3.5 Proposed functions of Doc2β in regulated exocytosis

Based on the effect of Doc2α in regulated exocytosis and the similarity between Doc2β and Doc2α, two functions of Doc2β in regulated exocytosis are proposed.

1.3.5.1 Vesicle recruitment and docking

This hypothesis is based on the Doc2β-Munc13 interaction. This interaction is induced by phorbol ester/diacylglycerol. The result of the interaction is the translocation of Doc2β and Munc13 to plasma membrane (Duncan, Betz et al. 1999a). Because Doc2β is associated with vesicles (Sakaguchi, Orita et al. 1995; Duncan, Betz et al. 1999a), such an interaction could lead to the increase in the number of docked vesicles (Figure 1-5). Several lines of evidence support this hypothesis. In PC12 cells, expression of N- or C-terminal deletion of Doc2α inhibit

high-K^+ induced secretion (Orita, Sasaki et al. 1996). This is because the N-terminal of Doc2 is important for the interaction with Munc13 while the C-terminal is responsible for the association with secretory vesicles. Introduction of Mid peptides, which disrupts the Doc2-Munc13 interaction, in superior cervical ganglion neurons inhibits synaptic transmission (Mochida, Orita et al. 1998). The onset of the inhibition by Mid peptides is slow and accelerated by increasing the frequency of stimulation consistent with the speculated function of Doc2-Munc13 interaction in vesicle recruitment.

The C-terminal domain of Doc2 also interacts with Munc18. Munc18 is normally bound to syntaxin at the plasma membrane. Recent studies in adrenal chromaffin cells suggest a role for Munc18 in vesicle docking, possibly through the interaction with one of the vesicle proteins (Voets, Toonen et al. 2001a). However, the possibility of Doc2 to be a docking molecule that recognises Munc18 at the plasma membrane is still questioned. This is because the Doc2α-Munc18-syntaxin complex has never been reported (Verhage, de Vries et al. 1997). However, it is possible that the specificity of Doc2-Munc13 translocation to plasma membrane is determined by Munc18-syntaxin complex at the plasma membrane. The recognition of Munc18 by Doc2 might direct the vesicles to the sites of exocytosis.

1.3.5.2 Vesicle priming

Doc2 competes with syntaxin for Munc18. The syntaxin-Munc18 interaction has a higher affinity than the Doc2-Munc18 interaction. However, the presence of other SNARE counterparts or Munc13 reduces the syntaxin-Munc18 interaction and promotes the Doc2-Munc18 interaction (Verhage, de Vries et al. 1997; Sassa, Harada

et al. 1999). Therefore, Doc2 might function by removing of Munc18 from syntaxin and presenting Munc13 to syntaxin at the same time. Such an interaction would promote the opened conformation of syntaxin and accelerate the SNARE complex formation (Figure 1-5). Based on a study in adrenal chromaffin cells, SNAREs are formed prior to the final Ca^{2+}-induced exocytosis (Xu, Rammner et al. 1999). The enhancement of SNARE complex formation would prime the vesicles and lead to an increase in number of fusion-competent vesicles.

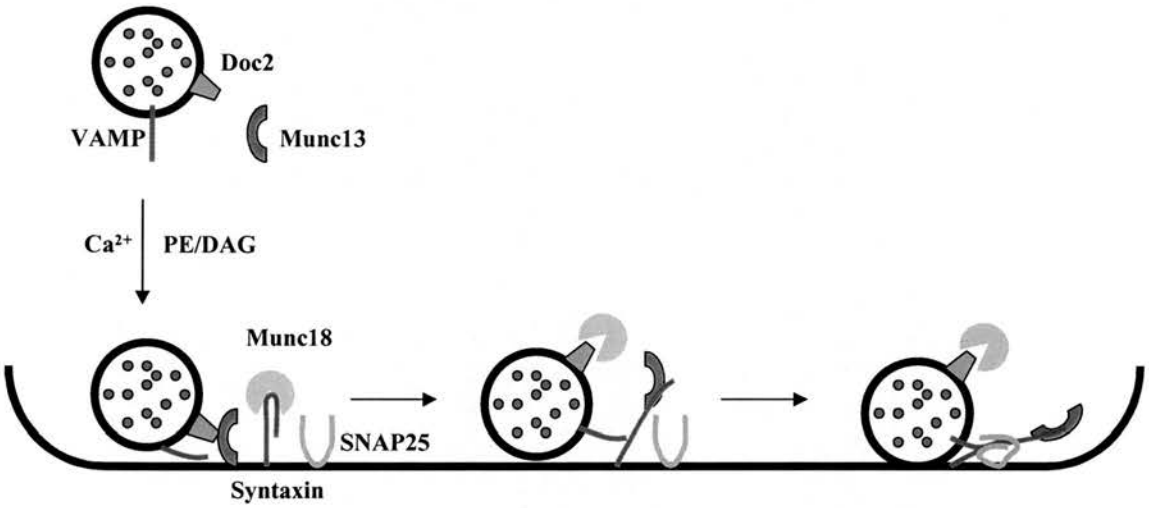

Figure 1-5 Hypothetical model of Doc2β function in regulated exocytosis

The Doc2-Munc13 interaction is induced by phorbol ester (PE) or diacylglycerol (DAG) in the presence of Ca^{2+}. The interaction recruits vesicles to the plasma membrane. Recognition of Munc18 by Doc2, Munc13 or both helps confine the location of vesicles at the plasma membrane to where the secretory machinery is. Doc2 can also accelerate the removal of Munc18 from syntaxin in the priming step. (VAMP=vesicle-associated membrane protein or synaptobrevin)

To test the hypotheses, the experiments were performed in bovine adrenal chromaffin cells. Adrenal chromaffin cells have served as a model for the understanding of exocytosis of neurons and endocrine cells. These cells are derived from neuroectoderm similar to all neurons. The adrenal chromaffin cells secrete catecholamines by regulated exocytosis of large dense-core vesicles using the conserved exocytotic machinery similar to that used in neurotransmission (Morgan and Burgoyne 1997). The cells are round with a diameter of 10-15 μM, permitting the application of high-resolution measurements of secretion at the single cell level.

Bovine adrenal chromaffin cells serve as a good model to study the effect of Doc2β expression. These cells do not express any known isoforms of Doc2 (Duncan, Apps et al. 2000a). However, both Munc13 and Munc18 are expressed in bovine adrenal chromaffin cells (Duncan, Don-Wauchope et al. 1999b; Ashery, Varoqueaux et al. 2000). Taking advantage of the Semliki forest virus (SFV) vector system, the mouse Doc2β gene was introduced into bovine adrenal chromaffin cells. The cells expressing Doc2β were identified by the co-expression of enhanced-green fluorescent protein (EGFP) reporter.

The secretion of catecholamines in cell-population was induced by high-K^+ depolarisation in intact cells or high Ca^{2+} in permeabilised cells. Single cell secretion was achieved by membrane capacitance measurements and electrochemical detection of catecholamine secretion. If Doc2 has a positive role in vesicle recruitment as speculated, expression of Doc2β in bovine adrenal chromaffin cells would increase catecholamine secretion. The number of fusion-competent vesicles (SRP and RRP) would also increase. This effect would be more significant after the

application of phorbol ester which induce Doc2β-Munc13 interaction. The single vesicle fusion kinetics are not expected to be different from control. On the other hand, expression of Doc2β C2-domain would have the opposite effects as shown in the case of Doc2α (Orita, Sasaki et al. 1996).

Chapter 2

Materials and Methods

2.1 MATERIALS

2.1.1 Bacterial strains

2.1.1.1 SCS110 (Stratagene, La Jolla, CA, US.)

rpsl (Str^r), *thr, leu, endA, thi-1, lacY, galK, galT, ara, tonA, tsx,* ***dam, dcm****, supE44, Δ(lac-proAB),* [F′ *traD36, proAB,* $lacI^qZ\Delta M15$]

2.1.1.2 DH5α (Clontech, Palo Alto, CA, US.)

deoR,endA1, gyrA96hsdR17($r_k^- m_k^+$), *recA1, supE44, thi-1, Δ(lacZYA-argFV169), ϕ80δlacZΔM15, F*$^-$, λ^-

2.1.2 Cell line

2.1.2.1 HEK293T (Dr. N. Kasahara, Institute of Genetic Medicine, University of Southern California, US.)

HEK293T cell line is a permanent line of primary human embryonic kidney transformed by Simian virus (SV40) large T-antigen. This T-antigen induces the replication of the plasmid containing the SV40 origin of replication.

2.1.3 Plasmid vectors

2.1.3.1 pIRES2-EGFP (Clontech, Palo Alto, CA, US.)

pIRES2-EGFP is designed for bicistronic plasmid construction. The multiple cloning sites (MCS) cassette is followed by the internal ribosome entry site (IRES)

from encephalomyocarditis virus which allows the translation of the downstream gene encoding enhanced green fluorescent protein (EGFP) independent of a 5′-cap. EGFP is a variant of wild-type green fluorescent protein which has brighter and higher expression in mammalian cells (maximum excitation = 488 nm, maximum emission = 507 nm). The vector contains a kanamycin/neomycin resistance gene for clone selection.

2.1.3.2 Superlinker Phagemid pSL1180 (Amersham Pharmacia Biotech, Piscataway, NJ, US.)

pSL1180 contains 64 uninterrupted hexamer recognition sequences. An ampicillin-resistant gene is used for clone selection.

2.1.3.3 pSCA1 and pSCAHelper (Dr. Rod Bremner, Eye Research Institute of Canada, Toronto, Canada)

All Semliki Forest Virus (SFV) vectors are derived from attenuated virus. pSCA1 and pSCAHelper are prepared from pSFV1 and pSFVHelper2 (Invitrogen, Carlsbad, California, US.), respectively, by substitution of the original SP6 promoter with a cytomegalovirus (CMV) immediate early promoter together with a T7 promoter (DiCiommo and Bremner 1998). The CMV promoter allows transcription in mammalian cells while the T7 promoter allows bacterial and *in vitro* transcription. The multiple cloning site of pSCA1 contains two restriction enzyme recognition sites, BamHI and SmaI. The plasmid contains an Ampicillin resistant gene for clone selection.

2.1.3.4 *Doc2β gene, Doc2β-EGFP fusion gene and C2AB-EGFP fusion gene (Dr.Rory R. Duncan, University of Edinburgh, UK.)*

The Doc2β gene was prepared by reverse transcription and polymerase chain reaction of mouse brain RNA as has been previously published (Duncan, Betz et al. 1999a; Duncan, Don-Wauchope et al. 1999b). The Doc2β gene was subcloned into the pIRES vector (Clontech, Cambridge, UK). Doc2β-EGFP was prepared by inframe insertion of Doc2β gene into pEGFPN1 (Clontech, Cambridge, UK), the fusion gene was then subcloned into the pSFV1 (Life technologies, UK). The gene encoding Doc2β C2 domains (C2AB) was prepared by PCR using the Doc2β gene as a template. The C2AB was then subcloned inframe with the EGFP into pEGFPN1.

2.1.4 Molecular biology reagents

2.1.4.1 *Plasmid DNA Purification kits*

Promega Corporation, Madison, WI, US.

Wizard™ *Plus* Minipreps DNA Purification System

Wizard™ *Plus* Midipreps DNA Purification System

Clontech, Palo Alto, CA, US.

NucleoBond Plasmid Maxi Kit

2.1.4.2 Enzymes

New England Biolabs, Beverly, MA, US.

Restriction enzymes and T4-DNA Ligase

USB Corporation, Cleveland, Ohio, US.

Shrimp Alkaline Phosphatase

2.1.4.3 DNA Electrophoresis

Invitrogen, Carlsbad, California, US.

Agarose powder

Ethidium bromide Solution

New England Biolabs, Beverly, MA, US.

λ-HindIII digested DNA Markers

Promega Corporation, Madison, WI, US.

1 kb and 100 bp DNA Markers

2.1.4.4 DNA extraction from agarose

Invitrogen, Carlsbad, California, US.

CONCERT Rapid Gel Extraction System

CONCERT Matrix Gel Extraction System

2.1.4.5 Protein Electrophoresis and Western Blotting

Invitrogen, Carlsbad, California, US.

Poly-acrylamide

Magic Mark

0.45 μm Nitrocellulose Membrane

WesternBreeze® Chromogenic Kit-Anti-Rabbit

Clontech, Palo Alto, CA, US.

A.V. peptide anti-EGFP antibody

2.1.5 Bacterial Culture Media and Related products

Invitrogen, Carlsbad, California, US.

All Bacterial culture supplies were from Invitrogen.

2.1.6 Mammalian Cell Culture media and Cell culture supplementary

Invitrogen, Carlsbad, California, US.

All mammalian cell culture supplies were purchased from Invitrogen.

2.1.7 Chemicals and Solutions

Worthington Biochemical Corporation, Lakewood, NJ, US.

Collagenase type II

BD Biosciences, Bedford, MA, US.

Matrigel Matrix

Molecular probes, Eugene, OR, US.

Fura-2, pentapotassium salt (cell impermeant)

Fura-2, AM (cell permeant)

Fura-6F, pentapotassium salt (cell impermeant)

Calbiochem-Novabiochem Corporation, La Jolla, CA, US.

Phorbol-12-myristate-13-acetate (PMA)

Dow Corning Corporation, Midland, MI, US.

Sylgard®184 Silicone elastomer kit

Sigma, St. Louis, MO, US.

All other chemicals were molecular biology grade and purchased from Sigma.

All solutions were made up in deionised-water prepared with Nanopure infinity™ ultrapure water system (Barnstead/Thermolyne, Iowa, US.).

2.2 METHODS

2.2.1 Construction of Recombinant plasmid vectors

The DNA recombinant protocols adopted were based on standard molecular biology protocols published elsewhere (Sambrook, Fritsch et al. 1989). The aim was to insert genes of interest, EGFP, Doc2β, Doc2β-EGFP and C2AB-EGFP, into DNA-based SFV vector, pSCA1.

i. Construction of Bicistronic SFV replicons

Bicistronic SFV replicons were constructed in order to express two genes independently. The internal ribosomal entry site (IRES) provided a translation of the second gene independent of a 5'cap. The first bicistronic SFV replicon (EGFP) was generated by subcloning the gene encoding IRES-EGFP as a *Bam*HI-*Hpa*I fragment from a commercially available vector pIRES2-EGFP (Clontech) into the *Bam*HI-*Sma*I sites of the DNA-based SFV vector (pSCA1). The second bicistronic SFV replicon (Doc2β-IRES-EGFP) was constructed in two steps. First, the Doc2β gene from pIRES-Doc2β was subcloned as a *Nhe*I-*Xho*I fragment into pIRES2-EGFP. The *Bam*HI-flanked Doc2β gene was then subcloned from the pIRES2-EGFP vector into the *Bam*HI site of the first bicistronic vector.

ii. Construction of SFV replicons containing the EGFP-fusion genes

The first replicon containing a Docβ gene fusion with a reporter EGFP gene (Doc2β-EGFP) was generated by replacing the SP6 promoter in the original RNA-based SFV

vector containing Doc2β-EGFP with a cytomegalovirus/T7 (CMV/T7) promoter from pSCA1. The CMV/T7 promoter was subcloned as a *Pvu*I-*Bsi*WI fragment into the RNA-based SFV vector containing Doc2β-EGFP. Another replicon containing a gene encoding Doc2β C2 domain fusion with a reporter EGFP gene (C2AB-EGFP) was generated by subcloning the C2AB-EGFP as a *Bgl*II-*Hpa*I fragment from the pEGFPN1-C2AB into the *Bam*HI-*Sma*I sites of pSCA1.

2.2.1.1 Preparation of Plasmids for Restriction Digests

The plasmid vectors were propagated in bacterial host SCS110 in order to amplify the plasmids and remove methylation at some restriction sites. SCS110 is a *dam* and *dcm* deficient strain of *E. Coli.* The plasmid DNA was purified from the transformants by using Wizard® *Plus* Midipreps DNA Purification System (Promega).

2.2.1.2 Restriction Digests

The restriction digest was performed as recommended by manufacturer. The restriction enzymes were supplied together with reaction buffers. In case of two or more enzymes used in the same reaction, the compatibility of buffers was considered based on the buffer compatibility table provided by manufacturer. Sequential restriction digests were used when there was no mutually compatible buffer for the restriction enzymes. The DNA was digested with the first enzyme, electrophoresed, extracted from agarose gel and digested with the second enzyme. Each reaction was performed in a 20-µl volume containing 1-2 µg of DNA and 2 units of restriction enzyme per 1 µg of DNA. The reactions were incubated at manufacturer-

recommended temperature for 2 hours in a PCR machine (MJ Research). The reaction was stopped by chilling on ice and addition of 5-μl gel loading buffer containing 65%(w/v) sucrose, 10 mM Tris-HCl (pH7.5), 10 mM EDTA and 0.3%(w/v) bromphenol blue.

2.2.1.3 DNA Electrophoresis

Agarose (Invitrogen) was dissolved in TBE buffer (containing Tris base 89 mM, Boric acid 89 mM and EDTA 1 mM) to give the concentration of 0.7% (w/v). The solution was heated up in a microwave until the agarose was completely dissolved. After the solution cooled down, ethidium bromide (Invitrogen) was added to give a final concentration of 50 μg/ml. The solution was poured into the electrophoresis chamber and left until the gel set. The DNA was loaded and the electrophoresis was started. After appropriate duration of electrophoresis, the gel was visualised under ultraviolet light. The amount of the DNA in each band was estimated by comparison the intensity of the DNA band with those of the DNA markers of known amounts.

2.2.1.4 DNA Extraction from Agarose Gel

Slices of gel containing DNA were excised from agarose gel and placed into microcentrifuge tubes, 300-400 mg in each tube. The CONCERT Rapid Gel Extraction System (Invitrogen) was used for DNA smaller than 10 kb and the CONCERT Matrix Gel Extraction System (Invitrogen) was used for DNA larger than 10 kb. The manufacturer-recommended protocol was followed. The DNA was eluted with deionised water (ddH_2O). A small amount of the eluted DNA was subjected to electrophoresis to determine the purity and amount of the extracted

DNA. Based on observation, both methods recovered about 70% of the total DNA in the bands.

2.2.1.5 Dephosphorylation of 5'-end

5' dephosphorylation was achieved by using Shrimp Alkaline Phosphatase (USB). The following protocol was used. Each 100 µl reaction contained 1 pmol of DNA ends, 10 µl of manufacturer-supplied 10x-reaction buffer (containing $MgCl_2$ 100 mM, Tris-HCl 200 mM, pH 8) and nuclease-free deionised water. One unit of shrimp alkaline phosphatase was added to the reaction. The reaction was incubated in a PCR machine at 30°C for 30 minutes followed by 70°C for 20 minutes to inactivate the enzymes.

2.2.1.6 DNA Ligation

Ligation was performed in a 20-µl reaction volume containing 200 ng of total DNA. A one-to-one molar ratio of plasmid and insert was used in each reaction. To each reaction, 6 Weiss-Units of T4 DNA ligase (New England Biolabs) was added. The reaction tubes were incubated at 12 °C for 12-14 hours in a PCR machine.

2.2.2 Bacterial Transformation

2.2.2.1 Preparation of Competent Bacteria

Competent bacterial cells were prepared by using the calcium precipitation method. Bacteria was grown overnight in 5 ml LB medium (Invitrogen) in a 37°C incubator shaking at 250 rpm. The overnight culture was transferred to a 100-ml Erlenmeyer

flask containing 50 ml of LB medium. The incubation was continued for 3 hours. The culture was then aliquoted into microcentrifuge tubes and centrifuged at 3000xg for 5 minutes. After the supernatant was decanted, the pellet was resuspended in 500 μl of ice-cold $CaCl_2$ solution (containing 50 mM $CaCl_2$ and 10 mM Tris-HCl, pH 8). The reaction tubes were incubated on ice for 30 minutes. The suspension was centrifuged at 3000xg for 5 minutes. The pellet was gently resuspended in 50 μl of iced-cold $CaCl_2$ solution and kept on ice. For long-term storage, glycerol was added to the competent cells to give the final concentration of 20%(v/v). The competent cells were then stored in a -80°C freezer for months.

2.2.2.2 Transformation

The ligation products or other plasmid vectors were added to the competent cells. The reaction was incubated for 30 minutes on ice followed by 1-minute incubation at 42°C. The reaction was then incubated for 2 minutes on ice. Warm LB medium without antibiotic was added to the reaction, 1 ml each. The reaction was incubated in a shaker incubator at 37°C for 1 hour. The transformation product was then plated on LB agar plate containing appropriate antibiotics and incubated at 37°C overnight.

2.2.3 Analysis of Transformants

Isolated colonies on the agar plates were transferred to 5-ml bacterial culture tubes containing LB medium and appropriate antibiotics (Ampicillin or Kanamycin 50 μg/ml). The tubes were incubated overnight in a shaking incubator at 37°C. Plasmids were purified from the bacterial culture by using Wizard™ *Plus* Minipreps DNA Purification System (Promega). The restriction mapping was performed by

digestion with particular restriction enzymes to yield information about the insertion and orientation of the inserts in the plasmid vectors.

2.2.4 DNA Sequencing

The DNA-based SFV replicons purified from the selected colonies were subjected to DNA sequencing. The forward primer based on the pSCA1 sequence proximal to the multiple cloning sites was 5'-ATGAGGTAGAGGGCTGCAAA-3'. The reward primer to verify the authenticity of Doc2β gene in the bicistronic construct was taken from the antisense sequence to the proximal end of the IRES (5'-AGACCCCTAGGAATGCTCGT-3'). The reward primer for the EGFP-fusion constructs was taken from the antisense sequence to the proximal end of the EGFP (5'-GTCCAGCTCGACCAGGATG-3'). The DNA was submitted to the central sequencing service (USC/Norris Comprehensive Cancer Centre, CA, US.). The sequencing procedure was a dye-based method where 3'-fluorescent-labelled dideoxynucleotide triphosphates were incorporated into the DNA extension products. The DNA sequences were compared with the database from GenBank (GenBank number for mouse Doc2β is NM 007873).

2.2.5 Large Scale DNA preparation

A bacterial colony containing the correct insertion was grown overnight in a 1-litre Erlenmeyer flask containing 500 ml of LB medium with appropriate antibiotics. Plasmid was purified from the bacterial culture by using NucleoBond Plasmid Maxi Kit (Clontech). The purified plasmid was kept in a -20°C freezer.

2.2.6 Long-term Storage of transformants

The overnight bacterial culture was aliquoted into cryotubes. Glycerol was added to a final concentration of 20%(v/v). The reaction was briefly mixed by vortexing and kept at -80°C.

2.2.7 Viral packaging

2.2.7.1 HEK293T cell culture

HEK293T cells were cultured in Iscove's Modified Eagle Medium (IMEM) supplemented with 10% fetal bovine serum. The cells were cultured in a 75-ml[3] tissue culture flask and maintained in an incubator at 37°C and 5% CO_2. The cells were passaged when the confluency reached 80-90%. The culture medium was removed from the tissue culture flask and the cells were washed once with 5 ml of phosphate buffer saline (PBS) pH 7.2. The cells were incubated with 3 ml of trypsin-EDTA solution (0.05% Trypsin, 0.53 mM EDTA) for 30 seconds at room temperature. The enzyme solution was then removed and the cell was further incubated for 3 minutes in an incubator. The cells were resuspended in complete medium, one-twentieth of the cell suspension was diluted and cultured in a new flask.

2.2.7.2 Calcium Phosphate transfection

HEK293T cells at a confluency of 80-90% in a 75-ml tissue culture flask were trypsinized as explained in the culture methods. The cells were plated in 6-well plates pre-coated with 0.001% poly-L-lysine at $4x10^5$ cells/well and maintained

overnight in an incubator at 37°C and 5% CO_2. The cells had attained 80% confluency the next day and were ready for calcium phosphate transfection. The culture medium was removed and replaced with 2 ml of fresh culture medium. The calcium phosphate transfection was started about 6 hours after the medium replacement. The replicon and helper plasmids at 10 μg each were diluted to a total volume of 263 μl with nuclease-free water in a 1.5-ml sterile microfuge tube. While gently agitating, 37 μl of 2 M $CaCl_2$ solution was added dropwise. The DNA-Ca^{2+} complex was added dropwise to another 1.5-ml sterile microfuge tube containing 300 μl of HEPES Buffer Solution (containing NaCl 280 mM, HEPES 50 mM and Na_2HPO_4 1.5 mM, pH 7.1). The reaction was incubated for 30 minutes at room temperature. While gently swirling, the culture plate, 300 μl of the DNA complex solution was added to each well of a 6-well plate. The cells were maintained overnight in an incubator at 37°C and 5% CO_2. The next morning after calcium phosphate transfection, the culture medium was removed and replaced with 2 ml of fresh medium supplemented with 0.5 mM of sodium butyrate. The cells were incubated with medium containing sodium butyrate for 6-8 hours. The medium containing sodium butyrate was removed and replaced with 0.8 ml of fresh medium without sodium butyrate. The medium was collected 24 hours after the last replacement and filtered through a 0.45-μm syringe filter. The filtrate was aliquoted and kept at –20°C for short-term or –80°C for long term storage.

2.2.8 Viral Activation

The viral stock was activated by incubation with one-twentieth of the total volume of α-chymotrypsin (10 mg/ml in HEPES-NaOH, pH 7.3) for 45 minutes at room temperature. The α-chymotrypsin was inactivated by addition of one-fortieth of the total volume of aprotinin (10 mg/ml in PBS pH 7.2, supplemented with 10 mM $MgCl_2$ and 20 mM $CaCl_2$) and incubated for 10 minutes at room temperature. The activated viral particles were used immediately or kept at -20°C.

2.2.9 Titering of viral particles

HEK293T cells were cultured on a 12-well plate pre-coated with poly-L-lysine. When the cells reached 90-100% confluency, the culture medium was removed and 100 μl of various dilutions of activated viral solution were added to the cells. The reaction was incubated for 1-2 hours in a tissue culture incubator. The viral solution was then removed and replaced with fresh medium. The numbers of fluorescent cells were counted under a fluorescent microscope at 24 hours post-infection.

Viral titer (/ml) = (numbers of fluorescent cells x 1000)/(dilution x 100)

The viral stock was diluted in IMEM medium and stored at the final titer of $3x10^8$/ml.

2.2.10 Detection of protein expression in SFV-infected cells

2.2.10.1 Preparation of cell lysate

Cell lysate was prepared from the cells at different time after infection. The culture medium was removed and the cells were washed once with cold PBS. The cells in each well were scraped from the bottom of the well in the presence of 0.5 ml of PBS. The cells were transferred to 1.5-ml microfuge tubes and centrifuged at 2000 g for 5 minutes. The pellet was resuspended in 60 µl of lysis buffer (50 mM Tris-HCl pH 7.8, 150 mM NaCl, 1% NP40, 1 mM PMSF, 1 µg/ml Pepstatin and 1 µg/ml Leupeptin) and incubated for 30 minutes on ice. The cell suspension was centrifuged at 10,000 g for 10 minutes. The lysate was transferred to new tubes and kept in -20°C freezer until used.

2.2.10.2 SDS Polyacrylamide Gel Electrophoresis (SDS-PAGE)

The 10% SDS-polyacrylamide gel was poured in a 1-mm thick cassette (Invitrogen). The separating and stacking gel were prepared as shown.

Separating gel :

50% Acrylamide/Bis (29:1)	5 ml
Separating Gel Buffer (1M Tris-HCl pH 8.8)	9.4 ml
10% SDS	250 µl
50% Sucrose	4 ml

H_2O	5.8 ml
Tetramethylethylenediamine (TEMED)	6.25 µl
50 mg/ml Ammonium Persulfate	625 µl

Stacking :

50% Acrylamide/Bis (29:1)	1 ml
Stacking Gel Buffer (0.375 M Tris-HCl oH 6.8)	4.2 ml
10% SDS	125 µl
H_2O	6.3 ml
TEMED	5 µl
50 mg/ml Ammonium Persulfate	1 ml

The SDS-PAGE was performed with the XCell *SureLock* Mini-Cell (Invitrogen). The running buffer contained 196 mM Glycine, 50 mM Tris-HCl pH 8.3 and 0.1% SDS. The lysate was mixed with the same volume of loading buffer (containing 125 mM Tris-HCl pH 6.8, 10% 2-Mercaptoethanol, 10% SDS, 10% Glycerol and bromphenol blue). The sample was heated up to 95°C for 5 minutes and loaded to the gel. A constant voltage of 100 Volts was applied for 2 hours.

2.2.10.3 *Electroblotting*

The method for transferring proteins from gel to solid membrane and immunological detection was based on standard protocol as previously published (Towbin, Staehelin et al. 1979). The semi-dry or horizontal blotting was achieved by using the X-cell *SureLock* blotting module (Invitrogen). The proteins were transferred to a 0.45-μm nitrocellulose membrane (Invitrogen). The gel-membrane pair was sandwiched between filter paper sheets soaked with transfer buffer (containing 96 mM Glycine, 12 mM Tris-HCl pH 8.3 and 20% methanol). A constant current of 500 mA was applied for 30 minutes. The membrane was removed from the blotting module and briefly rinsed in the transfer buffer before the detection step.

2.2.10.4 *Indirect Enzyme Immunoassay detection of proteins on membrane*

A primary antibody against EGFP (BD Living Colours A.V. Peptide Antibody, Clontech) was used for the detection of the proteins on the blotting membrane. Primary antibody binding to the EGFP on the membrane was detected with alkaline phosphatase-conjugated, goat anti-rabbit IgG provided with the WesternBreeze® Chromogenic Kit-Anti-Rabbit (Invitrogen). The protocol provided by the manufacturer was adopted. All steps were carried out at room temperature. Briefly, the membrane was incubated in a blocking solution (5% casein, 0.2% Tween-20 in PBS) for 1 hour. The membrane was then incubated for another hour in the blocking solution containing 1:500-1:1000 dilution of primary antibody. After a few rinses with a wash solution (0.2% Tween-20 in PBS), the membrane was incubated in the secondary antibody solution for 1 hour. The membrane was rinsed with the wash solution and stained with the chromogenic substrate containing 5-bromo-4-chloro-3-

indolyl phosphate (BCIP) and nitro blue tetrazolium (NTB). The protein G fusion molecular weight marker (MagicMark, Invitrogen) was used to identify the molecular weight of proteins.

2.2.11 Primary culture of bovine adrenal chromaffin cells

Chromaffin cells were prepared by a method modified from previous publication (Smith 1999). Bovine adrenal glands were collected fresh from a local slaughterhouse. The adrenal veins were infused immediately with ice-cold Locke's solution (containing 154.2 mM NaCl, 2.6 mM KCl, 2.2 mM K_2HPO_4, 0.85 mM KH_2PO_4, 20 mM HEPES, 10 mM glucose, 10 units/ml Penicillin and 10 μg/ml Streptomycin) to remove blood and prevent blood coagulation. The glands were carried in ice-cold Locke's solution to the laboratory. In the sterile cabinet, the surrounding fat was trimmed off the glands and the adrenal veins were infused with ice-cold Locke's solution until the fluid came out clear of red blood cells. The glands were then infused with pre-warmed collagenase Type II enzyme solution (0.25 mg/ml in DMEM/F12 supplement with 15 mM HEPES). The glands were placed in a container and incubated in a 37°C water bath for 5 minutes, the process was repeated three more times. After the collagenase treatment, the glands were cut along the border and the cortex was pulled out to separate it from the medulla. The yellowish medullary tissue was collected and placed in a Petridish containing 20 ml of collagenase enzyme solution. The medullary tissue was minced into small pieces and transferred to a sterile bottle containing a magnetic spin bar. The bottle was place in a 37°C water bath for 20 minutes with the magnetic spin bar spun at a moderate speed. After the dispersion step, the content was poured into a sterile

Petridish and the larger pieces of medullary tissue were removed. The suspension was filtered through a 70-μm cell strainer. The filtrate was centrifuged at 60 g for 8 minutes at room temperature in a swing-bucket rotor. The pellet was resuspended in 20-ml Locke's solution and centrifuged at 60 g for 5 minutes. This process was repeated twice. A drop of cell suspension was subjected to cell counting. After the final centrifugation, the pellet was resuspended in chromaffin cell culture media (DMEM/F12 supplemented with 15 mM HEPES, 1% (v/v) ITSX, 5 unit/ml of penicillin and 5 μg/ml of streptomycin) at a concentration about $1.5x10^5$cells/ml. One millilitre of cell suspension was aliquoted to each well of 24-well plate containing matrigel-coated cover glasses. For population assays, the cells were diluted to a concentration of $3x10^5$cells/ml and a 1-ml aliquot was added to each well of 24-well plate pre-coated with 0.01% poly-L-lysine. The cells were maintained in an incubator at 37°C and 5% CO_2. The culture medium was replaced the next day. The cells were used for experiment between 1-4 days after preparation.

2.2.12 Bovine adrenal chromaffin cells infection

Activated viral particles at a multiplicity of infection (MOI) of 50 were diluted with chromaffin cell culture media to a total volume of 200 μl. The culture medium was removed from the chromaffin cell culture and replaced with the viral-containing medium. The reaction was incubated for 2 hours. The viral-containing medium was then removed and replaced with fresh culture medium. The cells were used for experiments between 15-30 hours after infection.

2.2.13 Population Assay

The culture medium was removed and replaced with 0.5 ml of pre-warmed Locke's solution with or without 100-nM phorbol-12-myristate-13-acetate (PMA). The cells were then incubated for 10 minutes in a 37°C incubator.

2.2.13.1 High-K^+ stimulation

The Locke's solution was removed and replaced with 0.5 ml of pre-warmed high-K^+ solution (containing 98 mM NaCl, 50 mM KCl, 2 mM $CaCl_2$, 1 mM $MgCl_2$, 10 mM glucose, and 10 mM HEPES-NaOH pH 7.2, osmolarity 315 mOsmole) with or without 100-nM PMA. The cells were then incubated at 37°C for 3 minutes. The plate was chilled on ice and immediately centrifuged at 100g for 3 minutes at 4°C. A 50-µl duplicate was carefully removed from each well for the assay. The cells left on the culture plate were subjected to a lysis reaction by adding 50 µl of 10% nonidet P-40 (NP-40). The cells were incubated for 15 minutes at 37°C. The lysate was collected and centrifuged at 5000 g for 5 minutes. A 50-µl duplicate of the lysate was assayed for catecholamines.

2.2.13.2 β-escin permeabilisation

β-escin is a chemical permeabilising agent known to form complexes with cholesterol. Application of β-escin permeabilises cells in concentration dependent manner and pores of about 8-nm diameter are formed (Iizuka, Ikebe et al. 1994; Konishi and Watanabe 1995).

Permeabilising buffer

K-Glutamate	139 mM
PIPES	20 mM
K_2H_2EGTA	5 mM
MgATP	2 mM
Na_2GTP	0.3 mM
β-escin	60 μM
Bovine albumin	0.5%

pH was adjusted to 6.6 with KOH

Stimulating buffer

The stimulating buffer was similar to the permeabilisation buffer except that the EGTA was replaced with a combination of $CaCl_2$ and calcium buffer to give a desired free Ca^{2+} concentration. The Kd for Ca^{2+} of EGTA and HEDTA at pH 7.2 were 150 nM and 3.38 μM, respectively.

0.1-μM free Ca^{2+}	K_2H_2EGTA	5 mM
	$CaCl_2$	1.85 mM
1-μM free Ca^{2+}	K_2H_2EGTA	5 mM
	$CaCl_2$	4.3 mM

10-μM free Ca^{2+}	KH_2HEDTA	5	mM
	$CaCl_2$	3.5	mM

After 10-minute incubation with Locke's solution with or without PMA, the solution was replaced with a permeabilising buffer with or without PMA and incubated at 37°C for 5 minutes. The permeabilising buffer was replaced with a stimulating buffer with or without PMA. The cells were incubated at 37°C for 10 minutes. The plate was chilled on iced and immediately centrifuged at 100 g for 3 minutes at 4°C. A 50-μl duplicate was carefully pipetted from each well for the assay. The cells left on the culture plate were lysed with 1% NP-40 as previously discussed. The lysate was collected and centrifuged at 5000 g for 5 minutes. A 50-μl duplicate of the lysate was assayed for catecholamines.

2.2.13.3 Catecholamine assay

The assay for the catecholamines was based on the oxidation of catecholamines to produce a fluorescent derivative (von Euler and Lishajko 1959; von Euler and Lishajko 1961). The reaction was performed at room temperature. Each duplicate was mixed with 2 ml of acetate buffer (1 M sodium acetate, pH 6) and 100 μl of potassium ferricyanide solution (0.25% w/v) in a cuvette. The reaction was briefly mixed and incubated for 5 minutes. A 1-ml aliquot of one tenth dilution of freshly prepared ascorbate solution (2% w/v) in 5 M NaOH was added to each reaction. The reaction was thoroughly mixed and assayed with a fluorescent spectrophotometer. The excitation and emission wavelengths were 417 and 517 nm, respectively. The

concentration of catecholamines was calculated from the intensity of the reaction by using an equation obtained from a calibration with standard epinephrine.

2.2.13.4 Calibration of the catecholamine concentration

Various concentrations of epinephrine bitartrate (0-200 μM) were prepared. A 50-μl duplicate of each concentration was taken for the assay. The concentration of the epinephrine was plotted against the intensity and the graph was fitted with a linear function. This relation was used to calculate the catecholamine concentration from the population assay.

2.2.14 Electrophysiological recording

2.2.14.1 Patch clamp

Recording electrode

The recording pipettes were prepared from borosilicate-glass capillary tubes. Two-step pulling by a micropipette puller (Narashigi, Japan) was used to obtain a pipette tip of 1-2 μm in diameter. The pipette tip was coated with Sylgard and minimally fire polished. The pipette resistance was 1.5-3 MΩ after filling with the pipette solution.

Recording condition

A cover glass with attached chromaffin cells was transferred to a recording chamber continuously perfused with bath solution containing (in mM) 145 NaCl, 2.8 KCl, 5 $CaCl_2$, 1 $MgCl_2$, 10 HEPES-NaOH and 2 mg/ml glucose (pH 7.2, 315-320 mOsm).

The patch pipette solution contained (in mM) 145 CsGlutamate, 8 NaCl, 1 $MgCl_2$, 4 mM MgATP, 0.3 mM Na_2GTP, 0.1 mM fura-2, 10 HEPES-CsOH (pH 7.2, 305-310 mOsm). Conventional whole-cell recording was performed with an EPC-9 patch clamp amplifier together with Pulse software (HEKA, Lambrecht, Germany). The series resistance during recording was 5-10 MΩ. No series resistance compensation was used. The membrane potential was held at –70 mV. The data was acquired at 10 kHz and filtered at 3 kHz with an 8-pole Bessel filter. All experiments were done at 30°C.

For the Ca^{2+}-dialysis experiments, the bath solution containing 2 mM $CaCl_2$ was used instead of the one containing 5 mM $CaCl_2$. The internal solution containing 130 mM K-glutamate, 8 mM NaCl, 5 mM KH_2HEDTA, 3.5 mM $CaCl_2$, 1 mM $MgCl_2$, 2 mM MgATP, 0.3 mM Na_2GTP, 0.1 mM fura-6F, 10 mM HEPES-NaOH (pH 7.2, 305-310 mOsm). The free Ca^{2+} was calculated to be 10 μM. The Ca^{2+} dissociation constants (Kd) were as follow: 150 nM for EGTA, 3.38 μM for HEDTA, 140 nM for fura-2, 5.3 μM for fura-6F and 134 μM for ATP.

Identification of the EGFP-expressing cells

EGFP was used as a marker for protein expression. The infected cells expressing protein of interest were identified by the expression of the EGFP. A monochromator-based illumination system (T.I.L.L. Photonics, Germany) used for intracellular calcium measurement was also used to identify the EGFP-expressing cells. A 480/30-nm band-pass excitation filter and a 375-nm dichroic mirror were inserted into the light pathway. The monochromator was set to 488 nm for the

excitation. The emission light was filtered through a 535/40-nm band-pass emission filter.

2.2.14.2 *Membrane capacitance measurements*

Membrane capacitance measurements were achieved by using the "sine+DC" method (Lindau and Neher 1988). The software lockin extension of the Pulse software and EPC-9 were used. A 1-kHz 25-mV peak-to-peak sine wave was applied to the cell at the holding potential of –70 mV in the conventional whole-cell recording. The data was acquired at 10 kHz and filtered at 3 kHz with 8-pole Bessel filter. The data was also recorded at slow time scale (1 point per sweep) with the X-chart extension of the Pulse software.

2.2.14.3 *Measurement of the fusion-competent vesicle pool*

A simple whole-cell patch clamp and membrane capacitance measurement was used to estimate the size of the fusion-competent pool of vesicles in this experiment. Six 50-ms depolarisations were applied at an interval of 350 ms. The repetitive depolarisation readily depressed secretory response within few a stimuli (Figure 2-1).

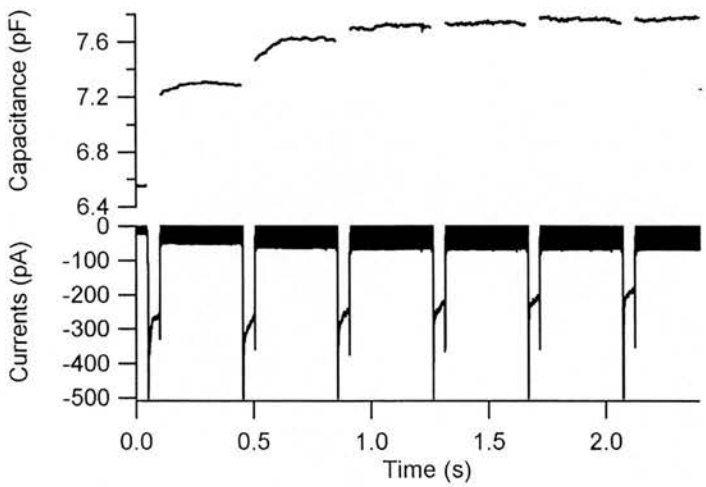

Figure 2-1 Capacitance response to train of depolarisation

Six 50-ms depolarisations to 10 mV from a holding potential of –70 mV were applied at 350-ms interval. The capacitance (*above*) showed significant reduction during the repetition while the calcium currents (*below*) were not significantly reduced.

The secretory response to each depolarisation was measured as a difference between the average of 100-ms of capacitance response after depolarisation and the average of 15-ms of capacitance baseline prior the depolarisation (Figure 2-2). Depolarisation induced secretion outlasts the duration of the stimulus (Seward, Chernevskaya et al. 1996). Therefore, the response was measured 50 ms after the end of each depolarisation.

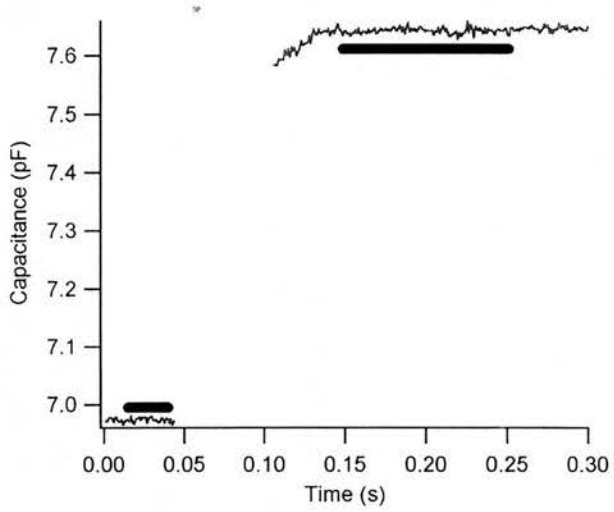

Figure 2-2 Measurement of capacitance response to each depolarisation

A capacitance response to a depolarisation is displayed. The gap in the capacitance recording indicates the application of the depolarisation voltage during which the capacitance meausement can not be recorded. The bars indicated the segments of the capacitance trace taken for averaging. The secretion was measured as a different between the average of the bar after and prior depolarisation.

Two methods of estimation of the fusion-competent pool were adopted from this stimulation protocols. First, the cumulative capacitance responses to the train of depolarisation was created. The fusion-competent pool was measured as the total secretion at the plateau of the cumulative capacitance response. This plateau was usually attained at the third depolarisation (Figure 2-3).

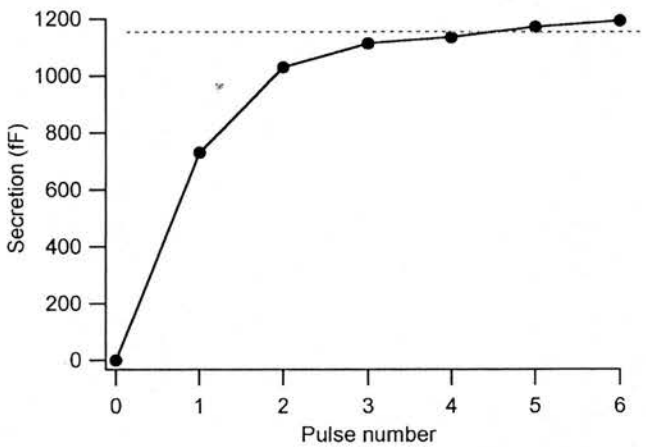

Figure 2-3 Cumulative capacitance responses

A cumulative secretion responded to a train of depolarisation is plotted against the stimulation number. Dashed line indicated the plateau of the secretion where the fusion-competent pool was measured.

Assuming that the calcium sensitivity did not change during the repetitive stimulation, the depression of the secretion was caused by the depletion of the fusion-competent pool. This protocol would give a good estimation of the fusion-competent pool provided that vesicle refilling and endocytosis are not significant during the stimulation. The refilling of the fusion-competent pool is Ca^{2+}-dependent and takes more than tens of seconds at the basal Ca^{2+} concentration (Heinemann, von Ruden et al. 1993; von Ruden and Neher 1993). A rapid endocytosis following Ca^{2+} -induced exocytosis was reported in adrenal chromaffin cells (Neher and Zucker 1993). However, this rapid endocytosis disappears within 2 minutes after the membrane patch was ruptured in whole-cell recording (Smith and Neher 1997). For this purpose, the recording was started 90-120 s after membrane rupture and the total stimulation time was less than 3 seconds.

To ensure that the depression of the secretory response occurred during the train of depolarisation, only when the total secretory response from the forth to sixth depolarisation was less than 25% of the total secretory response to six depolarisations that the data was included in the analysis (Figure 2-4). Using this criterion, about 35% of the data was excluded from the analysis. The size of the fusion-competent pool was measured from the average of the cumulative capacitance change from third to sixth depolarisations.

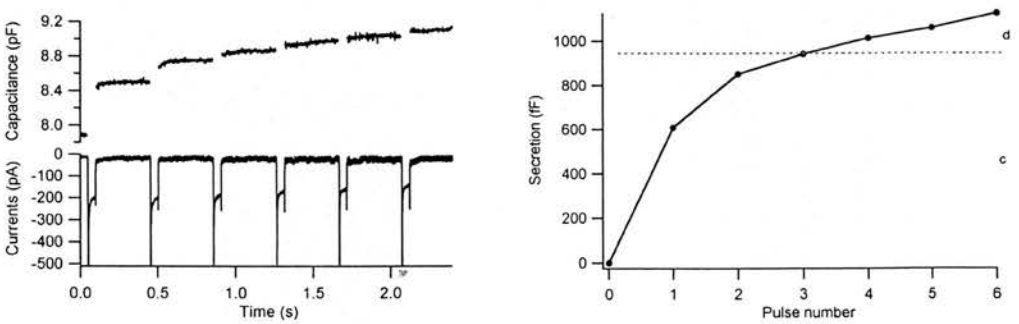

Figure 2-4 Depression of secretory response during train of depolarisation

The cumulative capacitance (*right*) was plotted from the capacitance responses to a train of depolarisation (*left*). c and d are the total capacitance change by first three depolarisations and forth to sixth depolarisations, respectively. The fusion-competent pool was calculated from the average of the third to sixth responses of the cumulative capacitance only when the readily depression occurred ($d/(c+d) < 0.25$).

The second method used to estimate the fusion-competent pool size was the paired-pulse protocol (Gillis, Mossner et al. 1996). The argument against using the train of depolarisation to estimate the fusion-competent pool is that the long stimulation might over estimate due to refilling or under estimate due to endocytosis and the reduction of calcium current during multiple stimulation. The paired-pulse protocol was designed to overcome that problem. The responses to the first two pulses were used for the calculation of the fusion-competent pool. The capacitance change induced by second depolarisation was depressed already while the calcium current did not reduce (Figure 2-5).

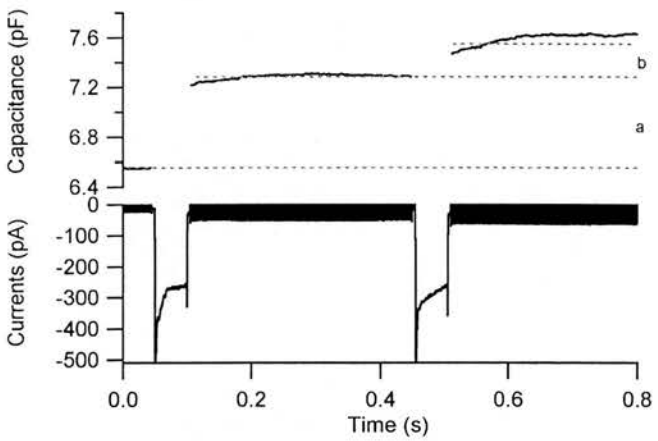

Figure 2-5 Paired-pulse depolarisation

An example of the capacitance response to the first two pulses of the train of depolarisation, the capacitance response to the second depolarisation (a) was significantly reduced compared to that of the first depolarisation (b). The calcium currents were not change during the depolarisation (*below*).

The fusion-competent pool was calculated from Gillis's equation.

$$\text{fusion-competent pool} = S/(1-R)^2$$

$$S = a+b$$

$$R = b/a$$

Where a and b are the capacitance changes in response to the first and second depolarisations, respectively.

The estimation of the fusion-competent pool is more reliable when R is small which indicates the significant depression of the secretion by second depolarisation. The fusion-competent pools calculated from both protocols were well correlated (Figure 2-6).

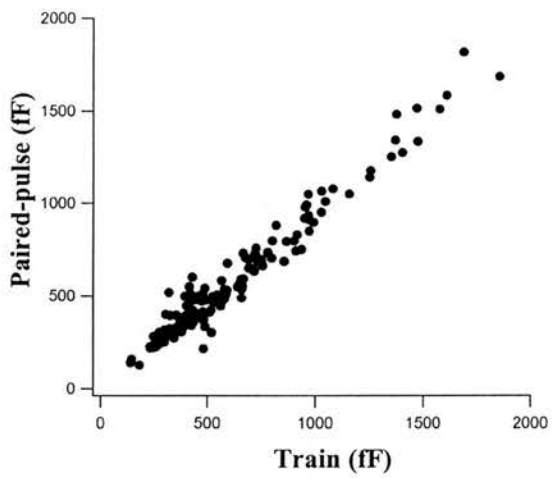

Figure 2-6 Correlation of the fusion-competent pool calculated from the train and pair-pulse protocols.

The fusion-competent pools were calculated from 155 experiments where R was less than 0.7. The correlation factor between both protocols was 0.98.

2.2.14.4 *Electrochemical detection of catecholamine release*

Recording Electrode

The carbon fiber microelectrodes (CFM) were prepared from 5-μm-diameter carbon fibers as previously published (Schulte and Chow 1996; Schulte and Chow 1998). A 3-cm long carbon fiber was attached to the tip of a 5-cm long copper wire with carbon paste. The carbon paste was allowed to dry. The carbon fiber-wire assembly was canulated into a borosilicate glass capillary tube by inserting the free end of the copper wire until the free end of the copper wire was 1 cm beyond the other end of the capillary tube. The copper wire was fixed within the capillary tube by application of a drop of epoxy glue. The epoxy glue was allowed to set. The assembly was placed on a micropipette puller by positioning the heat element of the puller at the carbon fiber just few millimeters from the carbon fiber-wire junction. A two-step pulling protocol was applied. The pulling protocol was designed to produce a capillary tip diameter just bigger than the diameter of the carbon fiber. The capillary tube containing a carbon fiber-wire assembly was collected. The carbon fiber was trimmed so that only 0.5 cm of carbon fiber protruded beyond the capillary tip. The Sylgard was applied to the tip of the capillary tube to seal the junction between carbon fiber and the capillary tip. The Sylgard was left to set overnight. After briefly rinsing with 70% alcohol and distilled water, the carbon fiber was coated with the anodic electrophoretic deposition paint (EDP; Cangard, BASF Farben und Lake GmbH, Muenster, Germany). The copper wire at the other end of the carbon fiber microelectrode was connected to the anode of the power supply while the EDP was connected to the cathode of the power supply through a coiled-

platinum wire. The carbon fiber was submerged into the EDP at the center of the coiled-platinum wire. A constant voltage of 5 V was applied for 3 minutes. The EDP-coated carbon fiber was heat-cured at 100°C for 3 minutes. The carbon fiber was cut to about 2-mm length from the tip of the capillary tube with a clean scalpel-blade before each use.

Recording condition

The CFM was connected to the headstage of a voltammeter. The CFM was lowered into a recording chamber containing cells. The tip of the CFM was placed as close as possible to the cell membrane of a selected cell. A constant voltage of 650 mV versus a silver/silverchloride reference electrode was applied to the CFM by the voltammeter. The output channel of the voltammeter was connected to the EPC-9 via an analogue-to-digital converter (AD-channel). The amperometric current was acquired at 10 kHz and filtered at 3 kHz with an 8-pole Bessel filter. The current was displayed on the oscilloscope window of the Pulse software.

2.2.14.5 Measurement of intracellular calcium

Intracellular calcium measurements were achieved by combined whole-cell patch clamp and fluorescence technique (Augustine and Neher 1992). A Ca^{2+}-sensitive dye fura-2 was dialysed into cell via patch pipette. Fura-2 is a Ca^{2+}-sensitive dye that shares the common Ca^{2+}-binding sites with those of EGTA (Tsien 1989). The dissociation constant (Kd) for Ca^{2+}-binding of fura-2 is 140 nM at pH 7.2. The affinity of fura-2 to Mg^{2+} is about five orders of magnitude weaker than the affinity for Ca^{2+} (Kd for Mg^{2+} is 6-10 mM). According to the Kd, the use of fura-2 is limited

to measurement of $[Ca^{2+}]_i$ at low micromolar range. Ca^{2+} binding to fura-2 shifts the fluorescence excitation spectrum to shorter wavelengths while the emission spectrum is hardly shifted (Figure 2-7).

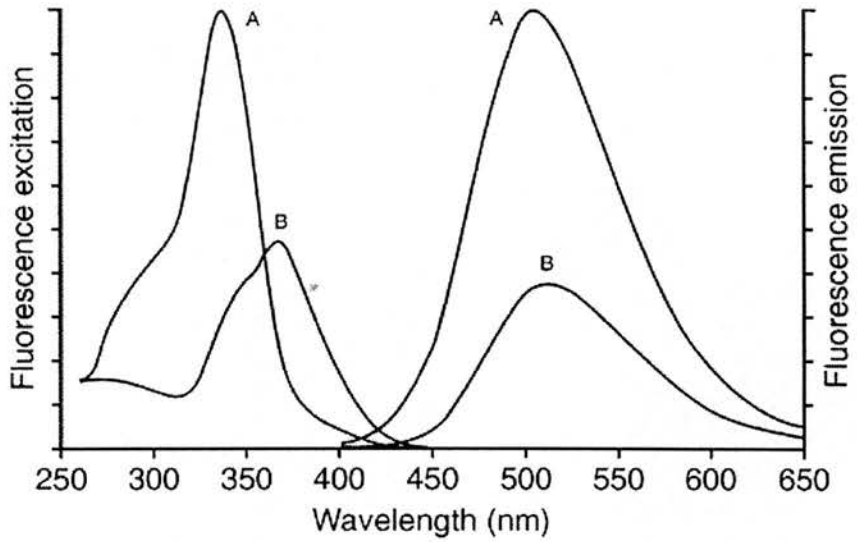

Figure 2-7 Fura-2 fluorescence excitation and emission spectrum (Molecular Probes, Eugene, OR, US.)

The fluorescence excitation spectrum of fura-2 (*left*) measured at the emission wavelength of 510 nm and the fluorescence emission spectrum (*right*) excited at 340 nm at low (B) and high (A) Ca^{2+} concentration. The excitation spectrum shifts to shorter wavelengths at higher Ca^{2+} concentration while the emission spectrum does not change.

Ca^{2+}-binding to fura-2 increases the fluorescence at the excitation wavelength of 340-350 nm while the fluorescence decreases at the excitation wavelength of 380-390 nm. The fluorescence at 360 nm excitation wavelength, the isosbestic point of fura-2, does not change with Ca^{2+}-binding. Taking advantage of the excitation wavelength shift by binding to Ca^{2+}, the dual-wavelength calcium measurement was

developed (Grynkiewicz, Poenie et al. 1985). The ratio of the fluorescence obtain at about 360 nm excitation (F1) and 380-390 nm excitation (F2) are used to calculate $[Ca^{2+}]_i$.

$$[Ca^{2+}]_i = Keff(R-Rmin)/(Rmax-R)$$

$$R = F1/F2$$

$$Rmin = F1/F2 \text{ measured at zero } Ca^{2+}$$

$$Rmax = F1/F2 \text{ measured at high } Ca^{2+}$$

$$Keff = \text{Effective binding constant}$$

$$= F2 \text{ (at zero } Ca^{2+})/F2 \text{ (at high } Ca^{2+})$$

The advantages of using dual wavelength for calculation of intracellular calcium concentration are that the effect of uneven dye loading, dye leaking or photo bleaching are reduced considerably.

In this experiment, the two wavelengths used were 355 and 390 nm. A monochromator-based illumination system (T.I.L.L. Photonics, Germany) coupling to a 63X water-immersion objective of an inverted microscope (Zeiss Axiovert 100, Germany) was used for the excitation. A 425-nm dichroic mirror was positioned in the light pathway to reflect the excitation light and transmit the emission light. The illumination area was restricted to a square of 40x40 μm. The excitation was alternated between 355 and 390 nm wavelength for 50-ms duration at each wavelength. The fluorescent emission transmitted through a 450-nm LP was

detected with a photomultiplier system (T.I.L.L. Photonics, Germany). The data was acquired with Fura-extension of Pulse software and EPC-9 amplifier.

Keff, Rmin and Rmax were obtained from *in vivo* calibration (Figure 2-8). Bovine adrenal chromaffin cells were dialysed with zero Ca^{2+} solution (10 mM EGTA), high Ca^{2+} solution (10 mM $CaCl_2$) or 300-nM Ca^{2+}solution (3.3 mM EGTA plus 6.6 mM Ca-EGTA) containing 0.1 mM fura-2 in whole-cell patch clamp experiment.

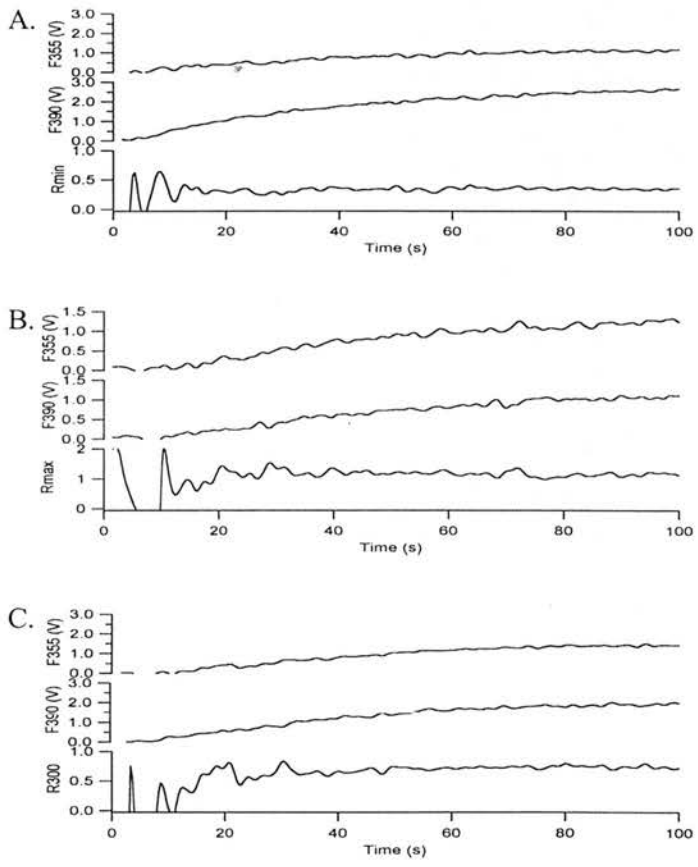

Figure 2-8 Fura-2 calibration

Examples of fura-2 fluorescence at 355 nm (F355), 390 nm (F390) excitation wavelengths recorded at zero Ca^{2+}(A), 10 mM Ca^{2+} (B) and 300 nM Ca^{2+} (C). The ratios of the two wavelengths are displayed at the lower panel of each recording.

Rmin, Rmax from the calibration were 0.364 and 1.102, respectively. Dialysis with a solution of known Ca^{2+} concentration (300 nM) yielded a fluorescence ratio (R300) of 0.749. The calculated Keff was 273 nM. Therefore, the equation used for calculation of $[Ca^{2+}]_i$ was:

$$[Ca^{2+}]_i = 273 \times (R-0.364)/(1.102-R) \quad nM$$

An example of intracellular calcium measurement is shown in Figure 2-9.

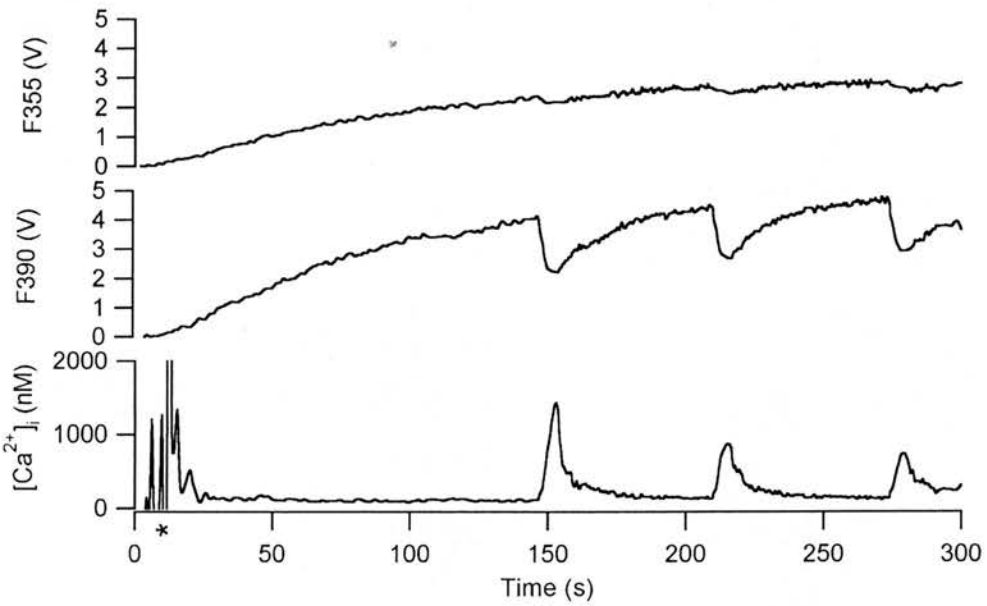

Figure 2-9 Intracellular calcium measurement

An example of $[Ca^{2+}]_i$ measured during a whole-cell patch clamp experiment. The fura-2 intensity at 355 and 390 nm excitation wavelengths are displayed in the *above* and *middle* panel, respectively. The fluorescence at 390 nm excitation wavelength decreased during the stimulation while the fluorescence at 355 nm excitation wavelength did not change significantly. The $[Ca^{2+}]_i$ calculated from the fluorescence ratio using the above equation is shown in the lower panel. The whole-cell was established as indicated by asterisk (*). Each peak of $[Ca^{2+}]_i$ corresponded to an application of a train of six depolarisation.

2.2.15 Imaging

Cells were washed once with PBS then fixed in 4% paraformaldehyde for 15 minutes. The cells were washed twice with PBS and mounted on microscopic slides with 95% glycerol in PBS. The slides were imaged with laser scanning confocal microscope (LSM510, Ziess, Germany) using a 40X oil immersion objective.

2.2.16 Analysis

2.2.16.1 Data Analysis

The data acquired with EPC-9 and Pulse software was exported to IGOR (WaveMetrics, Lake Oswego, OR, US.). The data was analysed offline with macros written on IGOR procedures.

2.2.16.2 Statistical Analysis

The data was analysed and displayed as Mean±SEM. The unpaired student's t test was used to compare the groups of data. A P-value of less than 0.05 was considered significant.

Chapter 3

Protein expression using DNA-based Semliki Forest Virus (SFV) vectors

3.1 Introduction

Several candidate proteins in exocytosis have been identified in the past decade. However, the functions of most proteins remain unclear. One factor that hampers the study of these proteins is the lack of an efficient method for transient expression of the proteins in eukaryotic cells especially in primary cell cultures such as neurons and adrenal chromaffin cells which are widely used to study exocytosis. The functions of these proteins have been mainly studied by using transgenic animals, introduction of externally synthesised proteins or low efficiency transfection methods. However, concerns have been raised regarding the development and the viability of the transgenic animals. Introduction of proteins into cells by dialysis through patch pipettes or cell permeabilisation causes the loss of some important cellular factors at the same time. The proteins or peptides synthesised *in vitro* or in other cells might not be subject to an accurate post-translational modification that normally occurs in eukaryotic cells. Transfection using chemical or physical methods yields a very low efficiency. Because of such low efficiency, the release of the co-expressed marker is assayed instead of the native secretory products themselves (Wick, Senter et al. 1993). Secretion of newly synthesised marker might not faithfully report the secretion of the native secretory products. The use of viral vector has proved to be the most efficient method for heterologous gene expression in eukaryotic cells. The ideal viral vector must have a high efficiency of infection and expression, be able to infect a wide range of host cells, have low cytotoxicity, be easy to prepare and not present a safety harzard to the user.

Semliki forest virus (SFV) is an RNA virus in the alphavirus family. It is a known pathogen in rodents. SFV has the ability to infect a wide range of host cells from arthropods to mammalian cells. The single-stranded RNA genome of positive polarity shares a common cap and polyadenylation with eukaryotic mRNAs. The 5'-end of the RNA genome contains genes encoding four nonstructural proteins (nsP1-nsP4). The 3'end contains genes encoding structural proteins, the capsid and envelope proteins. Upon entering host cell cytoplasm, the viral RNA starts the translation of nonstructural proteins by using the host's translation machinery. The nonstructural proteins form an RNA replicase complex responsible for the replication of the full-length viral genome (42S). Besides the 42s RNAs, smaller 26S RNAs encoding the structural genes are synthesised by using a subgenomic promoter at the 3'-end of nsP4. The capsid and envelope proteins are translated from the 26s RNAs. The envelope proteins are transported to the plasma membrane via the trans-Golgi network. The viral RNAs and capsid proteins form the nucleocapsids in the cytoplasm. The viral particles then bud from the host cells taking host cell plasma membrane as envelopes (review in Kaariainen and Soderlund 1978; Lundstrom, Schweitzer et al. 1999).

The Semliki Forest Virus (SFV) transduction system is a highly efficient method of gene expression (Ashery, Betz et al. 1999; Knight 1999; Duncan, Don-Wauchope et al. 1999b). The SFV vectors are derived from an attenuated strain of the virus. The viral genome is split between two plasmids, the cloning vector and the helper vector (Figure 3-1). The cloning vector contains the genes encoding nonstructural proteins followed by the multiple cloning sites (MCS). Transcription of the inserted genes is

driven by the subgenomic promoter at the 3'-end of nsP4. The helper vector contains genes encoding structural proteins.

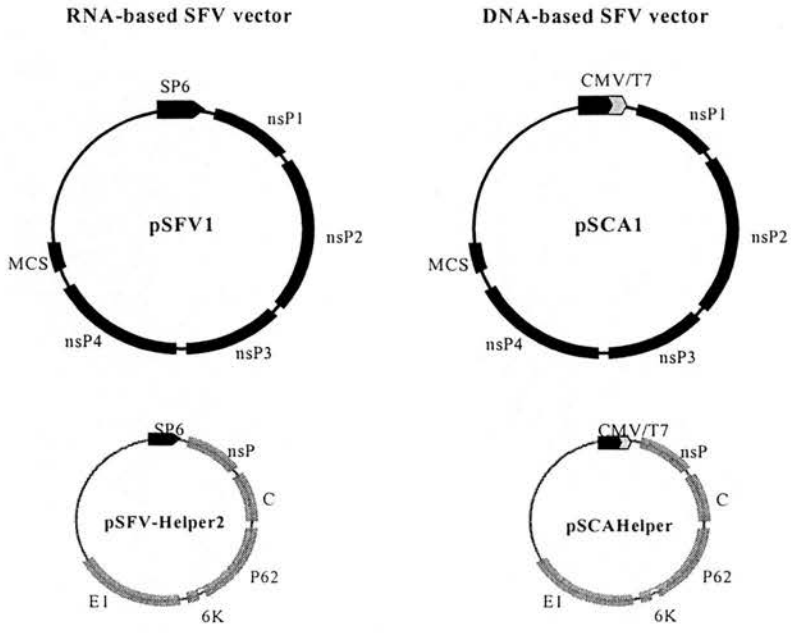

Figure 3-1 RNA and DNA-based SFV vectors

(DiCiommo and Bremner 1998)

The diagram of the SFV and SFV-helper plasmids in RNA and DNA-based systems. The SFV cloning vectors contain genes encoding nonstructural proteins (nsP1-4) which function as RNA-replicase complex. The helper plasmids contain genes encoding structural proteins including capsid protein (C) and envelope proteins important for viral infection (E1, P62). The SP6 promoters in RNA-based system are replaced with CMV/T7 promoters in DNA-based system. (MCS=multiple cloning sites)

Separation of the structural and nonstructural genes ensures that the virus is produced only when both plasmids are present in the same cell. The second level of safety measure is achieved by mutation of an envelope protein, P62 (Berglund, Sjoberg et al. 1993; Tubulekas and Liljestrom 1998). P62 forms a dimer with another envelope protein, E1. In the normal life cycle, P62 is cleaved into E2 and E3 in the Golgi complex. The E1-E2 complex is important for host cell-binding and membrane fusion during viral infection. In the absence of P62 cleavage, the virus is non-infectious (Liljestrom and Garoff 1991; review in Lundstrom, Schweitzer et al. 1999). However, the function of the E1-E2 complex can be restored by treatment with α-chymotrypsin.

The original SFV transduction system is RNA-based which needs an *in vitro* transcription prior to the transfection of eukaryotic cells (Figure 3-2). The DNA-based SFV transduction system simplifies the transfection processes by eliminating the *in vitro* transcription step (DiCiommo and Bremner 1998).

The aim of experiments was to study if the SFV transduction system would be useful for gene expression in bovine adrenal chromaffin cells. The efficiency of the SFV expression and the effects of viral infection on normal cell function were studied. To be able to use the SFV transduction system as a method for gene expression in the future, an efficient and easy method of viral preparation was also determined in these experiments.

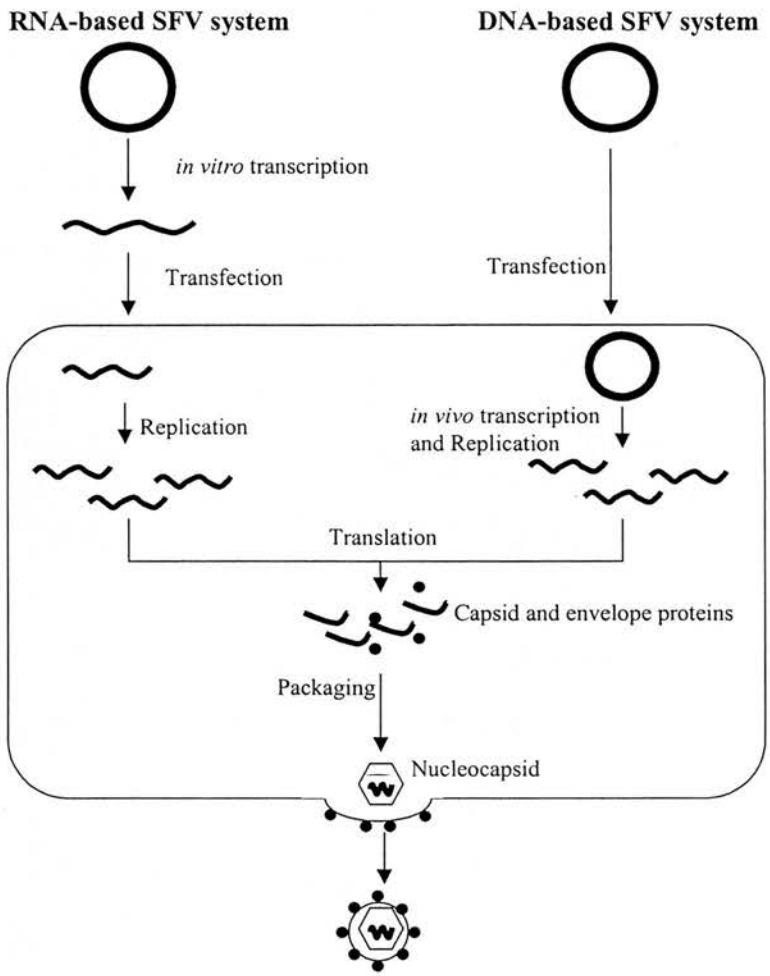

Figure 3-2 Viral packaging in RNA- and DNA-based SFV transduction system

Diagram demonstrates the processes to obtain SFV particles. The DNA-based system has an advantage over the original system that it does not need an *in vitro* transcription. The replicon and the helper plasmids are introduced into host cells. The viral nonstructural protein complex function as an RNA-replicase increasing the number of RNA copies. The viral proteins are translated using the host cell's translation machinery. The viral RNA and capsid proteins are packaged into viral nucleocapsids. The envelope proteins are transported to the plasma membrane via the ER-TGN-plasma membrane route. The viral particles bud from the plasma membrane taking host cell plasma membrane as viral envelopes.

3.2 Results

DNA-based SFV replicons were constructed using standard cloning strategies. The enhanced green fluorescent protein (EGFP) was used as a reporter for gene expression. For bicistronic replicons, the internal ribosomal entry site (IRES) inserted between the first and second genes provided the translation of the second gene independent of the 5'cap (Mountford, Zevnik et al. 1994; Havenga, Vogels et al. 1998). Four SFV replicons were constructed (Figure 3-3): a bicistronic replicon containing EGFP (EGFP), a bicistronic replicon containing Doc2β and EGFP (Doc2β-IRES-EGFP), a full-length Doc2β fusion with EGFP (Doc2β-EGFP) and Doc2β C2 domains fusion with EGFP (C2AB-EGFP). The EGFP was fused to the C-terminal of Doc2β and Doc2β C2 domains in the fusion constructs.

The authenticity of the replicons was verified by restriction mapping and DNA sequencing. The DNA sequences were compared with the data from GenBank. Doc2β from both the bicistronic construct (Doc2β-IRES-EGFP) and the fusion construct (Doc2β-EGFP) contained an open reading frame encoding the full-length Doc2β (Figure 3-3 and 3-4). The Doc2β C2 domains (C2AB) from the EGFP-fusion construct was a 990-bp sequence from the 3'-end of Doc2β encoding both Doc2β C2 domains.

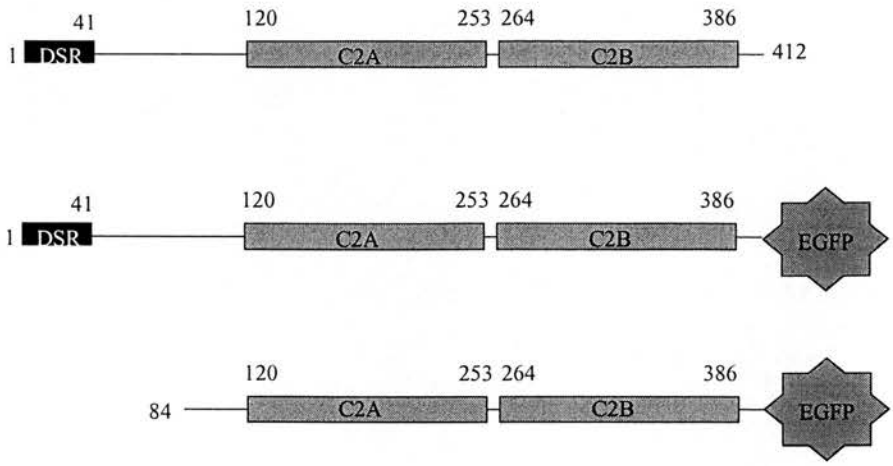

Figure 3-3 Domain structures of Doc2β and Doc2β C2-domain translation products from the DNA-based SFV replicons

Full-length Doc2β from the bicistronic construct is displayed above. The C-terminal EGFP fusion Doc2β and Doc2β C2 domains from the fusion constructs are displayed in the middle and lower panels, respectively. Doc2β contains the N-terminal Doc2-specific region (DSR) which is unique among isoforms of Doc2.

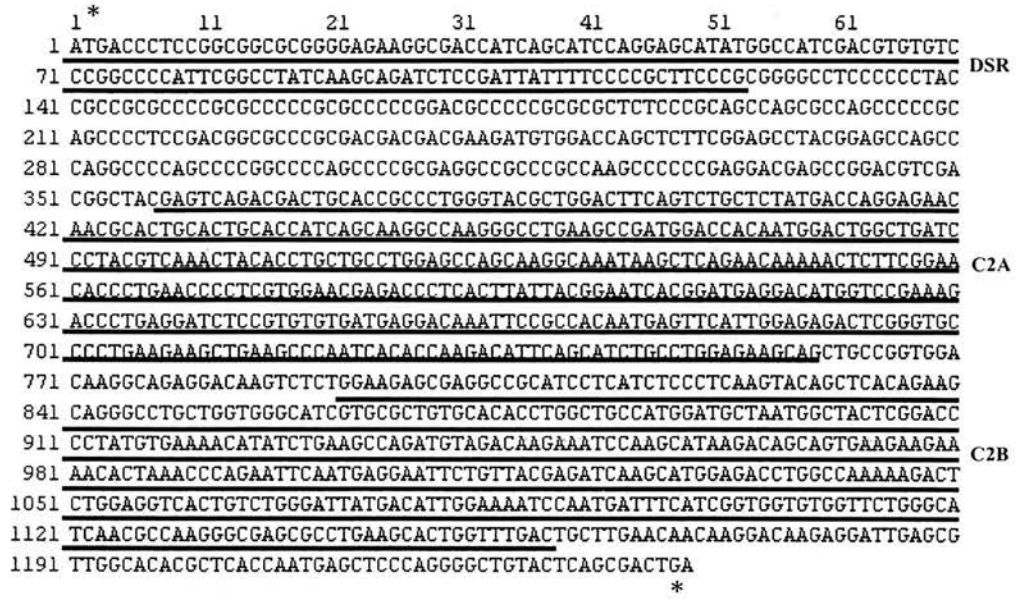

Figure 3-4 Doc2β sequence

The sequence of Doc2β has an open reading frame of 1239 base pairs. The start and stop codons are indicated (*). Underlines indicate Doc2-specific region (DSR), first (C2A) and second (C2B) C2 domains, respectively.

3.2.1 High viral titer was achieved by using calcium-phosphate transfection of HEK293T for viral packaging

The methods for SFV packaging commercially recommended or used by most laboratories are electroporation or cationic-lipid reagents. Both methods are expensive. The electroporation method also needs special equipment. Calcium phosphate transfection is a cheap and efficient method of gene transfer in many cell types. The SFV replicons and the helper vectors were delivered into HEK293T cells for viral packaging by a calcium phosphate transfection procedure. Incubation with sodium butyrate after transfection inhibited cell proliferation and enhanced viral protein expression (Iacomino, Tecce et al. 2001). The whole process took 48 hours after calcium phosphate transfection until the viral particles could be collected from the culture medium. A viral titer as high as 3-5 x 10^8 particles/ml was achieved. The titer was similar to that obtained by using the RNA-based SFV system (Pan, Jeromin et al. 2002). These viral particles were kept at –20°C without deterioration for months.

3.2.2 Efficiency of SFV transduction system in primary cultured bovine adrenal chromaffin cells

The viral particles produced were incapable of infection due to the mutation of the viral envelope protein. Reversion of this mutation was reported in previous studies (Berglund, Sjoberg et al. 1993; Tubulekas and Liljestrom 1998). The rate of reversion of the mutation in this experiment was less than 10^{-7} as no fluorescent cell was observed when HEK293T cells were infected with 10^7 viral particle containing the EGFP gene without α-chymotrypsin treatment. Treatment of the viral particles with α-chymotrypsin rendered the viral particles infectious.

Infection of primary cultures of bovine adrenal chromaffin cells with 50 multiplicity of infection (MOI) yielded more than 80% infected cells (Figure 3-5A). The fluorescence-expressing cells were detected as early as 6 hours after infection. The level of fluorescence expression varied among infected cells indicating differences in protein expression level. The protein expression detected by SDS-PAGE was consistent with the fluorescence expression (Figure 3-5B). Low level of protein expression was detected at 9 hours after infection. The level of the proteins was then increased during the course of the experiments. The expression of the larger proteins was slower than the expression of the small proteins. Low level of Doc2β-EGFP and C2AB-EGFP were detected at 12 hours after infection. Therefore, the experiments could be performed early after infection.

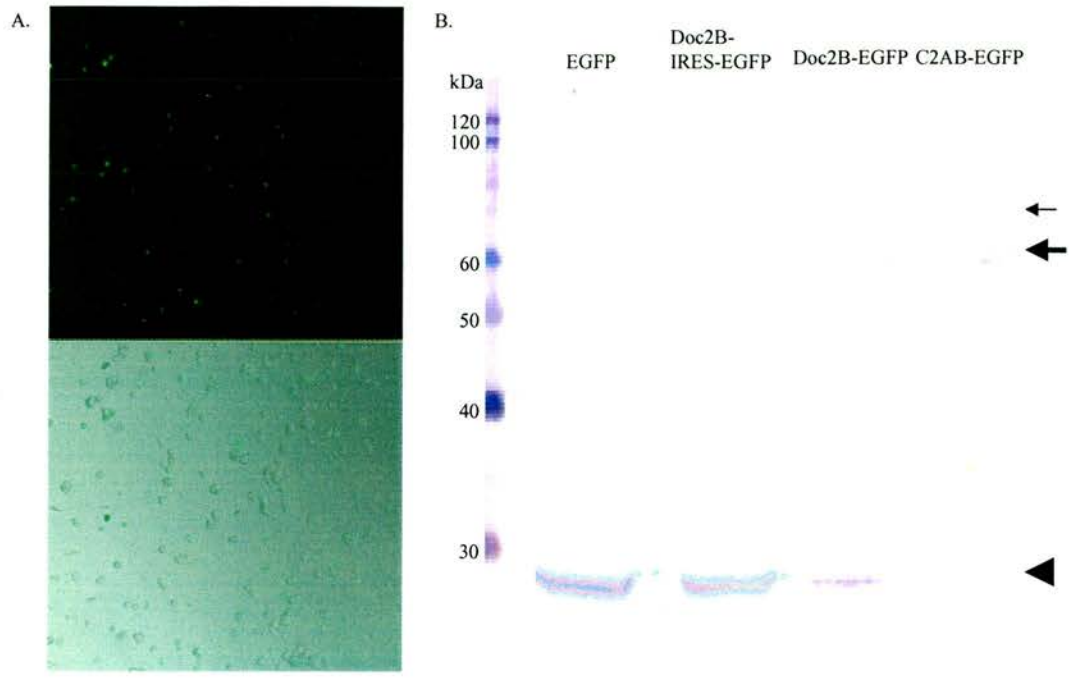

Figure 3-5 High efficiency expression by SFV system

Fluorescence microscopy and SDS-PAGE demonstrates protein expression in bovine adrenal chromaffin cells infected with 50 MOI of SFV particles.

A. Fluorescent microscopic images were taken from bovine adrenal chromaffin cells at 24 hours after infection with SFV containing the EGFP gene. The superimposed fluorescent and light microscopic image indicated that more than 80% of cells were infected (*below*).

B. SDS-PAGE from bovine adrenal chromaffin cells at 24 hours after infection with the indicated viral constructs. The proteins blotted on the nitrocellulose membrane were decorated with an antibody to EGFP (A.V peptide antibody, Clontech) and detected with alkaline phosphatase (AP)-conjugated secondary antibody. The purple colour was visualised after the AP-substrate reaction. The viral constructs used are indicated at the top and the molecular weight markers are indicated on the left. The *arrowhead*, *thin arrow* and *thick arrow* indicate the EGFP (27 kDa), Doc2-EGFP (73 kDa) and C2AB-EGFP (64 kDa), respectively. Doc2β-IRES-EGFP which expressed Doc2β and EGFP separately was detected at 27 kDa similar to EGFP. Both Doc2β-EGFP and C2AB-EGFP expressed the

proteins at the expected molecular weights. The level of protein expression was dependent on the size of the proteins. EGFP expressed at the highest level while the Doc2β fusion with EGFP expressed at the lowest level. Note that EGFP was also produced from Doc2β-EGFP and C2AB-EGFP by using the Kozak and initiation site at the beginning of the EGFP gene.

3.2.3 Subcellular distribution of proteins expressed by SFV expression system

Subcellular distribution of EGFP and Doc2β-EGFP expressed by the SFV transduction system was studied in bovine adrenal chromaffin, HEK293T and PC12 cells. EGFP was evenly distributed throughout the cytoplasm in adrenal chromaffin and HEK293T cells (Figure 3-6). Higher nuclear fluorescence was observed in most cells. This characteristic of EGFP distribution was similar to the distribution of GFP expressed by using SFV expression systems in bovine adrenal chromaffin cells reported previously (Ashery, Betz et al. 1999; Knight 1999). However, the distribution of EGFP in PC12 cells was different from the distribution in chromaffin and HEK293T cells. In PC12 cells, the fluorescence distribution was cytoplasmic with nuclear-sparing pattern. This difference was not a result of different expression levels because the pattern of distribution did not change when the cells were infected with lower multiplicity of infection or when the cells were imaged early after infection.

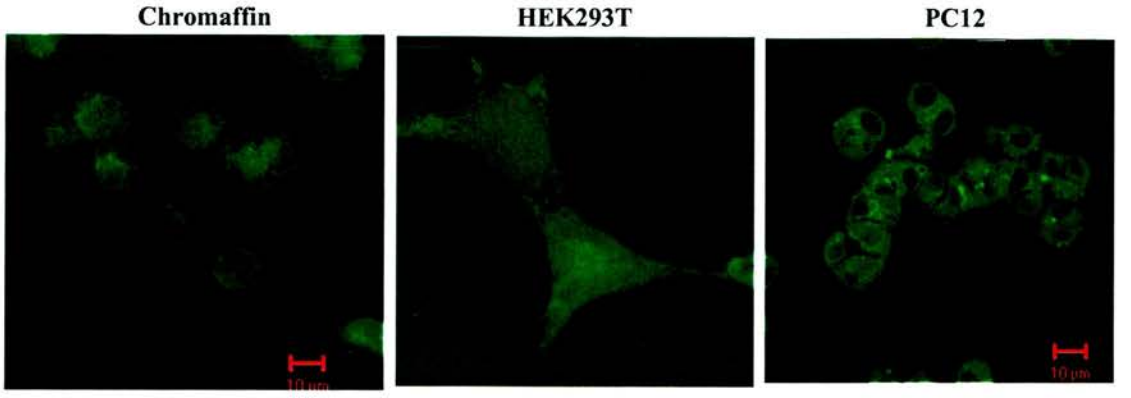

Figure 3-6 Subcellular distribution of EGFP

Bovine adrenal chromaffin, HEK293T and PC12 cells were infected with 50 MOI of SFV containing the EGFP gene. The cells were fixed with 4% paraformaldehyde at 24 hours after infection. EGFP was evenly distributed with high nuclear fluorescence in adrenal chromaffin and HEK293T while it was mainly cytoplasmic in PC12 cells.

The distribution of Doc2β-EGFP in PC12 cells was intracytoplasmic with a nuclear-sparing pattern similar to the result from previous study where the DEAE-dextran method was used to express mouse Doc2β in PC12 cells (Fukuda, Saegusa et al. 2001). When expressed in bovine adrenal chromaffin and HEK293T cells, Doc2β-EGFP showed both intracytoplasmic and nuclear distribution (Figure 3-7). Although the fluorescence distribution of Doc2β-EGFP was similar to that of EGFP alone, the expression of the Doc2β-EGFP in these cells was confirmed by SDS-PAGE. However, the cells infected with SFV containing Doc2β-EGFP expressed both Doc2β-EGFP and EGFP. This might explain the similarity of the fluorescence distribution between cells infected with SFV containing Doc2β-EGFP and SFV containing EGFP alone. The punctate cytoplasmic fluorescence was observed in

some chromaffin, HEK293T and PC12 cells as previously reported (Duncan, Betz et al. 1999a).

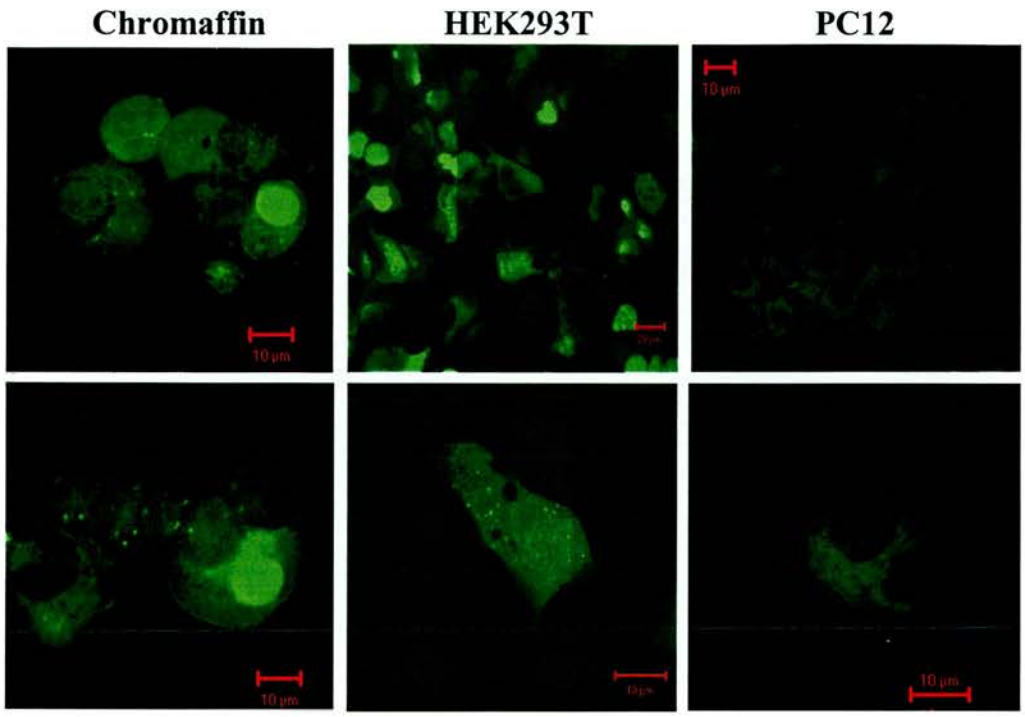

Figure 3-7 subcellular distribution of Doc2β-EGFP

The confocal images of bovine adrenal chromaffin, HEK293T and PC12 cells were taken at 24 hours after infection with 50 MOI of SFV containing Doc2β-EGFP. The fluorescence was mainly cytoplasmic in PC12 cells. In chromaffin and HEK293T cells, the fluorescence was distributed in both cytoplasm and nucleus. Lower panels show the punctate fluorescence distribution in chromaffin, HEK293T and PC12 cells.

The fluorescence distribution in bovine adrenal chromaffin cells infected with SFV containing C2AB-EGFP and Doc2β-IRES-EGFP was not different from that of cells infected with SFV containing Doc2β-EGFP and EGFP, respectively. The fluorescence was distributed throughout the cells (Figure 3-8). Nuclear fluorescence was always observed. Punctate fluorescence distribution was identified in some C2AB-EGFP expressing cells.

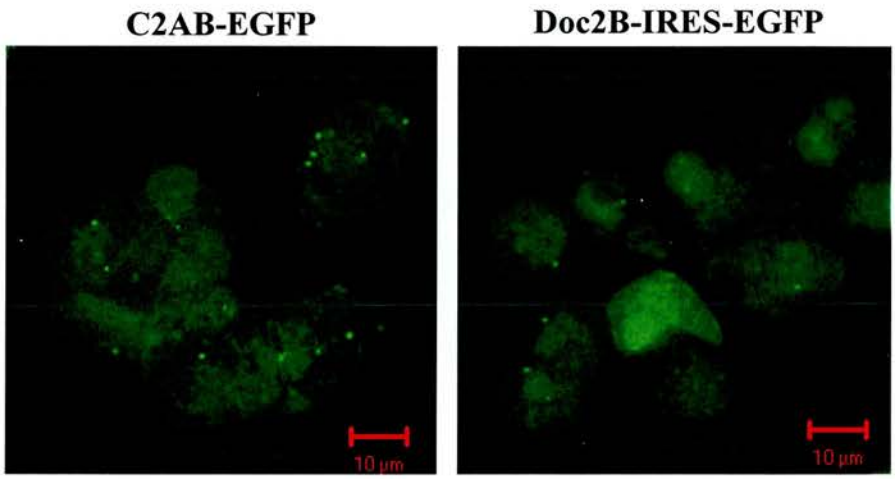

Figure 3-8 Distribution of C2AB-EGFP and EGFP from the bicistronic construct containing Doc2β and EGFP

Fluorescence distribution in bovine adrenal chromaffin cells expressing C2AB-EGFP and cells expressing Doc2β and EGFP from a bicistronic construct. The infected cells showed cytoplasmic and nuclear fluorescence. Some cytoplasmic punctate fluorescence was also observed in chromaffin cells expressing C2AB-EGFP (*left*).

3.2.4 No obvious cytotoxic effect was observed in SFV-infected cells

Among all methods for heterologous gene transfer in eukaryotic cells, viral vectors are the most efficient method. However, several viral vectors suffer from concerns regarding cellular cytotoxicity. SFV vector was proved to be an efficient method. The late onset of cytopathogenicity is one advantage of the SFV vector (Liljestrom and Garoff 1991; Glasgow, McGee et al. 1998; Ashery, Betz et al. 1999; Duncan, Don-Wauchope et al. 1999b). To verify that the SFV vectors would be a useful method for gene expression in bovine adrenal chromaffin cells, the effect of SFV infection was studied by comparing chromaffin cells infected with SFV virus containing the EGFP gene with non-infected cells. The EGFP and other members of green fluorescent protein have been used as markers for gene expression in a variety of preparations. Several studies showed no effect of EGFP on protein localisation and function (review in Zimmer 2002).

The cell morphology was not affected by viral infection, indicating that there was no obvious cytotoxic effect of viral infection during the course of the experiments. The initial membrane capacitance was measured after whole-cell establishment in patch clamp experiments. The distribution of the initial membrane capacitance from non-infected cells indicated that the chromaffin cells being studied came from a single population of cells (Figure 3-9). The size of the infected cells (7.4±0.2 pF, n=69) was not significantly different from the size of non-infected cells (7.7±0.1 pF, n=175) as shown in figure 3-10.

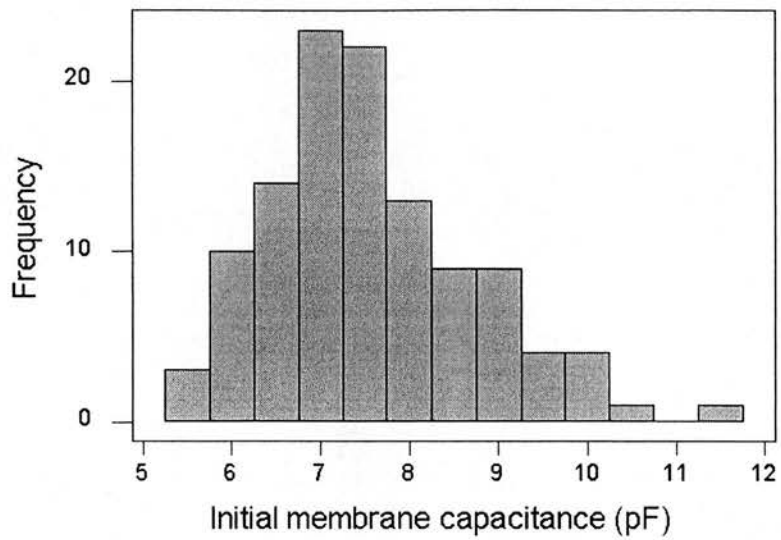

Figure 3-9 The distribution of initial membrane capacitance in non-infected cells

Membrane capacitance was measured in whole-cell patch clamp experiments. The initial membrane capacitance after whole-cell establishment indicated the cell size. The initial membrane capacitance from non-infected cells (n=175) shows a single peak normal distribution.

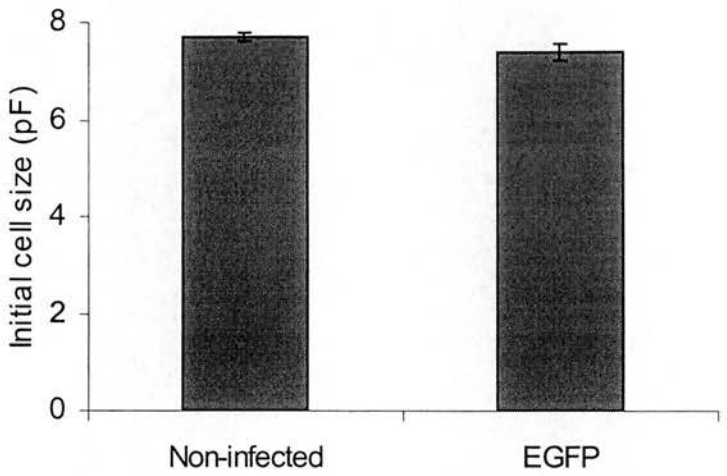

Figure 3-10 Histogram summarises the effect of SFV infection on initial cell size

The histogram displays the mean±s.e.m. of basal membrane capacitance from SFV-infected and non-infected cells. There was no statistical difference in the cell size between SFV-infected and non-infected cells.

The leak current during the whole-cell patch clamp experiments was used as an indicator for tight seal formation. The leak currents in SFV-infected cells (-24±1.9 pA, n=69) was not different from that of non-infected cells (-26±1.6, n=175) (Figure 3-11). Therefore, the SFV-infected cells can be used in patch clamp experiments.

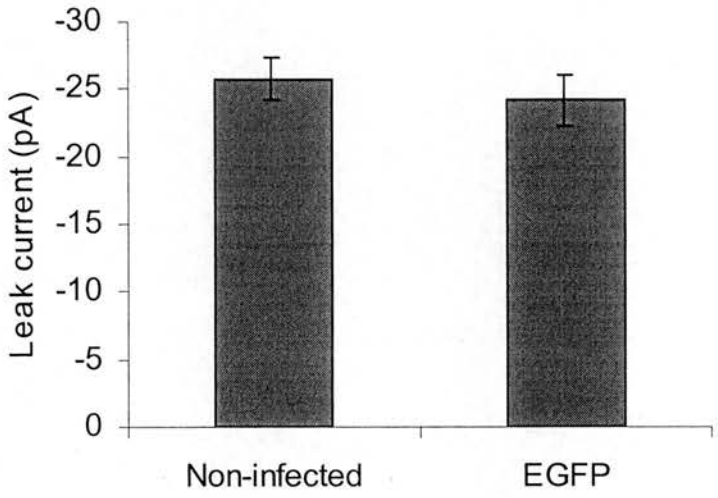

Figure 3-11 Histogram summarises the effect of SFV infection on the leak currents

The leak current was measured during the whole-cell patch clamp experiments. There was no statistical difference of leak currents between the SFV-infected and non-infected cells.

3.2.5 Basal intracellular Ca^{2+} concentration ($[Ca^{2+}]_i$) was increased in viral infected cells

Intracellular Ca^{2+}concentration ($[Ca^{2+}]_i$) is an important factor in regulated exocytosis. The amount of exocytosis depends on previous exposure to Ca^{2+} (von Ruden and Neher 1993). To study if the basal $[Ca^{2+}]_i$ was affected by SFV infection during the course of the experiment, the basal $[Ca^{2+}]_i$ was measured by using ratiometric fluorimetry. The average $[Ca^{2+}]_i$ in SFV-infected cells (233±25 nM, n=16) was significantly higher than that of non-infected cells (136±10 nM, n=76) as shown in figure 3-12. This result was different from a previous study where SFV infection did not affect basal $[Ca^{2+}]_i$ (Ashery, Betz et al. 1999). However, the level of $[Ca^{2+}]_i$ was well below the threshold for secretion predicted in bovine adrenal chromaffin cells (Heinemann, von Ruden et al. 1993). In experiments where the caged-Ca^{2+} compounds are used, the level of pre-stimulus $[Ca^{2+}]_i$ is as high as the level of basal $[Ca^{2+}]_i$ in the SFV-infected cells used in this experiment (Gillis, Mossner et al. 1996; Xu, Binz et al. 1998; Xu, Rammner et al. 1999).

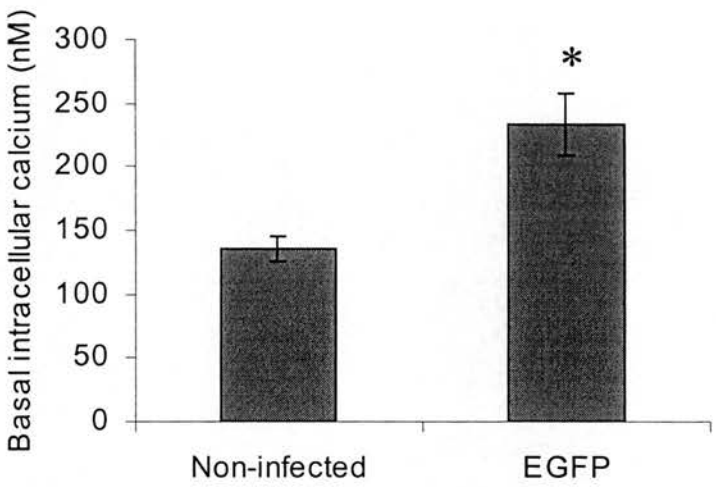

Figure 3-12 Histogram summarises the effect of SFV infection on basal $[Ca^{2+}]_i$

Intracellular calcium concentration ($[Ca^{2+}]_i$) was measured by using the Ca^{2+}-sensitive dye fura-2 in whole-cell patch clamp experiments. The cells with leak currents more than 25 pA were excluded from the analysis. The basal $[Ca^{2+}]_i$ in SFV-infected was higher than that of non-infected cells. Asterisk (*) indicates $p<0.05$ by student's t test.

3.2.6 SFV infection affected calcium currents in bovine adrenal chromaffin cells

Ca^{2+} influx through calcium channels is a physiological stimulus for secretion in adrenal chromaffin cells. To verify if SFV infection affected calcium currents, depolarisation-induced calcium currents were studied in whole-cell patch clamp experiments. The calcium currents in response to 50-ms depolarisation in non-infected cells showed a normal distribution with a single peak (Figure 3-13). This uniform distribution of calcium currents supports the idea that the chromaffin cells being studied came from a single population of cells.

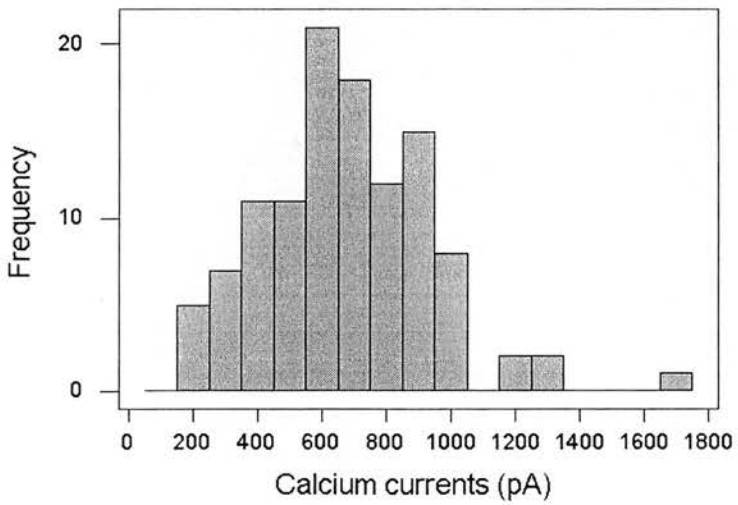

Figure 3-13 Distribution of calcium currents in non-infected cells

Bovine adrenal chromaffin cell was voltage clamped at a holding potential of –70 mV in the whole-cell configuration. A 50-ms depolarisation to 10 mV was applied. The distribution of calcium currents in response to the depolarisations was plotted. The single peak normal distribution was obtained.

SFV infection affected the calcium currents (Figure 3-14). The average calcium current in SFV-infected cells (322±28 pA, n=35) was only 50% of that of non-infected cells (674±24 pA, n=113). This effect was also reported in the previous studies (Ashery, Betz et al. 1999; Pan, Jeromin et al. 2002).

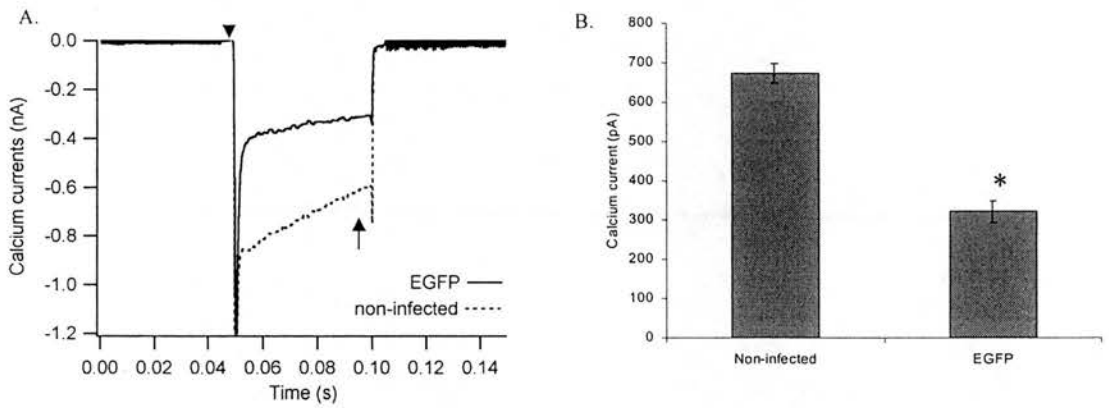

Figure 3-14 Effect of SFV infection on calcium currents

(A) Calcium currents in response to 50-ms depolarisations from SFV-infected and non-infected cells are superimposed. The magnitude of the calcium current was measured as a difference between the pre-depolarisation baseline (*arrowhead*) and the current at the end of the depolarisation prior to the capacitive transient (*arrow*). (B) The histogram shows the average calcium currents (mean±s.e.m). The calcium currents in SFV-infected cells were significantly smaller than that of non-infected cells (* indicates $p<0.05$).

The effect of SFV infection on calcium currents was observed throughout the course of the experiments. The calcium currents between 15-24 hours (330±43 pA, n=14) and between 24-30 hours (314±35 pA, n=21) post-infection was not different (Figure 3-15A). However, the calcium currents recorded at about 72 hours (163±21, n=5) post-infection were further reduced by 50% from the currents recorded between 15-24 hours post-infection (Figure 3-15B).

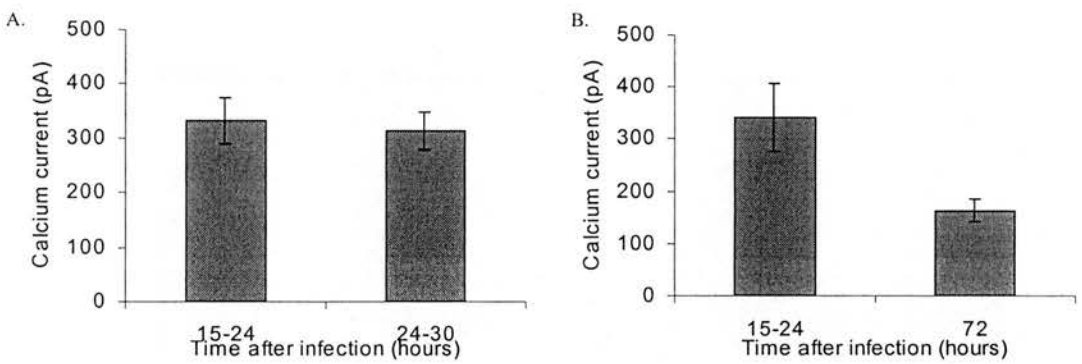

Figure 3-15 The rundown of calcium currents after SFV infection

Bovine adrenal chromaffin cells were infected with SFV containing the EGFP gene. The calcium currents were recorded as previously discussed. (A). The calcium currents were not different within 30 hours post-infection. (B). The calcium currents recorded at 72 hours post-infection were smaller than the calcium currents recorded at 24 hours post-infection.

3.2.7 Sodium current was reduced by SFV infection

The effect of SFV infection on ionic currents was not specific only to calcium currents. The sodium current in SFV-infected cells (1.38±0.1 nA, n=35) was also significantly smaller than that of non-infected cells (1.81±0.06 nA, n=114) (Figure 3-16).

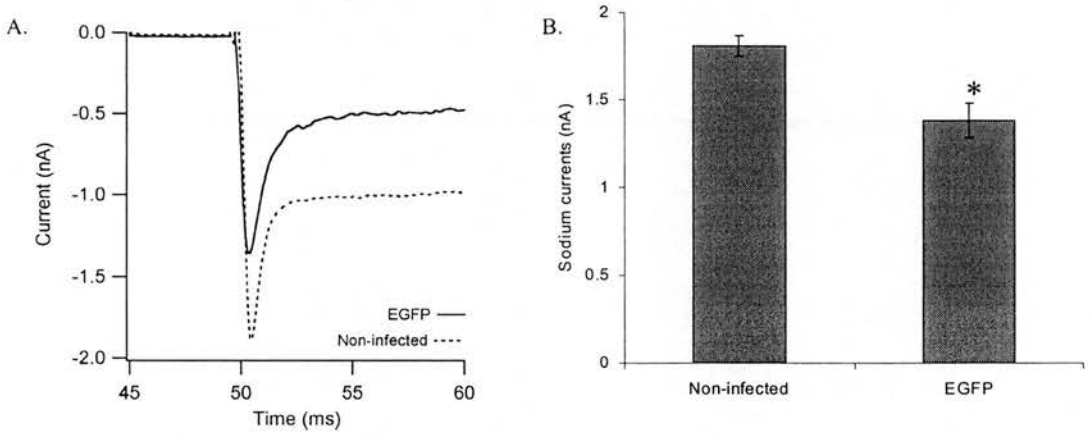

Figure 3-16 Effect of SFV infection on sodium currents

Sodium current was measured from the peak of the inward current within a few milliseconds after depolarisation. The initial inward current was mainly contributed by sodium current because of the slower activation kinetics of calcium channels. (A) Superimposed sodium currents from SFV-infected and non-infected cells. (B) Histogram summarises the effect of SFV infection on sodium currents. Asterisk (*) indicates $P<0.05$.

The mechanism for the increase of basal $[Ca^{2+}]_i$, the reduction of calcium and sodium currents are not well understood. The further reduction of the calcium currents at 72 hours post-infection indicated that these effects could be the result of the viral cytotoxicity, the viral protein expression or the expression of EGFP. SFV-induced apoptosis was reported in BHK21 cells (Glasgow, McGee et al. 1998). Ca^{2+} is an important messenger for the apoptosis. During apoptosis, the $[Ca^{2+}]_i$ increases. The effect of intracellular Ca^{2+} on calcium and sodium channels has been reported (Brehm and Eckert 1978; Gera and Byerly 1999; Pan, Jeromin et al. 2002). Ca^{2+} induces inactivation of calcium and sodium channels. Sustained elevation of $[Ca^{2+}]_i$ also reduces the number of sodium channels (Kobayashi, Shiraishi et al. 2002). The reduction of calcium and sodium currents could be the result of the increase of basal $[Ca^{2+}]_i$ in SFV-infected cells. To verify the correlation between $[Ca^{2+}]_i$ and the calcium and sodium currents, the calcium and sodium currents were taken from the selected group of non-infected cells which had basal $[Ca^{2+}]_i$ similar to that of SFV-infected cells. The calcium and sodium currents from this selected group of non-infected cells were not significantly different from that of SFV-infected cells (Figure 3-17). This result indicated that the $[Ca^{2+}]_i$ is an important factor that alters other cellular properties.

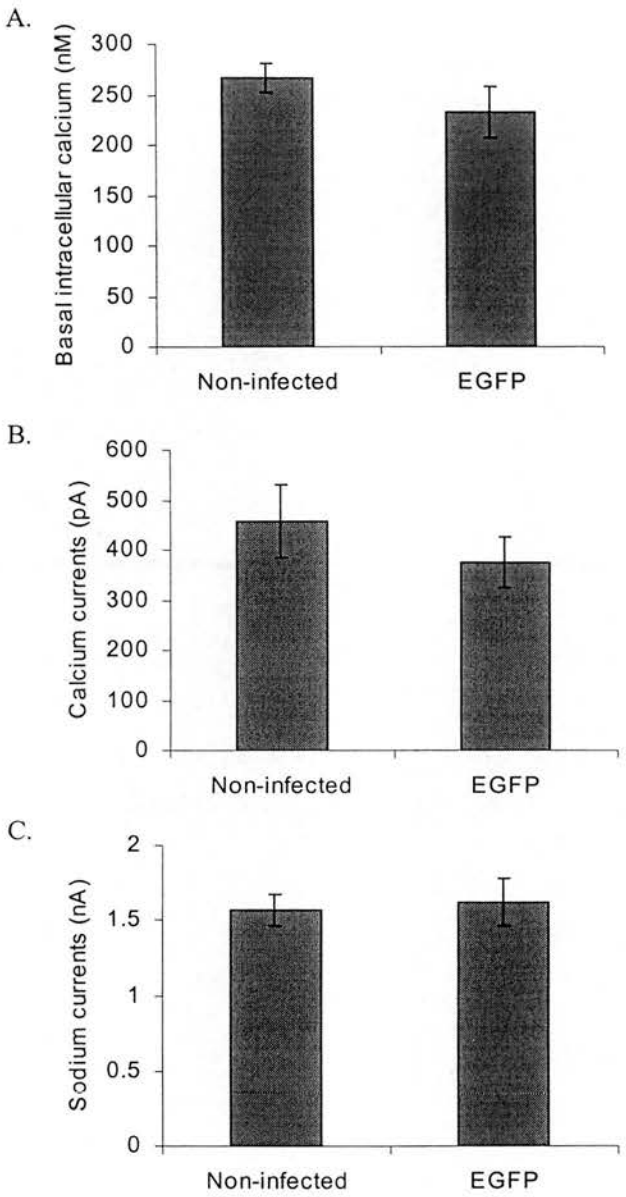

Figure 3-17 Effect of $[Ca^{2+}]_i$ on calcium and sodium currents

The average $[Ca^{2+}]_i$ from a selected population of non-infected cells (n=17) with high basal $[Ca^{2+}]_i$ was not different from that of SFV-infected cells (A). The calcium (B) and sodium (C) currents in this group were not significantly different from that of SFV-infected cells (n=16).

3.2.8 The catecholamine content was not affected by SFV infection

To verify if the SFV infection affected the synthesis and metabolism of catecholamines in bovine adrenal chromaffin cells, the total cellular catecholamine content was compared between SFV-infected and non-infected cells. The total catecholamine content of SFV-infected cells (0.16±0.004 pMol/cell, n=12) was not significantly different from that of non-infected cells (0.16±0.01 pMol/cell, n=8).

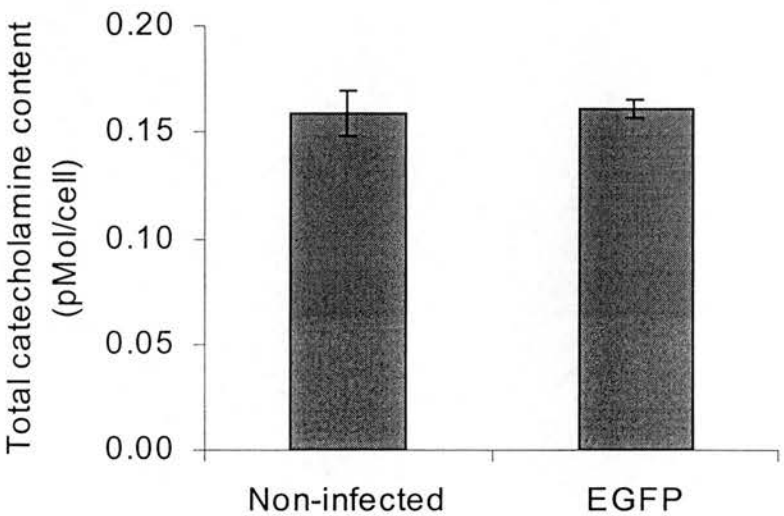

Figure 3-18 Total catecholamine content in SFV-infected and non-infected bovine adrenal chromaffin cells

Bovine adrenal chromaffin cells ($3x10^5$ cells/sample) were lysed with a detergent solution (1% NP40). The catecholamine in the cell lysate was assayed with a spectrofluorimetric method. The histogram shows the catecholamine content per cells (pMol/cell). There was no difference in the catecholamine content of SFV-infected and non-infected cells.

3.2.9 SFV infection did not affect catecholamine secretion

Catecholamine secretion in bovine adrenal chromaffin was assayed by several methods both at the single cell and cell-population level. The aim was to verify if the SFV transduction system could be used as a mean to deliver genes for study of exocytotic in bovine adrenal chromaffin cells.

3.2.9.1 Effect of SFV infection on catecholamine secretion in cell-populations

3.2.9.1.1 High-K^+ stimulation

High-K^+ stimulation was used to study catecholamine secretion in the bovine adrenal chromaffin cell population. High-K^+ induces membrane depolarisation based on Nernst's theory. Membrane depolarisation induces the opening of voltage-gated calcium channels. The influx of Ca^{2+} through the calcium channels raises the $[Ca^{2+}]_i$ which then stimulates the exocytotic cascades. The high-K^+-induced catecholamine secretion in SFV-infected cells (11.8±0.75%, n=27) was slightly reduced when compared to that of non-infected cells (14.3±1%, n=24) (Figure 3-19). The reduction of high-K^+-induced catecholamine secretion in SFV-infected cells may seem inconsistent with the reduction of the calcium currents. One reason that can explain this discrepancy is that the secretion shown here includes both the basal and Ca^{2+}-activated secretion. Therefore, the effect of calcium current reduction on high-K^+-induced catecholamine secretion in SFV-infected cells may be obscured by the basal secretion. However, the possible direct effect of SFV infection on secretory machinery has to be studied.

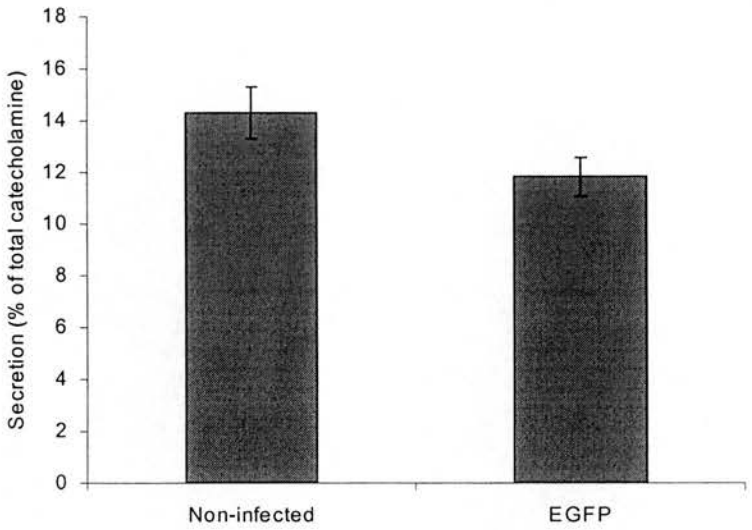

Figure 3-19 High-K^+ induced similar catecholamine secretion in SFV-infected and non-infected bovine adrenal chromaffin cells

Bovine adrenal chromaffin cells (3 x 10^5cells/sample) were stimulated with solution containing high K^+(98 mM NaCl, 50 mM KCl, 2 mM $CaCl_2$, 1 mM $MgCl_2$, 10 mM glucose, and 10 mM HEPES-NaOH pH 7.2, osmolarity 315 mOsmole) for 3 minutes at 37°C. The catecholamine secreted into the medium was assayed by using a spectrofluorimetric method. The release was displayed as percentages of total catecholamine content in the same sample. The catecholamine secretion from SFV-infected cells was not statistically different from that of non-infected cells.

3.2.9.1.2 β-escin permeabilisation

Despite the reduction of calcium currents by 50% in SFV-infected cells, the reduction of the high-K^+ induced secretion was very marginal. This could indicate the modification of the release probability in SFV-infected cells. To verify if the secretory machinery was affected by SFV infection, Ca^{2+} was introduced into cells via dialysis so that the effect of SFV infection on the calcium currents would be bypassed and the cells were stimulated with the same concentrations of Ca^{2+}. In the population assay of catecholamine secretion, bovine adrenal chromaffin cells were permeabilised by β-escin in the presence of various concentrations of free Ca^{2+}. Both SFV-infected and non-infected cells showed similar Ca^{2+}-dependent catecholamine secretion at all concentration of Ca^{2+} tested. The catecholamine secretion induced by 1-μM Ca^{2+} was not different statistically between SFV-infected (30±1.2%, n=12 for 1μM Ca^{2+}) and non-infected cells (33±2.2%, n=12 for 1μM Ca^{2+}). The Ca^{2+}-dependency of catecholamine secretion was also not different (Figure 3-20). This finding indicated that the secretory machinery was not affected by SFV infection.

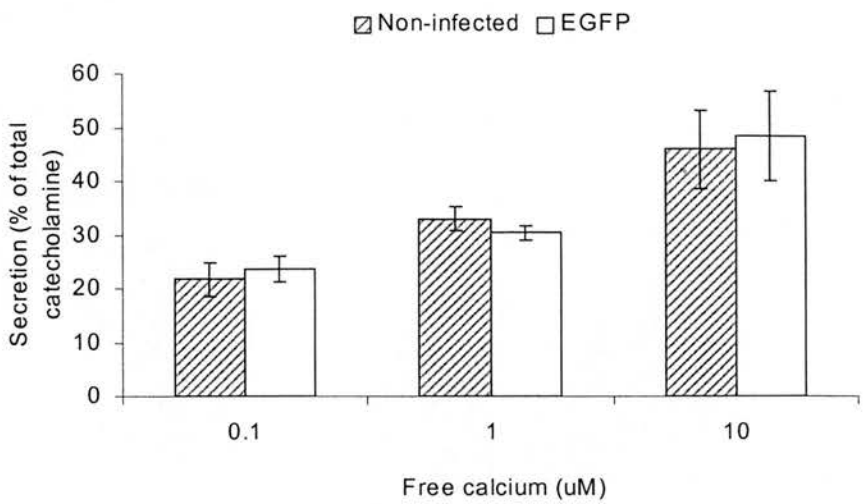

Figure 3-20 Catecholamine secretion from β-escin permeabilised cells

Bovine adrenal chromaffin cells were permeabilised with β-escin in the presence of the indicated Ca^{2+} concentration. The cells were incubated for 5 minutes in the permeabilising solution (139 mM K-Glutamate, 20 mM PIPES, 5 mM K_2H_2EGTA, 2 mM MgATP, 0.3 mM Na_2GTP, 60 μMβ-escin and 0.5% Bovine albumin; pH was adjust to 6.6 with KOH). The permeabilising solution was replaced with fresh permeabilising solution with the indicated Ca^{2+} concentration. The stimulation was continued for 10 minutes at 37°C. The catecholamine release into the media was assayed and displayed as percentages of total catecholamine content in the same sample. The amount and Ca^{2+}-dependency of secretion was not affected by SFV-infection.

3.2.9.2 Effect of SFV infection on single cell exocytosis

3.2.9.2.1 Ca^{2+} dialysis

Single-cell secretion of catecholamine was monitored with membrane capacitance measurement and amperometry (Figure 3-21). Bovine adrenal chromaffin cells were stimulated with buffered-Ca^{2+} solution dialysed into cells via patch pipettes. Carbon-fiber microelectrodes were positioned close to the plasma membrane to detect the catecholamine release from the cells.

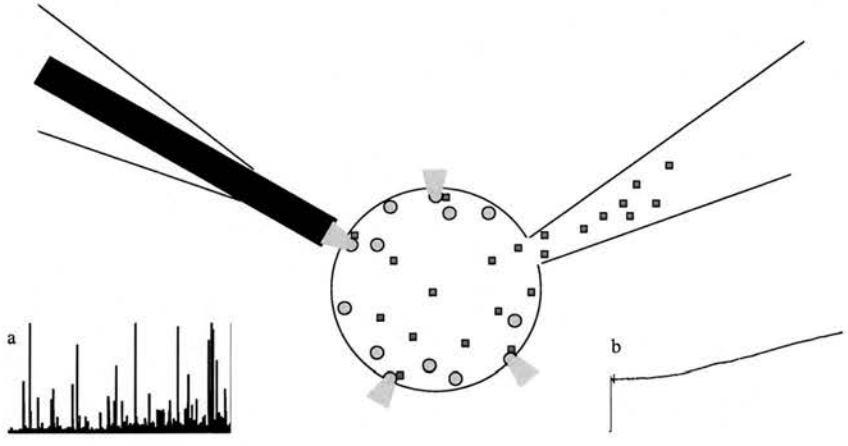

Figure 3-21 Cell membrane capacitance measurement and amperometry

A diagram shows the recording condition during single cell study. In this case, Ca^{2+}(*red squares*) was dialysed into cells via a patch pipette in whole-cell configuration (*right*). A carbon-fiber microelectrode was placed close to the plasma membrane (*left*). Catecholamine secretion (*gray zone*) was picked up by the carbon fiber microelectrode as amperometric spikes (*inset a*). Simultaneous increase of plasma membrane from vesicle fusion was detected as an increase in membrane capacitance (*inset b*).

The secretion started with a few seconds delay after the whole-cell was established (Figure 3-22A). This delay was contributed by several factors including rate of Ca^{2+} diffusion from the patch pipette to the exocytotic machinery, the protein-protein and protein-membrane phospholipids interaction during exocytosis and the catecholamine diffusion from the release sites to the carbon fiber microelectrode. This delay was longer than the delay measured when cells were stimulated with step-depolarization (Chow, von Ruden et al. 1992). Therefore, the delay in the Ca^{2+} dialysis experiment was contributed primarily by the diffusion of Ca^{2+} from the patch pipette as seen when fura-6F was included in the pipette solution. In most experiments with access resistant about 5-10 MΩ, the fura-6F reached the maximal level within 2 minutes. However, the diffusion of Ca^{2+} was faster than that of Fura-6F due to the smaller size. The secretion was Ca^{2+} concentration-dependent as the amount of secretion induced by 1.5-μM free Ca^{2+} was smaller than that of 10-μM free Ca^{2+} (Figure 3-22B).

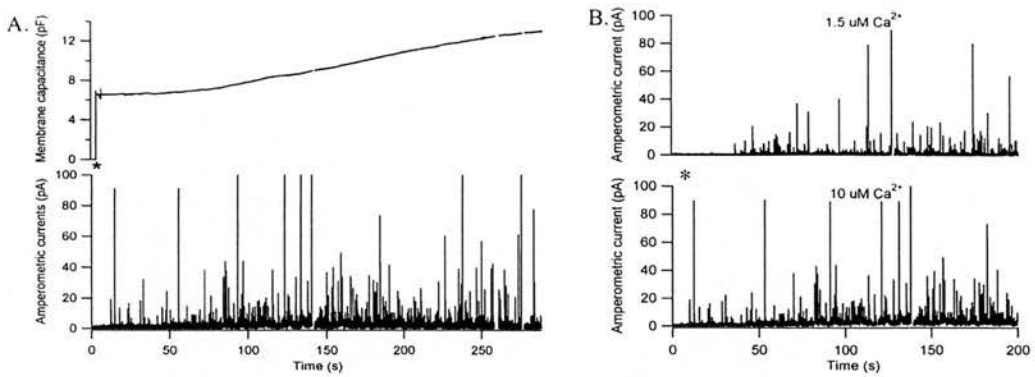

Figure 3-22 Single cell secretion during whole-cell Ca^{2+}-dialysis experiments

Typical response to intracellular dialysis with pipette solution containing 10 μM Ca^{2+} in bovine adrenal chromaffin cell (A), the membrane capacitance and amperometric current are shown in upper and lowe panel, respectively. The membrane patch was ruptured at the time indicated by an Asterisk (*). Note the delay between membrane rupture and the amperometric spikes. The amperometric responses to dialysis with different Ca^{2+} concentration are shown in (B). Each amperometric recording was taken from different cells. Catecholamine secretion was Ca^{2+}-dependent, the number of amperometric spikes with 10-μM Ca^{2+} dialysis (*lower panel*) was higher than that of 1.5 μM Ca^{2+}(*upper panel*). The delay between the membrane rupture and the beginning of the secretion was also shorter with higher Ca^{2+}.

The amount and time course of catecholamine secretion was measured from the cumulative latency histogram constructed from the amperometric recording (Figure 3-23).

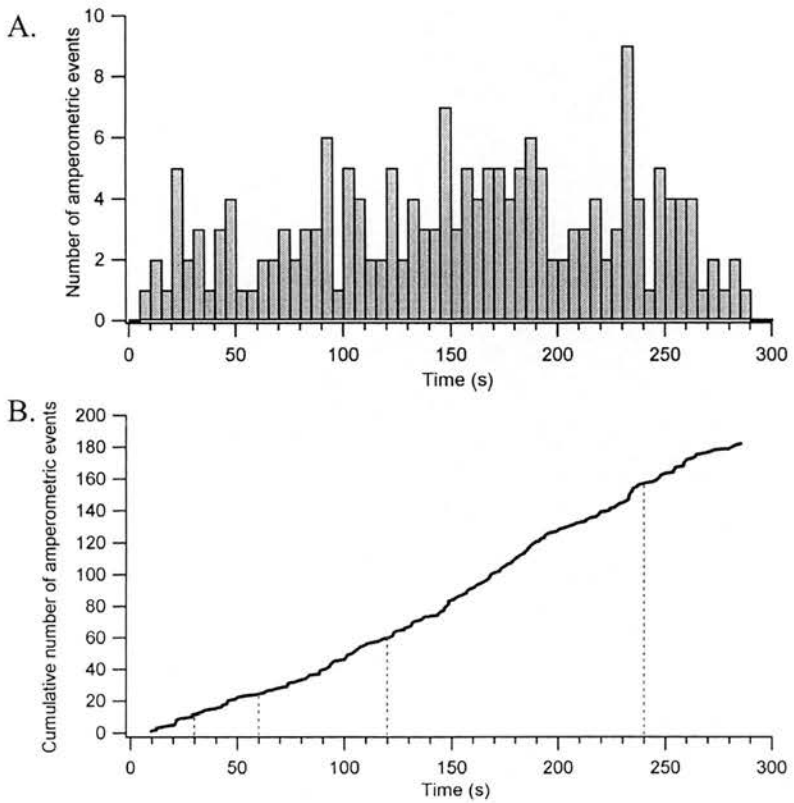

Figure 3-23 Latency histogram of amperometric current

The delay between whole-cell establishment to each amperometric spike was measured by using a program written on IGOR (WaveMetrics, Lake Oswego, OR, US.). The latency histogram (A) was then constricted from the delay. The cumulative latency graph (B) was constructed by integration of the latency histogram. The vertical dash lines on the cumulative latency graph indicate the time (30, 60, 120 and 240 s) after the membrane patch rupture where the secretion was measured.

The secretion was measured at 10, 30, 60, 120, 180 and 240 seconds after the whole-cell was established. There was no significant difference in the amount and time course of secretion between SFV-infected and non-infected cells (Figure 3-24). The secretion at 120 seconds after whole-cell establishment was not different between SFV-infected (68±18 events, n=12) and non-infected cells (69±18 events, n=12).

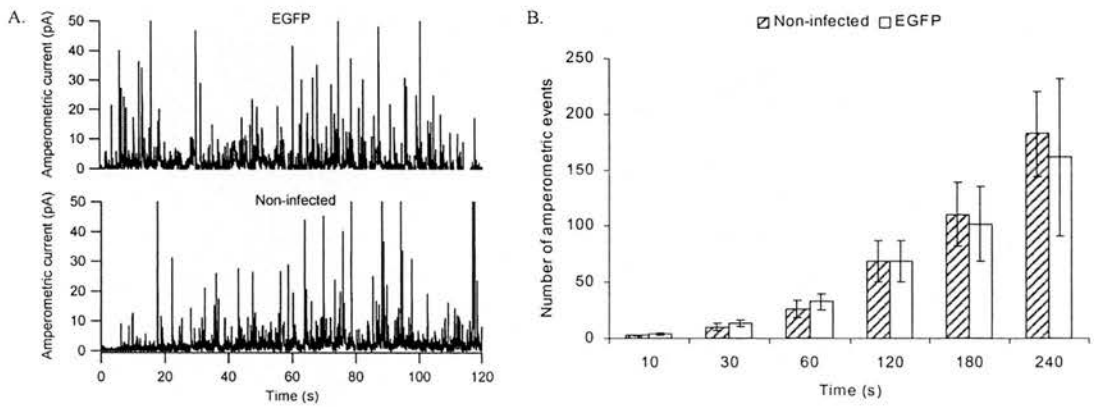

Figure 3-24 Amperometric currents from SFV-infected and non-infected cells during Ca^{2+} dialysis experiments

Examples of amperometric recording from EGFP-expressing cell and non-infected cell are shown in (A). The secretion (number of the amperometric spikes) were measured from cumulative latency graph at indicated time and shown in (B). There was no difference in secretion between SFV-infected and non-infected cells.

Exocytosis was also measured from the membrane capacitance changes during the Ca^{2+}dialysis experiment. The capacitance changes were measured at 30, 60, 120 and 240 s after membrane patch rupture (Figure 3-25A). Consistent with the

amperometric measurement, there was no difference in capacitance changes between SFV-infected cells and non-infected cells during Ca^{2+} dialysis experiments (Figure 3-25B).

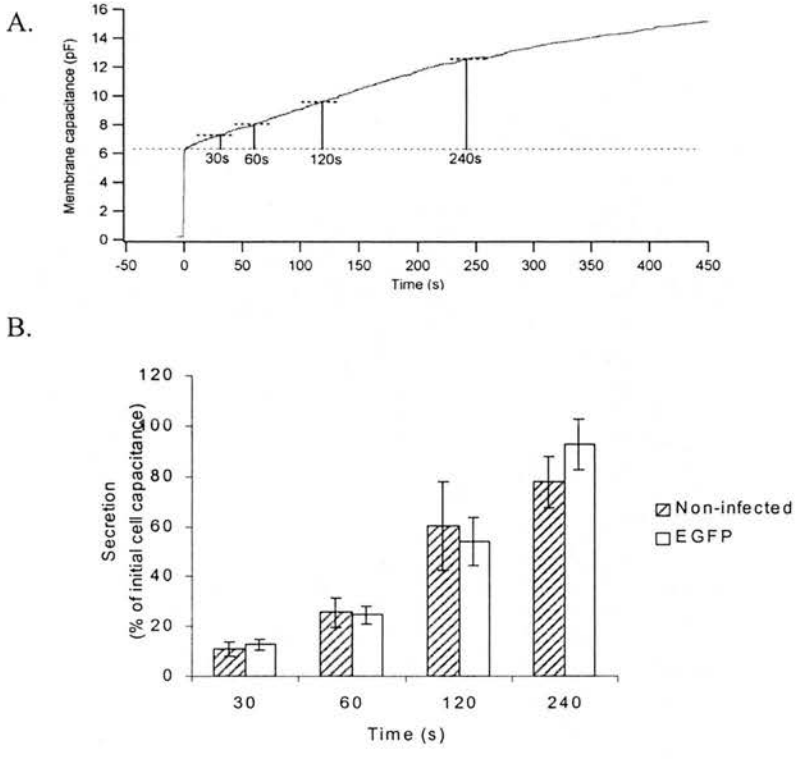

Figure 3-25 Membrane capacitance responses from SFV-infected and non-infected cells during Ca^{2+} dialysis experiments

The course of the membrane capacitance changes during Ca^{2+} dialysis is shown in (A). The membrane patch was ruptured at time zero. The capacitance was measured at the indicated time (vertical dash line in A). The capacitance changes as a percentage of initial membrane capacitance were displayed in (B). There was no difference in capacitance change in response to Ca^{2+} stimulation among the SFV-infected and non-infected cells.

3.2.9.2.2 Step depolarization

Secretory vesicles reside in different functional pools. Only a small number of vesicles are releasable (the fusion-competent vesicles) and rapidly released upon elevation of $[Ca^{2+}]_i$. These small functional pools of vesicles were overlooked in the population assay due to slow diffusion of Ca^{2+} into cells. Therefore, adrenal chromaffin cells were stimulated with step depolarisations in whole-cell patch clamp experiments. Depolarisation induces calcium influx through calcium channels which leads to a substantial increase in $[Ca^{2+}]_i$ near the plasma membrane. The secretion induced by this stimulation protocol is contributed mainly by the small pool of vesicles near the plasma membrane (the RRP and SRP). Six 50-ms depolarisations were applied at an interval of 350 ms. Despite the reduction of calcium currents by 50% in SFV-infected cells, the average membrane capacitance response to the first depolarisation of the train from SFV-infected cells (317±34, n=35) was only 20% reduced when compared with that of non-infected cells (391±29 fF, n=113). This effect was not statistically different (Figure 3-26). The amount of secretion in response to a single depolarisation was similar to the size of the RRP estimated from caged-Ca^{2+} experiments (Xu, Rammner et al. 1999).

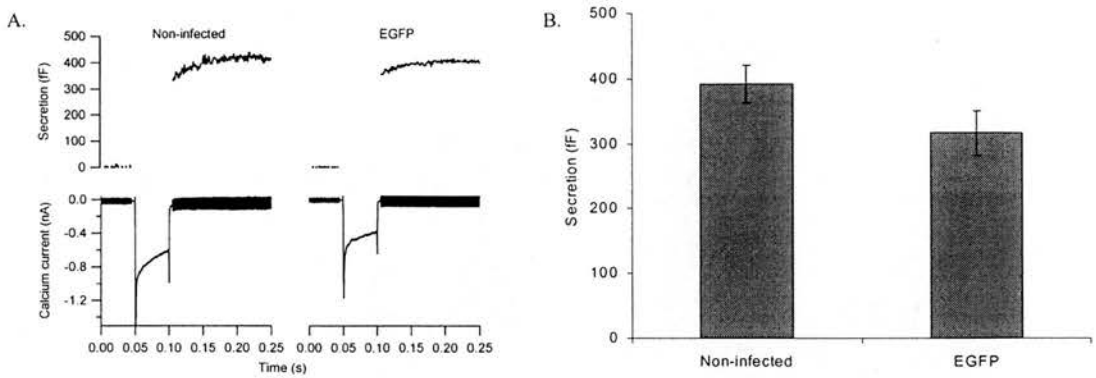

Figure 3-26 Effect of SFV infection on depolarisation-induced secretion

Membrane capacitance and calcium currents in response to 50-ms depolarisations to 10 mV from a holding potential of –70 mV were measured in whole-cell patch clamp experiments. (A) Calcium currents and capacitance changes from SFV-infected and non-infected cells. The capacitance and calcium currents are shown in the upper and lower panels, respectively. Note that the calcium current is smaller in SFV-infected cells. Exocytosis was determined by the change in the membrane capacitance after depolarisation relative to the basal membrane capacitance prior to stimulation. (B) Histogram shows mean±s.e.m. There was no significant difference in membrane capacitance changes between SFV-infected cells (n=35) and non-infected cells (n=113).

Upon repetitive depolarisations, the secretion showed significant rundown within each train due to the depletion of the fusion-competent vesicles by each successive depolarisation. The plateau of the capacitance response to the train of depolarisations implied the number of fusion-competent vesicles (Figure 3-27).

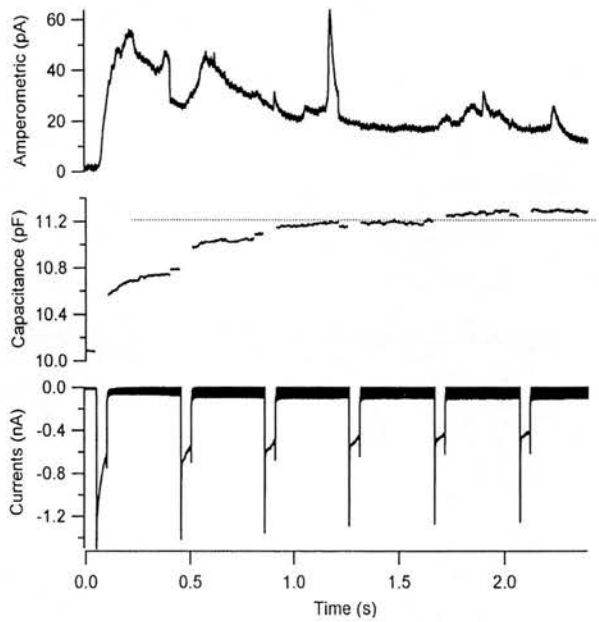

Figure 3-27 Capacitance and amperometric response to a train of depolarisations

A bovine adrenal chromaffin cell was stimulated with a train of 50-ms depolarisations at 350-ms intervals in whole-cell patch clamp recording. The calcium currents and capacitance are displayed in lower and middle panels, respectively. The capacitance response showed significant reduction during repetitive stimulation while calcium currents were not significantly reduced. The dash line on the capacitance trace indicated the plateau of capacitance response. The amperometric current recorded from a carbon-fiber microelectrode is shown in the upper panel. The membrane capacitance increase was consistent with the increase of the amperometric current, implying the fusion of catecholamine containing vesicles.

The size of the fusion-competent vesicle pool measured by this protocol in non-infected cells was 590±33 fF (n=113). This number was consistent with the size of the fusion-competent vesicle pool estimated by flash photolysis of caged-Ca^{2+} experiment in bovine adrenal chromaffin cells (Xu, Binz et al. 1998; Xu, Rammner et al. 1999; Ashery, Varoqueaux et al. 2000). The distribution of the fusion-competent vesicle pool sizes from non-infected cells was plotted. The distribution showed a single peak consistent with the distribution of initial membrane capacitance and calcium currents (Figure 3-28).

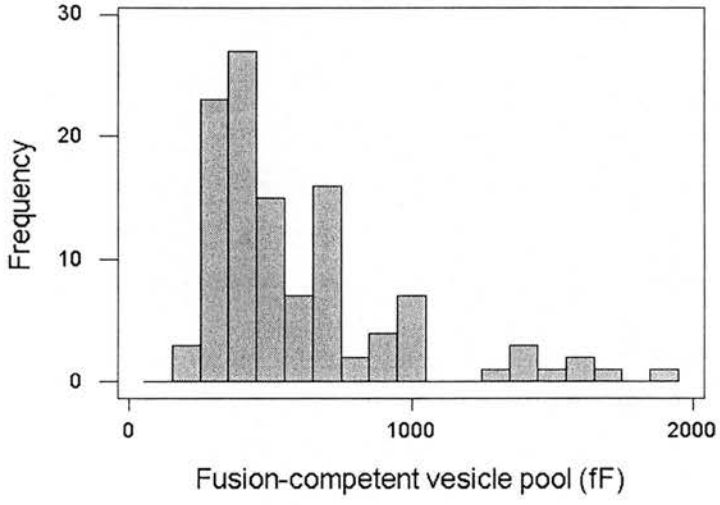

Figure 3-28 distribution of the fusion-competent vesicle pool sizes in non-infected cells

The fusion-competent vesicle pool was measured using the train of depolarisation protocol. The distribution of the pools showed a single peak indicating that the chromaffin cells being studied came from a single population.

The size of the fusion-competent vesicle pool was not significantly different between SFV-infected (611±55 fF, n=35) and non-infected cells (Figure 3-29).

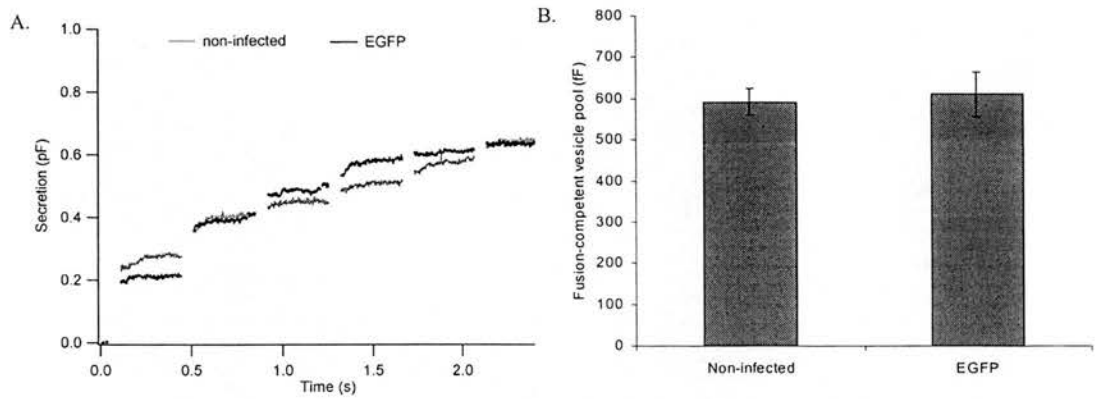

Figure 3-29 The fusion-competent vesicle pool was not affected by SFV-infection

Capacitance responses to a train of depolarisations from SFV-infected and non-infected cells are superimposed (A). The histogram (B) shows no difference in the fusion-competent vesicle pool size in SFV-infected and non-infected cells.

To study how the SFV-infected cells were able to maintain the secretory responses to 50-ms depolarisations despite the reduction of calcium currents, the correlation between calcium currents and secretion from non-infected cells were analysed in detail. Previous studies showed that the depolarization-induced secretion was exponentially dependent on the integral calcium current with a power of 1.5 (Engisch and Nowycky 1996). Non-infected cells were separated into two groups based on their calcium currents, one group having calcium currents less than 400 pA and another group having calcium currents more than 400 pA. The size of the fusion-competent vesicle pools was only slightly and not significantly increased in the group having calcium currents less than 400 pA (682±91 fF versus 568±33 fF in

group having calcium currents more than 400 pA) as shown in figure 3-30B. The capacitance changes induced by 50-ms depolarisations for the group having calcium currents less than 400 pA (386±68 fF, n=21) were not significantly different from that of the group having calcium currents more than 400 pA (380±31 fF, n=98) (Figure 3-30A). This result could indicate the saturation of secretion by the single depolarization. Studies using flash photolysis of caged-Ca^{2+} compounds reveal that the fusion competent vesicle pool is further divided into the rapidly releasable pool (RRP) and slowly releasable pool (SRP) based on the rate constant of exocytosis. The Ca^{2+}entry during the single depolarization might be enough to stimulate secretion from the RRP. The increased Ca^{2+}entry during this short depolarization was not able to induce significant additional secretion from the SRP. Another possibility was that the RRP was increased in the group having calcium currents less than 400 pA. As shown in figure 3-30C, the basal $[Ca^{2+}]_i$ in the group having calcium currents less than 400 pA (238±23 nM, n=14) was significantly higher than that of the group having calcium currents more than 400 pA (113±8 nM, n=62). It is known that Ca^{2+} is not only important for the final step of exocytosis but also the recruitment of vesicles. The precise molecular mechanism of Ca^{2+} in vesicle recruitment is still unclear. It was reported that Ca^{2+} induces SNARE complex formation (Quetglas, Leveque et al. 2000; Lawrence and Dolly 2002a; Lawrence and Dolly 2002b). The transition between SRP and RRP is also dependent on SNARE complex formation (Xu, Rammner et al. 1999; Voets 2000). Therefore, a high level of $[Ca^{2+}]_i$ in chromaffin cells might increase the RRP and be responsible for the discrepancy between calcium currents and capacitance changes as observed in SFV-infected cells.

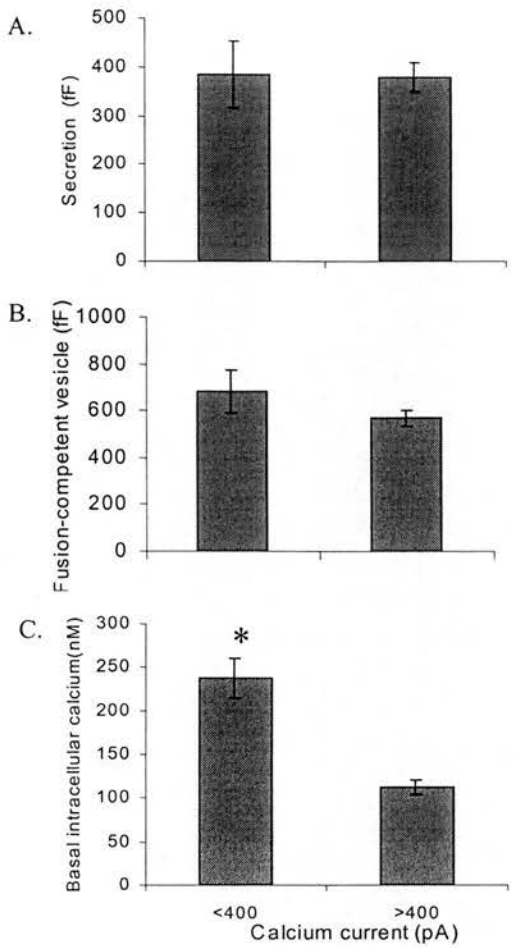

Figure 3-30 Histogram summarizes the secretion from non-infected cells with different calcium currents

Non-infected cells were separated into a group having calcium currents less than 400 pA and a group having calcium currents more than 400 pA. The 50-ms depolarisations elicited similar responses in both groups (A). The fusion-competent vesicle pools were not different between the two groups (B). The basal $[Ca^{2+}]_i$ was significantly higher in the group having calcium currents less than 400 pA (C).

3.2.9.3 Single vesicle exocytosis

Individual amperometric currents in response to intracellular dialysis with 10 μM Ca^{2+} were analysed. The amplitude of the amperometric spikes were not different between SFV-infected (13.8±0.7 pA, n=549 from 11 cells) and non-infected cells (14.8±0.7 pA, n=546 from 8 cells) (Figure 3-31).

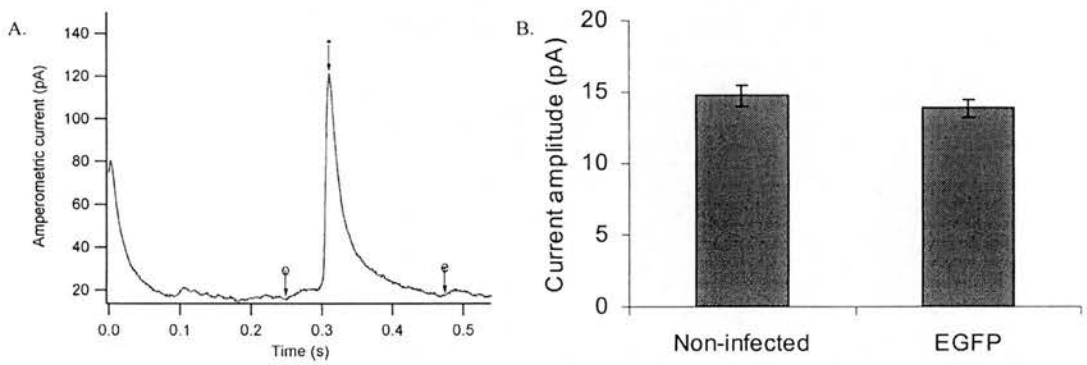

Figure 3-31 Amperometric current amplitude in SFV-infected and non-infected cells

(A) The amperometric current amplitude was defined as the peak current (*) minus the baseline current at the beginning of the amperometric event (o). (B) The histogram shows no difference of the amperometric current amplitude between SFV-infected and non-infected cells.

The individual amperometric events with an amplitude of 20 pA or more were studied in more detail for the characteristics of single vesicle and kinetics of single vesicle exocytosis. In this selected group of responses the amperometric current amplitude was not significantly different between SFV-infected (42.5±1.9 pA, n=201 from 11 cells) and non-infected cells (47.5±2.5 pA, n=178 from 7 cells) (Figure 3-

32B). The integral of the individual amperometric event indicated the amount of catecholamine released from each vesicle was also similar between SFV-infected (1.54±0.08 pC, n=201 from 11 cells) and non-infected cells (1.64±0.08 pC, n=178 from 7 cells) (Figure 3-32B). This result indicated that a similar amount of catecholamine was released from each vesicle.

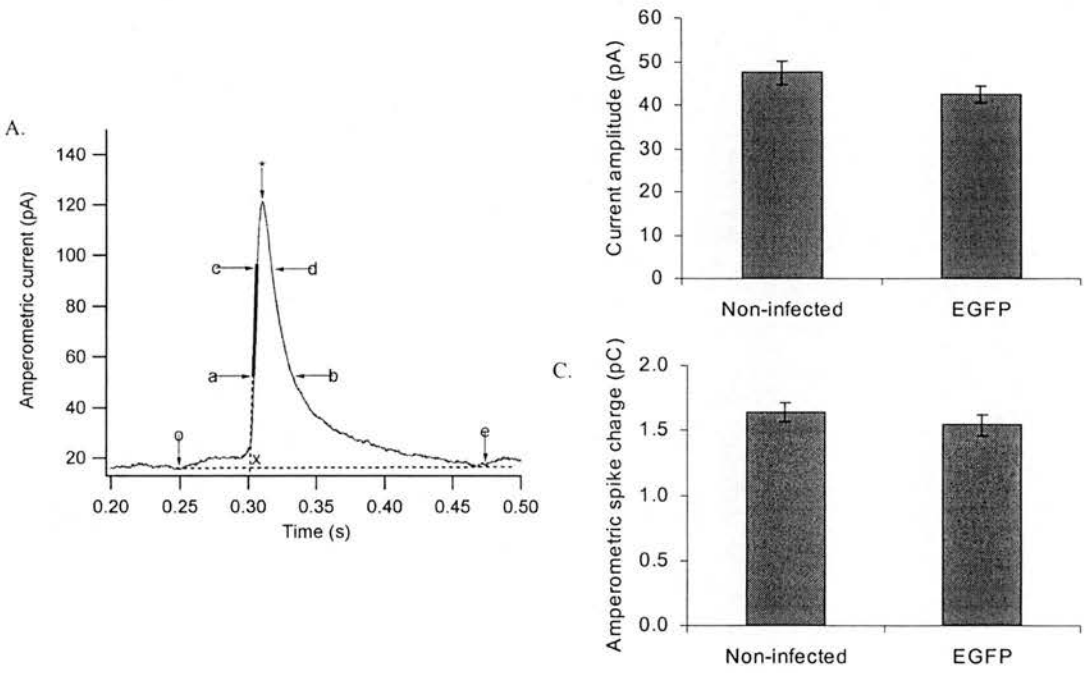

Figure 3-32 Amperometric current amplitude and charge from selected responses with amplitude higher than 20 pA

The single amperometric current (A) was identified with a program written on IGOR (WaveMetrics, Lake Oswego, OR, US.). The total charge was calculated by integration of the amperometric current above the baseline (horizontal dash line in A) from the beginning (o) to the end (e) of the event. The histograms show that neither the amplitude (B) nor total charge (C) was affected by SFV infection.

The release of catecholamines from single vesicles was determined from the characteristics of the individual amperometric current. An individual amperometric event began with a small amplitude foot signal. The foot signal indicated the leakage of catecholamine from the initial fusion pore. Because the foot signals were very small in amplitude, only the amperometric recordings that had very low noise level were analysed. The duration, amplitude and charge of the foot signals were measured. None of the foot parameters of SFV-infected cells was statistically different from that of non-infected cells (figure 3-33).

After an initial foot signal, the individual amperometric current proceeded with an abrupt increase of the current to the maximum followed by an exponential dacay to the baseline. The sudden increase of the amperometric current indicated the release of catecholamine after fusion pore expansion. The risetime, halfwidth and the decay time constant indicated the kinetics of the catecholamine release. The risetime, halfwidth and the decay time constant were not affected by SFV infection (figure 3-34).

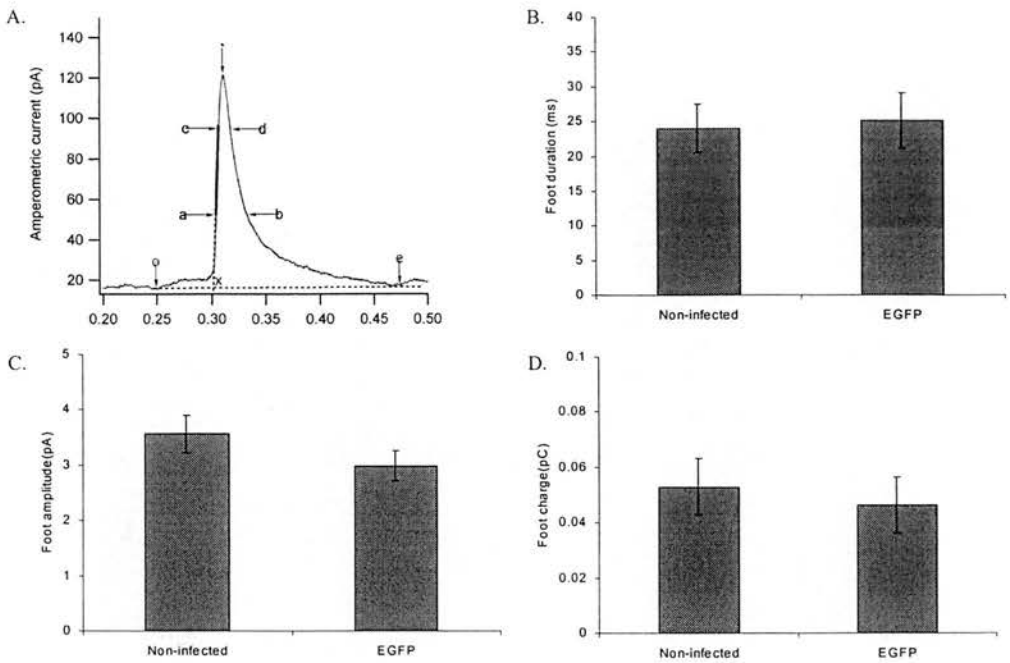

Figure 3-33 The amperometric foot signal was not affected by SFV infection

A line was extrapolated from the rising limb of the amperometric current (A). The foot duration was measured from the beginning of the amperometric current (o) to where the extrapolated line met the baseline (x). The foot amplitude was the peak amplitude within the duration of the foot signal. The integral of the signal within the foot duration was the foot charge. The foot duration (B) was not different between SFV-infected (25±3.9 ms, n=61 from 5 cells) and non-infected cells (24±0.3 ms, n=76 from 5 cells). The foot amplitude (C) of SFV-infected cells (3±0.27 pA, n=61 from 5 cells) was not different from that of non-infected cells (3.6±0.33 ms, n=76 from 5 cells). The foot charge (D) were similar between SFV-infected (0.05±0.01 pC, n=61 from 5 cells) and non-infected cells (0.046±0.01 pC, n=76 from 5 cells).

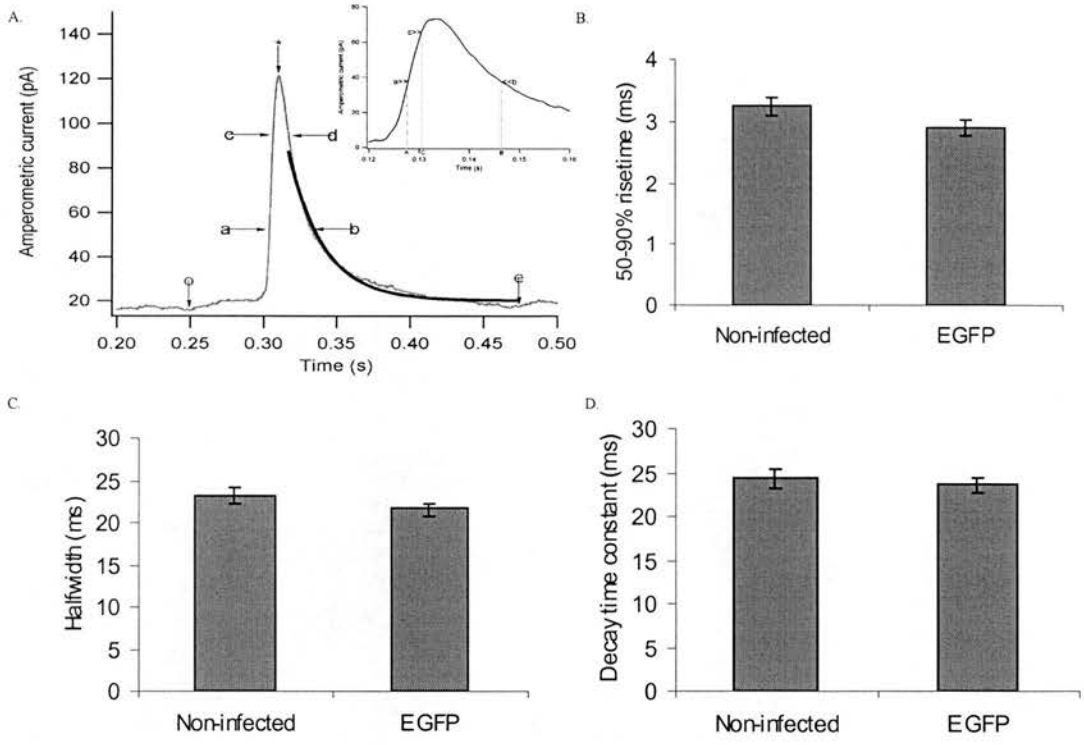

Figure 3-34 Effects of SFV infection on risetime, halfwidth and decay time constant of amperometric currents

The risetime, halfwidth and decay time constant were measured with a program written on IGOR (WaveMetrics, Lake Oswego, OR, US.). The risetime was determined from the duration taken for the current to increase from 50% (a) to 90% (c) of amplitude (*C-A* in the inset). The risetime (B) for SFV-infected cells (2.9±0.13 ms, n=201 from 11 cells) was not different from that of non-infected cells (3.2±0.17 ms, n=178 from 7 cells). The halfwidth was measured as the duration from 50% of the amplitude at the ascending limb to the same level at the descending limb of the amperometric current at (*B-A* in the inset). The halfwidth (C) in SFV-infected cells cells (21.5±0.8 ms, n=201 from 11 cells) was not different from that of non-infected cells (23.3±1 ms, n=178 from 7 cells). The decay of the amperometric current from 90% of amplitude (d) until the end of the signal (e) was fitted with single exponential function. The decay time constant (D) was similar between SFV-infected cells (23.5±0.9 ms, n=201 from 11 cells) and non-infected cells (24.3±1.1 ms, n=178 from 7 cells).

3.3 Conclusion

It was shown in the experiments that Semliki Forest virus (SFV) vector system was an efficient method for gene expression in primary cultured bovine adrenal chromaffin cells. The system was easy to prepare. A high level of protein expression was achieved within 24 hours after infection. However, this viral vector system still had some drawbacks. The calcium currents were significantly affected by viral-mediated expression of EGFP. The calcium currents were reduced by 50% in SFV-infected cells. This effect was more pronounced at 72 hours after infection. The reduction of the calcium currents could be the result of the viral infection or the expression of EGFP. The correlation between the high basal $[Ca^{2+}]_i$ and the reduction of calcium currents indicated that the $[Ca^{2+}]_i$ might be the main messenger for the calcium current reduction. The high basal $[Ca^{2+}]_i$ could be the result of viral-induced apoptosis as previously reported (Glasgow, McGee et al. 1998). Despite the effects of the SFV vector system on calcium currents and $[Ca^{2+}]_i$, the catecholamine synthetic pathway , the fusion-competent pool of secretory vesicles and the catecholamine secretion were not affected. Therefore, the effect of protein expression could be studied early after infection and there was a reasonably long window that the exocytosis could be studied in these cells.

Chapter 4

Effects of Doc2β expression in bovine adrenal chromaffin cells

4.1 Introduction

Doc2β is a promising candidate in regulated exocytosis. This protein is associated with secretory vesicles and highly enriched in brain. Doc2β contains two C2 domains that interact with Ca^{2+} and phospholipids (Sakaguchi, Orita et al. 1995; Kojima, Fukuda et al. 1996). Doc2β interacts with the synaptic proteins Munc13 and Munc18, both of which are important for synaptic transmission and regulated exocytosis in other secretory cells (Orita, Naito et al. 1997; Verhage, de Vries et al. 1997). The significant role of Doc2 in regulated exocytosis comes from studies of the brain-specific isoform Doc2α. Expression of Doc2α enhances secretion in PC12 cells (Orita, Sasaki et al. 1996; Orita, Naito et al. 1997). Study in superior cervical ganglion neurons indicates that the secretory enhancement is mediated by the Doc2α-Munc13 interaction which plays a substantial part in vesicle recruitment (Mochida, Orita et al. 1998). Consistently, application of phorbol ester in HEK293 cells expressing both Doc2β and Munc13 induces translocation of both proteins to the plasma membrane. The function of Doc2β in regulated exocytosis is not known but it is hypothesised that Doc2β performs a similar function as Doc2α because of the high homology, the complementary distribution in brain and the similarities in Ca^{2+}-dependent activity between these two isoforms. Besides, Doc2β may be important for regulated exocytosis in non-neuronal cells because it is expressed ubiquitously.

In these experiments, the effect of Doc2β and Doc2β C2 domain expression in bovine adrenal chromaffin cells was studied. The aims were to determine the

function of Doc2β in regulated exocytosis of large dense-core vesicles in bovine adrenal chromaffin cells and to identify the mechanism of action. Two hypotheses were proposed for the function of Doc2β based on the studies of Doc2α. First, Doc2β enhances exocytosis by interaction with Munc18 and increases the rate of vesicle supply to the plasma membrane (vesicle recruitment and docking). Second, Doc2β increases the rate of vesicle priming through the interaction with Munc13.

The proteins were expressed in bovine adrenal chromaffin cells by using the SFV transduction system. The cells expressing Doc2β or Doc2β C2 domains were identified from the expression of the reporter EGFP. The experiments were performed at 15-30 hours after infection. Within this time window, the proteins were expressed at high level and the viral cytotoxicity was not substantial as shown in the previous chapter.

4.2 Results

4.2.1 Doc2β did not affect cell morphology

Expression of Doc2β or Doc2β C2 domains (C2AB) did not have an obvious cytotoxic effect on bovine adrenal chromaffin cells. The cell morphology was not distinguishable from EGFP-expressing or non-infected cells. The cell size as indicated by the membrane capacitance in Doc2β-expressing cells (7.4±0.1 pF, n=50) and C2AB-expressing cells (7.7±0.3 pF, n=16) were not different from that of EGFP-expressing cells (7.4±0.2 pF, n=69) (Figure 4-1A). The leak currents during patch clamp experiments were similar to that of EGFP-expressing cells (-24±1.9 pA, n=69 for EGFP-expressing cells; –23±2.5 pA, n=50 for Doc2β-expressing cells and -22±4.4 pA, n=16 for C2AB-expressing cells) (Figure 4-1B).

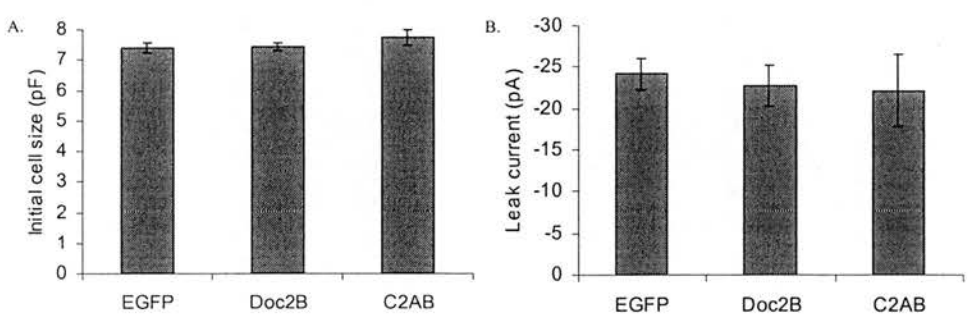

Figure 4-1 Effect of Doc2β and Doc2β C2 domains on basal cellular properties

Whole-cell patch clamp in bovine adrenal chromaffin cells expressing EGFP, Doc2β and C2AB. The initial membrane capacitance was not significantly different among these cells (A). The leak currents were not affected by the protein expression (B).

4.2.2 Basal intracellular Ca^{2+} ($[Ca^{2+}]_i$) concentration was not altered by Doc2β expression

Expression of Doc2β did not affect the basal $[Ca^{2+}]_i$. The basal $[Ca^{2+}]_i$ in Doc2β-expressing cells (199±15 nM, n=6) was not different from that of EGFP-expressing cells (233±25 nM, n=16). This was also not significantly different in cells expressing Doc2β C2 domains (218±25 nM, n=4) (Figure 4-2).

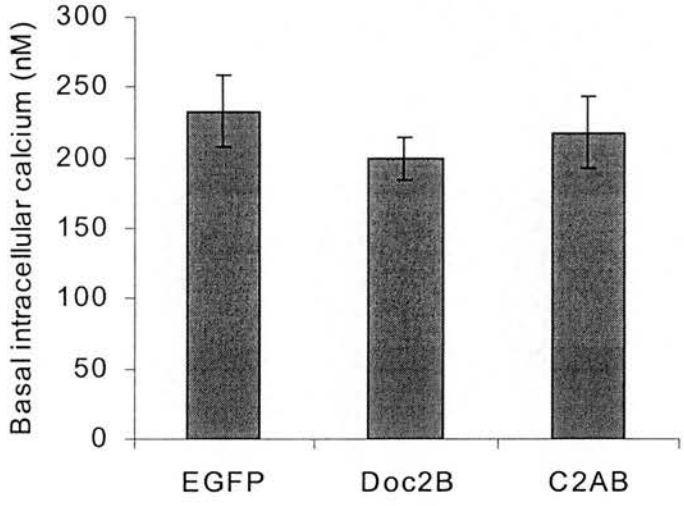

Figure 4-2 Basal intracellular calcium concentration in Doc2β-, C2AB- and EGFP-expressing cells

The basal intracellular calcium concentration $[Ca^{2+}]_i$ was measured in whole-cell patch clamp by including fura-2 in the pipette solution. Histogram shows no significant effect of Doc2β or Doc2β C2 domains on basal $[Ca^{2+}]_i$.

4.2.3 Doc2β did not affect calcium and sodium currents

Calcium and sodium currents were recorded in whole-cell patch clamp experiments. Both the calcium and sodium currents recorded from adrenal chromaffin cells expressing Doc2β individually from the bicistronic construct (Doc2β-IRES-EGFP) or as a fusion protein with EGFP (Doc2-EGFP) were not different. The calcium currents (Figure 4-3A) from cells expressing Doc2β-IRES-EGFP and Doc2β-EGFP were 363±41 pA (n=15) and 378±61 pA (n=7). The sodium currents (Figure 4-3A) were 1.55±0.20 nA (n=15) and 1.71±0.18 nA (n=7) for cells expressing Doc2β-IRES-EGFP and Doc2β-EGFP, respectively. Therefore, the data from both constructs were pooled.

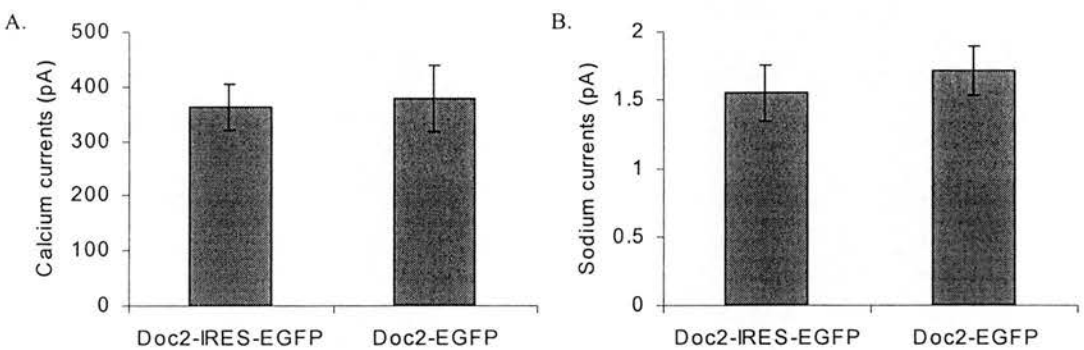

Figure 4-3 The calcium and sodium currents from cells expressing Doc2β and Doc2β-EGFP

Calcium and sodium currents in response to 50-ms depolarisations were recorded from cells expressing Doc2β from the bicistronic construct (Doc2β-IRES-EGFP) or the EGFP-fusion construct (Doc2β-EGFP). The calcium and sodium currents from cells expressing Doc2β-IRES-EGFP and Doc2β-EGFP were not significantly different.

Expression of Doc2β did not affect the calcium current in bovine adrenal chromaffin cells (Figure 4-4). The calcium current in Doc2β-expressing cells was 367±33 pA (n=22) similar to those of EGFP-expressing cells (322±28 pA, n= 35). Calcium current recorded from cells expressing Doc2β C2 domains (418±74 pA, n=7) was not different from those of Doc2β- or EGFP-expressing cells.

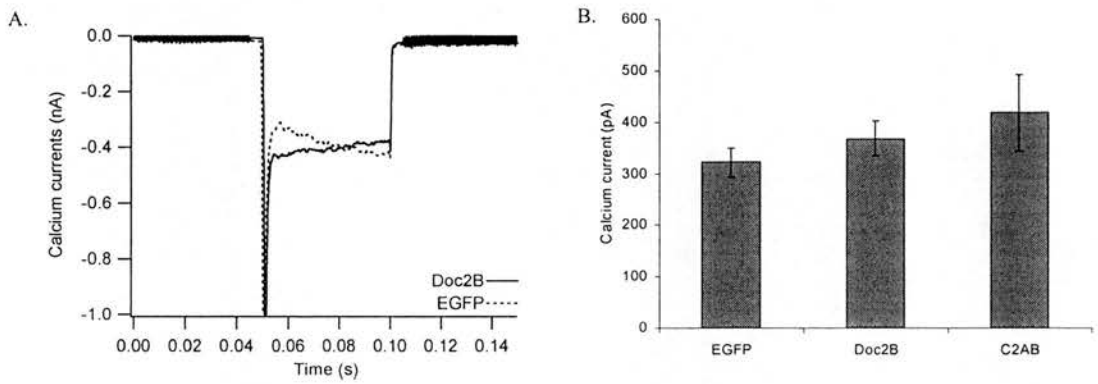

Figure 4-4 Effect of Doc2β and Doc2β C2 domains on calcium currents

The calcium currents were recorded in whole-cell patch clamp experiments. A 50-ms depolarisation induced similar calcium current in both Doc2β- and EGFP-expressing cells (A). Histogram shows that the calcium currents from each group of cells were not significantly different (B).

The sodium currents were measured as previously discussed. Expression of Doc2β or Doc2β C2 domains did not affect sodium currents. The sodium currents were 1.6±0.15 nA (n=22) for Doc2β-expressing cells, 1.59±0.19 nA (n=7) for C2AB-expressing cells and 1.38±0.1 nA (n=35) for EGFP-expressing cells (Figure 4-5).

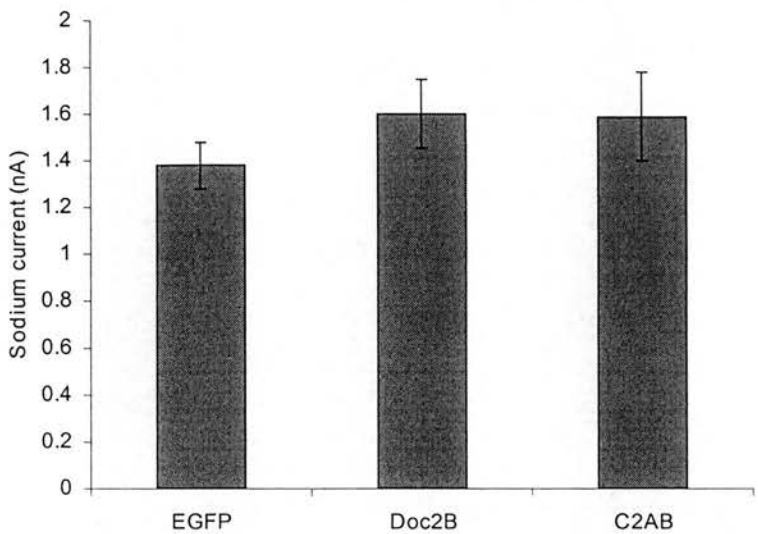

Figure 4-5 Histogram summarizes the effect of Doc2β and Doc2β C2 domains on sodium currents

The inward currents in response to 50-ms depolarisations were recorded in whole-cell patch clamp experiments. Sodium currents were measured from peaks of initial inward currents. Histograms show no significantly difference of sodium currents among cells expressing EGFP, Doc2β and Doc2β C2 domains.

4.2.4 Doc2β did not affect the total catecholamine content

The total catecholamine content in cells expressing Doc2β or Doc2β C2 domains was not altered. The total catecholamine content in Doc2β-expressing cells was 0.16± 0.003 pMol/cell (n=16) which was similar to that of EGFP-expressing cells (0.16±0.004 pMol/cell, n=12). The catecholamine content in cells expressing Doc2β C2 domain (0.16±0.01pMol/cell, n=8) was not different from those of Doc2β- and EGFP-expressing cells (Figure 4-6).

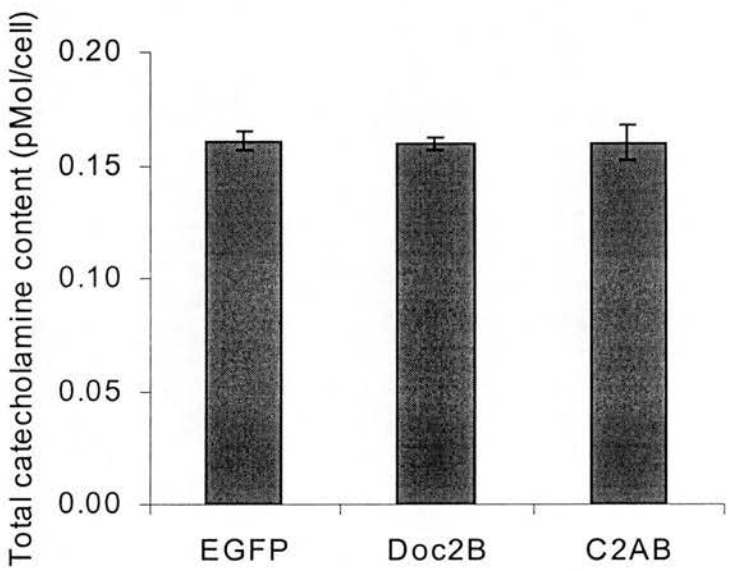

Figure 4-6 Total catecholamine content was not affected by Doc2β and Doc2β C2 domains

Bovine adrenal chromaffin cells expressing EGFP, Doc2β or Doc2β C2 domains were lysed with detergent solution (1% NP40). The cell lysate was assayed for catecholamines. The catecholamine content in Doc2β- and C2AB-expressing cells was not different from that of EGFP-expressing cells.

4.2.5 Doc2β expression did not affect secretion

Several methods of secretion assay were employed in order to study the effect of Doc2β and Doc2β C2 domains on different functional pools of vesicles.

4.2.5.1Effect of Doc2β on catecholamine secretion in cell-population

4.2.5.1.1 High-K^+ stimulation

Previous studies show that expression of Doc2α in PC12 cells enhances high K^+-induced secretion. To study the effect of Doc2β and Doc2β C2 domains on catecholamine secretion, high-K^+ stimulation was adopted in this study. Bovine adrenal chromaffin cells expressing Doc2β, Doc2β C2 domains or EGFP were stimulated with high-K^+ solution for 3 minutes. The catecholamine secretion in response to the stimulation in Doc2β-expressing cells (12±0.8%, n=39) and C2AB-expressing cells (11.7±1%, n=28) was not significantly different from that of EGFP-expressing cells (11.8±0.7%, n=27) as shown in figure 4-7.

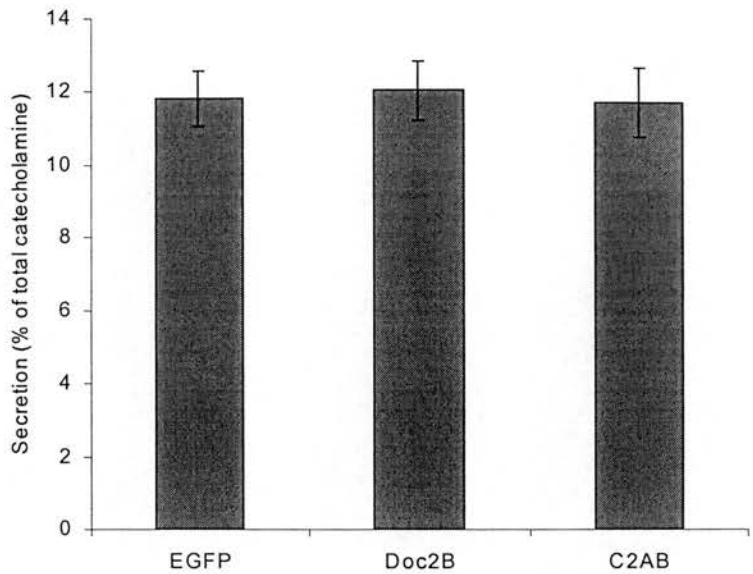

Figure 4-7 Histogram summarizes the effect of Doc2β and Doc2β C2 domains on high-K^+ stimulated catecholamine secretion

Bovine adrenal chromaffin cells expressing the indicated proteins ($3x10^5$cells/sample) were stimulated for 3 minutes at 37°C with a solution containing 50-mM KCl (98 mM NaCl, 50 mM KCl, 2 mM $CaCl_2$, 1 mM $MgCl_2$, 10 mM glucose, and 10 mM HEPES-NaOH pH 7.2, osmolarity 315 mOsmole). The secretion of catecholamines was assayed and displayed as percentages of the total catecholamine content in each sample. Histogram shows that expression of Doc2β or Doc2β C2 domains did not significantly affect secretion.

4.2.5.1.2 β-escin permeabilisation

Catecholamine release was also studied in β-escin permeabilised cells. Bovine adrenal chromaffin cells permeabilised with β-escin in the presence of Ca^{2+} released catecholamine in a Ca^{2+}-dependent manner. The amount of secretion was not significantly different among cells expressing different proteins at all Ca^{2+} concentrations studied (Figure 4-8). This result indicated that the Ca^{2+}-dependency of secretion was not affected in cells expressing Doc2β and Doc2β C2 domains. The catecholamine secretion in response to 1 μM Ca^{2+} for cells expressing Doc2β, Doc2β C2 domains and EGFP were 32±1.5% (n=12), 34±1.5% (n=12) and 30±1.4% (n=12), respectively.

Both high K^+ stimulation in intact cells and Ca^{2+} stimulation in β-escin permeabilised cells induced secretion of more than 10 % of total catecholamine content. This amount of secretion is larger than the fraction of docked vesicles estimated in bovine adrenal chromaffin cells (Parsons, Coorssen et al. 1995). Therefore, more vesicles must be recruited to the plasma membrane for secretion during the stimulation. Based on the results from this study, expression of Doc2β or Doc2β C2 domains did not affect the rate of vesicle recruitment.

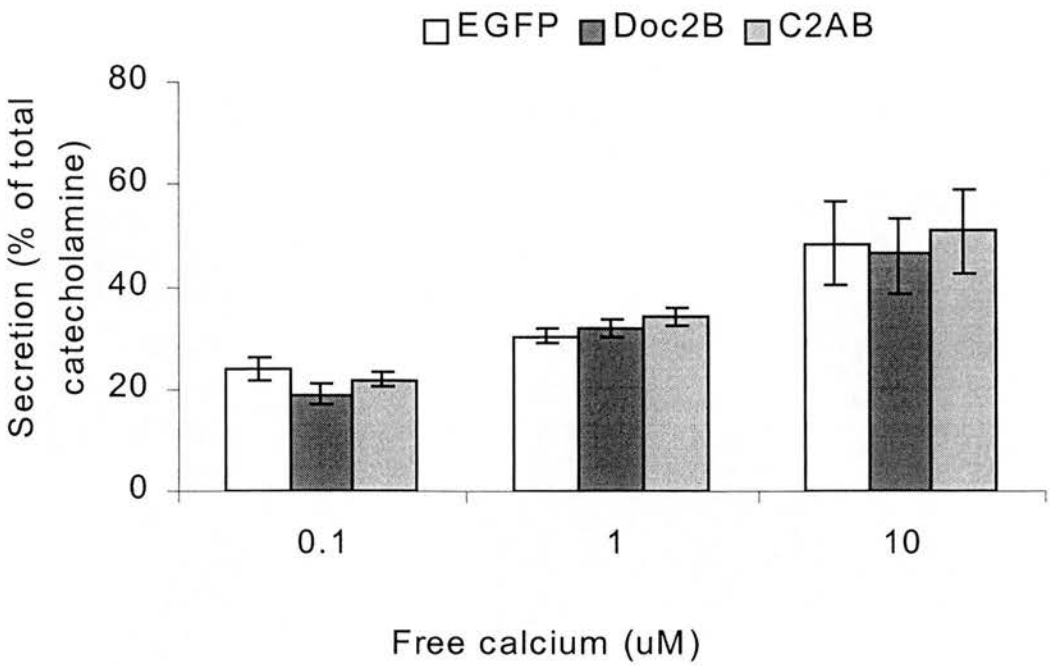

Figure 4-8 Effect of Doc2β and Doc2β C2 domains on catecholamine secretion in β-escin permeabilised cells

Bovine adrenal chromaffin cells were incubated for 5 minutes in the permeabilising solution (139 mM K-Glutamate, 20 mM PIPES, 5 mM K_2H_2EGTA, 2 mM MgATP, 0.3 mM Na_2GTP, 60 μM β-escin and 0.5% Bovine albumin; pH was adjust to 6.6 with KOH). The solution was replaced with fresh permeabilising solution containing the indicated Ca^{2+} for 10 minutes at 37°C. The catecholamine release into the media was assayed and displayed as percentages of total catecholamine content in the same sample. The secretion was Ca^{2+}-dependent. The catecholamine secretion was not different among cells expressing Doc2β, Doc2β C2 domains and EGFP at all Ca^{2+} levels tested.

4.2.5.2 Effect of Doc2β expression on single cell exocytosis

4.2.5.2.1 Ca^{2+} dialysis

Simultaneous membrane capacitance and amperometric currents were recorded during whole-cell dialysis with pipette solution containing 10 μM Ca^{2+}. The Ca^{2+} dialysis induced extensive secretion in adrenal chromaffin cells. The cells were nearly double in size at 240 seconds after whole-cell establishment. The time course of secretion was monitored by measurement of the membrane capacitance changes or the number of amperometric events at variable times after whole-cell establishment. The membrane capacitance changes were not significantly affected in cells expressing Doc2β or Doc2β C2 domains (Figure 4-9). The catecholamine release detected with the carbon fiber microelectrodes placed in proximity to the cell surface was consistent with the membrane capacitance measurements. Expression of Doc2β did not affect the amount or time course of exocytosis during whole-cell dialysis with 10 μM Ca^{2+} (Figure 4-10). The secretion at 120 seconds after whole-cell establishment was 65±11 events (n=11) for Doc2β-expressing cells and 68±18 events (n=12) for EGFP-expressing cells.

The results here were consistent with the population study that expression of Doc2β did not affect the rate of vesicle recruitment despite the massive secretion. More over, the initial secretion after whole-cell establishment indicating the secretion from the smaller functional pools were not affected by the expression of Doc2β and Doc2β C2 domains.

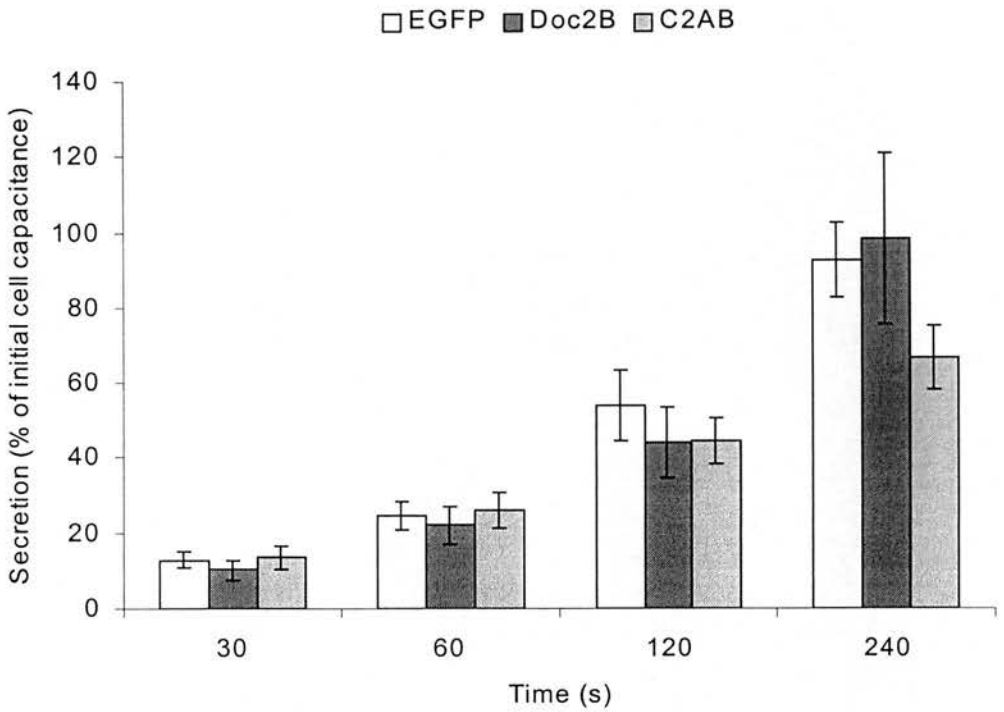

Figure 4-9 Effect of Doc2β and Doc2β C2 domains on membrane capacitance changes in Ca^{2+}dialysis experiments

Bovine adrenal chromaffin cells expressing Doc2β, Doc2β C2 domains or EGFP were stimulated with 10 μM Ca^{2+} introduced into cells via the patch pipette in whole-cell patch clamp. The histogram shows the membrane capacitance changes at the indicated time after the whole cell was achieved. The changes were not significantly affected by expression of Doc2β or Doc2β C2 domains.

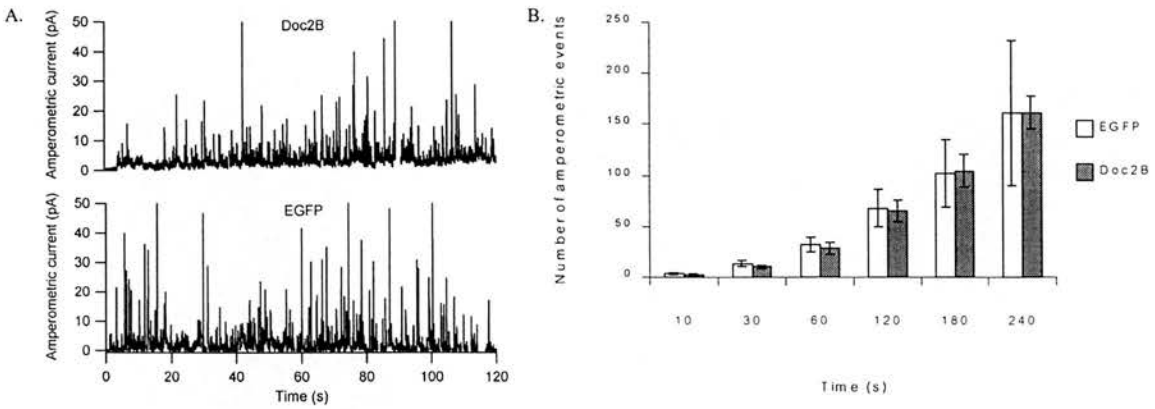

Figure 4-10 Amperometric response to Ca^{2+}dialysis in Doc2β-expressing cells

The examples of amperometric current in response to dialysis with 10 μM Ca^{2+} from Doc2β- and EGFP-expressing cells were compared (A). The delay and the amount of secretion were not different. Histogram shows number of amperometric events at the indicated time after the membrane patch was ruptured (B). There was no significant difference in secretion observed throughout the course of the dialysis (n=13 each).

4.2.5.2.2 Step depolarisation

Population assay or slow dialysis would overlook the small functional pool of vesicles near the plasma membrane (RRP and SRP). To study these functional pools of vesicles, trains of depolarisations were applied to adrenal chromaffin cells in whole-cell patch clamp experiments. The capacitance response to the first depolarisation of the train were compared. A 50-ms depolarisation induced secretion primarily from a small pool of vesicles near the plasma membrane (RRP) as discussed in the previous chapter. The capacitance responses to 50-ms depolarisations in cells expressing Doc2β from the bicistronic construct (291±44 fF, n=15) and cells expressing Doc2β-EGFP (307±90 fF, n=7) was not different (Figure 4-11).

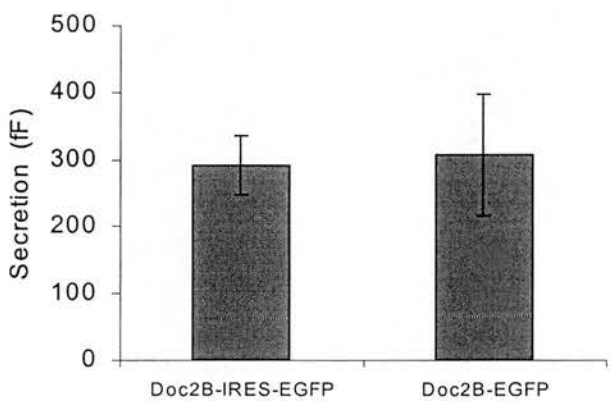

Figure 4-11 Depolarization-induced secretion in cells expressing Doc2β and Doc2β-EGFP

The histogram summarizes the capacitance response to 50-ms depolarization from chromaffin cells infected with SFV expressing Doc2β-IRES-EGFP and Doc2β-EGFP. The capacitance changes were not significantly different.

The capacitance changes in cells expressing Doc2β (296±40 fF, n=22) and Doc2β C2 domains (270±50 fF, n=7) were not significantly different from that of EGFP-expressing cells (317±34 fF, n=35) (Figure 4-12).

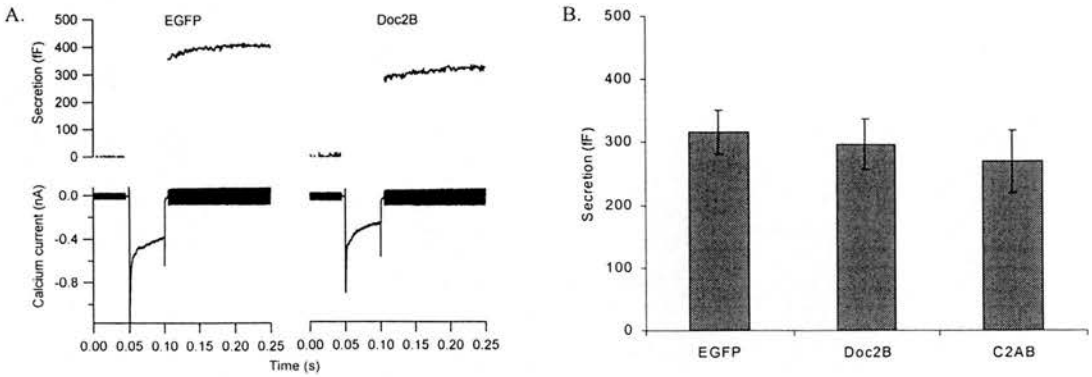

Figure 4-12 Effect of Doc2β and Doc2β C2 domains on depolarization-induced secretion

Bovine adrenal chromaffin cells were stimulated with 50-ms depolarisations in whole-cell patch clamp experiments. The capacitance changes (*above*) and the calcium currents (*below*) from cells expressing Doc2β and EGFP were displayed (A). The histogram summarizes the effect of EGFP, Doc2β and C2AB on secretion. The secretion was not significantly different among cells expressing different proteins.

The size of the fusion-competent vesicle pool was measured from the plateau of the capacitance response to a train of depolarisations. The size of the fusion-competent vesicle pool (Figure 4-13) was not different between cells expressing Doc2β from the bicistronic (582±71 fF, n=15) and the fusion construct (567±127 fF, n=7).

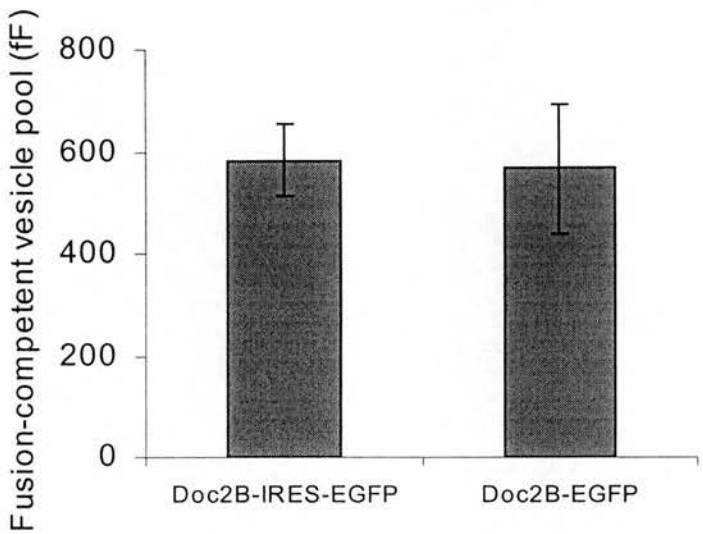

Figure 4-13 The size of the fusion-competent vesicle pool in cells expressing Doc2β from the bicistronic and the fusion construct

The size of the fusion-competent vesicle pool was measured using a train of depolarisations as previously discussed. Histogram shows that the size of the fusion-competent vesicle pools was not different in cells expressing Doc2β and Doc2β-EGFP.

The size of the fusion-competent vesicle pool (Figure 4-14) in cells expressing Doc2β (577±61 fF, n=22) and Doc2β C2 domain (549±164 fF, n=7) were not different from that of EGFP-expressing cells (611±55 fF, n=35).

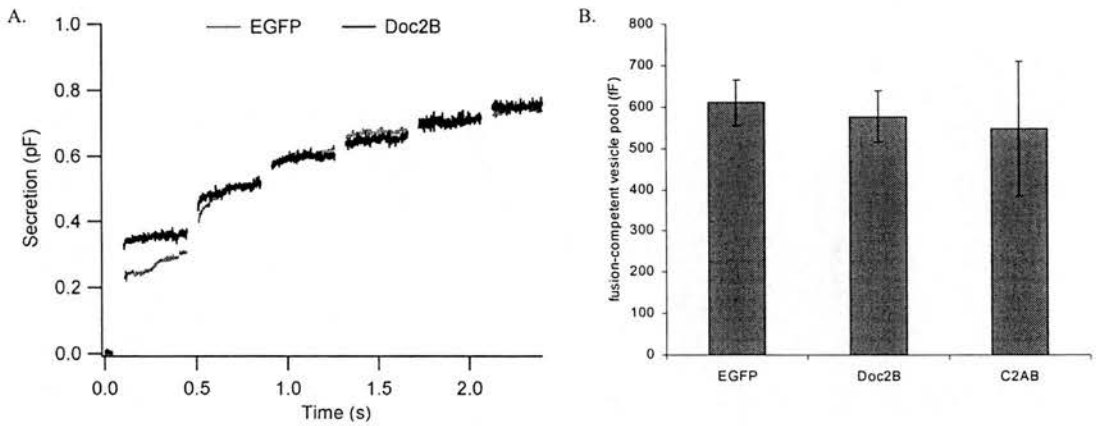

Figure 4-14 The effect of Doc2β on the fusion-competent vesicle pool

(A) Examples of capacitance responses to the stimulation from cells expressing Doc2β and EGFP are superimposed. Histogram shows that the fusion-competent vesicle pool was not affected by expression of Doc2β or Doc2β C2 domain (B).

4.2.6 Effect of Doc2β expression on single vesicle exocytosis

The characteristics and kinetics of individual amperometric events were analysed. The overall amperometric current amplitude in cells expressing Doc2β was 14±0.5 pA (n=663 from 11 cells) which was not significantly different from that of cells expressing Doc2β C2 domain (16±1.2 pA, n=182 from 3 cells) or EGFP (14±0.6 pA, n=549 from 11 cells) (Figure 4-15).

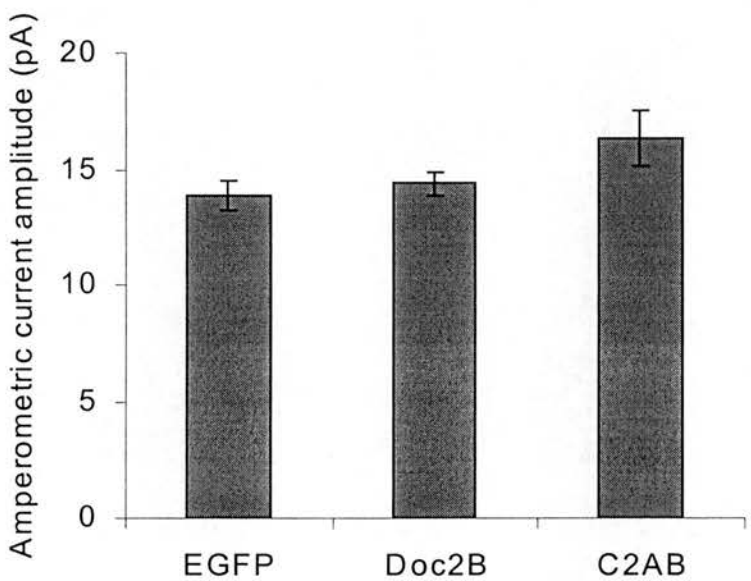

Figure 4-15 Overall amperometric current amplitude

Histogram shows the amperometric current amplitude from cells expressing Doc2β, Doc2β C2 domain and EGFP. The amplitude was not statistically different.

The individual amperometric currents with amplitude higher than 20 pA were analysed in detail. In this selected group of amperometric events, the current amplitude (Figure 4-16A) was not different among cells expressing Doc2β (43±3 pA, n=184 from 11 cells), Doc2β C2 domains (40±3 pA, n=35 from 3 cells) and EGFP (43±2 pA, n=201 from 11 cells). The amperometric charge (Figure 4-16B) in cells expressing Doc2β (1.43±0.07 pC, n=184 from 11 cells) was not different from those of cells expressing EGFP (1.54±0.08 pC, n=201 from 11 cells) and Doc2β C2 domains (1.33±0.09 pC, n=35 from 3 cells). Therefore, the vesicular catecholamine content was not different among cells expressing different proteins in this experiment.

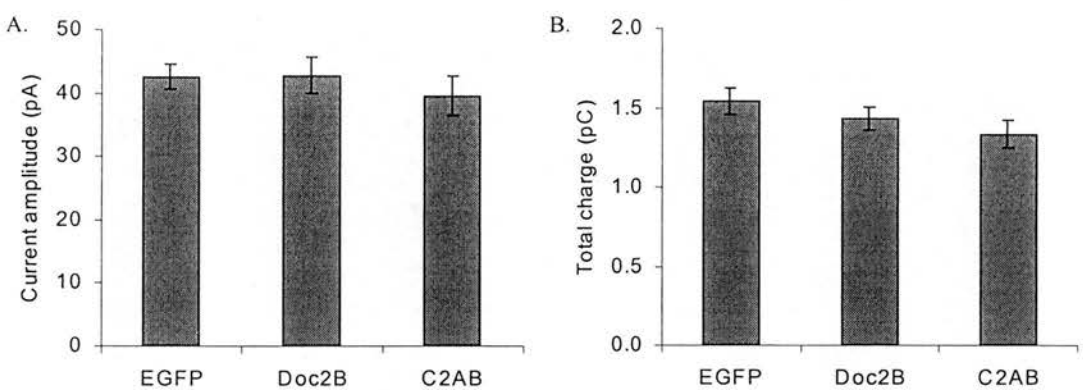

Figure 4-16 Effect of Doc2β on amperometric current amplitude

Histograms show the average amperometric current amplitude (A) and charge (B) from cells expressing different proteins. Both the amplitude and charge from cells expressing Doc2β or Doc2β C2 domain were not significantly different from those of EGFP-expressing cells.

The risetime, halfwidth and the decay time constant were not affected by Doc2β or Doc2β C2 expression (Figure 4-17). These results indicated that the release of catecholamines from single vesicles was not affected by the expression of these proteins.

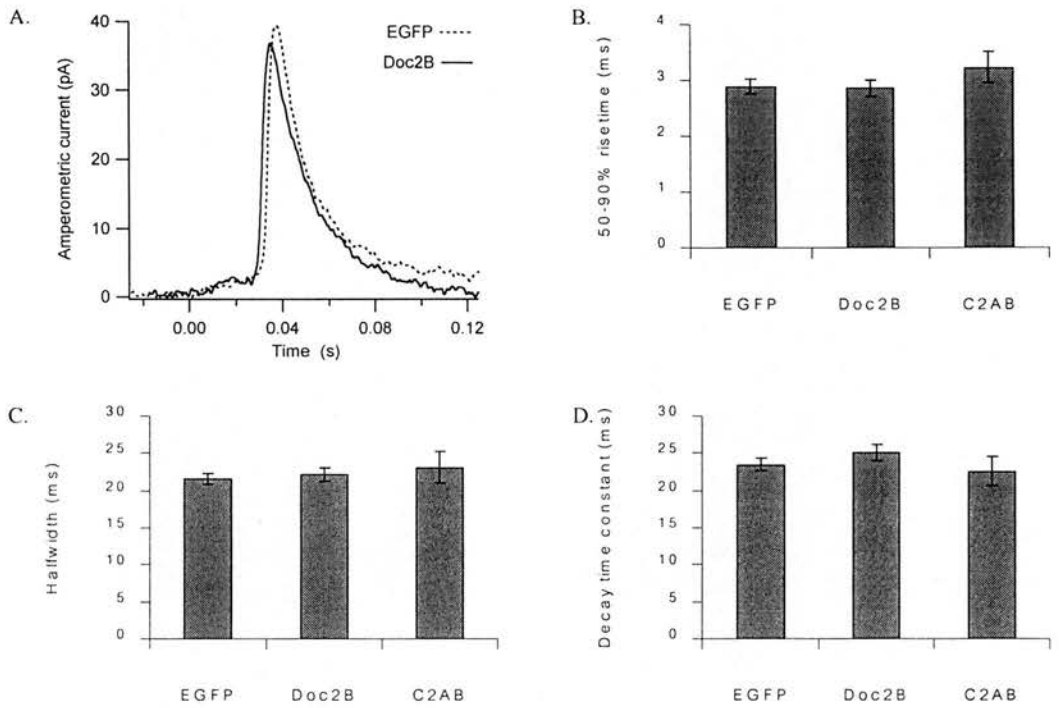

Figure 4-17 Effect of Doc2β on kinetics of single vesicle exocytosis

The amperometric currents from EGFP- and Doc2β-expressing cells were superimposed (A). The 50-90% risetime (B), halfwidth (C) and decay time constant (D) were not affected by expression of Doc2β or Doc2β C2 domains.

The amperometric foot signals were analysed. The amperometric foot amplitude, duration and charge in cells expressing Doc2β and Doc2β C2 domains were not significantly different from those of EGFP-expressing cells (Figure 4-18).

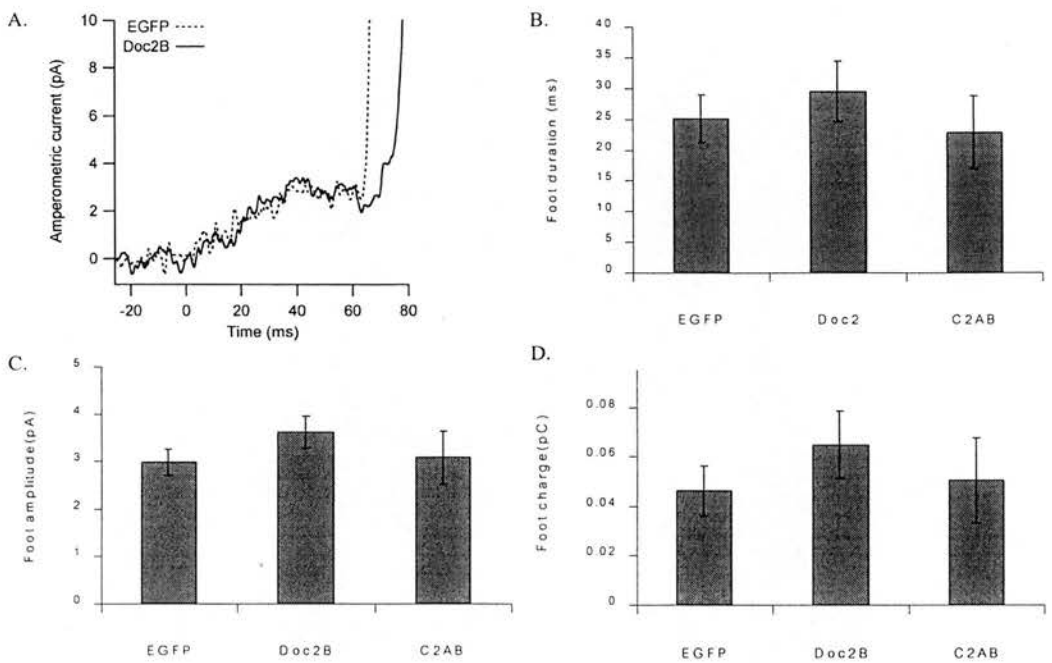

Figure 4-18 The amperometric foot signal was not affected by Doc2β and Doc2β C2 domains

Examples of amperometric foot currents from cells expressing EGFP and Doc2β were superimposed (A). The foot duration (B), amplitude (B) and charge were not significantly different among cells expressing Doc2β, Doc2β C2 domains and EGFP.

4.3 Conclusion

The effect of Doc2β and Doc2β C2 domain (C2AB) expression was studied in primary cultured bovine adrenal chromaffin cells. Expression of Doc2β or C2AB did not affect basal $[Ca^{2+}]_i$, calcium and sodium currents in these cells. Catecholamine secretion was not affected by expression of Doc2β or C2AB. To test if the fusion-competent pool of vesicles was affected by the expression of Doc2β or C2AB, the fusion-competent pool of vesicles was measured by using train of depolarisations. The fusion-competent pool of vesicles was not altered in bovine adrenal chromaffin cells expressing Doc2β or C2AB. The vesicle fusion kinetics was not affected by Doc2β or C2AB expression. These results indicate that Doc2β is not essential for regulated exocytosis of LDCVs in bovine adrenal chromaffin cells.

Chapter 5

Effects of phorbol ester

5.1 Introduction

Diacylglycerol (DAG) is one of the most important second messengers in cellular processes including exocytosis. In chromaffin cells, activation of the muscarinic receptor acts through IP3/DAG pathway to stimulate catecholamine secretion. Phorbol ester (PE) is a tumour enhancer that potently stimulates DAG receptors. Several downstream effectors of PE/DAG have been identified. In bovine adrenal chromaffin cells, stimulation with phorbol ester increases the size of the RRP and highly Ca^{2+}-sensitive pool (HCSP) through activation of protein kinase C (Gillis, Mossner et al. 1996; Yang, Udayasankar et al. 2002). Phorbol ester also induces disruption of cortical actin network and increases the number of docked vesicles (Vitale, Seward et al. 1995; Tsuboi, Kikuta et al. 2001). Another PE/DAG receptor reported lately is Munc13. Munc13 contains a C1 (PE/DAG interacting) domain similar to that of protein kinase C (PKC). The effect of phorbol ester-enhanced synaptic transmission is completely abolished in PE/DAG binding-deficient Munc13 mutant mice (Rhee, Betz et al. 2002). Interestingly, the Doc2-Munc13 interaction is enhanced by phorbol ester. Application of phorbol ester induces the translocation of both Doc2 and Munc13 to plasma membrane. Studies in PC12 cells demonstrate that phorbol ester –induced secretion is enhanced in cells expressing Doc2α (Orita, Naito et al. 1997). To study if the phorbol ester-enhanced exocytosis is potentiated by the expression of Doc2β, the cells were pre-incubated with phorbol ester prior to the stimulation.

5.2 Results

5.2.1 The fluorescence distribution in cells expressing Doc2β-EGFP was not affected by phorbol ester

Phorbol ester enhances the Doc2-Munc13 interaction both *in vitro* and *in vivo*. Munc13 is translocated to plasma membrane after application of phorbol ester. In cells expressing both Doc2β and Munc13, application of phorbol ester mobilises Doc2β and Munc13 to plasma membrane (Duncan, Betz et al. 1999a). To verify if phorbol ester changed the distribution of Doc2β in bovine adrenal chromaffin and PC12 cells, cells expressing Doc2β-EGFP were incubated with 100 nM Phorbol-12-myristate-13-acetate (PMA). The fluorescence distribution in chromaffin and PC12 did not change by PMA incubation (Figure 5-1). However, the cells expressing Doc2β-EGFP also expressed EGFP as discussed earlier. The distribution of EGFP was not changed by PMA and might obscure the distribution of Doc2β-EGFP. Another possibility is that adrenal chromaffin cells express low level of Munc13. Therefore, the interaction between Doc2β and Munc13 might be undetectable in this experiment.

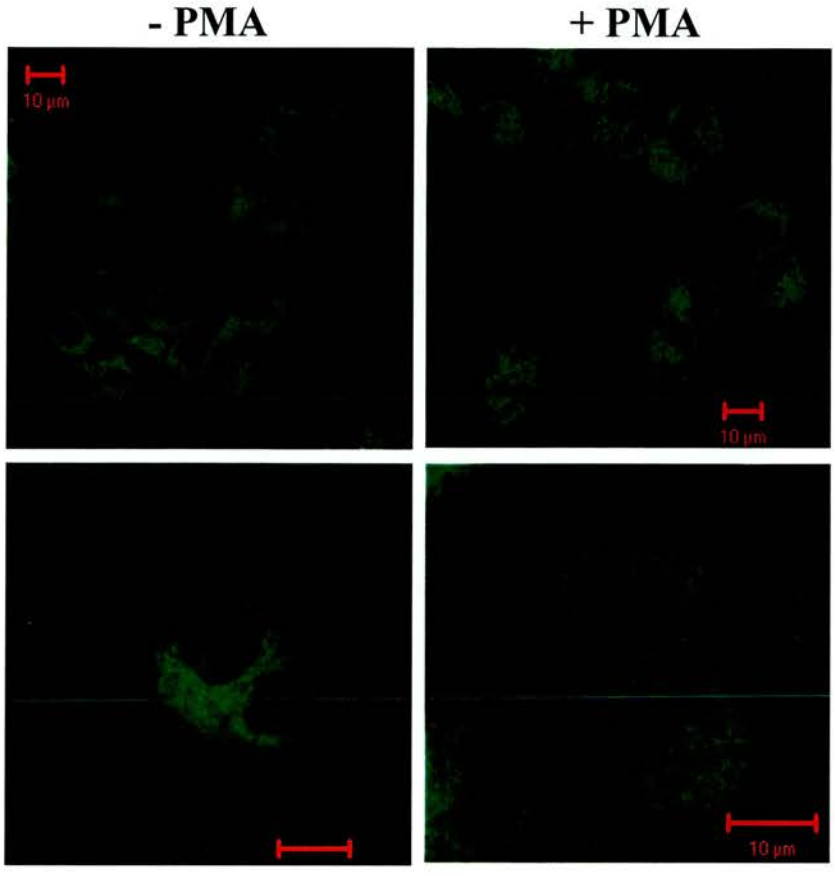

Figure 5-1 Effect of phorbol ester on distribution of Doc2β-EGFP

PC12 cells expressing Doc2β-EGFP were incubated with 100 nM PMA for 10 minutes at 37°C. The cells were fixed with 4% paraformaldehyde and imaged with a confocal microscope. The fluorescence distribution did not change after PMA incubation.

5.2.2 Effect of Phorbol ester on exocytosis

5.2.2.1 High-K^+ stimulation

Catecholamine secretion from a cell-population was studied. Bovine adrenal chromaffin cells were pre-incubated for 10 minutes in Locke's solution with and without 100 nM PMA. The cells were then stimulated for 3 minutes with high-K^+ solution with or without 100 nM PMA. The catecholamine secretion was not enhanced by PMA incubation. The catecholamine secretion with and without PMA incubation in EGFP-expressing cells were11.8±0.7 (n=27) and 11.6±1.5 (n=10) % of total catecholamine. The catecholamine secretion with and without PMA incubation in Doc2β-expressing cells were12.1±0.8 (n=39) and 13.5±1.1 (n=18) % of total catecholamine. The catecholamine secretion with and without PMA incubation in C2AB-expressing cells were11.7±1 (n=28) and 12.1±1.2 (n=10) % of total catecholamine. The secretion after PMA incubation from cell expressing different proteins was not significantly different (Figure 5-2).

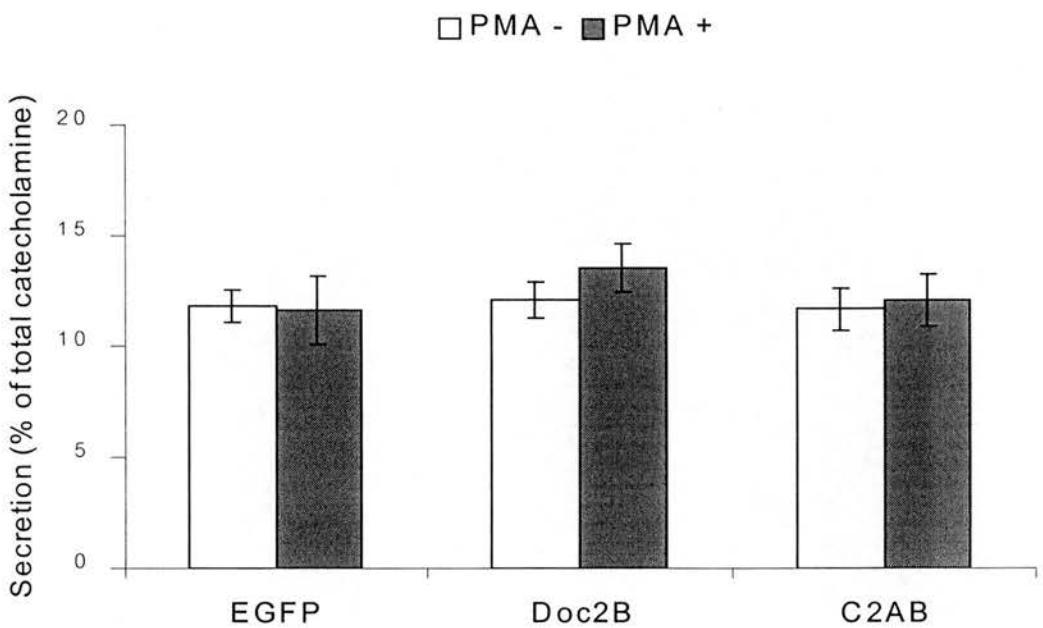

Figure 5-2 Effect of phorbol ester on catecholamine secretion induced by high-K^+ stimulation

Bovine adrenal chromaffin cells were stimulated with high-K^+ solution as discussed previously. For the PMA-incubated group, PMA was present during incubation and stimulation. The secretion was measured as percentages of total catecholamine. The histograms show mean±s.e.m. in cells expressing indicated proteins. PMA did not enhance secretion induced by high-K^+ solution.

5.2.2.2 β-escin permeabilisation

Phorbol ester has been shown to reduce calcium currents in adrenal chromaffin cells (Gillis, Mossner et al. 1996). The effect of phorbol ester on calcium currents might affect the high-K^+ induced secretion. To overcome the effect of phorbol ester on calcium currents, the β-escin permeabilisation method was used. In PMA-incubated group, 100 nM PMA was present before and during stimulation. The permeabilised cells were stimulated by solution containing 1 μM Ca^{2+}. The average catecholamine secretion was similarly enhanced by about 30% in cells expressing different proteins. The catecholamine secretion with and without PMA incubation in EGFP-expressing cells were 30±1.4 (n=12) and 46±5.9 (n=6) % of total catecholamine. The catecholamine secretion with and without PMA incubation in Doc2β-expressing cells were 32±1.5 (n=12) and 43±5.5 (n=6) % of total catecholamine. The catecholamine secretion with and without PMA incubation in C2AB-expressing cells were 34±1.5 (n=12) and 44±1.5 (n=6) % of total catecholamine. The catecholamine secretion after PMA incubation was not significantly different among those groups (Figure 5-3).

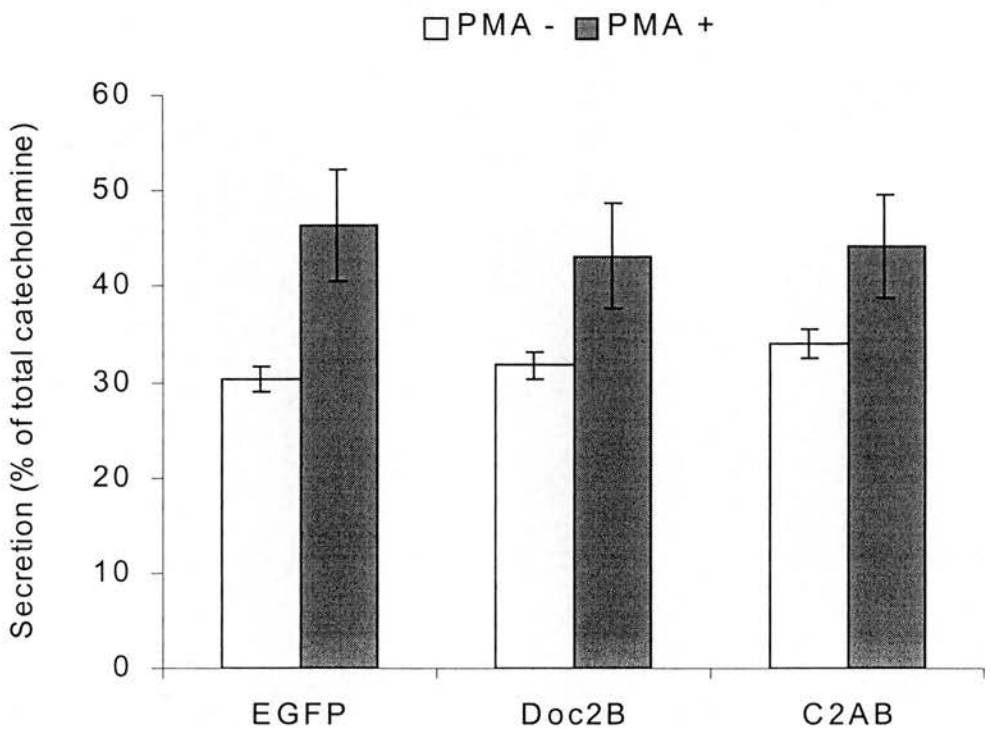

Figure 5-3 Effect of phorbol ester on catecholamine secretion in β-escin permeabilised cells

Permeabilisation was performed as previously discussed. PMA was included during permeabilisation and stimulation in PMA-incubated groups. The secretion was induced by 1 μM Ca^{2+}. The catecholamine secretion was enhanced by PMA. The secretion after PMA incubation were not different among cells expressing Doc2β, Doc2β C2 domain and EGFP.

5.2.2.3 Step depolarisation

To study the small functional pool of vesicles near the plasma membrane (the RRP and SRP), the cells were stimulated with step depolarisations to 10 mV from a holding potential of –70. Calcium currents responded to 50-ms depolarisations were recorded in whole-cell patch clamp. For the PMA-incubated group, the cells were pre-incubated with 100 nM PMA for 5 minutes at 30°C. The calcium currents in cells pre-incubated with PMA showed varying degree of reduction when compared with cells in the same group without PMA incubation (Figure 5-4). The calcium currents with and without PMA incubation in EGFP-expressing cells were 322±28 (n=35) and 217±29 (n=14) pA. The calcium currents with and without PMA incubation were 367±33 (n=22) and 268±34 (n=11) pA in cells expressing Doc2β. The calcium currents with and without PMA incubation were 418±74 (n=7) and 332±60 (n=9) pA in cells expressing Doc2β C2 domains. Similar to the calcium current without PMA incubation, the calcium currents with PMA incubation were not statistically different among cells expressing different proteins. This reduction of calcium current was the reason why the PMA did not enhance high K^+-induced secretion.

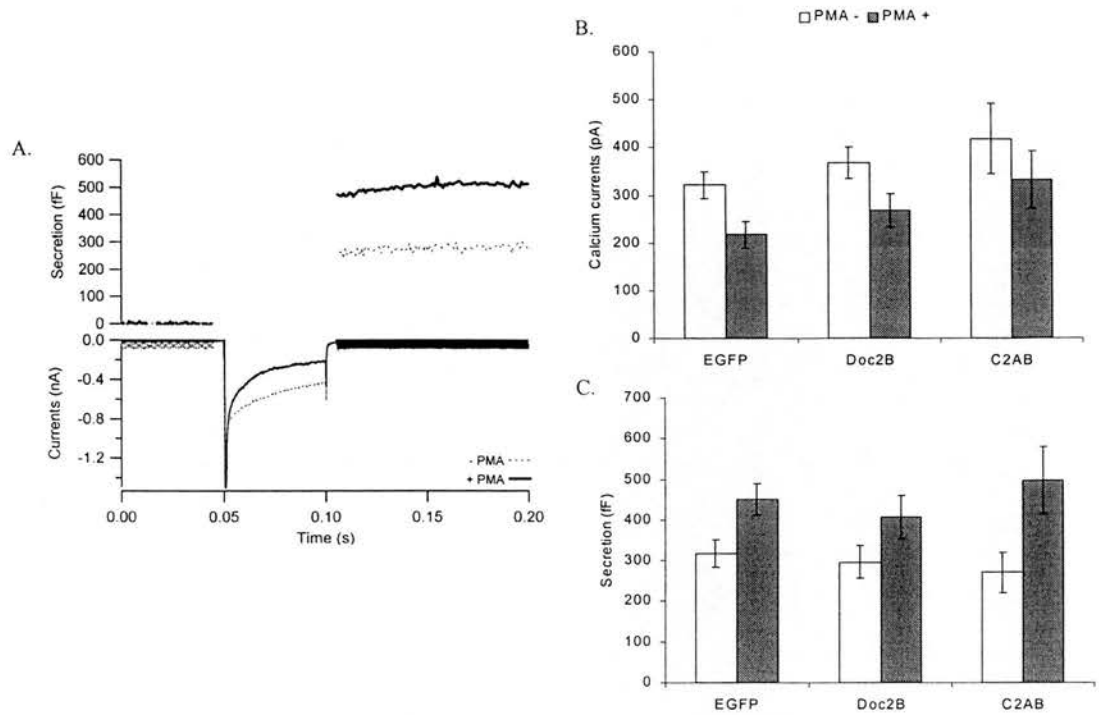

Figure 5-4 Effect of phorbol ester on calcium currents and secretion responded to 50-ms depolarisation

Bovine adrenal chromaffin cells were pre-incubated with 100 nM PMA for 5 minutes at 30°C in PMA-incubated group. The cells were stimulated with a 50-ms depolarisation to 10 mV from a holding potential of –70 mV in whole-cell patch clamp experiments. The calcium currents and membrane capacitance recorded from EGFP-expressing cells with and without PMA incubation were superimposed (A). Note the secretion increases after PMA incubation while the calcium current decreases. The histograms display mean±s.e.m. of calcium currents (B) and capacitance changes (C) from EGFP-, Doc2β- and C2AB-expressing cells with and without PMA incubation. The calcium currents and membrane capacitance changes after PMA incubation were not significantly different among cells expressing EGFP, Doc2β and Doc2β C2 domains.

Despite the reduction of calcium currents, the secretory responses to 50-ms depolarisations were enhanced by PMA. As discussed in the previous chapter, this single depolarisation induced secretion from the RRP. This result was consistent with previous study which application of phorbol ester increases the RRP (Gillis, Mossner et al. 1996). The secretion without and with PMA incubation in EGFP-expressing cells were 317±34 fF (n=35) and 451±38 fF (n=14), respectively. The secretion without and with PMA incubation were 296±40 fF (n=22) and 405±54 fF (n=11) in Doc2β-expressing cells. The secretion without and with PMA incubation in cells expressing Doc2β C2 domains were 270±50 fF (n=7) and 496±83 fF (n=7), respectively. The secretion after PMA incubation was not significantly different among cells expressing different proteins (figure 5-4).

The fusion-competent vesicle pool was estimated by using trains of depolarisations. The fusion-competent vesicle pool was significantly increased by PMA incubation in all cell groups (Figure 5-5). However, the size of this pool after PMA incubation was not significantly different among cells expressing EGFP, Doc2β and Doc2β C2 domains. The size of the fusion-competent vesicle pool with PMA incubation in EGFP-, Doc2β- and C2AB-expressing cells were 1015±86 fF (n=144), 971±106 fF (n=11 and 1136±141 fF (n=7), respectively.

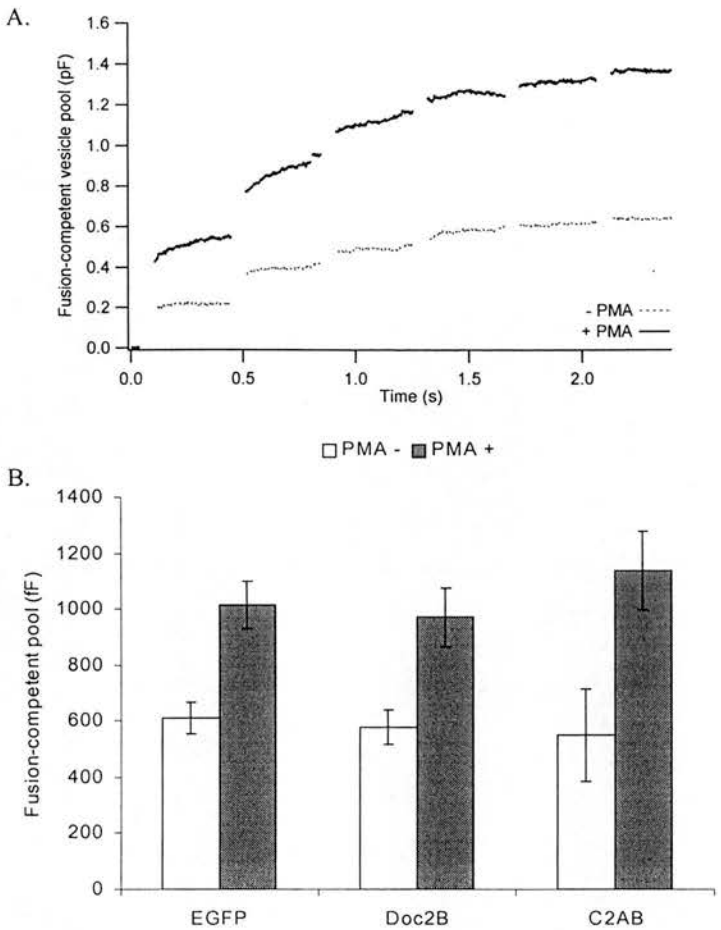

Figure 5-5 Effect of phorbol ester on the size of the fusion-competent vesicle pool

The size of the fusion-competent vesicle pool was measured as previously described. The groups denoted "+PMA" were pre-incubated with 100 nM PMA for 5 minutes at 30°C. Capacitance responses to train of depolarisations from EGFP-expressing cells with and without PMA incubation are superimposed (A). The histograms show the size of the fusion-competent vesicle pool (mean±s.e.m.) from EGFP-, Doc2β- and C2AB-expressing cells. The fusion-competent pools both before and after PMA incubation were not different between cells expressing EGFP, Doc2β and Doc2β C2 domains.

5.3 Conclusion

The effect of phorbol ester on exocytosis in bovine adrenal chromaffin cells was studied. Incubation of bovine adrenal chromaffin cells with 100 nM Phorbol-12-myristate-13-acetate (PMA) enhanced cathecholamine secretion while the calcium currents were reduced. The enhancement of cathecholamine secretion after incubation with PMA was a result of the increase in the size of the fusion-competent vesicle pool. Expression of Doc2β or C2AB did not alter the secretory-enhancement effect of PMA. The fusion-competent vesicle pool similarly increased by nearly 100% in cells expressing EGFP, Doc2β and C2AB.

Summarised results

Table 1: Leak currents

Cells	Mean (pA)	S.E.M.	N
Non-infected	-25.8	1.6	175
EGFP	-24.2	1.9	69
Doc2β	-22.7	2.5	50
Doc2β C2 domains	-22.1	4.4	16

Table 2: Initial membrane capacitance

Cells	Mean (pF)	S.E.M.	N
Non-infected	7.71	0.09	175
EGFP	7.41	0.18	69
Doc2β	7.44	0.13	50
Doc2β C2 domains	7.73	0.26	16

Table 3: Basal intracellular calcium concentration

Cells	- PMA			+ PMA		
	Mean (nM)	S.E.M.	N	Mean (nM)	S.E.M.	N
Non-infected	136	10	76	123	20	11
EGFP	233	25	16	-	-	-
Doc2β	199	15	6	-	-	-
Doc2β C2 domains	218	25	4	-	-	-

Table 4: Calcium currents

Cells	- PMA			+ PMA		
	Mean (pA)	S.E.M.	N	Mean (pA)	S.E.M.	N
Non-infected	673	24	113	401	33	15
EGFP	322	28	35	217	29	14
Doc2β	367	33	22	268	35	11
Doc2β C2 domains	418	74	7	332	60	7

Table 5: Sodium currents

Cells	- PMA			+ PMA		
	Mean (nA)	S.E.M.	N	Mean (nA)	S.E.M.	N
Non-infected	1.81	0.06	113	1.60	0.17	15
EGFP	1.38	0.10	35	1.22	0.09	14
Doc2β	1.60	0.15	22	1.62	0.19	11
Doc2β C2 domains	1.59	0.19	7	1.54	0.22	7

Table 6: Total catecholamine content

Cells	Mean(pMol/cell)	S.E.M.	N
Non-infected	0.16	0.011	8
EGFP	0.16	0.004	12
Doc2β	0.16	0.003	16
Doc2β C2 domains	0.16	0.008	12

Table 7: High-K^+ induced catecholamine secretion

Cells	- PMA			+ PMA		
	Mean (%)	S.E.M.	N	Mean (%)	S.E.M.	N
Non-infected	14.27	1.01	24	14.85	1.22	10
EGFP	11.82	0.75	27	11.60	1.54	10
Doc2β	12.05	0.81	39	13.53	1.07	18
Doc2β C2 domains	11.70	0.96	28	12.08	1.18	10

Table 8: Catecholamine secretion by β-escin permeabilisation in the presence of 1 μM Ca^{2+}.

Cells	- PMA			+ PMA		
	Mean (%)	S.E.M.	N	Mean (%)	S.E.M.	N
Non-infected	32.97	2.25	12	42.07	5.23	6
EGFP	30.32	1.35	12	46.37	5.86	6
Doc2β	31.75	1.47	12	43.15	5.54	6
Doc2β C2 domains	34.06	1.47	12	44.22	5.46	6

Table 9: Capacitance changes in response to 50-ms depolarization

Cells	- PMA			+ PMA		
	Mean (fF)	S.E.M.	N	Mean (fF)	S.E.M.	N
Non-infected	391	29	113	550	93	15
EGFP	317	34	35	451	38	14
Doc2β	296	40	22	407	54	11
Doc2β C2 domains	270	50	7	496	83	7

Table 10: Fusion-competent vesicle pool size

Cells	- PMA			+ PMA		
	Mean (fF)	S.E.M.	N	Mean (fF)	S.E.M.	N
Non-infected	590	33	113	1010	113	15
EGFP	611	55	35	1015	86	14
Doc2β	577	61	22	972	106	11
Doc2β C2 domains	549	164	7	1136	141	7

Table 11: Capacitance response to intracellular dialysis with 10 μM Ca^{2+}.

Cells	30 s		60 s		120 s		N
	Mean (%)	S.E.M.	Mean (%)	S.E.M.	Mean (%)	S.E.M.	
Non-infected	11.03	2.93	25.59	6.18	60.19	17.84	10
EGFP	12.84	2.17	24.62	3.70	53.83	9.60	11
Doc2β	10.19	2.78	22.08	5.09	43.79	9.46	13
Doc2β C2 domains	13.53	3.14	26.06	4.90	44.59	6.24	6

Table 12: Amperometric current response to intracellular dialysis with 10 μM Ca^{2+}.

Cells	30 s		60 s		120 s		N
	Mean (events)	S.E.M.	Mean (events)	S.E. M.	Mean (events)	S.E.M.	
Non-infected	9.8	3.3	26.3	8.0	68.5	18.2	12
EGFP	13.6	2.8	32.4	7.3	68.1	18.3	12
Doc2β	10.2	2.3	28.6	5.6	65.5	10.8	11
Doc2β C2 domains	11.3	7.9	21.0	16.0	38.3	26.2	3

Table 13: Amperometric current amplitude

Cells	Mean (pA)	S.E.M.	N
Non-infected	14.8	0.7	546 (8 cells)
EGFP	13.8	0.7	549 (11 cells)
Doc2β	14.4	0.5	663 (11 cells)
Doc2β C2 domains	16.3	1.2	182 (3 cells)

Table 14: Amperometric current charge

Cells	Mean (pC)	S.E.M.	N
Non-infected	1.64	0.08	178 (7 cells)
EGFP	1.54	0.08	201 (11 cells)
Doc2β	1.43	0.07	184 (11 cells)
Doc2β C2 domains	1.33	0.09	35 (3 cells)

Table 15: Amperometric current 50-90%risetime

Cells	Mean (ms)	S.E.M.	N
Non-infected	3.24	0.17	178 (7 cells)
EGFP	2.89	0.14	201 (11 cells)
Doc2β	2.86	0.15	184 (11 cells)
Doc2β C2 domains	3.23	0.28	35 (3 cells)

Table 16: Amperometric current halfwidth

Cells	Mean (ms)	S.E.M.	N
Non-infected	23.31	0.96	178 (7)
EGFP	21.59	0.79	201 (11)
Doc2β	22.10	0.95	184 (11)
Doc2β C2 domains	23.10	2.11	35 (3)

Table 17: Amperometric current decay time constant

Cells	Mean (ms)	S.E.M.	N
Non-infected	24.35	1.12	178 (7)
EGFP	23.51	0.91	201 (11)
Doc2β	25.12	1.08	184 (11)
Doc2β C2 domains	22.51	1.92	35 (3)

Table 18: Amperometric foot amplitude

Cells	Mean (pA)	S.E.M.	N
Non-infected	3.56	0.33	76 (6)
EGFP	2.99	0.27	61 (4)
Doc2β	3.61	0.34	56 (4)
Doc2β C2 domains	3.08	0.56	28 (3)

Table 19: Amperometric foot duration

Cells	Mean (ms)	S.E.M.	N
Non-infected	24.0	3.44	76 (6)
EGFP	25.1	3.93	61 (4)
Doc2β	29.5	4.94	56 (4)
Doc2β C2 domains	22.9	5.95	28 (3)

Table 20: Amperometric foot charge

Cells	Mean (fC)	S.E.M.	N
Non-infected	52.8	10.29	76 (6)
EGFP	46.2	10.18	61 (4)
Doc2β	64.8	13.70	56 (4)
Doc2β C2 domains	50.4	17.23	28 (3)

Chapter 6

DISCUSSION

Discussion

6.1 Semliki forest virus (SFV) transduction system for Exocytosis study

The semliki forest virus (SFV) transduction system has been used for heterologous gene expression in wide range of host cells. The method is safe because two levels of safety measures are introduced into the system, the separation of the viral structural and nonstructural proteins and the mutation of the viral envelope protein. The reversion of the mutation was less than 10^{-7} in this experiment consistent with previously reported (Berglund, Sjoberg et al. 1993). The viral particles are easy to prepare. Introduction of the DNA-based system simplifies the preparation of viral particles (DiCiommo and Bremner 1998). Using calcium phosphate transfection method in HEK293T cells, the viral production obtained was as high as that obtained by using electroporation. This method will be useful because the calcium phosphate transfection method is not expensive and needs no special equipment.

The adrenal chromaffin cells are a good model cell for studying exocytosis. The cells possess the exocytotic machinery similar to neurons. The relatively large cells permit the use of high resolution techniques to study of exocytosis. However, the study of exocytosis in these cells is hindered by the lack of a reliable method to express genes. Primary cultures of bovine adrenal chromaffin cells are normally difficult for heterologous gene expression. Using the SFV vector system, a very high efficiency of infection and protein expression was obtained. The protein expression was detected early after SFV infection. The process took longer for the larger proteins. However, proteins as large as 73 kDa (Doc2β-EGFP) were detected within

12 hours post-infection. The level of protein expression was heterogeneous among infected cells. This is probably due to the differences in the multiplicity of infection (MOI). However, this pattern of expression did not change when lower MOI was used. The viral infected cells will eventually die due to apoptosis. As shown in the experiment, the deterioration of calcium currents was prominent at 72 hours after infection. This result is consistent with a previous report in BHK21 cells where SFV infection leads to apoptosis at 48 hours after infection (Glasgow, McGee et al. 1998). Therefore, there is a reasonably long window in which the experiments can be performed on SFV-infected cells.

The enhanced green fluorescent protein (EGFP) was used as a reporter for gene expression. EGFP is a red-shifted variant of wild-type green fluorescent protein (GFP). The EGFP has been optimised for brighter and higher fluorescence expression in mammalian cells. EGFP is 239 residues. However, expression of EGFP does not alter the function and localisation of proteins (Ashery, Betz et al. 1999; Ashery, Varoqueaux et al. 2000; Tsuboi, Zhao et al. 2000; Molinete, Dupuis et al. 2001). The distribution and function of Doc2β-EGFP were not disturbed when expressed in HEK293 cells (Duncan, Betz et al. 1999a). The distribution of EGFP in bovine adrenal chromaffin cells in this experiment was similar to previously reported (Ashery, Betz et al. 1999; Knight 1999). The fluorescence was evenly distributed in cytoplasm. High nuclear fluorescence was common. This pattern is also observed when EGFP is expressed in pancreatic β-cells using adenovirus vector (Molinete, Dupuis et al. 2001). The fluorescence distribution in PC12 cells expressing EGFP was different from that of chromaffin and HEK293T cells. PC12 cells expressing

EGFP were devoided of nuclear fluorescence. This phenomenon was not a result of differences in protein expression level or multiplicity of infection because imaging at different times or using different multiplicity of infection did not affect the fluorescence distribution.

Despite the late onset of cytotoxicity reported previously and no obvious morphological change observed in this experiment, the SFV-infected cells showed some deterioration early after infection. The basal intracellular Ca^{2+} concentration ($[Ca^{2+}]_i$) , the calcium and sodium currents were affected by SFV infection during the course of the experiments. This might indicate the early sign of cytotoxicity. It is proposed that viral infected cells initiate a program cell death or apoptosis to prevent viral replication and distribution. The apoptosis induced by SFV infection is reported in BHK21 cells at 48 hours after transfection with SFV vectors (Glasgow, McGee et al. 1998). Ca^{2+} is a major messenger in the apoptotic cascades (Ermak and Davies 2002). The release of Ca^{2+} from intracellular stores or the influx of Ca^{2+} from extracellular fluid during the apoptosis increases the concentration of intracellular Ca^{2+}. Although, the level of $[Ca^{2+}]_i$ was well below the threshold for secretion reported for chromaffin cells, several changes in the SFV-infected cells were related to the increase in $[Ca^{2+}]_i$. The calcium and sodium currents were significantly affected by SFV infection. This effect was also observed early after infection. The reduction of calcium currents was observed previously in SFV-infected bovine adrenal chromaffin cells (Ashery, Betz et al. 1999; Pan, Jeromin et al. 2002). However, the mechanism of the inhibition of calcium and sodium currents is still unclear. It was shown in this experiment that the reduction of calcium and sodium currents was correlated with the increase in $[Ca^{2+}]_i$. This result is consistent with

previous reports that Ca^{2+} induces inactivation of calcium and sodium channel and sustained elevation of $[Ca^{2+}]_i$ reduces the number of surface sodium channels (Brehm and Eckert 1978; Gera and Byerly 1999; Kobayashi, Shiraishi et al. 2002; Tan, Kupershmidt et al. 2002).

Although, the increase of intracellular Ca^{2+} concentration is able to explain the effects of SFV infection, others explanations are possible. Previous studies show that calcium currents are reduced in SFV-infected cells despite a normal basal $[Ca^{2+}]_i$ (Ashery, Betz et al. 1999). However, the reduction of calcium currents in that experiment is only slight and non-significant. The further reduction of calcium currents at 72 hours after infection indicated that the effect was correlated with the viral protein expression, the EGFP expression and viral-induced apoptosis. It was proposed that the viral infected-cells eventually die because of virus takes over the cellular expression machinery. However, the expression of native proteins in SFV infected chromaffin cells is not affected as long as 48 hours after infection (Duncan, Don-Wauchope et al. 1999b). Therefore, the reduction of calcium and sodium current is unlikely to be the result of the decreased production of channel proteins by such a mechanism. It is possible that the viral proteins or the EGFP used as a reporter for gene expression affected the calcium and sodium currents. This is evidenced in ventricular myocyte where expression of GFP using lipid transfection method inhibits calcium currents (Tateyama, Zong et al. 2001).

Despite the effect on $[Ca^{2+}]_i$, calcium and sodium currents, SFV infection did not affect the catecholamine secretion in bovine adrenal chromaffin cells. This result is consistent with previous studies which demonstrate that SFV infection does not

interfere with vesicle trafficking in adrenal chromaffin cells (Ashery, Betz et al. 1999; Knight 1999; Duncan, Don-Wauchope et al. 1999b). The total catecholamine content was not affected by SFV infection. The vesicular catecholamine content was also not affected by SFV infection as determined from the integral amperometric currents. Therefore, the metabolic cascades of catecholamine synthesis are preserved in SFV-infected cells. Single vesicle exocytosis was not affected by SFV infection. The number of fusion-competent vesicles estimated by repetitive stimulation was not affected by SFV infection. The size of this pool estimated by this protocol was about 500-600 fF. This number is consistent with the size of the pool estimated by flash photolysis of caged-Ca^{2+} experiments. The depolarization protocol also revealed another smaller pool of vesicles consistent with the readily releasable pool (RRP) reported earlier (Xu, Rammner et al. 1999; Voets 2000). This pool contributed to the secretion in response to a 50-ms depolarization. The fact that the secretion induced by a 50-ms depolarization in SFV infected cells was not significantly reduced despite the reduction of calcium currents by 50% indicated either the stimulus was sufficient to deplete the pool or this pool was increased in SFV infected cells. The increase of the RRP in SFV-infected cells is possible because the higher basal $[Ca^{2+}]_i$. The time course of secretion during Ca^{2+}dialysis through patch pipettes argues against the increase of the RRP because the course of the catecholamine secretion was not affected in SFV-infected cells. However, the slow dialysis might overlook the small RRP. More studies are needed before one can conclude the precise effect of SFV infection on the RRP. Sustained stimulation by Ca^{2+}dialysis through patch pipettes or in β-escin permeabilised cells elicited similar amount and course of secretion in SFV-infected and non-infected cells. Such stimulation not only induced secretion

from the small fraction of vesicles near plasma membrane but also those inside the cells. Therefore, this result indicated that the vesicle recruitment was not affected by SFV infection. The Ca^{2+}-dependency of secretion in β-escin permeabilised cells was not affected by SFV infection. The responses to the application of phorbol ester indicate that the phorbol ester/diacylglycerol cascades are preserved in SFV infected cells. Phorbol ester enhances secretion by several mechanisms. The RRP, fusion-competent pool and the rate of vesicle supply are increased by phorbol ester.

Therefore, the SFV is an efficient method for expression that can be used for exocytosis study. This method provides a reasonably long window that the experiment can be performed. However, the effects of the SFV infection on $[Ca^{2+}]_i$, calcium and sodium currents have to be considered. The development of new generation of SFV with lower cytotoxicity would diminish the side effect of this method and provides a better means for gene expression.

6.2 Role of Doc2β in regulated exocytosis of large dense-core vesicles in bovine adrenal chromaffin cells

Proteins in the family of Doc2 are promising candidates in regulated exocytosis because they are vesicle-associated proteins containing C2 domains that Ca^{2+}-dependently interact with phospholipids. Moreover, these proteins interact with Munc13 and Munc18, both of which are important for synaptic transmission. The discoveries that Doc2α and the Doc2α-Munc13 interaction are important for regulated exocytosis in PC12 cells and synapses suggest the role of Doc2 in regulated exocytosis. Most proteins that participate in regulated exocytosis have both neuronal isoforms as well as the ubiquitous counterparts. Doc2β is a ubiquitous isoform of Doc2 whose function in regulated exocytosis remains mysterious. There are several convincing evidence that this protein performs a similar function in regulated exocytosis as its neuronal-specific counterpart. Previous studies in PC12 cells reveals that expression of full-length Doc2α enhances exocytosis while expression of Doc2α C2 domains inhibits exocytosis. Therefore, the effect of both full-length Doc2β and Doc2β C2 domains was studied in this experiment. Doc2β is highly homologous among different species (Naito, Orita et al. 1997; Verhage, de Vries et al. 1997). The mouse Doc2β was used in this experiment. Bovine adrenal chromaffin cells do not express any known isoform of Doc2 but they are good models for studying the effect of Doc2β because adrenal chromaffin cells express Doc2β interacting proteins, Munc13 and Munc18. Full-length Doc2β was expressed either individually or as a fusion protein with EGFP (Doc2-EGFP). Adrenal chromaffin cells expressing either Doc2β or Doc2β-EGFP were not different

functionally. Doc2β C2 domains (C2AB) was expressed as a fusion protein with EGFP. Bovine adrenal chromaffin cells expressing Doc2β-EGFP showed both intracytoplasmic and nuclear distribution. This pattern of fluorescence distribution was similar to cell expressing EGFP alone. However, SDS-PAGE confirmed that Doc2β-EGFP was actually expressed in these cells. The similarity of fluorescence distribution between cells expressing Doc2β-EGFP and EGFP alone was probably because of the cells expressing Doc2β-EGFP also expressed EGFP as shown in SDS-PAGE. Previous studies reported that HEK293 cells expressing Doc2β-EGFP showed cytoplasmic punctate fluorescence. Some cells did show the punctate distribution in this experiment. However, most cells did not. This was probably because the background fluorescence of the EGFP. The distribution of Doc2β C2 domains was similar to that of Doc2β. Expression of Doc2β or Doc2β C2 domains did not alter cellular functions studied in this experiments. The basal intracellular Ca^{2+} concentration, the calcium and sodium currents were not significantly different from that of cell expressing EGFP alone.

The effect of Doc2β and Doc2β C2 domains on exocytosis was studied. Based on the hypothesis that Doc2β is involved with vesicle recruitment, Doc2β expression should enhance secretion and increase the functional pools of vesicles near plasma membrane (the fusion-competent vesicle or primed-pool). However, secretion was not enhanced by Doc2β expression. The fusion competent-vesicle pool and the rapidly releasable pool (RRP) were not altered in this study. The Ca^{2+}-dependency of catecholamine secretion was not different from that of control cells. The effect of phorbol ester enhancement of secretion was not potentiated by the expression of

Doc2β. The expression of Doc2β C2 domains did not alter the secretory function in adrenal chromaffin cells. These results indicate that Doc2β is not involved in the regulated exocytosis of large dense-core vesicles in bovine adrenal chromaffin cells. However, it does not exclude the possible role of Doc2β in regulated exocytosis in other cells especially neurons. Adrenal chromaffin cells do not express any known isoform of Doc2 and express only a low level of Munc13 (Ashery, Varoqueaux et al. 2000; Duncan, Apps et al. 2000a). Therefore, these cells may not use Doc2 and Doc2-Munc13 mechanisms in regulated exocytosis. The low level of Munc13 in adrenal chromaffin cells could be the reason why expression of Doc2β did not potentiate catecholamine secretion. A previous study demonstrates that expression of Munc13 enhances secretion in bovine adrenal chromaffin cells by increasing the rate of vesicle priming while the number of docked vesicles is not affected (Ashery, Varoqueaux et al. 2000). The mechanism of Munc13-enhanced priming is through the interaction with syntaxin (Richmond, Weimer et al. 2001). The Munc13-syntaxin interaction is neither Ca^{2+} nor phorbol ester dependent. Therefore, the function of the Munc13-phorbol ester interaction in physiological condition whether it is just to mobilise Munc13 to plasma membrane for the interaction with syntaxin or to induce the Munc13-Doc2 interaction needs to be clarified. It would be interesting to see if the expression of both Doc2β and Munc13 in adrenal chromaffin cells would potentiate the secretory enhancement effect of Munc13 alone.

Doc2β also interacts with Munc18. Recent studies in adrenal chromaffin cells revealed that Munc18 is important for vesicle docking. Overexpression of Munc18-1 in bovine adrenal chromaffin cells increases the fusion-competent vesicle pool and

accelerates vesicle supply (Voets, Toonen et al. 2001a). It is proposed that the mechanism of Munc18-enhanced docking is through the interaction with some vesicular proteins. Although Doc2β is a vesicle-associated protein that interacts with Munc18, the results from this experiment do not support the role of Doc2β in vesicle docking.

Several lines of evidence indicate that Doc2 function may not be specific only to regulated exocytosis. Doc2β is expressed not only in tissue having regulated exocytosis but also in other tissues that do not use regulated exocytosis such as heart, lung and spleen (Sakaguchi, Orita et al. 1995). Doc2α is also expressed in testis (Orita, Sasaki et al. 1995). The third ubiquitous isoform of Doc2, Doc2γ, was discovered recently (Fukuda and Mikoshiba 2000b). Doc2γ does not have Ca^{2+}-dependent activity. It is possible that Doc2 participates in other intracellular transportation pathways. This is supported by a study in BHK cells where both Doc2α and Doc2β interact with cytoplasmic dynein. The role of cytoplasmic dynein in regulated exocytosis is not well understood but it is involved in intracellular membrane transport (Aniento, Emans et al. 1993). The spatiotemporal distribution of Doc2β also suggests a non-secretory function for Doc2β. The expression of Doc2β early before the detection of synaptogenesis in rat embryos implies the other functions of Doc2β in neuronal development such as cell proliferation or synaptogenesis (Korteweg, Denekamp et al. 2000). Further studies are necessary to clarify the cellular functions of Doc 2β and others Doc2 isoforms.

Conclusion

1. Semliki Forest Virus (SFV) transduction system is an efficient method for gene expression in primary cultures of adrenal chromaffin cells. Almost 100% of cells can be transfected by this method. The expression can be detected as early as 6 hours after infection. The expression of larger proteins is slower than the expression of smaller proteins. Proteins as large as 73 kDa can be detected within 12 hours after infection.

2. Semliki Forest Virus infection does not affect the secretory pathway in bovine adrenal chromaffin cells within 30 hours after infection. The catecholamine content and the secretion are not affected by SFV infection within this time window.

3. Semliki Forest Virus infection affects the basal intracellular calcium concentration ($[Ca^{2+}]_i$), calcium and sodium currents. These effects are observed already at 15 hours after infection and progress with time. The reduction of calcium and sodium currents are possibly secondary to the increase in $[Ca^{2+}]_i$.

4. High titer of Semliki Forest Virus can be achieved by using calcium phosphate transfection method. The titer of $5x10^8$/ml is obtained in this experiment.

5. Doc2β is not essential for regulated exocytosis of large dense-core vesicles in bovine adrenal chromaffin cells. Expression of full-length Doc2β or the N-terminal deletion of Doc2β (C2AB) did not affect catecholamine secretion in these cells.

Perspectives

The results from these experiments demonstrated that overexpression of Doc2β or Doc2β C2 domain (C2AB) did not have any effect on regulated exocytosis of large-dense core vesicles in bovine adrenal chromaffin cells. This is likely that Doc2β is not essential for regulated secretion in these cells. However, the function of Doc2β in regulated exocytosis in other secretory cells especially neurons is still promising. The studies here generate several ideas for further studies the effect of Doc2β in regulated exocytosis.

1. Bovine adrenal chromafiin cells do not express any know isoform of Doc2. Therefore, it might be interesting to study the effect of Doc2β expression in neurons which are known to express Doc2β.

2. Doc2β has been shown to interacts with Munc13 (Orita, Naito et al. 1997; Mochida, Orita et al. 1998) and Munc18 (Verhage, de Vries et al. 1997). It would be useful to study if the Doc2β-EGFP used in these experiments are able to interact with Munc13 and Munc18 *in vitro* or *in vivo*.

3. The distribution of Doc2β could not be precisely determined in these experiments. This was because of the cells expressing Doc2β-EGFP also expressed EGFP. The distribution of Doc2β could be determined by using Doc2β-specific antibody. Unfortunately, there is no commercially available Doc2β-specific antibody. Therefore, a new vector that expresses only a fusion

protein of Doc2β and a marker such as HA or EGFP should be used so that the Doc2β distribution can be detected with anti-HA or anti-EGFP antibodies.

4. The importance of Doc2-Munc13 interaction in regulated exocytosis has been demonstrated in PC12 cells and neurons (Orita, Sasaki et al. 1996; Mochida, Orita et al. 1998). Although no known Doc2 isoform has been discovered in bovine adrenal chromaffin cells and overexpression of Doc2β in these cells did not affect exocytosis, it can not be excluded that bovine adrenal chromaffin cells might express other isoforms of Doc2. Therefore, it is interesting to identify if the Doc2-Munc13 interaction is essential for regulated exocytosis in these cells. This can be achieved by overexpression of Munc13-interacting domain of Doc2 (Mid). Mid is highly conserved among members of Doc2 family. Mid domain interrupts Doc2-Munc13 interaction both *in vitro* and *in vivo* (Orita, Naito et al. 1997; Mochida, Orita et al. 1998). If the Doc2-Munc13 interaction is important for regulated exocytosis, overexpression of Mid would inhibit secretion.

5. The level of Munc13 expression in bovine adrenal chromaffin cells is very low (Ashery, Varoqueaux et al. 2000). Expression of Doc2β alone in these cells might not significantly increase Doc2β-Munc13 interaction. Therefore, the effect of Doc2β expression alone might not be seen. Overexpression of Munc13-1 in bovine adrenal chromaffin cells enhanced rate of vesicle priming and secretion (Ashery, Varoqueaux et al. 2000). It might be interesting to study if expression of both Doc2β and Munc13-1 in these cells would produce more secretion than overexpression of Munc13-1 alone.

Chapter 7

APPENDICES

Appendix I

Patch clamp Membrane Capacitance Measurements

Membrane capacitance measurements have been used in combination with patch clamp to study exocytosis and endocytosis at high resolution. The general background of the membrane capacitance measurement comes from the three-component equivalent circuit proposed for the pipette-cell assembly in whole-cell or perforated configuration (Neher and Marty 1982). The membrane lipid bilayer, which separates the intracellular and extracellular ions, is equivalent to the capacitor (Figure 7-1). Change in membrane surface area by exocytosis or endocytosis is accompanied by the corresponding change of membrane capacitance.

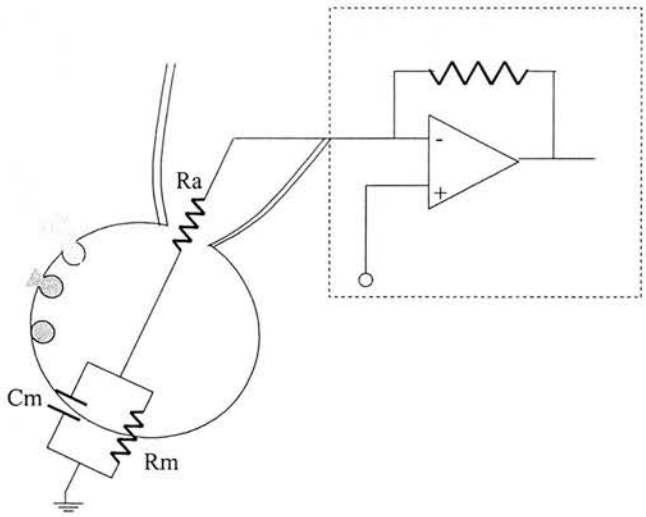

Figure 7-1 Three-component equivalent circuit

A simplified three-component equivalent circuit of pipette-cell assembly in whole-cell or perforated configuration consists of two resistors and a capacitor. Ra is the access resistance at the pipette tip, Rm is membrane resistance and Cm is membrane capacitance.

Several methods for membrane capacitance measurement have been developed. The most popular method is using the sinusoidal wave and a phase-sensitive detector or lock-in amplifier (Lindau and Neher 1988). A sinusoidal voltage is applied to a cell at a hyperpolarised holding potential. The phase and the magnitude of the resulting current are analysed with the implemented hardware or software lock-in. The resulting sinusoidal current consists of a component in phase and a component 90° out of phase with the sinusoidal voltage (Figure 7-2).

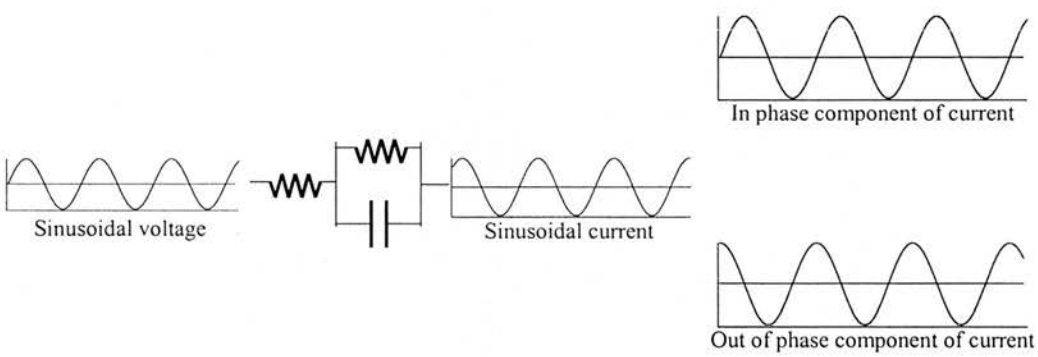

Figure 7-2 Current response to a sinusoidal voltage stimulus of the resistor-capacitor (RC) circuit

The current response to a sinusoidal voltage stimulus of a RC circuit is a sinusoidal wave of the same frequency as the voltage stimulus. The lock-in amplifier deciphers the current into the component in phase and 90° out of phase with the voltage stimulus.

The admittance (Y), the ratio of the sinusoidal current to the sinusoidal voltage stimulus, can be rewritten in a form of complex number.

$$Y(\omega) = (1+j\omega RmCm)/Rt(1+j\omega RpCm)$$

$$Rt = Ra+Rm$$

$$Rp = RaRm/(Ra+Rm)$$

Or $$Y(\omega) = Ga(Gm + j\omega Cm)/(Ga + Gm + j\omega Cm)$$

$$Ga = 1/Ra$$

$$Gm = 1/Rm$$

Or $$Y(\omega) = A + jB$$

$$A = b(1 + x^2a)/(1 + x^2a^2)$$

$$B = bx(1 - a)/(1 + x^2a^2)$$

$$b = 1/(1/Ga + 1/Gm)$$

$$a = b/Ga$$

$$x = \omega Cm/Gm$$

The in phase and out of phase outputs from the phase-sensitive detector are proportional to the real and imaginary component of the admittance, respectively. The access conductance, membrane conductance and membrane capacitance are calculated from the admittance (Gillis 1995).

$$Ga = A + B^2/(A - b)$$

$$Gm = bGa/(Ga - b)$$

$$Cm = 1/\omega Ga^2/(Ga - b)(A - b)/B$$

There are some considerations for using this method of membrane capacitance measurement. The sinusoidal voltage amplitude must not induce a non-linear membrane conductance change during the capacitance measurement. Therefore, the sinusoidal voltage amplitude should not be too high. The admittance of the capacitor depends on the sinusoidal frequency. At the very low frequency, the total admittance of the three-component circuit is close to 1/Rt and at high frequency this value approaches 1/Ra. Normally a sinusoidal voltage of about 25-mV amplitude and 1 kHz is used. The EPC-9 and a software lock-in extension of Pulses program were used in this experiment. The circuit parameter was calculated according to Lindau-Neher technique implementing sine+DC method (Figure 7-3).

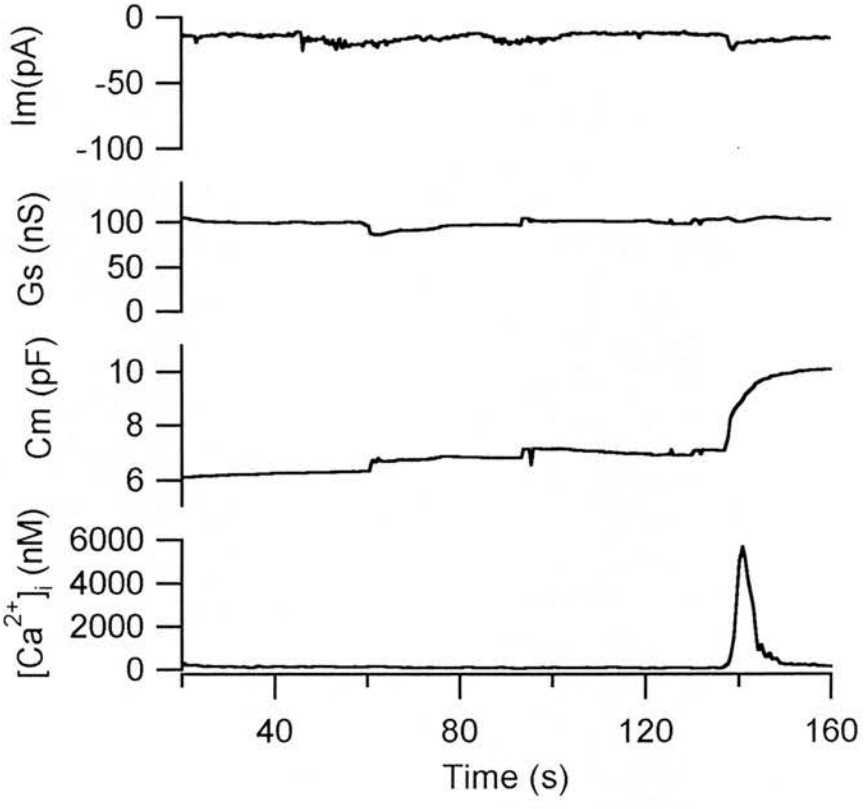

Figure 7-3 Low resolution capacitance recording

The membrane current (Im), Series (access) conductance (Gs), membrane capacitance (Cm) and $[Ca^{2+}]_i$ recorded with the X-chart extension of pulse software. The capacitance increase was observed where the $[Ca^{2+}]_i$ increase without significant change of Gs.

Appendix II

Electrochemical detection of catecholamines release from single bovine adrenal chromaffin cells

Epinephrine and norepinephrine released from adrenal chromaffin cells are among several secreted products that are oxidisable. At the redox potential, half of the catecholamines are in oxidised form and another half in reduced form. Application a potential exceeding the redox potential favours the conversion of the catecholamines to oxidised form (Figure 7-4).

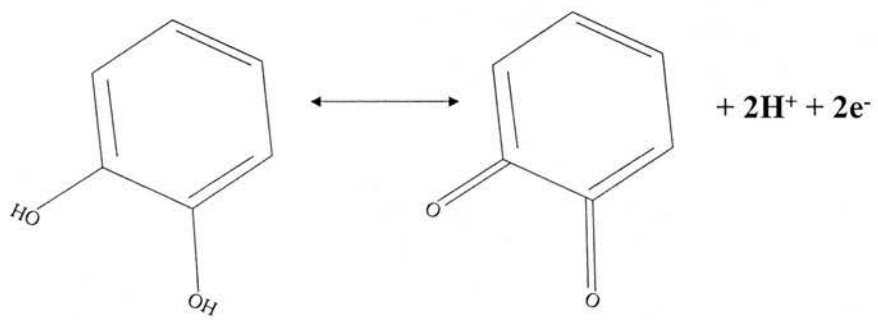

Figure 7-4 Oxidation of catechol from catecholamine to a quinone derivatives.

Catechol nucleus of the catecholamines can be oxidised to its quinone products. Each catechol molecule gives two electrons in the oxidation reaction.

The release of catecholamine from adrenal chromaffin cells can be detected by using electrochemical detection method. A carbon-fiber microelectrode is placed close to plasma membrane with a constant voltage at least 200 mV beyond the redox potential of catecholamine applied. The catecholamines released from the vesicles diffuse to the electrode. The electron transfer at the surface of the carbon fiber microelectrode produces the amperometric current (Figure 7-5).

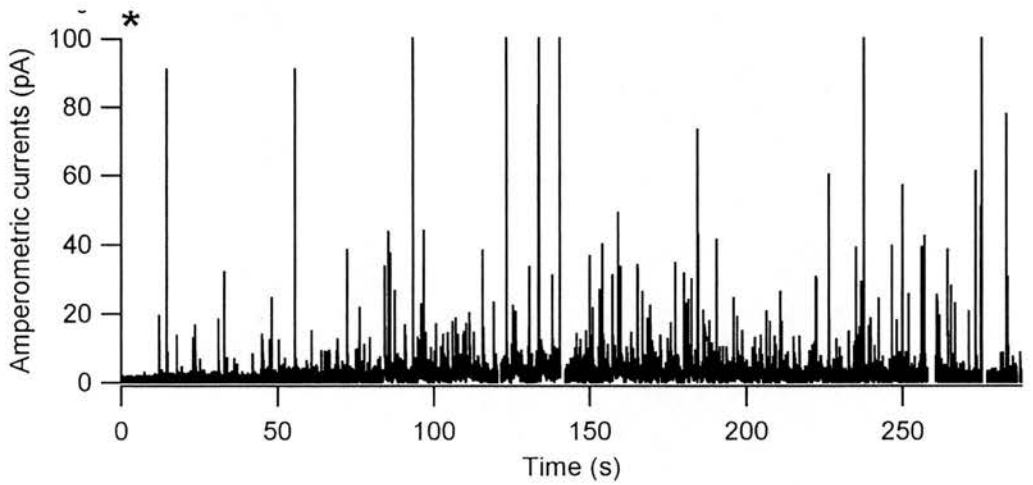

Figure 7-5 Amperometric current recording from a chromaffin cell

A bovine adrenal chromaffin cell was dialysed with pipette solution containing 10 μM Ca^{2+} in the whole-cell patch clamp. A carbon-fiber microelectrode placed close to plasma membrane detected the catecholamine release. Asterisk indicates the time when whole-cell was achieved. Each spike indicated the fusion of single vesicle.

The advantages of the electrochemical detection are that the released products are directly monitored and it is not interfered by concomitant endocytosis. The amperometric currents are detected with a certain delay after stimulation despite the electrode being close to the plasma membrane (Chow, von Ruden et al. 1992). In adrenal chromaffin cells, this delay is much longer than in synapses. Adrenal chromaffin cells utilise the same secretory machinery as synapses. The synaptic vesicles are co-localised with calcium channel in synapses to allow rapid release. Such localisation is not existed in adrenal chromaffin cells so the secretion occurs with a longer delay. The latency of each amperometric event is measured as the time between the beginning of the stimulation to the beginning of the amperometric event. The latency distribution of the amperometric events gives the information about the frequency and amount of secretion.

Characteristics of individual amperometric event are determined by the time course of catecholamine release, the diffusion from the release site to the electrode surface and the rate of electron transfer at the surface of the electrode. The rate of electron transfer at the surface of the electrode is very fast so that it can be negligible. Therefore the characteristic of the amperometric current is determine mainly by the time course of the catecholamine release and the diffusion from the release site to the electrode surface. The electrode can be placed very close to plasma membrane so that the diffusion from the release site to the electrode can be disregard.

A typical individual amperometric response in adrenal chromaffin cell is preceded with a slow rising signal called the foot signal (Figure 7-6). The foot signal is usually small in amplitude and variable in duration. The mechanism underlined the

foot signal is the slowly release of catecholamines through fusion pore (Chow and Von Ruden 1995). The initial pore size is small and only few catecholamine molecules that free to diffuse through the pore (Schroeder, Borges et al. 1996; Albillos, Dernick et al. 1997; Ales, Tabares et al. 1999). The rest of the catecholamine molecules are in complex with the intravesicular matrix mainly chromogranin A. The response proceeds with an abrupt increase of the signal indicates the sudden releases of the catecholamine. The abrupt increase in catecholamine release is consistent with the sudden expansion of the fusion pore (Ales, Tabares et al. 1999). However, the time course of the rising to the maximum of the amperometric signal is not instantaneous despite the electrode being in touch with the plasma membrane (Schroeder, Borges et al. 1996). The rising phase of the amperometric signal is determined by the rate of fusion pore expansion and the dissolution of the catecholamine from the complex matrix. The signal then decays with an exponential function. The rate of decay is consistent with the diffusion theory which includes diffusion within the complex matrix and the diffusion from the release site to the electrode.

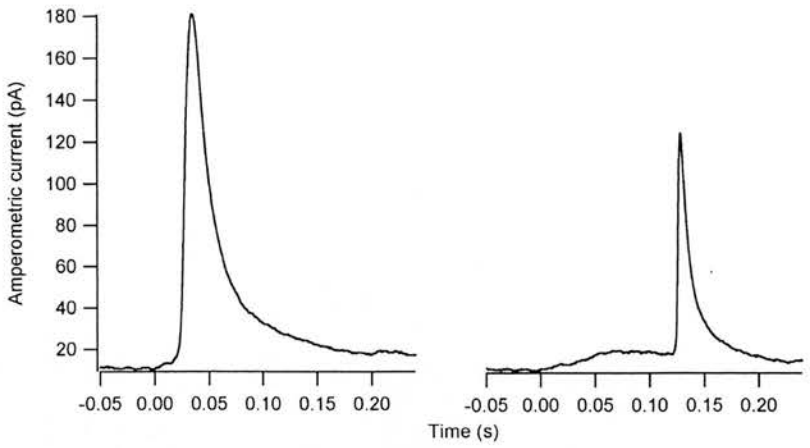

Figure 7-6 Individual amperometric currents

The individual amperometric currents are from the same cell in response to intracellular dialysis with pipette solution containing 10-μM Ca^{2+}. The response is preceded by a foot signal which can be large (*right*) or small (*left*) or even discernible in some responses. The response then proceeds with an abrupt increase signal follows by an exponential decay.

Simple parameters are extracted from the individual amperometric events to get information about vesicle fusion kinetics. The foot duration, amplitude and charge give information about fusion pore opening and the release through the fusion pore. The risetime gives the information about the rate of fusion pore expansion and the dissolution of the vesicular matrix. To avoid the complication by the foot signal, the 50-90% (of the amplitude) risetime is measured. The decay time constant also indicates the rate of matrix dissolution. However, these parameters are subjected to the filtering effect of the distance separating the release site and electrode based on the diffusion theory. Integral of amperometric current yields the total charge. The number of catecholamine release can be calculated from the total charge, taken into account that two electrons per molecule of catecholamine are transferred during the oxidation reaction.

$$Q = zeM$$

Where Q=total charge from integral amperometric current, z=number of electron transfer per molecule, e=elementary charge (1.6×10^{-19} coulomb) and M=number of molecule released.

Appendix III

Analysis of amperometric currents

Amperometric currents were analysed with a macro written on IGOR (WaveMetrics, Lake Oswego, OR, US.). The combination of automatic and manual data management helped the identification of the amperometric events more reliable especially in case of high noise, baseline unstability or high frequency secretion. The macro was tailored to particular experimental design in this work but it was easy to adapt for a different experimental design.

Data acquisition

In whole-cell Ca^{2+}-dialysis experiment, the amperometric current and membrane capacitance were simultaneously acquired with an EPC-9 together with Pulse software (HEKA Elektronik, Lambrecht, Germany). This multi-channel data acquisition limited the duration for each acquisition to only 540 milliseconds. Therefore, the data was repetitively acquired and several wave outputs were generated within one experiment. These waves were systematically named by the program. Due to the computational delay, the wave outputs were interrupted by gaps of about 200 milliseconds. To be more complicated, these gaps were not fixed values. The data was exported to IGOR to perform an analysis. The capacitance was exported as an ASCII file while the amperometric currents were exported as IGOR binary waves. The capacitance data from the ASCII file was copied into the IGOR table and saved as an IGOR-packed experiment in the same folder as the IGOR binary waves.

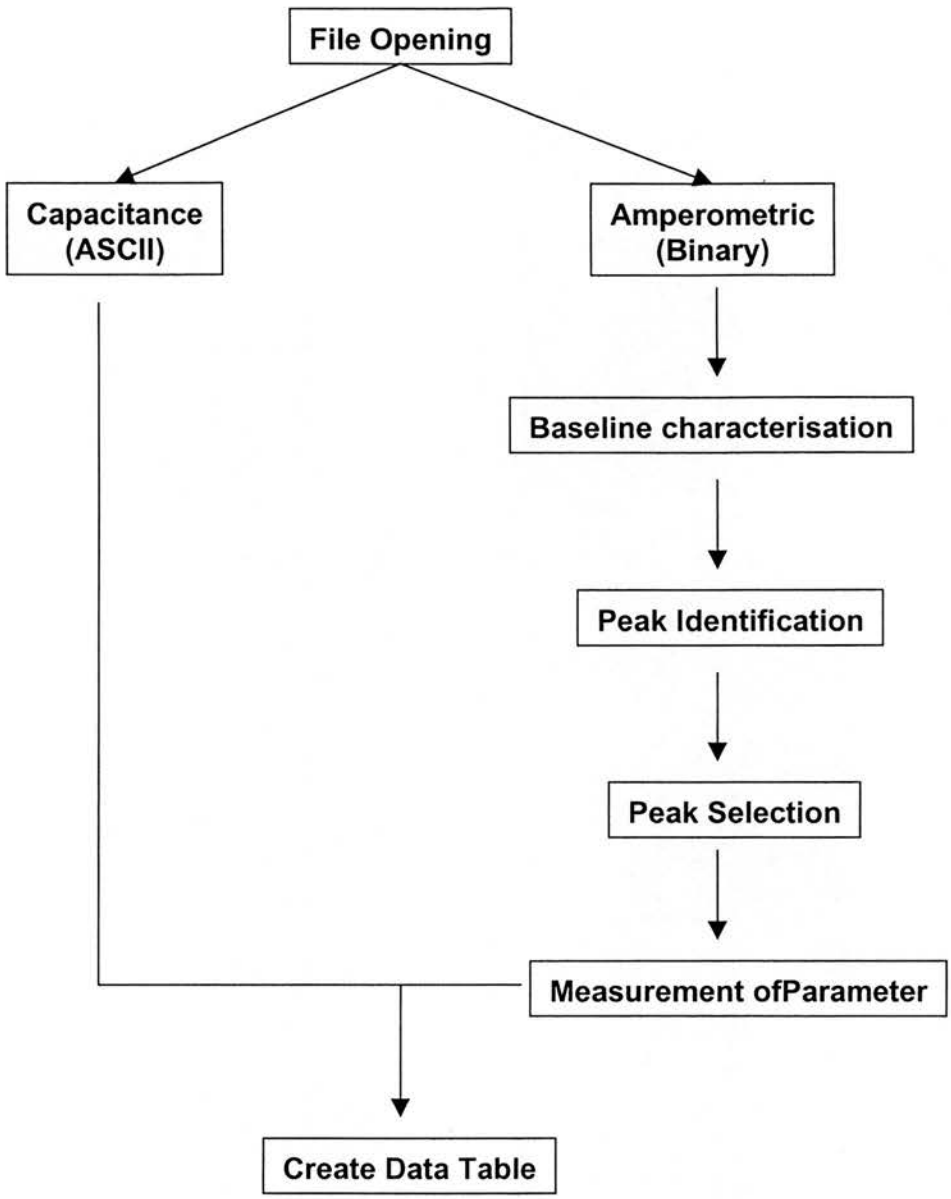

Figure 7-7 Structure of the macro for amperometric analysis

Flow chart displays the process of amperometric current analysis.

File opening

The macro located the folder and opened the capacitance file into the program window. A table of the time at the beginning of each acquisition was generated from the capacitance file (Figure 7-8). This table was later used for creating a latency histogram. The amperometric IGOR binary files were loaded into the same window.

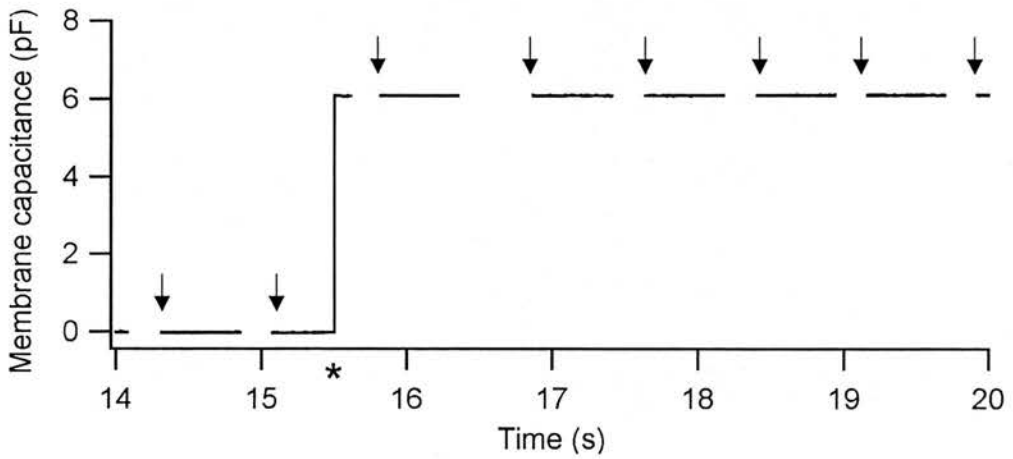

Figure 7-8 Capacitance recording

An example of capacitance recording from a Ca^{2+}-dialysis experiment. The graph was created from an ASCII data exported from an experiment. The whole-cell was established at time indicated by asterisked (*). A gap was introduced between two adjacent acquisitions due to a computational delay. *Arrow* indicated the beginning of each acquisition used for creating a table. The beginning of each capacitance acquisition was consistent with the beginning of each amperometric acquisition.

Baseline characterisation

After the files were loaded into the program window, the amperometric current was filtered with a smooth operation of the IGOR. The smooth operation behaved as a low-pass filter by computing the output value for a given point using the neighbour points. The baseline average and standard deviation (SD) were measured from a segment of amperometric current recorded prior to whole-cell establishment which was free of amperometric event.

Identification of peak

The peaks higher than baseline average plus five standard deviation were identified by a FindPeak operation of the IGOR. This operation identified a peak by taking first and second derivative of the wave. The peak was identified where the first derivative zero-crossing and the negative second derivative.

Peak selection

The IGOR FindPeak operation detected every single peak that met the condition. The noise peaks superimpose on the real amperometric events were also identified as peak. To exclude the noise peaks, a conditioning that the peaks must be at least five standard deviation from the lowest point between a given peak and the previous one was applied.

Identification of the actual peak, the beginning and the end of the amperometric event

The macro then searched for the beginning and the end of individual amperometric event by using an IGOR FindLevel operation. The beginning of the amperometric event was identified where the lowest point within 200 ms to the left of the peak was. The end of the amperometric event was identified as the point within 200 ms to the right of the peak where the level was the same as that of the beginning of the amperometric event. The maximum value within the beginning and the end of the amperometric event was identified by an IGOR WaveStats operation (Figure 7-9).

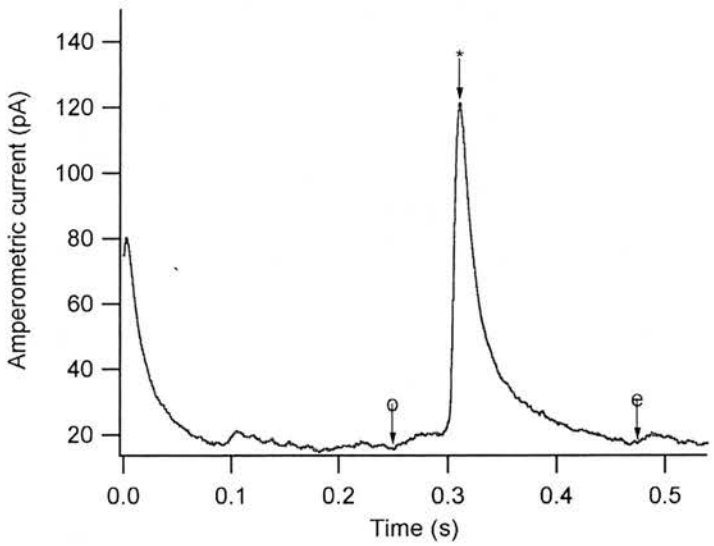

Figure 7-9 Identification of an individual amperometric event

An individual amperometric event identified by the macro. The beginning (o) and the end (e) of the amperometric event were identified. The actual peak (*) was identified from the peak of the amperometric current within the beginning and the end of the amperometric event.

Measurement of amperometric parameters

The amperometric amplitude was measured as a difference between the maximum value (*) and the value at the beginning (o) of the amperometric event. Integration of the amperometric current between the beginning and the end of the amperometric current yielded the total charge (Figure 7-10). The latency of the amperometric event was obtained from the equation below.

Latency = [The time at the start of a given acquisition] +

[the location of the peak within a given acquisition] –

[the time of whole-cell establishment]

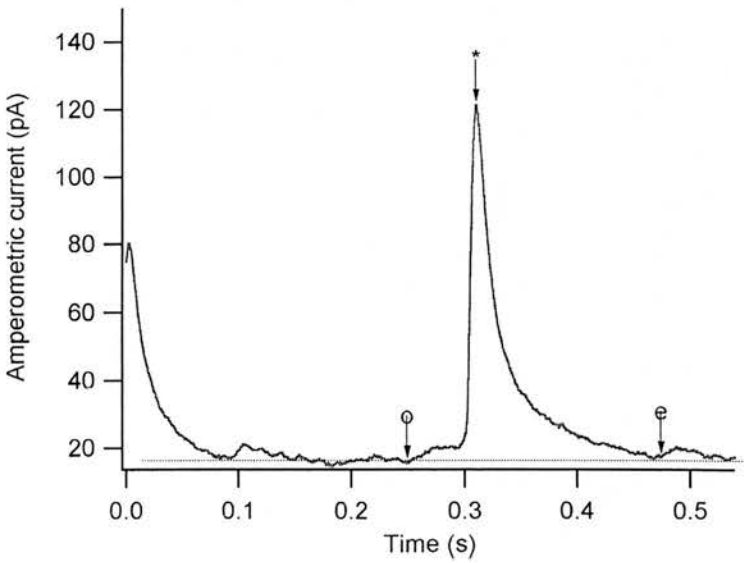

Figure 7-10 Measurement of amperometric charge

The amperometric charge was obtained from the integration of the amperometric current above the baseline (dash line) between the beginning (o) and the end (e) of the amperometric current.

The macro next identified the 50 and 90% level of the amplitude on the ascending and descending limbs of the amperometric event (Figure 7-11).

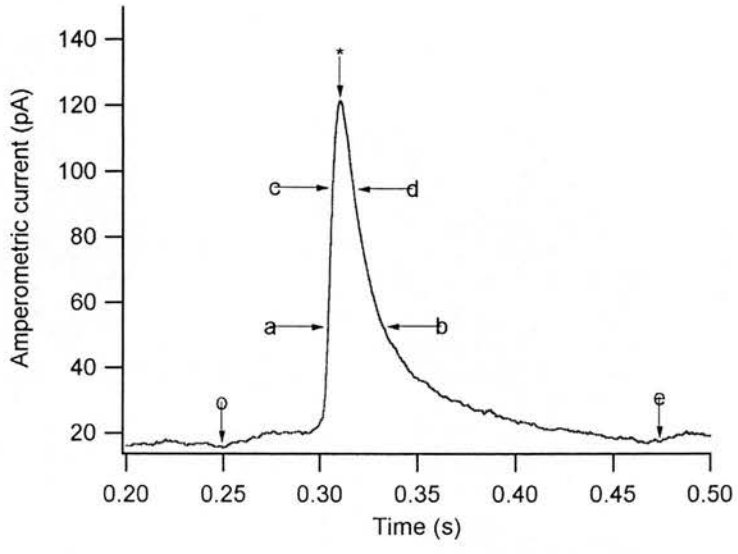

Figure 7-11 Identification of 50 and 90% of the amperometric amplitude

a and *b* were the location of the 50% level of the amplitude on the ascending and descending limbs of the amperometric event. *c* and *d* were the location of the 90% level of the amplitude on the ascending and descending limbs of the amperometric event, respectively.

50-90% risetime = c-a

Halfwidth = b-a

The descending limb of the amperometric event from 90% level of the amplitude to the end of the amperometric event was fitted with single exponential function (Figure 7-12).

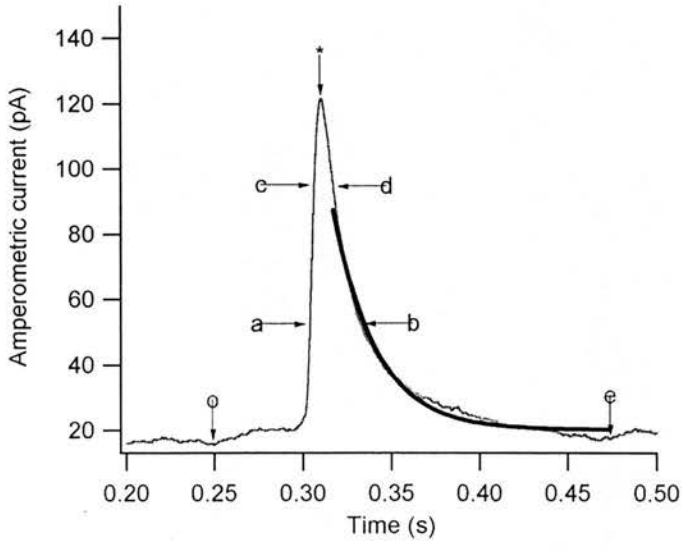

Figure 7-12 Exponential fitting of the amperometric current

The descending limb of the amperometric event from *d* to *e* was fitted with a single exponential function. The fitted curve (dark) is superimposed on the amperometric current.

Measurement of foot parameters

The ascending limb of the amperometric event from 50 to 90% level of the amplitude was fitted with a linear function. The fitted line was extrapolated to the baseline of the amperometric event to identify the end of the foot signal (Figure 7-13).

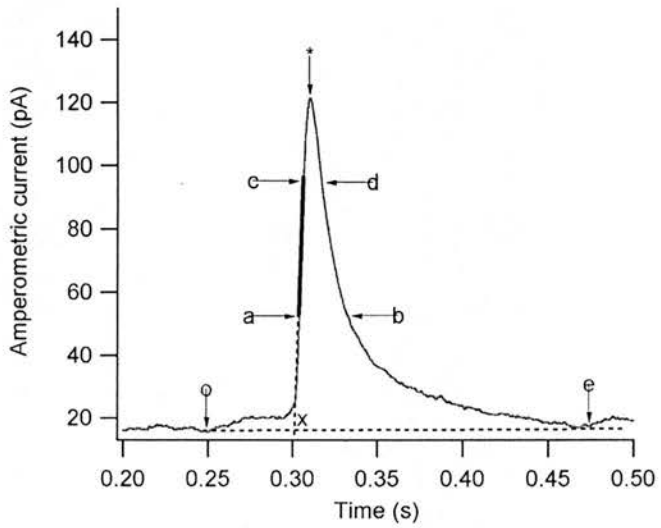

Figure 7-13 Determination of foot parameter

The ascending limb of the amperometric event from *a* to *c* was fitted with a linear function (dark line). The fitted line was extrapolated to the baseline of the amperometric event to identify the time at the end of the foot (x).

Foot duration = the end of foot signal -the beginning of the event

Foot charge = Integral of amperometric current between the beginning of the event and the end of the foot above the baseline

Foot amplitude = maximum value between the beginning of the event and the end of the foot – the base line

The macro finally created a latency histogram for measurement of the amount and frequency of secretion.

The macro allowed user to modified the conditions for amperometric analysis at several levels. The detected amperometric events were displayed so that the user could proceed with the measurement of the amperometric parameters or discard the peak and start a new cycle of peak identification.

Acknowledgements

This work was performed at Department of Biomedical Sciences, University of Edinburgh, UK. and Department of Physiology and Biophysics, University of Southern California, US.

I would like to express my sincere gratitude to people who helped this work succeed.

Dr. Robert H Chow who introduced me to the works in this field and always supports me in every steps of my Ph.D.

Dr. Michael J. Shipston, my supervisor, who always gives helpful advise.

Dr. Rory R Duncan and Dr. Rod Bremner who provided the DNA and Vectors for the viral expression.

My colleagues at both University of Edinburgh and University of Southern California who gave a helpful discussion.

The Department secretary offices at both University of Edinburgh and University of Southern California who helped my work more convenient.

My Thai friends at Edinburgh and US. who gave me comfort and great time abroad.

Finally, I would like to thank my family especially my parents, Mr. Anan and Mrs. Charoon Tapechum, who always have faith in me.

The financial support during this work was provided by Faculty of Medicine Siriraj Hospital, Thailand. and University of Southern California, US.

Chapter 8

Bibliography

Albillos, A., G. Dernick, et al. (1997). "The exocytotic event in chromaffin cells revealed by patch amperometry." Nature **389**(6650): 509-12.

Ales, E., L. Tabares, et al. (1999). "High calcium concentrations shift the mode of exocytosis to the kiss- and-run mechanism." Nat Cell Biol **1**(1): 40-4.

Aniento, F., N. Emans, et al. (1993). "Cytoplasmic dynein-dependent vesicular transport from early to late endosomes." J Cell Biol **123**(6 Pt 1): 1373-87.

Aravamudan, B., T. Fergestad, et al. (1999). "Drosophila UNC-13 is essential for synaptic transmission." Nat Neurosci **2**(11): 965-71.

Ashery, U., A. Betz, et al. (1999). "An efficient method for infection of adrenal chromaffin cells using the Semliki Forest virus gene expression system." Eur J Cell Biol **78**(8): 525-32.

Ashery, U., F. Varoqueaux, et al. (2000). "Munc13-1 acts as a priming factor for large dense-core vesicles in bovine chromaffin cells." Embo J **19**(14): 3586-96.

Augustin, I., A. Betz, et al. (1999a). "Differential expression of two novel Munc13 proteins in rat brain." Biochem J **337**(Pt 3): 363-71.

Augustin, I., C. Rosenmund, et al. (1999b). "Munc13-1 is essential for fusion competence of glutamatergic synaptic vesicles." Nature **400**(6743): 457-61.

Augustine, G. J. and E. Neher (1992). "Calcium requirements for secretion in bovine chromaffin cells." J Physiol **450**: 247-71.

Aunis, D. (1998). "Exocytosis in chromaffin cells of the adrenal medulla." Int Rev Cytol **181**: 213-320.

Aunis, D. and K. Langley (1999). "Physiological aspects of exocytosis in chromaffin cells of the adrenal medulla." Acta Physiol Scand **167**(2): 89-97.

Banerjee, A., V. A. Barry, et al. (1996). "N-Ethylmaleimide-sensitive factor acts at a prefusion ATP-dependent step in Ca2+-activated exocytosis." J Biol Chem **271**(34): 20223-6.

Barnard, R. J., A. Morgan, et al. (1997). "Stimulation of NSF ATPase activity by alpha-SNAP is required for SNARE complex disassembly and exocytosis." J Cell Biol **139**(4): 875-83.

Berghs, C. A., N. Korteweg, et al. (1999). "Co-expression in Xenopus neurons and neuroendocrine cells of messenger RNA homologues of exocytosis proteins DOC2 and munc18-1." Neuroscience **92**(2): 763-72.

Berglund, P., M. Sjoberg, et al. (1993). "Semliki Forest virus expression system: production of conditionally infectious recombinant particles." Biotechnology (N Y) **11**(8): 916-20.

Betz, A., U. Ashery, et al. (1998). "Munc13-1 is a presynaptic phorbol ester receptor that enhances neurotransmitter release." Neuron **21**(1): 123-36.

Betz, A., M. Okamoto, et al. (1997). "Direct interaction of the rat unc-13 homologue Munc13-1 with the N terminus of syntaxin." J Biol Chem **272**(4): 2520-6.

Betz, A., P. Thakur, et al. (2001). "Functional interaction of the active zone proteins Munc13-1 and RIM1 in synaptic vesicle priming." Neuron **30**(1): 183-96.

Biederer, T. and T. C. Sudhof (2000). "Mints as adaptors. Direct binding to neurexins and recruitment of munc18." J Biol Chem **275**(51): 39803-6.

Brehm, P. and R. Eckert (1978). "Calcium entry leads to inactivation of calcium channel in Paramecium." Science **202**(4373): 1203-6.

Brose, N., K. Hofmann, et al. (1995). "Mammalian homologues of Caenorhabditis elegans unc-13 gene define novel family of C2-domain proteins." J Biol Chem **270**(42): 25273-80.

Brose, N., A. G. Petrenko, et al. (1992). "Synaptotagmin: a calcium sensor on the synaptic vesicle surface." Science **256**(5059): 1021-5.

Brose, N., C. Rosenmund, et al. (2000). "Regulation of transmitter release by Unc-13 and its homologues." Curr Opin Neurobiol **10**(3): 303-11.

Burgess, T. L. and R. B. Kelly (1987). "Constitutive and regulated secretion of proteins." Annu Rev Cell Biol **3**: 243-93.

Chapman, E. R. and R. Jahn (1994). "Calcium-dependent interaction of the cytoplasmic region of synaptotagmin with membranes. Autonomous function of a single C2- homologous domain." J Biol Chem **269**(8): 5735-41.

Chow, R. H., J. Klingauf, et al. (1994). "Time course of Ca2+ concentration triggering exocytosis in neuroendocrine cells." Proc Natl Acad Sci U S A **91**(26): 12765-9.

Chow, R. H. and L. Von Ruden (1995). Electrochemical Detection of Secretion from Single Cells, Plenum Pub Corp.

Chow, R. H., L. von Ruden, et al. (1992). "Delay in vesicle fusion revealed by electrochemical monitoring of single secretory events in adrenal chromaffin cells." Nature **356**(6364): 60-3.

Chung, S. H., W. J. Song, et al. (1998). "The C2 domains of Rabphilin3A specifically bind phosphatidylinositol 4,5-bisphosphate containing vesicles in a Ca2+-dependent manner. In vitro characteristics and possible significance." J Biol Chem **273**(17): 10240-8.

Chung, S. H., P. Stabila, et al. (1997). "Importance of the Rab3a-GTP binding domain for the intracellular stability and function of Rabphilin3a in secretion." J Neurochem **69**(1): 164-73.

Chung, S. H., Y. Takai, et al. (1995). "Evidence that the Rab3a-binding protein, rabphilin3a, enhances regulated secretion. Studies in adrenal chromaffin cells." J Biol Chem **270**(28): 16714-8.

Conesa-Zamora, P., J. C. Gomez-Fernandez, et al. (2000). "The C2 domain of protein kinase calpha is directly involved in the diacylglycerol-dependent binding of the C1 domain to the membrane." Biochim Biophys Acta **1487**(2-3): 246-54.

Coussens, L., P. J. Parker, et al. (1986). "Multiple, distinct forms of bovine and human protein kinase C suggest diversity in cellular signaling pathways." Science **233**(4766): 859-66.

Darchen, F., J. Senyshyn, et al. (1995). "The GTPase Rab3a is associated with large dense core vesicles in bovine chromaffin cells and rat PC12 cells." J Cell Sci **108**(Pt 4): 1639-49.

Davis, A. F., J. Bai, et al. (1999). "Kinetics of synaptotagmin responses to Ca2+ and assembly with the core SNARE complex onto membranes." Neuron **24**(2): 363-76.

Davletov, B. A. and T. C. Sudhof (1993). "A single C2 domain from synaptotagmin I is sufficient for high affinity Ca2+/phospholipid binding." J Biol Chem **268**(35): 26386-90.

De Robertis, E. D. P. and H. S. Bennett (1954). "Submicroscopic vesicular compartment in the synapse." Fed. Proc. **13**: 35.

de Vries, K. J., A. Geijtenbeek, et al. (2000). "Dynamics of munc18-1 phosphorylation/dephosphorylation in rat brain nerve terminals." Eur J Neurosci **12**(1): 385-90.

Del Castillo, J. and B. Katz (1954a). "The effect of magnesium on the activity of motor nerve endings." J. Physiol. **124**: 553-559.

Del Castillo, J. and B. Katz (1954b). "Quantal components of the ending plate potential." J. Physiol. **124**: 560.

DiCiommo, D. P. and R. Bremner (1998). "Rapid, high level protein production using DNA-based Semliki Forest virus vectors." J Biol Chem **273**(29): 18060-6.

Dinkelacker, V., T. Voets, et al. (2000). "The readily releasable pool of vesicles in chromaffin cells is replenished in a temperature-dependent manner and transiently overfills at 37 degrees C." J Neurosci **20**(22): 8377-83.

Dobrunz, L. E. and C. F. Stevens (1997). "Heterogeneity of release probability, facilitation, and depletion at central synapses." Neuron **18**(6): 995-1008.

Dulubova, I., S. Sugita, et al. (1999). "A conformational switch in syntaxin during exocytosis: role of munc18." Embo J **18**(16): 4372-82.

Duncan, R. R., D. K. Apps, et al. (2000a). "Is double C2 protein (DOC2) expressed in bovine adrenal medulla? A commercial anti-DOC2 monoclonal antibody recognizes a major bovine mitochondrial antigen." Biochem J **351**(Pt 1): 33-7.

Duncan, R. R., A. Betz, et al. (1999a). "Transient, phorbol ester-induced DOC2-Munc13 interactions in vivo." J Biol Chem **274**(39): 27347-50.

Duncan, R. R., A. C. Don-Wauchope, et al. (1999b). "High-efficiency Semliki Forest virus-mediated transduction in bovine adrenal chromaffin cells." Biochem J **342 Pt 3**: 497-501.

Eberhard, D. A., C. L. Cooper, et al. (1990). "Evidence that the inositol phospholipids are necessary for exocytosis. Loss of inositol phospholipids and inhibition of secretion in permeabilized cells caused by a bacterial phospholipase C and removal of ATP." Biochem J **268**(1): 15-25.

Engisch, K. L. and M. C. Nowycky (1996). "Calcium dependence of large dense-cored vesicle exocytosis evoked by calcium influx in bovine adrenal chromaffin cells." J Neurosci **16**(4): 1359-69.

Ermak, G. and K. J. Davies (2002). "Calcium and oxidative stress: from cell signaling to cell death." Mol Immunol **38**(10): 713-21.

Essen, L. O., O. Perisic, et al. (1996). "Crystal structure of a mammalian phosphoinositide-specific phospholipase C delta." Nature **380**(6575): 595-602.

Fatt, P. and B. Katz (1952). "Spontaneous subthreshold activity at motor nerve endings." J. Physiol. **117**: 109-128.

Fernandez-Chacon, R., A. Konigstorfer, et al. (2001). "Synaptotagmin I functions as a calcium regulator of release probability." Nature **410**(6824): 41-9.

Fischer von Mollard, G., G. A. Mignery, et al. (1990). "rab3 is a small GTP-binding protein exclusively localized to synaptic vesicles." Proc Natl Acad Sci U S A **87**(5): 1988-92.

Fischer von Mollard, G., B. Stahl, et al. (1994). "Rab proteins in regulated exocytosis." Trends Biochem Sci **19**(4): 164-8.

Fischer von Mollard, G., B. Stahl, et al. (1994). "Localization of Rab5 to synaptic vesicles identifies endosomal intermediate in synaptic vesicle recycling pathway." Eur J Cell Biol **65**(2): 319-26.

Fukuda, M. and K. Mikoshiba (2000b). "Doc2gamma, a third isoform of double C2 protein, lacking calcium- dependent phospholipid binding activity." Biochem Biophys Res Commun **276**(2): 626-32.

Fukuda, M., J. E. Moreira, et al. (2000a). "Role of the conserved WHXL motif in the C terminus of synaptotagmin in synaptic vesicle docking." Proc Natl Acad Sci U S A **97**(26): 14715-9.

Fukuda, M., C. Saegusa, et al. (2001). "The C2A domain of double C2 protein gamma contains a functional nuclear localization signal." J Biol Chem **276**(27): 24441-4.

Geppert, M., Y. Goda, et al. (1994). "Synaptotagmin I: a major Ca2+ sensor for transmitter release at a central synapse." Cell **79**(4): 717-27.

Geppert, M., Y. Goda, et al. (1997). "The small GTP-binding protein Rab3A regulates a late step in synaptic vesicle fusion." Nature **387**(6635): 810-4.

Gera, S. and L. Byerly (1999). "Voltage- and calcium-dependent inactivation of calcium channels in Lymnaea neurons." J Gen Physiol **114**(4): 535-50.

Gillis, K. D. (1995). Techniques for Membrane Capacitance Measurements, Plenum Pub Corp.

Gillis, K. D., R. Mossner, et al. (1996). "Protein kinase C enhances exocytosis from chromaffin cells by increasing the size of the readily releasable pool of secretory granules." Neuron **16**(6): 1209-20.

Glasgow, G. M., M. M. McGee, et al. (1998). "The Semliki Forest virus vector induces p53-independent apoptosis." J Gen Virol **79**(Pt 10): 2405-10.

Grynkiewicz, G., M. Poenie, et al. (1985). "A new generation of Ca2+ indicators with greatly improved fluorescence properties." J Biol Chem **260**(6): 3440-50.

Gumbiner, B. and R. B. Kelly (1982). "Two distinct intracellular pathways transport secretory and membrane glycoproteins to the surface of pituitary tumor cells." Cell **28**(1): 51-9.

Hata, Y., C. A. Slaughter, et al. (1993). "Synaptic vesicle fusion complex contains unc-18 homologue bound to syntaxin." Nature **366**(6453): 347-51.

Hata, Y. and T. C. Sudhof (1995). "A novel ubiquitous form of Munc-18 interacts with multiple syntaxins. Use of the yeast two-hybrid system to study interactions between proteins involved in membrane traffic." J Biol Chem **270**(22): 13022-8.

Havenga, M. J., R. Vogels, et al. (1998). "Second gene expression in bicistronic constructs using short synthetic intercistrons and viral IRES sequences." Gene **222**(2): 319-27.

Hay, J. C. and T. F. Martin (1992). "Resolution of regulated secretion into sequential MgATP-dependent and calcium-dependent stages mediated by distinct cytosolic proteins." J Cell Biol **119**(1): 139-51.

Heald, R., R. Tournebize, et al. (1996). "Self-organization of microtubules into bipolar spindles around artificial chromosomes in Xenopus egg extracts." Nature **382**(6590): 420-5.

Heidelberger, R., C. Heinemann, et al. (1994). "Calcium dependence of the rate of exocytosis in a synaptic terminal." Nature **371**(6497): 513-5.

Heinemann, C., R. H. Chow, et al. (1994). "Kinetics of the secretory response in bovine chromaffin cells following flash photolysis of caged Ca2+." Biophys J **67**(6): 2546-57.

Heinemann, C., L. von Ruden, et al. (1993). "A two-step model of secretion control in neuroendocrine cells." Pflugers Arch **424**(2): 105-12.

Hori, T., Y. Takai, et al. (1999). "Presynaptic mechanism for phorbol ester-induced synaptic potentiation." J Neurosci **19**(17): 7262-7.

Hosono, R. and Y. Kamiya (1991). "Additional genes which result in an elevation of acetylcholine levels by mutations in Caenorhabditis elegans." Neurosci Lett **128**(2): 243-4.

Hosono, R., T. Sassa, et al. (1987). "Mutations affecting acetylcholine levels in the nematode Caenorhabditis elegans." J Neurochem **49**(6): 1820-3.

Hu, K., J. Carroll, et al. (2002). "Action of complexin on SNARE complex." J Biol Chem **277**(44): 41652-6.

Iacomino, G., M. F. Tecce, et al. (2001). "Transcriptional response of a human colon adenocarcinoma cell line to sodium butyrate." Biochem Biophys Res Commun **285**(5): 1280-9.

Iizuka, K., M. Ikebe, et al. (1994). "Introduction of high molecular weight (IgG) proteins into receptor coupled, permeabilized smooth muscle." Cell Calcium **16**(6): 431-45.

Jahn, R. and T. C. Sudhof (1999). "Membrane fusion and exocytosis." Annu Rev Biochem **68**: 863-911.

Katz, B. and R. Miledi (1965). "The effect of calcium on acetylcholine release from motor nerve terminals." Proc. R. Soc. B. **161**: 496-503.

Kawasaki, F., A. M. Mattiuz, et al. (1998). "Synaptic physiology and ultrastructure in comatose mutants define an in vivo role for NSF in neurotransmitter release." J Neurosci **18**(24): 10241-9.

Kazanietz, M. G., N. E. Lewin, et al. (1995). "Characterization of the cysteine-rich region of the Caenorhabditis elegans protein Unc-13 as a high affinity phorbol ester receptor. Analysis of ligand-binding interactions, lipid cofactor requirements, and inhibitor sensitivity." J Biol Chem **270**(18): 10777-83.

Kelly, R. B. (1985). "Pathways of protein secretion in eukaryotes." Science **230**(4721): 25-32.

Kelly, R. B. (1991). "Secretory granule and synaptic vesicle formation." Curr Opin Cell Biol **3**(4): 654-60.

Klenchin, V. A. and T. F. Martin (2000). "Priming in exocytosis: attaining fusion-competence after vesicle docking." Biochimie **82**(5): 399-407.

Knight, D. E. (1999). "Secretion from bovine chromaffin cells acutely expressing exogenous proteins using a recombinant Semliki Forest virus containing an EGFP reporter." Mol Cell Neurosci **14**(6): 486-505.

Kobayashi, H., S. Shiraishi, et al. (2002). "Regulation of voltage-dependent sodium channel expression in adrenal chromaffin cells: involvement of multiple calcium signaling pathways." Ann N Y Acad Sci **971**: 127-34.

Koch, H., K. Hofmann, et al. (2000). "Definition of Munc13-homology-domains and characterization of a novel ubiquitously expressed Munc13 isoform." Biochem J **349**(Pt 1): 247-53.

Kojima, T., M. Fukuda, et al. (1996). "Calcium-dependent phospholipid binding to the C2A domain of a ubiquitous form of double C2 protein (Doc2 beta)." J Biochem (Tokyo) **120**(3): 671-6.

Konishi, M. and M. Watanabe (1995). "Resting cytoplasmic free Ca2+ concentration in frog skeletal muscle measured with fura-2 conjugated to high molecular weight dextran." J Gen Physiol **106**(6): 1123-50.

Korteweg, N., F. A. Denekamp, et al. (2000). "Different spatiotemporal expression of DOC2 genes in the developing rat brain argues for an additional, nonsynaptic role of DOC2B in early development." Eur J Neurosci **12**(1): 165-71.

Lawrence, G. W. and J. O. Dolly (2002a). "Ca2+-induced changes in SNAREs and synaptotagmin I correlate with triggered exocytosis from chromaffin cells: insights gleaned into the signal transduction using trypsin and botulinum toxins." J Cell Sci **115**(Pt 13): 2791-800.

Lawrence, G. W. and J. O. Dolly (2002b). "Multiple forms of SNARE complexes in exocytosis from chromaffin cells: effects of Ca(2+), MgATP and botulinum toxin type A." J Cell Sci **115**(Pt 3): 667-73.

Liljestrom, P. and H. Garoff (1991). "A new generation of animal cell expression vectors based on the Semliki Forest virus replicon." Biotechnology (N Y) **9**(12): 1356-61.

Lindau, M. and E. Neher (1988). "Patch-clamp techniques for time-resolved capacitance measurements in single cells." Pflugers Arch **411**(2): 137-46.

Martelli, A. M., G. Baldini, et al. (2000). "Rab3A and Rab3D control the total granule number and the fraction of granules docked at the plasma membrane in PC12 cells." Traffic **1**(12): 976-86.

Martin, T. F. and J. A. Kowalchyk (1997). "Docked secretory vesicles undergo Ca2+-activated exocytosis in a cell- free system." J Biol Chem **272**(22): 14447-53.

Mizoguchi, A., Y. Yano, et al. (1994). "Localization of Rabphilin-3A on the synaptic vesicle." Biochem Biophys Res Commun **202**(3): 1235-43.

Mochida, S., S. Orita, et al. (1998). "Role of the Doc2 alpha-Munc13-1 interaction in the neurotransmitter release process." Proc Natl Acad Sci U S A **95**(19): 11418-22.

Molinete, M., S. Dupuis, et al. (2001). "Role of clathrin in the regulated secretory pathway of pancreatic beta- cells." J Cell Sci **114**(Pt 16): 3059-66.

Morgan, A. and R. Burgoyne (1997). "Common mechanisms for regulated exocytosis in chromaffin cell and synapse." Seminars Cell Dev Biol **8**: 141-149.

Mountford, P., B. Zevnik, et al. (1994). "Dicistronic targeting constructs: reporters and modifiers of mammalian gene expression." Proc Natl Acad Sci U S A **91**(10): 4303-7.

Murthy, V. N. and C. F. Stevens (1998). "Synaptic vesicles retain their identity through the endocytic cycle." Nature **392**(6675): 497-501.

Murthy, V. N. and C. F. Stevens (1999). "Reversal of synaptic vesicle docking at central synapses." Nat Neurosci **2**(6): 503-7.

Nagano, F., S. Orita, et al. (1998). "Interaction of Doc2 with tctex-1, a light chain of cytoplasmic dynein. Implication in dynein-dependent vesicle transport." J Biol Chem **273**(46): 30065-8.

Naito, A., S. Orita, et al. (1997). "Molecular cloning of mouse Doc2alpha and distribution of its mRNA in adult mouse brain." Brain Res Mol Brain Res **44**(2): 198-204.

Nakata, T., S. Terada, et al. (1998). "Visualization of the dynamics of synaptic vesicle and plasma membrane proteins in living axons." J Cell Biol **140**(3): 659-74.

Nalefski, E. A. and J. J. Falke (1996). "The C2 domain calcium-binding motif: structural and functional diversity." Protein Sci **5**(12): 2375-90.

Neher, E. and A. Marty (1982). "Discrete changes of cell membrane capacitance observed under conditions of enhanced secretion in bovine adrenal chromaffin cells." Proc Natl Acad Sci U S A **79**(21): 6712-6.

Neher, E. and R. S. Zucker (1993). "Multiple calcium-dependent processes related to secretion in bovine chromaffin cells." Neuron **10**(1): 21-30.

Newton, A. C. (1995). "Protein kinase C: structure, function, and regulation." J Biol Chem **270**(48): 28495-8.

Nielander, H. B., F. Onofri, et al. (1995). "Phosphorylation of VAMP/synaptobrevin in synaptic vesicles by endogenous protein kinases." J Neurochem **65**(4): 1712-20.

Niemann, H., J. Blasi, et al. (1994). "Clostridial neurotoxins: new tools for dissecting exocytosis." Trends Cell Biol **4**: 179-185.

Nishizaki, T., J. H. Walent, et al. (1992). "A key role for a 145-kDa cytosolic protein in the stimulation of Ca(2+)-dependent secretion by protein kinase C." J Biol Chem **267**(33): 23972-81.

Nonet, M. L., K. Grundahl, et al. (1993). "Synaptic function is impaired but not eliminated in C. elegans mutants lacking synaptotagmin." Cell **73**(7): 1291-305.

Nonet, M. L., J. E. Staunton, et al. (1997). "Caenorhabditis elegans rab-3 mutant synapses exhibit impaired function and are partially depleted of vesicles." J Neurosci **17**(21): 8061-73.

Oheim, M., D. Loerke, et al. (1998). "The last few milliseconds in the life of a secretory granule. Docking, dynamics and fusion visualized by total internal reflection fluorescence microscopy (TIRFM)." Eur Biophys J **27**(2): 83-98.

Okamoto, M., T. Matsuyama, et al. (2000). "Ultrastructural localization of mint1 at synapses in mouse hippocampus." Eur J Neurosci **12**(8): 3067-72.

Orita, S., A. Naito, et al. (1997). "Physical and functional interactions of Doc2 and Munc13 in Ca2+- dependent exocytotic machinery." J Biol Chem **272**(26): 16081-4.

Orita, S., T. Sasaki, et al. (1996). "Doc2 enhances Ca2+-dependent exocytosis from PC12 cells." J Biol Chem **271**(13): 7257-60.

Orita, S., T. Sasaki, et al. (1995). "Doc2: a novel brain protein having two repeated C2-like domains." Biochem Biophys Res Commun **206**(2): 439-48.

Ossig, R., C. Dascher, et al. (1991). "The yeast SLY gene products, suppressors of defects in the essential GTP-binding Ypt1 protein, may act in endoplasmic reticulum-to-Golgi transport." Mol Cell Biol **11**(6): 2980-93.

Palade, G. (1975). "Intracellular aspects of the process of protein synthesis." Science **189**(4200): 347-58.

Pan, C. Y., A. Jeromin, et al. (2002). "Alterations in exocytosis induced by neuronal Ca2+ sensor-1 in bovine chromaffin cells." J Neurosci **22**(7): 2427-33.

Parker, P. J., L. Coussens, et al. (1986). "The complete primary structure of protein kinase C--the major phorbol ester receptor." Science **233**(4766): 853-9.

Parsons, T. D., J. R. Coorssen, et al. (1995). "Docked granules, the exocytic burst, and the need for ATP hydrolysis in endocrine cells." Neuron **15**(5): 1085-96.

Perin, M. S., V. A. Fried, et al. (1990). "Phospholipid binding by a synaptic vesicle protein homologous to the regulatory region of protein kinase C." Nature **345**(6272): 260-3.

Petrenko, A. G., M. S. Perin, et al. (1991). "Binding of synaptotagmin to the alpha-latrotoxin receptor implicates both in synaptic vesicle exocytosis." Nature **353**(6339): 65-8.

Plattner, H., A. R. Artalejo, et al. (1997). "Ultrastructural organization of bovine chromaffin cell cortex-analysis by cryofixation and morphometry of aspects pertinent to exocytosis." J Cell Biol **139**(7): 1709-17.

Pyle, J. L., E. T. Kavalali, et al. (2000). "Rapid reuse of readily releasable pool vesicles at hippocampal synapses." Neuron **28**(1): 221-31.

Pyott, S. J. and C. Rosenmund (2002). "The effects of temperature on vesicular supply and release in autaptic cultures of rat and mouse hippocampal neurons." J Physiol **539**(Pt 2): 523-35.

Quetglas, S., C. Leveque, et al. (2000). "Ca2+-dependent regulation of synaptic SNARE complex assembly via a calmodulin- and phospholipid-binding domain of synaptobrevin." Proc Natl Acad Sci U S A **97**(17): 9695-700.

Reist, N. E., J. Buchanan, et al. (1998). "Morphologically docked synaptic vesicles are reduced in synaptotagmin mutants of Drosophila." J Neurosci **18**(19): 7662-73.

Rhee, J. S., A. Betz, et al. (2002). "Beta phorbol ester- and diacylglycerol-induced augmentation of transmitter release is mediated by Munc13s and not by PKCs." Cell **108**(1): 121-33.

Richmond, J. E., R. M. Weimer, et al. (2001). "An open form of syntaxin bypasses the requirement for UNC-13 in vesicle priming." Nature **412**(6844): 338-41.

Risinger, C. and M. K. Bennett (1999). "Differential phosphorylation of syntaxin and synaptosome-associated protein of 25 kDa (SNAP-25) isoforms." J Neurochem **72**(2): 614-24.

Sabatini, B. L. and W. G. Regehr (1996). "Timing of neurotransmission at fast synapses in the mammalian brain." Nature **384**(6605): 170-2.

Sakaguchi, G., T. Manabe, et al. (1999). "Doc2alpha is an activity-dependent modulator of excitatory synaptic transmission." Eur J Neurosci **11**(12): 4262-8.

Sakaguchi, G., S. Orita, et al. (1995). "Molecular cloning of an isoform of Doc2 having two C2-like domains." Biochem Biophys Res Commun **217**(3): 1053-61.

Sambrook, J., E. F. Fritsch, et al. (1989). Molecular cloning: a laboratory manual, Cold Spring Habor Laboratory Press, N.Y.

Sassa, T., S. Harada, et al. (1999). "Regulation of the UNC-18-Caenorhabditis elegans syntaxin complex by UNC- 13." J Neurosci **19**(12): 4772-7.

Schekman, R. (1992). "Genetic and biochemical analysis of vesicular traffic in yeast." Curr Opin Cell Biol **4**(4): 587-92.

Schiavo, G., Q. M. Gu, et al. (1996). "Calcium-dependent switching of the specificity of phosphoinositide binding to synaptotagmin." Proc Natl Acad Sci U S A **93**(23): 13327-32.

Schikorski, T. and C. F. Stevens (1997). "Quantitative ultrastructural analysis of hippocampal excitatory synapses." J Neurosci **17**(15): 5858-67.

Schneggenburger, R., A. C. Meyer, et al. (1999). "Released fraction and total size of a pool of immediately available transmitter quanta at a calyx synapse." Neuron **23**(2): 399-409.

Schroeder, T. J., R. Borges, et al. (1996). "Temporally resolved, independent stages of individual exocytotic secretion events." Biophys J **70**(2): 1061-8.

Schulte, A. and R. H. Chow (1996). "A Simple Method for Insulating Carbon-Fiber Microelectrodes Using Anodic Electrophoretic Deposition of Paint." Analytical Chemistry **68**(17): 3054-3058.

Schulte, A. and R. H. Chow (1998). "Cylindrically Etched Carbon-Fiber Microelectrodes for Low-Noise Amperometric recording." Analytical Chemistry **70**(5): 985-990.

Schulze, K. L., J. T. Littleton, et al. (1994). "rop, a Drosophila homolog of yeast Sec1 and vertebrate n-Sec1/Munc-18 proteins, is a negative regulator of neurotransmitter release in vivo." Neuron **13**(5): 1099-108.

Seward, E. P., N. I. Chernevskaya, et al. (1996). "Ba2+ ions evoke two kinetically distinct patterns of exocytosis in chromaffin cells, but not in neurohypophysial nerve terminals." J Neurosci **16**(4): 1370-9.

Shao, X., B. A. Davletov, et al. (1996). "Bipartite Ca2+-binding motif in C2 domains of synaptotagmin and protein kinase C." Science **273**(5272): 248-51.

Shimazaki, Y., T. Nishiki, et al. (1996). "Phosphorylation of 25-kDa synaptosome-associated protein. Possible involvement in protein kinase C-mediated regulation of neurotransmitter release." J Biol Chem **271**(24): 14548-53.

Smith, C. (1999). "A persistent activity-dependent facilitation in chromaffin cells is caused by Ca2+ activation of protein kinase C." J Neurosci **19**(2): 589-98.

Smith, C. and E. Neher (1997). "Multiple forms of endocytosis in bovine adrenal chromaffin cells." J Cell Biol **139**(4): 885-94.

Sollner, T., M. K. Bennett, et al. (1993). "A protein assembly-disassembly pathway in vitro that may correspond to sequential steps of synaptic vesicle docking, activation, and fusion." Cell **75**(3): 409-18.

Stevens, C. F. and J. M. Sullivan (1998). "Regulation of the readily releasable vesicle pool by protein kinase C." Neuron **21**(4): 885-93.

Stevens, C. F. and T. Tsujimoto (1995). "Estimates for the pool size of releasable quanta at a single central synapse and for the time required to refill the pool." Proc Natl Acad Sci U S A **92**(3): 846-9.

Stevens, C. F. and J. H. Williams (2000). ""Kiss and run" exocytosis at hippocampal synapses." Proc Natl Acad Sci U S A **97**(23): 12828-33.

Steyer, J. A., H. Horstmann, et al. (1997). "Transport, docking and exocytosis of single secretory granules in live chromaffin cells." Nature **388**(6641): 474-8.

Sudhof, T. C. (1995). "The synaptic vesicle cycle: a cascade of protein-protein interactions." Nature **375**(6533): 645-53.

Sun, L., M. A. Bittner, et al. (2001). "Rab3a binding and secretion-enhancing domains in Rim1 are separate and unique. Studies in adrenal chromaffin cells." J Biol Chem **276**(16): 12911-7.

Sutton, R. B., B. A. Davletov, et al. (1995). "Structure of the first C2 domain of synaptotagmin I: a novel Ca2+/phospholipid-binding fold." Cell **80**(6): 929-38.

Tan, H. L., S. Kupershmidt, et al. (2002). "A calcium sensor in the sodium channel modulates cardiac excitability." Nature **415**(6870): 442-7.

Tateyama, M., S. Zong, et al. (2001). "Properties of voltage-gated Ca(2+) channels in rabbit ventricular myocytes expressing Ca(2+) channel alpha(1E) cDNA." Am J Physiol Cell Physiol **280**(1): C175-82.

Tellam, J. T., S. McIntosh, et al. (1995). "Molecular identification of two novel Munc-18 isoforms expressed in non- neuronal tissues." J Biol Chem **270**(11): 5857-63.

Tolar, L. A. and L. Pallanck (1998). "NSF function in neurotransmitter release involves rearrangement of the SNARE complex downstream of synaptic vesicle docking." J Neurosci **18**(24): 10250-6.

Towbin, H., T. Staehelin, et al. (1979). "Electrophoretic transfer of proteins from polyacrylamide gels to nitrocellulose sheets: procedure and some applications." Proc Natl Acad Sci U S A **76**(9): 4350-4.

Tsien, R. Y. (1989). "Fluorescent indicators of ion concentrations." Methods Cell Biol **30**: 127-56.

Tsuboi, T., T. Kikuta, et al. (2001). "Protein kinase C-dependent supply of secretory granules to the plasma membrane." Biochem Biophys Res Commun **282**(2): 621-8.

Tsuboi, T., C. Zhao, et al. (2000). "Simultaneous evanescent wave imaging of insulin vesicle membrane and cargo during a single exocytotic event." Curr Biol **10**(20): 1307-10.

Tubulekas, I. and P. Liljestrom (1998). "Suppressors of cleavage-site mutations in the p62 envelope protein of Semliki Forest virus reveal dynamics in spike structure and function." J Virol **72**(4): 2825-31.

Turner, K. M., R. D. Burgoyne, et al. (1999). "Protein phosphorylation and the regulation of synaptic membrane traffic." Trends Neurosci **22**(10): 459-64.

Varoqueaux, F., A. Sigler, et al. (2002). "Total arrest of spontaneous and evoked synaptic transmission but normal synaptogenesis in the absence of Munc13-mediated vesicle priming." Proc Natl Acad Sci U S A **99**(13): 9037-42.

Verhage, M., K. J. de Vries, et al. (1997). "DOC2 proteins in rat brain: complementary distribution and proposed function as vesicular adapter proteins in early stages of secretion." Neuron **18**(3): 453-61.

Verhage, M., A. S. Maia, et al. (2000). "Synaptic assembly of the brain in the absence of neurotransmitter secretion." Science **287**(5454): 864-9.

Vitale, M. L., E. P. Seward, et al. (1995). "Chromaffin cell cortical actin network dynamics control the size of the release-ready vesicle pool and the initial rate of exocytosis." Neuron **14**(2): 353-63.

Voets, T. (2000). "Dissection of three Ca2+-dependent steps leading to secretion in chromaffin cells from mouse adrenal slices." Neuron **28**(2): 537-45.

Voets, T., T. Moser, et al. (2001b). "Intracellular calcium dependence of large dense-core vesicle exocytosis in the absence of synaptotagmin I." Proc Natl Acad Sci U S A **98**(20): 11680-5.

Voets, T., R. F. Toonen, et al. (2001a). "Munc18-1 promotes large dense-core vesicle docking." Neuron **31**(4): 581-91.

von Euler, U. S. and F. Lishajko (1959). "The Estimation of Catechol Amines in Urine." Acta Physiol Scand **45**: 122.

von Euler, U. S. and F. Lishajko (1961). "Improved Technique for the Fluorimetric Estimation of Catecholamines." Acta Physiol Scand **51**: 348.

von Ruden, L. and E. Neher (1993). "A Ca-dependent early step in the release of catecholamines from adrenal chromaffin cells." Science **262**(5136): 1061-5.

Wang, Y., M. Okamoto, et al. (1997). "Rim is a putative Rab3 effector in regulating synaptic-vesicle fusion." Nature **388**(6642): 593-8.

Wick, P. F., R. A. Senter, et al. (1993). "Transient transfection studies of secretion in bovine chromaffin cells and PC12 cells. Generation of kainate-sensitive chromaffin cells." J Biol Chem **268**(15): 10983-9.

Wiedemann, C., T. Schafer, et al. (1996). "Chromaffin granule-associated phosphatidylinositol 4-kinase activity is required for stimulated secretion." Embo J **15**(9): 2094-101.

Wu, M. N., J. T. Littleton, et al. (1998). "ROP, the Drosophila Sec1 homolog, interacts with syntaxin and regulates neurotransmitter release in a dosage-dependent manner." Embo J **17**(1): 127-39.

Xu, T., U. Ashery, et al. (1999). "Early requirement for alpha-SNAP and NSF in the secretory cascade in chromaffin cells." Embo J **18**(12): 3293-304.

Xu, T., T. Binz, et al. (1998). "Multiple kinetic components of exocytosis distinguished by neurotoxin sensitivity." Nat Neurosci **1**(3): 192-200.

Xu, T., B. Rammner, et al. (1999). "Inhibition of SNARE complex assembly differentially affects kinetic components of exocytosis." Cell **99**(7): 713-22.

Yamaguchi, T., H. Shirataki, et al. (1993). "Two functionally different domains of rabphilin-3A, Rab3A p25/smg p25A- binding and phospholipid- and Ca(2+)-binding domains." J Biol Chem **268**(36): 27164-70.

Yang, B., M. Steegmaier, et al. (2000). "nSec1 binds a closed conformation of syntaxin1A." J Cell Biol **148**(2): 247-52.

Yang, Y., S. Udayasankar, et al. (2002). "A highly Ca2+-sensitive pool of vesicles is regulated by protein kinase C in adrenal chromaffin cells." Proc Natl Acad Sci U S A **99**(26): 17060-17065.

Zhang, W., A. Efanov, et al. (2000). "Munc-18 associates with syntaxin and serves as a negative regulator of exocytosis in the pancreatic beta -cell." J Biol Chem **275**(52): 41521-7.

Publications

Biochem. J. (1999) **342**, 497–501 (Printed in Great Britain)

RESEARCH COMMUNICATION

High-efficiency Semliki Forest virus-mediated transduction in bovine adrenal chromaffin cells

Rory R. DUNCAN, Andrew C. DON-WAUCHOPE, Sompol TAPECHUM, Michael J. SHIPSTON, Robert H. CHOW and Peter ESTIBEIRO[1]

Membrane Biology Group, Biomedical Sciences, University of Edinburgh Medical School, Teviot Place, Edinburgh, EH8 9XD, U.K.

Adrenal chromaffin cells are commonly used in studies of exocytosis. Progress in characterizing the molecular mechanisms has been slow, because no simple, high-efficiency technique is available for introducing and expressing heterologous cDNA in chromaffin cells. Here we demonstrate that Semliki Forest virus (SFV) vectors allow high-efficiency expression of heterologous protein in chromaffin cells.

Key words: acidic vesicle, confocal, double C2 protein β-isoform, exocytosis, SFV.

INTRODUCTION

Adrenal chromaffin cells have long been a model system of choice for studies of exocytosis. These neuroendocrine cells, like neurons, fire action potentials, exhibit calcium-dependent exocytosis, and express many proteins closely related to synaptic proteins.

An important barrier to the advance in understanding of the molecular mechanisms underlying exocytosis is the lack of a high-efficiency technique for introducing heterologous DNA or RNA into chromaffin cells. 'Traditional' methods for mammalian cell transfection, such as calcium phosphate precipitation, lipid-mediated transfection and electroporation have met with limited success and have variable efficiencies [1–4].

A number of viral transduction systems have been developed to permit the efficient transduction of cDNA into eukaryotic cells. The ideal viral-vector system would be easy to use, have a broad host range but low human pathogenicity, and permit efficient infection of target cells with high-level protein expression and low cytotoxicity. Of the existing expression systems for higher eukaryotic cells, perhaps the most efficient in terms of protein production is the baculovirus system for insect cell hosts [5]. Efficient viral transduction systems for mammalian cells based on a recombinant vaccinia virus, adenovirus or defective herpes simplex virus-1 have been developed (for a review, see [6]), but these require considerable expertise for use and can be time-consuming and expensive. In addition, adequate containment facilities may not be available.

The recently introduced Semliki Forest virus (SFV) transduction system [7,8] has several potential benefits over other viral transduction systems, in particular, minimal containment requirements and ease of use. The gene of interest may be ligated directly to a DNA cloning vector encoding non-structural SFV genes for replicase, reverse transcriptase and helicase. After *in vitro* transcription, resultant capped RNA is co-electroporated alongside structural gene RNA into a permissive host cell line, commonly baby-hamster kidney (BHK)-21 cells. Attenuated, non-infectious packaged viral particles are assembled in the host cells, secreted into the extracellular medium and can be stored for future use. Treatment of these viral particles with a protease renders them infectious [7–8].

The SFV transduction system has already been used to express a number of proteins in a broad range of mammalian cells, including cultured rat hippocampal neurons, BHK-21, HeLa, and Madin–Darby canine kidney cells [7–10,11]. This broad host cell range, the ability to sub-clone directly into the expression vector without the need for *in vivo* recombination steps, and the excellent attenuation of recombinant SFV together make this system a particularly attractive candidate for transducing cDNA into chromaffin cells. In the present study, we examine the efficacy of SFV transduction of green fluorescent protein (GFP) mut3 and double C2 protein β-isoform-enhanced GFP (DOC2β-EGFP) in chromaffin cells. DOC2β is a protein that has been shown to associate with secretory vesicles previously [12], and which may play a role in exocytosis [13]. Efficient SFV transduction of chromaffin cells is obtained with the modification of previously published procedures.

MATERIALS AND METHODS

Isolation of a cDNA encoding mouse brain DOC2β

A reverse-transcription PCR strategy was used to amplify a cDNA encoding the open reading frame of mouse brain DOC2β. mRNA (1 μg) was used as a template in a first-strand cDNA synthesis directed from an anchored deoxyoligo d(T) (5′-TTCTAGAATTCAGCGGCCGC$(T)_{30}N_1N_2$) primer, using Superscript II reverse transcriptase (Gibco BRL Life Technologies). The resultant cDNA was diluted and used in a PCR reaction between forward (5′-CTGCCTGCATGACCCTCCG-GC) and reverse (5′-TCAGTCGCTGAGYACAGCCCCTG-

Abbreviations used: BHK, baby-hamster kidney; DOC2β, double C2 protein β-isoform; GFP, green fluorescent protein; EGFP, enhanced GFP; SFV, Semliki Forest virus.

[1] To whom correspondence should be addressed (e-mail Peter.Estibeiro@ed.ac.uk).

GG) deoxyoligonucleotides, using Expand polymerase cocktail (Boehringer Mannheim). The PCR product(s) were ligated to a T/A vector (pCR2.1, Invitrogen) and completely sequenced on both strands (Oswel DNA Services, Southampton, U.K.).

Cell culture

Bovine adrenal chromaffin cells were prepared from adrenal glands freshly obtained from an abattoir. The standard approach [14] involved collagenase digestion and mechanical dispersion. The dispersed cells were maintained in culture for up to 5 days in 30 mm diameter plastic culture chambers and on glass coverslips in Dulbecco's modified Eagle's medium supplemented with 1% (v/v) 1× insulin/transferrin/selenium supplement (ITS-X), 0.1% penicillin/streptomycin and 1% (w/v) sodium pyruvate (all from Gibco BRL Life Technologies) at 37 °C in 95% air, 5% CO_2. BHK-21 cells were cultured in Glasgow Modified Eagle's medium supplemented with 10% (v/v) tryptose phosphate broth, 10% (v/v) foetal bovine serum, 2 mM glutamine and 100 units/ml of penicillin/streptomycin (all from Gibco BRL Life Technologies) at 37 °C in 95% air, 5% CO_2, and used between passage numbers 5 and 15.

Generation of recombinant SFV particles

PCR was used to generate an *Eco*RI-*Bam*HI flanked DOC2β fragment for ligation to pEGFPN1 (Clontech). DOC2β-EGFP cDNA was sub-cloned into the *Sma*I site of pSFV1 expression vector (Life Technologies) as a T4 DNA polymerase blunt-ended *Eco*RI-*Not*I fragment from pEGFPN1. A GFPmut3 insert was amplified by PCR using forward (5′-CGGAGATCTATGAGTAAAGGAGAAGAACTTTTCACT) and reverse (5′-GCCGGATCCCATATGTTTGTATAGTTCATCCATGCCATGTGTAAT) deoxyoligonucleotides, and a GFPmut3 plasmid as a template. The PCR product was treated with Klenow enzyme and ligated to the *Eco*RV site of pBluescript II KS (Stratagene). The insert was subcloned as a *Bam*HI-*Bgl*II fragment into pSFV1. The orientation and integrity of the cDNA inserts were confirmed by DNA sequencing. Capped mRNA was generated from these constructs and pSFV2 helper vector (Gibco BRL Life Technologies) by linearizing both vectors with *Spe*I and transcribing *in vitro* using SP6 RNA polymerase according to the manufacturer's instructions. Five to ten micrograms of each *in vitro*-transcribed mRNA were electroporated into approx. 1×10^7 BHK-21 cells in Glasgow modified Eagle's medium supplemented with 2 mM glutamine at 2125 V/cm, 25 μF and pulsed twice using a Bio-Rad GenePulser apparatus. Cells were allowed to recover for 5 min, resuspended in 24 ml of complete medium and plated for culture for a further 48 h. Medium was recovered from these plates, and filtered through a 0.25 μm-pore-size filter before storage at −20 °C.

Infection of chromaffin cells with recombinant SFV particles

Approx. 1×10^6 freshly prepared chromaffin cells were plated in 90-mm diameter tissue-culture plates containing sterile glass coverslips. After 24 h of culture at 37 °C, the conditioned culture medium was removed and stored for later use. Virus stock was activated by the addition of chymotrypsin A4 (250 μg/ml; Sigma Aldrich) and digestion for 10 min on ice. Proteolysis was halted by the addition of aprotinin (0.67 mg/ml; Sigma–Aldrich). A 1:10 dilution of the virus stock was made in conditioned chromaffin cell medium, and approx. 1 ml of this was overlaid on to the cells. The cells were incubated with the virus for 2 h, then the medium was removed and replaced again with conditioned chromaffin cell medium. The infected cells were cultured for specific times post infection before harvesting for immunoblot analysis and confocal fluorescence microscopy.

Immunoblotting

Cells were removed from culture at appropriate time points after infection and washed three times with ice-cold PBS, pH 7.4 (Gibco BRL Life Technologies). Cells were homogenized in the plate by the addition of 500 μl of lysis buffer [10 mM Tris/HCl, 0.1% (w/v) SDS, 1μg/ml leupeptin, 1 μg/ml aprotinin, 0.2 mM 4-(2 aminoethyl)benzenesulphonyl fluoride, pH 7.4] and scraping into a fresh tube. The protein concentration was determined by assaying a 1 in10 dilution of the mixture using the Bradford method according to the manufacturer's instructions (Bio-Rad). Approx. 10 μg of protein per sample were electrophoresed in an SDS/10% polyacrylamide gel using the method of Laemmli [15]. Proteins were transferred to poly(vinylidene difluoride) (Bio-Rad) using a Trans-Blot SD (Bio-Rad) semi-dry electroblotter at 20 V for 30 min. Following transfer, excess binding sites on the membrane were blocked by incubating in blotting buffer (PBS, 5% (w/v) non-fat skimmed milk) for 1 h. Monoclonal anti-synaptotagmin, anti-rSEC8, anti-rabphilin-3A, anti-munc-18 (Transduction Laboratories), monoclonal anti-GFP (Clontech) or polyclonal anti-dopamine-β-hydroxylase (D-β-H) were diluted in blocking buffer and incubated with the membranes for 1 h. Membranes were washed extensively with PBS before incubation with horseradish peroxidase-conjugated anti-mouse IgG (Transduction Laboratories, for monoclonals) or horseradish-peroxidase conjugated anti-rabbit IgG (Amersham–Pharmacia Biotech, for polyclonal), diluted in blocking buffer as before. Decorated proteins were revealed by ECL® (Amersham–Pharmacia Biotech) according to the manufacturer's instructions.

Single-cell fluorescence and electrophysiology

Cells expressing GFP or EGFP fusion proteins were identified by their green fluorescence. The cells attached to glass coverslips were mounted in a perfusion chamber located on the stage of an inverted microscope (Zeiss Axiovert 100), and illuminated via the epi-illumination pathway by a monochromated light source (TILL Photonics, Planegg, Germany). Excitation was at 488 nm for EGFP and 395 nm for the mut3.1GFP. The filter combination was a dichroic mirror Q500L and the emission filter HQ500LP (Chroma Technology, Brattleboro, VT, U.S.A.).

Fluorescent cells were subjected to perforated-patch recording with an EPC-9 patch clamp system (HEKA Elektronik, Germany); a system which performs automated on-line measurements of ionic currents, membrane capacitance, membrane conductance and series conductance. Membrane capacitance is proportional to cell-membrane-surface area and serves as a measure of secretion, since the surface area increases upon exocytotic addition of vesicular membrane and decreases upon endocytosis [14]. The patch pipette solution contained 135 mM caesium glutamate, 9 mM NaCl, 1 mM triethylammonium chloride, 10 mM Hepes (pH 7.3, titrated with CsOH). For perforation of the membrane patch, standard protocols were followed [16] and the amphotericin (Sigma–Aldrich) concentration was 200 μg/ml. After seal formation, the series resistance was measured continuously and recordings were started when the series resistance dropped below 20 MΩ. The external bath solution contained 145 mM NaCl, 2.8 mM KCl, 5 mM $CaCl_2$, 1 mM $MgCl_2$, 10 mM Hepes (pH 7.3, titrated with NaOH) and 10 mM glucose. The external bath solution was constantly perfused at 0.5–1 ml/min. Recordings were made at room

temperature (approx. 20 °C). The values of membrane current and capacitance responses are reported as the mean ± S.E.M. in the text.

Confocal microscopy

Cells cultured on glass coverslips were washed twice with PBS supplemented with Ca^{2+} and Mg^{2+} before fixation for 5 min with ice-cold 4% (w/v) buffered paraformaldehyde, or living cells were imaged using a Leica TCS NT Confocal System (Leica Lasertechnik GmbH, Heidelberg, Germany) with a PL APO 63 × /1.32–0.6 oil immersion lens, also made by Leica. If required, cells were counter-stained using the acidotropic dye LysoTracker Red according to the manufacturer's instructions (Molecular Probes).

RESULTS

Highly efficient SFV infection of adrenal chromaffin cells

Previously published procedures for SFV transduction yielded low efficiencies of infection/expression (10–20%) in chromaffin cells. Adding the step of inactivating the chymotrypsin A (used to activate the viral particles) increased the number of cells that survived viral incubation, but the numbers of cells expressing GFP still remained low (< 30%). The further modification using conditioned chromaffin cell medium rather than PBS or BHK-21 medium for both the virus incubation and recovery stages dramatically improved the final percentage of cells observed to have a fluorescent phenotype 48–72 h post-infection. Approx. 90–100% of all cells were observed to fluoresce, estimated by directly counting the fluorescent cells compared with the total number of cells counted under visible light (Figure 1B). Immunoblot studies of viral-infected chromaffin cells demonstrated that DOC2β-EGFP could be detected using a monoclonal anti-GFP antibody between 16–19 h post-infection. These observations were supported by the development of a fluorescent-chromaffin-cell phenotype in infected cells between these time-points. The levels of detectable decorated DOC2β-EGFP increased steadily up to 72 h post-infection, with no apparent change in cellular morphology (Figures 1A and 1B).

In this study, we used a 1:10 dilution of one-sixtieth of the virus stock (approx. 8×10^6 infectious units) to infect approx. 1×10^5 cells. This provided a multiplicity of infection of approx. 8, assuming that all the viral particles were competent to infect chromaffin cells. In practice, the dilution of the viral stock could have been greater.

Chromaffin cell biology after SFV infection

Immunoblot studies of the endogenous chromaffin cell proteins synaptotagmin, D-β-H, rSEC8, rabphilin-3A and munc-18 demonstrated that the steady-state levels of these proteins did not decrease throughout this time course (Figure 1A). The stabilities of synaptic proteins are variable [11], although no data is available relating to these proteins in bovine adrenal chromaffin

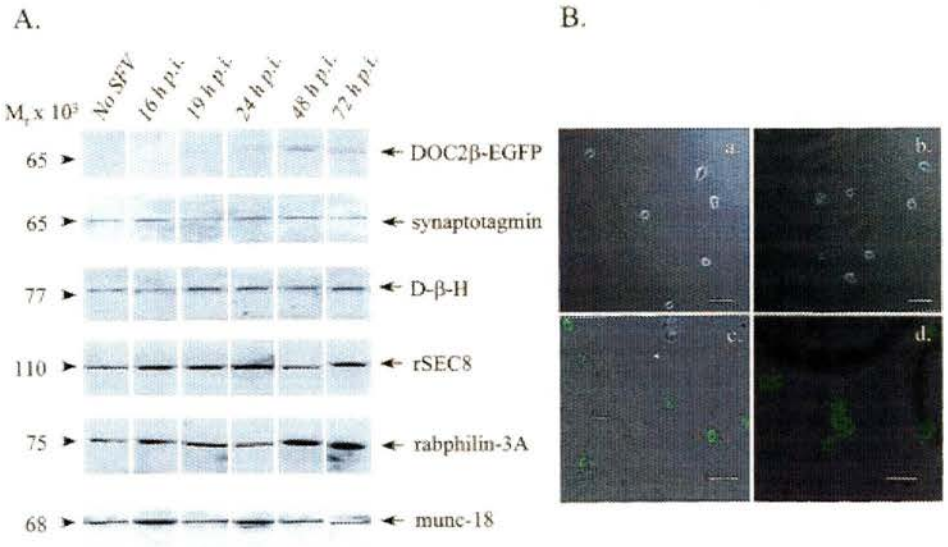

Figure 1 (A) Immunoblot analysis of DOC2β-EGFP fusion protein expression in SFV-infected bovine adrenal chromaffin cells, and (B) low-power confocal images superimposed on bright-field images of SFV-infected bovine adrenal chromaffin cells

(**A**) DOC2β-EGFP fusion protein was first detected between 16 h and 19 h post-infection (p.i.), with the level of detectable protein increasing with time up to 72 h post-infection. The levels of synaptotagmin, dopamine-β-hydroxylase (D-β-H), rSEC8, rabphilin-3A and munc-18 did not decrease over the time of the study. The time course of expression is in contrast with the time course of SFV-transduced expression, reported previously, where host-cell protein synthesis was sequestered as early as 9 h post-infection (see text for references). (**B**) Cells grown on sterile glass coverslips were removed from the same cultures used for immunoblot analysis and examined under 488 nm illumination as described in Materials and methods section. DOC2β-EGFP could be seen from 19 h post-infection, and increased in intensity up to 72 h post-infection. No EGFP fluorescence could be detected in non-infected cells. (a) At 16 h post-infection, no fluorescence is visible. (b) At 19 h post-infection, some EGFP fluorescence is just visible. This correlates with immunoblot analyses, which first detected decorated DOC2β-EGFP between 16 h and 19 h. (c) and (d) The intensity of the EGFP-fluorescence appeared to increase between 24 h and 72 h post-infection. The relative percentage of cells with the green fluorescent phenotype can be judged by comparing fluorescent cells with non-infected cells, revealed by the superimposition of the bright-field image. At 24 h post-infection, a single cell (arrow) that is not expressing DOC2β-EGFP can be seen in this field. In these experiments, we judged the efficiency of infection and expression to be 90–100% by 48–72 h post-infection. These images are representative of several independent experiments, where the observed transduction efficiencies were comparable ($n > 25$ experiments). Scale bars: 10 μm.

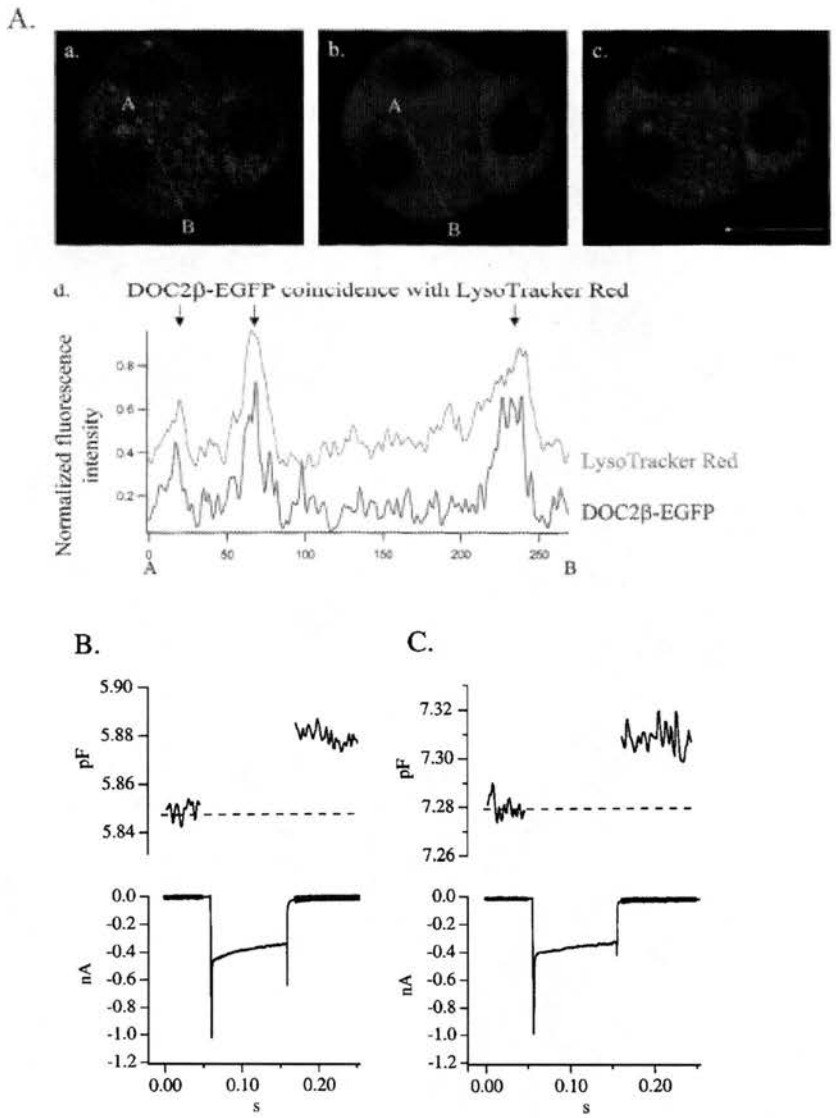

Figure 2 Confocal microscopy and electrophysiology of DOC2β-EGFP-expressing chromaffin cells

(**A**) High-power confocal images of a group of three DOC2β-EGFP-expressing chromaffin cells 48 h post-infection. A single 1 μm-thick confocal optical section, illuminated at 488 nm and 577 nm, was used to produce these images. (a) The EGFP fluorescence is seen distributed throughout the chromaffin cell in a punctate distribution with nuclear sparing, reminiscent of a vesicular localization. This coincides with the distribution of LysoTracker Red in the same cell (b), which also shows a punctate distribution with nuclear sparing. (c) Superimposition of the two images revealed the fluorescent spots to be overlapping, as indicated by yellow. A yellow line AB shown on (a) and (b), was measured for fluorescence intensity. (d) Shows the normalized intensity under the line proceeding in arbitrary distance units from point A to point B. Similar vertical lines were drawn through 55 vesicular areas in 5 cells. DOC2β-EGFP peaks were coincident with LysoTracker Red peaks in 98% of cells. Conversely LysoTracker Red peaks were coincident with DOC2β-EGFP peaks in 76% of cells. The arrows mark peaks that are representative of vesicular fluorescence. Scale bar: 10 μm with bold inset (yellow square on left hand end of scale bar in panel c; 0.39 μm) representing the approximate size of a large dense core vesicle. Membrane currents and capacitance responses in response to depolarizations of 100-ms duration to +10 mV, from a holding potential of −70 mV for (**B**) non-infected cells and (**C**) infected cells. The solutions have been designed to isolate the inward currents – an initial rapidly inactivating sodium current, followed by a maintained calcium current. The membrane capacitance increases in response to the injections of calcium due to the depolarizations. There is a gap during the depolarizations, during which the capacitance measurements are not calculated.

cells. Interestingly, the half-life of synaptotagmin I in neurons has recently been shown to be within 8–22 h during 1–3 days of culture [11]. The stable synaptotagmin level in our experiments suggest that the ability of SFV-infected cells to synthesize new proteins remains unaffected over the course of this experiment. Biophysical studies of cells expressing GFP and DOC2-EGFP constructs 48 h after SFV infection revealed that the cell membranes were intact, with no significant increase in the leak current [2.8 ± 0.4 pA ($n = 18$) compared with 3.2 ± 0.5 pA ($n = 18$) in non-infected cells], and the cells displayed significant calcium currents and capacitance increases, indicative of exocytosis (Figures 2B and 2C). When subjected to 100-ms depolarizations to +10 mV, the chromaffin cells displayed a mean calcium current amplitude of 297 ± 23 pA ($n = 18$), which is approx.

25% less than the current measured in non-infected chromaffin cells at 407 ± 37 pA ($n = 18$). In response to the injection of calcium current, the transduced cells responded with an increase in membrane capacitance of 14 ± 2 fF ($n = 18$), compared with 31 ± 4 ($n = 18$) in non-infected cells. Thus, 48 h after viral infection, all the infected cells are expressing heterologous protein, and they continue to carry out normal physiological processes of calcium current conduction and exocytosis.

DOC2β is localized to an acidic, vesicular compartment in chromaffin cells

Confocal microscopy revealed that DOC2β-EGFP fluorescence was distributed throughout the cell in a characteristic punctate pattern with nuclear sparing, reminiscent of a vesicular localization. Cells that were loaded with the acidic compartment probe LysoTracker Red showed a similar fluorescence distribution. The vesicular distribution of DOC2β-EGFP shows 98% coincidence with LysoTracker Red in double-labelled cells, suggesting that the DOC2β-EGFP fusion protein was directed to an acidic compartment in these cells (Figure 2A). In contrast, transduced GFPmut3 displayed a homogeneous cytoplasmic distribution (results not shown).

DISCUSSION

We have developed a modification of the SFV transduction approach that efficiently introduces heterologous cDNA into bovine adrenal chromaffin cells. The steady-state levels of several endogenous chromaffin cell proteins remain unaffected up to 72 h post-infection. This result is surprising because SFV has been shown to sequester host-cell protein-synthesis machinery after infection, effectively halting endogenous protein synthesis in favour of viral protein production; however, the observation suggests that there may be a time window over which meaningful biophysical studies of exocytosis can be carried out. Indeed, our preliminary results with patch-clamp measurements have demonstrated that the cells still have significant calcium currents and secretion, though somewhat depressed compared with non-infected cells. These data are in agreement with a recent paper describing the use of SFV vectors to express synaptic proteins in cultured neurons without cytotoxic effects [11].

The time course of heterologous protein expression in chromaffin cells appeared to be slower than in cultured cell-lines such as BHK-21 cells, COS-7 cells and Chinese hamster ovary cells (e.g. [17]), where it has been reported that expressed protein can be detected as early as 9 h post-infection, at which point host endogenous protein synthesis is already depressed. Furthermore, the levels of heterologous protein expression, judged by immunoblotting and GFP fluorescence intensity, are relatively low compared with those in other cell types reported previously [8–10].

The observation here that DOC2β-EGFP is directed to an intracellular acidic compartment, in support of earlier work on DOC2 intracellular localization (e.g. [12]), provides evidence that proteins expressed from SFV-based vector systems in chromaffin cells can be correctly processed and targeted. Furthermore, this is the first direct visualization of DOC2-EGFP *in vivo*. Additional experiments using SFV-GFPmut3 alone confirmed the high-efficiency of transduction using these conditions, and the ability of SFV-expressed proteins to be directed to the appropriate intracellular localization.

SFV transduction systems have, until now, been used for large-scale, high-efficiency protein production in mammalian cells. The slow time course, high-efficiency of infection and expression, and reduced expression levels seen in bovine chromaffin cells should make the SFV transduction system a valuable tool in the study of chromaffin cell biology.

We thank Dr. David Apps for his gift of the rabbit polyclonal anti-bovine dopamine-β-hydroxylase antibody. We also thank Ms. Linda Sharp for her expert assistance with the confocal microscopy. This work was funded by a Wellcome Trust Project grant to R.H.C and M.J.S.

REFERENCES

1 Ma, W. J., Holz, R. W. and Uhler, M. D. (1992) J. Biol. Chem. **267**, 22728–22732
2 Liu, F., Housley, P. R. and Wilson, S. P. (1996) J. Neurochem. **67**, 1457–1462
3 Wick, P. F., Senter, R. A., Parsels, L. A., Uhler, M. D. and Holz, R. W. (1993) J. Biol. Chem. **268**, 10983–10989
4 Wilson, S. P., Liu, F., Wilson, R. E. and Housley, P. R. (1995) Anal. Biochem. **226**, 212–220
5 Moss, B., Elroystein, O., Mizukami, T., Alexander, W. A. and Fuerst, T. R. (1990) Nature (London) **348**, 91–92
6 Moss, B. and Flexner, C. (1989) Annals N.Y. Acad. Sci. **569**, 86–103
7 Berglund, P., Sjoberg, M., Garoff, H., Atkins, G. J., Sheahan, B. J. and Liljestrom, P. (1993) Bio/Technology **11**, 916–920
8 Liljestrom, P. and Garoff, H. (1991) Bio/Technology **9**, 1356–1361
9 Olkkonen, V. M., Liljestron, P., Garoff, H., Simons, K. and Dotti, C. G. (1993) J. Neuroscience Res. **35**, 445–451
10 Olkkonen, V. M., Dupree, P., Killisch, I., Zerial, M. and Simons, K. (1993) J. Cell Sci. **106**, 1249–1261
11 Daly, C. and Ziff, E. B. (1997) J. Neurosci. **17**, 2365–2755
12 Verhage, M., deVries, K. J., Roshol, H., Burbach, J. P. H., Gispen, W. H. and Sudhof, T. C. (1997) Neuron **18**, 453–461
13 Orita, S., Naito, A., Sakaguchi, G., Maeda, M., Igarashi, H., Sasaki, T. and Takai, Y. (1997) J. Biol. Chem. **272**, 16081–16084
14 Lindau, M. and Neher, E. (1988) Pfluegers Arch. **411**, 137–146
15 Laemmli, U. K. (1970) Nature (London) **277**, 680–668
16 Zhou, Z. and Neher, E. (1993) J. Physiol. (London) **469**, 245–273
17 Cicciarone, V., Anderson, D. and Jesse, J. (1997) Focus **16**, 94–98

Received 7 May 1999/30 June 1999; accepted 16 July 1999

Efficacy of Semliki Forest Virus Transduction of Bovine Adrenal Chromaffin Cells

An Analysis of Heterologous Protein Targeting and Distribution

RORY R. DUNCAN, JENNIFER GREAVES, SOMPOL TAPECHUM, DAVID K. APPS, MICHAEL J. SHIPSTON, AND ROBERT H. CHOW[a]

University of Edinburgh, Division of Biomedical and Clinical Laboratory Sciences, Membrane Biology Group, Edinburgh EH8 9XD, Scotland

ABSTRACT: **In using chromaffin cells as a model for studying the mechanism of regulated exocytosis, there is a requirement for an efficient, safe, and robust system for the transduction and expression of heterologous cDNA in these cells. We have used Semliki Forest virus to transduce cDNAs encoding various proteins fused to enhanced green fluorescent protein (EGFP) into cultured bovine adrenal cells. Transduction is highly efficient but has no significant effect on the steady state levels of several endogenous proteins or of catecholamines in the transfected cells. Furthermore, the transfected cells show depolarization-induced calcium currents and nicotine-induced catecholamine release. We present data to show that virally transduced proteins are targeted to their intracellular locations correctly in chromaffin cells. The fusion protein pro-ANF-EGFP is specifically targeted to large dense-core vesicles as shown by its colocalization with acidophilic dyes and chromogranin A, making this a useful system for the study of secretory vesicle dynamics.**

KEYWORDS: **GFP; exocytosis; confocal laser scanning microscopy; three-dimensional image analysis**

INTRODUCTION

Adrenal chromaffin cells have proved to be a model system for studies of regulated exocytosis. These neuroendocrine cells, like neurones, fire action potentials, exhibit calcium-dependent exocytosis, and express many proteins closely related to synaptic proteins.

Address for correspondence: Rory R. Duncan, University of Edinburgh, Division of Biomedical and Clinical Laboratory Sciences, Membrane Biology Group, George Square, Edinburgh EH8 9XD, Scotland. Voice: +44-1316502864; fax: +44-1316503711.
rd@srv4.med.ed.ac.uk

[a]Robert H. Chow's current address: Keck University Medical School, University of Southern California, Los Angeles, CA 90089-9142, USA.

Ann. N.Y. Acad. Sci. 971: 641–646 (2002).

An important barrier to the advance in understanding of the molecular mechanisms underlying exocytosis has been the lack of a high-efficiency technique for introducing heterologous DNA or RNA into chromaffin cells. The more "traditional" methods for mammalian cell transfection, such as electroporation, lipid-mediated transfection, and calcium phosphate precipitation have variable efficiencies and limited success.[1–3]

The desire to achieve the efficient transduction of cDNA into eukaryotic cells has driven the development of several viral transduction systems. The ideal viral-vector system would permit efficient infection of target cells with high-level protein expression and low cytotoxicity, would be easy to use, and would have a broad host range but low human pathogenicity. Efficient viral transduction systems for mammalian cells based on a recombinant vaccinia virus, adenovirus, or defective HSV1 have been developed (for review, see Moss *et al.*[4]), but these can be time consuming and expensive and require considerable expertise. In addition, adequate containment facilities are essential for these systems. The Semliki Forest virus (SFV) transduction system[5,6] has several potential benefits over other viral transduction systems, including minimal containment requirements and ease of use.

The SFV transduction system already has been used to express several proteins in a broad range of mammalian cells, including cultured rat hippocampal neurons, BHK, HeLa, and MDCK cells.[5–7] This broad host cell range, the ability to subclone directly into the expression vector without the need for *in vivo* recombination steps, and the excellent attenuation of recombinant SFV together make this system a particularly attractive candidate for transducing cDNA into chromaffin cells. Recently, a variant of the vector carrying two point mutations was developed. This showed lower cytotoxicity and much higher expression levels in primary neurons compared with the wild-type SFV vector. A triple mutant vector demonstrated temperature-sensitive expression in both BHK cells and primary neurons.[8] Recent work has seen the extensive use of green fluorescent protein (GFP), a soluble inherently fluorescent protein isolated and cloned from the pacific jellyfish *Aequoria victoria*. Spectral variants and "humanized" (i.e., mammalian codons replace the jellyfish preferred codons) forms of GFP such as enhanced GFP (EGFP) subsequently have been described. GFP and its relatives are widely used as noninvasive fluorescent markers to study fusion protein dynamics and localization. In this article, we examine the efficacy of SFV transduction of a soluble, cytoplasmic protein (GFP), a vesicle membrane peripherally associated protein (double C2 protein (DOC2β)-EGFP), a plasma membrane/vesicle associated *trans*-membrane protein (syntaxin 1a-EGFP), and a vesicle lumen cargo protein (atrial natriuretic factor [pro-ANF]-EGFP)[9] in chromaffin cells. We present data to demonstrate the accurate targeting of these proteins to their appropriate intracellular locations.

SFV INFECTION OF ADRENAL CHROMAFFIN CELLS IS HIGHLY EFFICIENT

Previously published procedures for SFV transduction achieved only low efficiencies of infection/expression (10–20%) in chromaffin cells. Adding the step of inactivating the chymotrypsin A (used to activate the viral particles) increased the number of cells that survived viral incubation, but the numbers of cells expressing

GFP still remained low (<30%). The further modification of using conditioned chromaffin cell medium rather than phosphate-buffered saline or BHK-21 medium for both the infection and recovery stages drastically improved the fraction of fluorescent cells 48–72 hours after infection. Approximately 90–100% of all cells were observed to fluoresce, estimated by directly counting the fluorescent cells compared with the total number of cells counted under visible light. Immunoblot studies of viral-infected chromaffin cells demonstrated that DOC2β-EGFP could be detected using a monoclonal anti-GFP antibody between 16 and 19 hours after infection. These observations were supported by the development of a fluorescent chromaffin cell phenotype in infected cells between these time points. The levels of detectable decorated DOC2β-EGFP increased steadily up to 72 hours after infection, with no change in cellular morphology.[10]

CHROMAFFIN CELL BIOLOGY IS UNPERTURBED AFTER SFV INFECTION

Western blot studies of endogenous chromaffin cell exocytotic proteins demonstrated that the steady state levels of these proteins did not decrease throughout a 0- to 72-h transduction time course,[10] suggesting that the ability of SFV-infected cells to synthesize new proteins remains unaffected during this time. Biophysical studies of cells expressing GFP and Doc2-EGFP constructs 48 hours after SFV infection revealed that the cell membranes are intact, with no significant increase in the leak current, and the cells display significant calcium currents and capacitance increases, indicative of exocytosis. When subjected to 100-ms depolarizations to +10 mV, the transduced chromaffin cells displayed a mean calcium current amplitude approximately 25% less than the current measured in noninfected chromaffin cells.[10] In response to calcium inflow, the transduced cells responded with an increase in membrane capacitance similar to that in noninfected cells.[10] A fluorescent assay of catecholamine release revealed no significant difference between total catecholamine content and release from mock- and SFV-transduced chromaffin cells 16–24 hours after infection (R.R. Duncan, J. Greaves, D.K. Apps, M.J. Shipston, and R.H. Chow, unpublished data). Thus, at 48 hours after viral infection, all the infected cells are expressing heterologous protein, and they continue to perform normal physiological processes such as depolarization-induced calcium influx, catecholamine synthesis, and exocytosis. These data are in close agreement with another study of SFV transduction in chromaffin cells.[11]

HETEROLOGOUS PROTEIN TARGETING

Confocal laser scanning confocal microscopy of living or fixed chromaffin cells transduced to express fluorescently tagged synaptic proteins demonstrated that the introduced fusion proteins could be directed to the appropriate intracellular compartments. Data deconvolution, three-dimensional image reconstruction, and quantitation were used to further analyze protein distributions in chromaffin cells. Syntaxin 1a-EGFP was found to be distributed in a punctate pattern, with a significant fraction of the expressed protein present in raft-like structures on the cell surface, as revealed

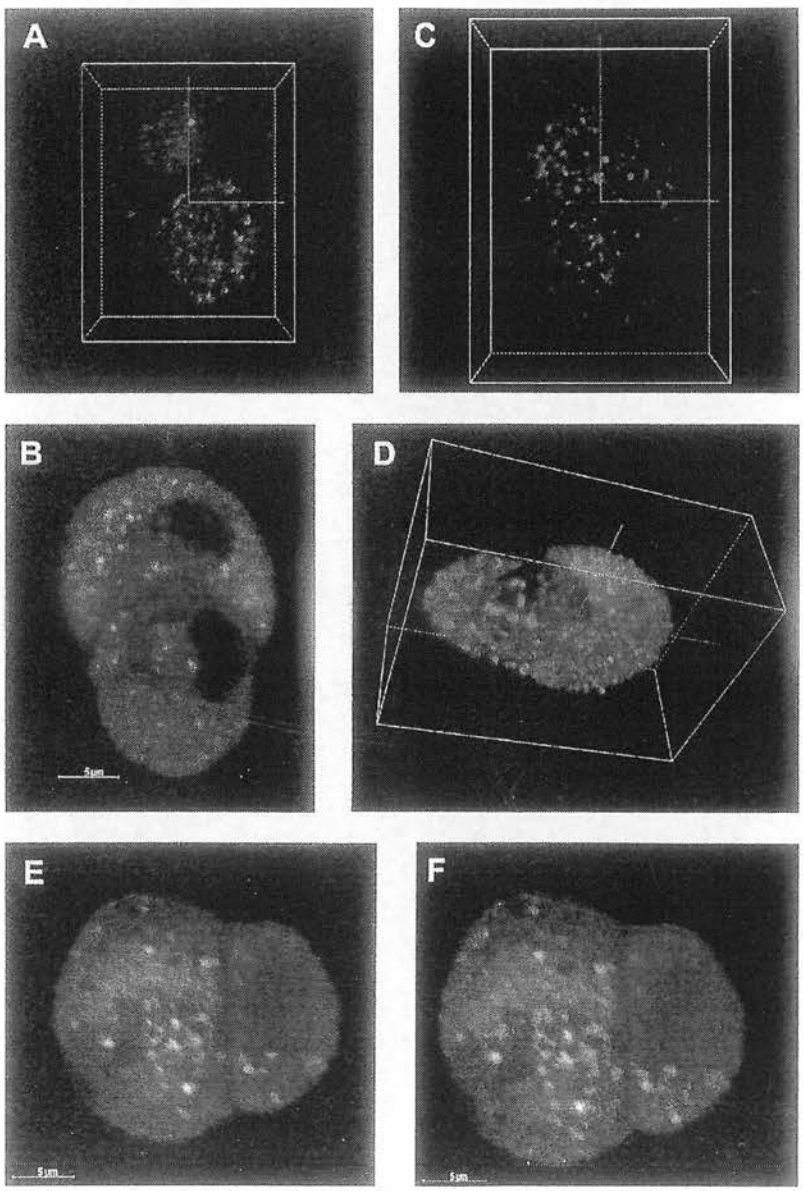

FIGURE 1. *See following page for legend.*

by three-dimensional image reconstruction (FIG. 1A). This distribution is similar to that previously reported for native syntaxin 1a in Baby Hamster Kidney (BHK-21) and PC12 cells.[12] The targeting of pro-ANF-EGFP to the lumen of LDCVs was subjected to a particularly detailed analysis. Analyses based on a pixel-by-pixel comparison of thresholded green and red fluorescence intensities in living cells demonstrated that 96.5 ± 0.2% of the green channel pixels colocalized in 3D with red channel pixels in LDCV-sized structures, whereas 1.040 ± 0.002% of red pixels colocalized with pro-ANF-EGFP labeling (FIG. 1B–D). The latter figure leads to a rough estimate of up to 15,000 LDCVs per cell, bearing in mind that not all acidic organelles are presumed to be LDCVs. Consistent with their being LDCVs, the labeled structures had a calculated diameter of approximately 380 nm (mean volume, 0.0281 ± 0.0002 μm^3; $n = 760$ single objects from seven cells). In addition, the ANF-EGFP fluorescence colocalized with immunostaining for chromogranin A in fixed cells (not shown), a secretory protein found in the lumen of LDCVs. The direction of SFV-transduced pro-ANF to the lumen of LDCVs in chromaffin cells is in agreement with previous reports of pro-ANF distribution.[9,13] Confocal microscopy revealed the DOC2β-EGFP fluorescence to be distributed throughout the cell in a characteristic punctate pattern with nuclear sparing, reminiscent of a vesicular localization (FIG. 1E). The fluorescence distributions of DOC2β-EGFP pixels Lysotracker red DND-99 pixels were found to be greater than 99% colocalized in double-labeled cells, suggesting that the DOC2β-EGFP fusion protein was directed to an acidic compartment in these cells (FIG. 1F).[10] In contrast, transduced GFP displayed a homogeneous cytoplasmic distribution (not shown).

SFV transduction systems have, until now, been used for large-scale, high-efficiency protein production in mammalian cells. The high efficiency of infection and expression and reduced expression levels seen in bovine chromaffin cells should make the SFV transduction system a valuable tool in the study of chromaffin cell biology. Recent work[14] has cast doubt on the use of acidophilic dyes such as acridine orange to image exocytotic events. These dyes accumulate in acidic organelles but become membrane permeant if the intralumenal pH increases, leading to a loss of fluorescence and rapid probe diffusion. This effect appears identical to images of fluorescent vesicle fusion.[14] Furthermore, the restoration of the acidic pH inside the vesicle leads to further accumulation of cytoplasmic dye, causing the impression of

---

FIGURE 1. Confocal images of bovine adrenal chromaffin cells transduced with SFV to express synaptic proteins tagged with EGFP. (**A**) A three-dimensional reconstruction showing an EGFP-syntaxin 1a vesicular distribution with a significant fraction of the punctate fluorescence located on the cell surface. (**B**) A single, 0.4-μm–thick confocal optical section showing pro-ANF-EGFP to occupy a punctate pattern concentrated at the base the cell, as previously described for LDCV distribution in bovine adrenal chromaffin cells.[15] These structures colocalized with Lysotracker red–extracted pixels. (**C, D**) The colocalization map of extracted pixels superimposed upon a three-dimensional reconstruction of pro-ANF-EGFP–transduced cells demonstrates that the colocalization of pro-ANF-EGFP with Lysotracker is almost complete by the lack of any remaining green or yellow pixels. Colocalization is represented by gray or white structures. (**E**) A three-dimensional reconstruction of three cells expressing DOC2β-EGFP and costained with Lysotracker red. (**F**) A three-dimensional reconstruction of colocalizing pixels superimposed onto the original image, as in **D**, reveals almost complete coincidence between the EGFP and the Lysotracker red fluorescence.

the appearance of a "new" vesicle recruited to the site of the previous "flash". Fluorescent pro-ANF comprises an excellent and specific marker for LDCVs in chromaffin cells, which is not membrane permeant, and specificity problems associated with acidophilic dyes.

Highly efficient SFV transduction of bovine adrenal chromaffin cells, high-resolution confocal fluorescence microscopy, combined with three-dimensional image analysis will permit the investigation of the dynamics of exocytosis in living primary cell cultures.

REFERENCES

1. LIU, F., P.R. HOUSLEY & S.P. WILSON. 1996. Initial processing of human proenkephalin in bovine chromaffin cells. J. Neurochem. **67:** 1457–1462.
2. WICK, P.F., R.A. SENTER, L.A. PARSELS, *et al.* 1993. Transient transfection studies of secretion in bovine chromaffin cells and PC12 cells—generation of kainate-sensitive chromaffin cells. J. Biol. Chem. **268:** 10983–10989.
3. WILSON, S.P., F. LIU, R.E. WILSON & P.R. HOUSLEY. 1995. Optimization of calcium-phosphate transfection for bovine chromaffin cells—relationship to calcium-phosphate precipitate formation. Anal. Biochem. **226:** 212–220.
4. MOSS, B., O. ELROYSTEIN, T. MIZUKAMI, *et al.* 1990. New mammalian expression vectors. Nature **348:** 91–92.
5. BERGLUND, P. *et al.* 1993. Semliki Forest Virus expression system: production of conditionally-infectious recombinant particles. Biotechnology **11:** 916–920.
6. LILJESTROM, P. & H. GAROFF. 1991. A new generation of animal cell expression vectors based on the semliki forest virus replicon. Biotechnology **9:** 1356–1361.
7. OLKKONEN, V.M. *et al.* 1993. Molecular cloning and subcellular localization of three GTP-binding proteins of the rab subfamily. J. Cell Sci. **106:** 1249–1261.
8. LUNDSTROM, K., D. ROTMANN, D. HERMANN, *et al.* 2001. Novel mutant Semliki Forest virus vectors: gene expression and localization studies in neuronal cells. Histochem. Cell Biol. **115:** 83–91.
9. BURKE, N.V. *et al.* 1997. Neuronal peptide release is limited by secretory granule mobility. Neuron **19:** 1095–1102.
10. DUNCAN, R.R. *et al.* 1999. High-efficiency Semliki Forest virus-mediated transduction in bovine adrenal chromaffin cells. Biochem. J. **342:** 497–501.
11. KNIGHT, D.E. 1999. Secretion from bovine chromaffin cells acutely expressing exogenous proteins using a recombinant Semliki Forest Virus containing an EGFP reporter. Mol. Cell. Neurosci. **14:** 486–505.
12. LANG, T. *et al.* SNAREs are concentrated in cholesterol-dependent clusters that define docking and fusion sites for exocytosis. EMBO J. **20:** 2202–2213.
13. JOHNS, L.M., E.S. LEVITAN, E.A. SHELDEN, *et al.* Restriction of secretory granule motion near the plasma membrane of chromaffin cells. J. Cell Biol. **153:** 177–190.
14. WILLIAMS, R.M. & W.W. WEBB. 2000. Single granule pH cycling in antigen-induced mast cell secretion. J. Cell Sci. **113:** 3839–3850.
15. CUCHILLO-IBANEZ, I., P. MICHELENA, A. ALBILLOS & A.G. GARCIA. 1999. A preferential pole for exocytosis in cultured chromaffin cells revealed by confocal microscopy. FEBS Lett. **459:** 22–26.

Use of ANF-EGFP for the Visualization of Secretory Vesicles in Bovine Adrenal Chromaffin Cells

JENNIFER GREAVES, RORY R. DUNCAN, SOMPOL TAPECHUM, DAVID K. APPS, MICHAEL J. SHIPSTON, AND ROBERT H. CHOW[a]

Division of Biomedical and Clinical Laboratory Sciences, Membrane Biology Group, University of Edinburgh, Edinburgh EH8 9XD, United Kingdom

KEYWORDS: **GFP; exocytosis; fluorescence; confocal laser scanning microscopy**

Much of the recent progress in the study of regulated exocytosis in chromaffin cells has depended on the evolution of technologies designed to solve the problems of analyzing secretory vesicle movement. The tools now available include methods for introducing heterologous DNA or RNA into chromaffin cells, probes to label the various cell components, and imaging systems capable of resolving the movement of individual vesicles in real time. In particular, interest has focused on fluorescent probes that specifically label the secretory vesicles in these cells (chromaffin granules). Antibodies directed against secretory vesicle proteins can only be used in fixed, permeabilized cells. Most nonprotein labels, which are typically small organic molecules, have poor subcellular specificity and resolution. For example, acidophilic probes such as acridine orange label chromaffin granules, but do not allow them to be distinguished from the many other acidic compartments within the cell. Furthermore, recent results have called into question the use of acidophilic dyes in the study of exocytosis because, in some cell types at least, the intravesicular pH may increase following an exocytotic stimulus, but without fusion. Such luminal deacidification leads to loss of the probe into the cytoplasm, which may be recorded as an exocytotic event,[1] while subsequent reacidification results in reuptake of the probe, which may be recorded as the appearance of a new vesicle. It is not yet clear whether these difficulties apply to chromaffin cells.

Recently, a gene transduction system has been developed that uses recombinant Semliki Forest virus (SFV) to introduce Green Fluorescent Protein (GFP)–fusion proteins efficiently into bovine chromaffin cells.[2] The heterologously expressed protein needs no additional cofactors, does not affect cell growth or function, and emits

Address for correspondence: Jennifer Greaves, Division of Biomedical and Clinical Laboratory Sciences, Membrane Biology Group, University of Edinburgh, George Square, Edinburgh EH8 9XD, United Kingdom.

[a]Current address: Keck University Medical School, University of Southern California, Los Angeles, CA 90089-9142.

Ann. N.Y. Acad. Sci. 971: 275–276 (2002).

a green fluorescence on irradiation with near-UV or blue light.[3] Furthermore, GFP cDNA can be genetically fused to other proteins and expressed in eukaryotic cells with no alteration in its fluorescent properties, thereby producing an endogenous probe for gene expression or protein localization.[4]

We have used this system in chromaffin cells to express a fusion protein containing rat prepro-atrial natriuretic factor (ANF) and EGFP, a red-shifted variant of GFP.[5] Other groups have found this to be processed efficiently in PC12 cells and targeted to secretory vesicles.[6] Imaging of bovine chromaffin cells by confocal microscopy at 48 h after transduction revealed that ANF-EGFP fluorescence occurred throughout the cells with a punctate distribution; the size of the labeled organelles was consistent with their being large dense cored vesicles (chromaffin granules). They were labeled by the acidophilic probe, LysoTracker Red, suggesting that the ANF-EGFP fusion protein was directed to an intracellular acidic compartment; however, the number of red objects greatly exceeded the number of green, reflecting the low rate of secretory vesicle turnover and assembly. Immunocytochemistry of fixed cells showed that the labeled organelles contained chromogranin A, the major cargo protein of the granules. Biochemical assays showed no significant difference between control cells and cells transduced with ANF-EGFP, either in their total catecholamine content or in the fraction of catecholamine released on stimulation of the cells with nicotine. We were able to record exocytosis of the vesicle contents by total internal reflection fluorescence microscopy (TIRFM, or evanescent wave microscopy), where membrane fusion events with consequent release and dequenching of the fusion protein appeared as bright flashes. The fact that only a small subset of the chromaffin granules (~1% of the total) became labeled was a distinct advantage in that it permitted tracking of this entire vesicle population within a cell.

REFERENCES

1. WILLIAMS, R.M. & W.W. WEBB. 2000. Single granule pH cycling in antigen-induced mass cell secretion. J. Cell Sci. **113**(part 21): 3839–3850.
2. DUNCAN, R.R., A.C. DON-WAUCHOPE, S. TAPECHUM, *et al.* 1999. High-efficiency Semliki Forest virus–mediated transduction in bovine adrenal chromaffin cells. Biochem. J. **342:** 497–501.
3. CHALFIE, M., Y. TU, G. EUSKIRCHEN, *et al.* 1994. Green fluorescent protein as a marker for gene expression. Science **263:** 802–804.
4. PATTERSON, G.H., S.M. KNOBEL, W.D. SHARIF, *et al.* 1997. Use of the green fluorescent protein and its mutants in quantitative fluorescence microscopy. Biophys. J. **73:** 2782–2790.
5. ZHANG, G., V. GURTU & S.R. KAIN. 1996. An enhanced green fluorescent protein allows sensitive detection of gene transfer in mammalian cells. Biochem. Biophys. Res. Commun. **227:** 707–711.
6. BURKE, N.V., W. HAN, D. LI, *et al.* 1997. Neuronal peptide release is limited by secretory granule mobility. Neuron **19:** 1095–1102.